THE UNIVERSITY OF CALGARY

A Prototype Portable Vehicle Navigation System Utilizing Map Aided GPS

by

James Blake Bullock

A THESIS

SUBMITTED TO THE FACULTY OF GRADUATE STUDIES

IN PARTIAL FULFILMENT OF THE REQUIREMENTS FOR THE

DEGREE OF MASTER OF SCIENCE

DEPARTMENT OF GEOMATICS ENGINEERING

CALGARY, ALBERTA

JUNE, 1995

ABSTRACT

The author has developed a prototype portable vehicle navigation system (PortaNav) based on a notebook computer, a PCMCIA-type GPS receiver, and a digital road map. The system is completely autonomous and can be operated in any vehicle. The market for such a system includes business travellers, real estate agents, sales people, and tourists.

For positioning, a Kalman filter is used to combine GPS measurements with observations derived from the digital road map. Test results show that the map aided GPS solution is smoother and more accurate than stand-alone GPS, particularly in tree canopy and urban canyon environments.

The thesis describes the complete design of PortaNav. Included are details on computing platforms, GPS technology, Kalman filtering, and digital road map databases. The mathematical basis for the map aiding process is presented. Test results from various urban environments are used to illustrate the improved performance.

ACKNOWLEDGEMENTS

There are many to thank without whom this project would never have come to fruition.

First of all to Dr. Edward J. Krakiwsky, who was my friend first and supervisor second. His never-ending support, ideas, encouragement and dreams are greatly appreciated and admired. He has always shown faith in my abilities by sharing responsibilities and opportunities with me.

A special thanks to Mr. Mohamed A. Abousalem, an esteemed colleague, for having the patience to listen to my sometimes crazy ideas. His wealth of knowledge and understanding coupled with a true love of science proved to be an invaluable resource.

For technical support, thanks to Peter Loomis at Trimble Navigation and Rama Aysola at Etak, whose assistance went far beyond the call of duty.

The Natural Science and Engineering Research Council of Canada, The Province of Alberta, and The University of Calgary are gratefully acknowledged for funding this research.

To my parents, Brian and Cheryl Bullock, who have raised me to love God and those around me, to believe in myself, and to work hard to achieve my goals. Their financial and emotional support throughout my schooling will forever be appreciated.

To my dear wife Kandyce, who expects nothing but the best from me and gives everything in return. Thank you for your patience, love, and support which has inspired and buoyed me up through these years. Most of all, thank you for your friendship.

And finally, to my precious daughter Melissa, who always brings a smile to my face and a tear of joy to my heart.

To my two sweethearts,

my wife Kandyce and my daughter Melissa

TABLE OF CONTENTS

APPROVAL PAGE ii

ABSTRACT iii

ACKNOWLEDGEMENTS iv

DEDICATION v

TABLE OF CONTENTS vi

LIST OF TABLES x

LIST OF FIGURES xi

NOTATION xvi

1.0 INTRODUCTION 1

1.1 Vehicle Navigation Systems 1

1.2 Historical Review 1

1.3 Recent Technological Advances 4

1.4 Current Navigation Trends 6

1.5 Market for Portable Navigation 8

1.6 Definition of Research Project 9

2.0 PORTABLE NAVIGATION DEVICES 11

2.1 Personal Digital Assistants (PDAs) 11

2.2 Personal Navigation Assistants (PNAs) 13

2.3 Notebook Computer Based PNAs 14

3.0 GPS TECHNOLOGIES 15

3.1 Single Point GPS versus Differential GPS (DGPS) 16

3.2 Single Frequency versus Dual Frequency Receivers 17

3.3 Pseudorange versus Carrier Phase Measurements 17

3.4 PCMCIA GPS Receivers 19

3.5 Design Implications for PortaNav 19

4.0 DIGITAL ROAD MAPPING TECHNOLOGIES 20
4.1 Digital Map-Related Functions 20
4.1.1 Map Display 20
4.1.2 Address Matching 21
4.1.3 Map Matching 22
4.1.4 Best Route Calculation 24
4.1.5 Route Guidance 25
4.2 Digital Road Map Suppliers and Standards 26
4.2.1 Etak 27
4.2.2 NavTech 29
4.2.3 JDRMA 30
4.2.4 EGT and EDRA 31
4.3 Design Implications for PortaNav 33

5.0 PROTOTYPE SYSTEM DESIGN 34
5.1 Hardware and Software Components 34
5.2 Functionality 37
5.3 Performance 38
5.4 Software Design Considerations 39

6.0 POSITIONING MODULE 41
6.1 Global Positioning System 41
6.1.1 GPS Pseudoranges 41
6.1.2 Code Phase Observable 46
6.1.3 Doppler Observable 48
6.2 Positioning Solutions 51
6.2.1 Unique Solution 51
6.2.2 Least Squares Solution 52
6.2.3 Kalman Filtering 57
6.3 Map Aiding 64

6.3.1 Weighted Point Model 64
6.3.2 Slope-Intercept Model 66
6.4 Post-Mission Precise Orbit Processing 68
6.5 Positioning Module Overview 70

7.0 DATABASE ENGINE MODULE 71
7.1 Digital Road Map Coordinate Frame 71
7.2 Road Finding Algorithm 74
7.2.1 Nearest Feature Search 74
7.2.2 Confidence Regions 76
7.2.3 Road Selection and Elimination 78
7.2.4 Map Aided Updates 79

8.0 USER INTERFACE 81
8.1 Hardware Interface 81
8.2 Software Interface 81
8.3 Capabilities 83
8.4 Limitations 84
8.5 Suitability of Use 85

9.0 TESTING RESULTS 86
9.1 Solutions Compared 86
9.2 Environments Tested 87
9.3 Kalman Filter for Map Aided GPS 88
9.3.1 Kalman Filter Parameters 88
9.3.2 Kalman Filter Constraints 90
9.4 Test Descriptions 93
9.4.1 Static Tests 93
9.4.2 Open Road Tests 95
9.4.3 Tree Canopy Tests 110

9.4.4 Urban Canyon Tests 124
9.5 Performance Summary of Solution Types 137
9.5.1 Best DOP Unique Solution 137
9.5.2 Least Squares Solution 138
9.5.3 Map Aided GPS Solution 139
9.5.4 Precise Solution 140

10.0 CONCLUSIONS AND RECOMMENDATIONS 142
10.1 Conclusions From Operational Tests 142
10.2 Recommendations For Future Development Directions 144

REFERENCES 146

LIST OF TABLES

3.1 Summary of Single Point and Differential GPS Range Errors 16

4.1 Digital Road Map Feature Content Requirements for Map-Related Functions 26

4.2 Map-Related Functions Supported by Major Digital Road Map Formats/Suppliers 27

6.1 Typical Error Budget for Single Point C/A-Code GPS Pseudoranges 44

9.1 Parameters Used in Kalman Filter 89

9.2 Variances of Observations Used 89

9.3 Summary of Constraints Used in Kalman Filter 91

9.4 Static Test Comparison Between Trimble MobileGPS and Ashtech Z-12 94

9.5 Summary of Data Rates Achieved 140

LIST OF FIGURES

1.1 Position versus Location 2

1.2 The Etak Navigator 4

1.3 GPS Usage in Various Types of Vehicle Navigation Systems 7

2.1 Typical Personal Digital Assistant (PDA) Form Factors 11

2.2 Basic Elements of a PDA 13

2.3 Typical Personal Navigation Assistants (PNAs) 14

3.1 Concept of GPS Positioning 15

4.1 Map Matching for Display 23

5.1 PortaNav System Components 35

5.2 Main Software Modules in PortaNav 39

5.3 Screen Capture of the PortaNav User Interface 40

6.1 Confidence Ellipse for Computed Position 56

6.2 Recursive Kalman Filtering Algorithm 59

6.3 Sequential Updates in a Kalman Filter 64

6.4 A Weighted Point Observation 65

6.5 A Straight Line Slope-Intercept Observation 67

6.6 PortaNav Positioning Module Block Diagram 70

7.1 Geometry of a Nearest Feature Search 75

7.2 Combined GPS and Map Congidence Region 77

7.3 Road Acceptance and Rejection 78

8.1 Trimble MobileGPS Control Panel 84

9.1 Precise Fix Static Test 94
9.2 Effect of Static Map Constraint in Map Aided GPS 95
9.3 Map Aided GPS on Open Road 97
9.4 Best DOP Fix on Open Road 97
9.5 Least Squares Fix on Open Road 98
9.6 Precise Fix on Open Road 98
9.7 HDOP on Open Road, May 28, 1995 99
9.8 Number of Satellites Available on Open Road, May 28, 1995 99
9.9 Difference in Northing Between Map Aided GPS and Precise Fix on Open Road, May 28, 1995 101
9.10 Difference in Northing Between Best DOP Fix and Precise Fix on Open Road, May 28, 1995 101
9.11 Difference in Easting Between Map Aided GPS and Precise Fix on Open Road, May 28, 1995 102
9.12 Difference in Easting Between Best DOP Fix and Precise Fix on Open Road, May 28, 1995 102
9.13 Difference in Height Between Map Aided GPS and Precise Fix on Open Road, May 28, 1995 103
9.14 Difference in Height Between Best DOP Fix and Precise Fix on Open Road, May 28, 1995 103
9.15 Map Aided GPS on Open Road 105
9.16 Best DOP Fix on Open Road 105

9.17 Least Squares Fix on Open Road 106
9.18 Precise Fix on Open Road 106
9.19 HDOP on Open Road, May 29, 1995 107
9.20 Number of Satellites Available on Open Road, May 29, 1995 107
9.21 Map Aided GPS on Open Road 109
9.22 Best DOP Fix on Open Road 109
9.23 Number of Satellites Available on Open Road, June 2, 1995 110
9.24 Map Aided GPS in Tree Canopy 112
9.25 Best DOP Fix in Tree Canopy 112
9.26 Least Squares Fix in Tree Canopy 113
9.27 Precise Fix in Tree Canopy 113
9.28 HDOP in Tree Canopy, May 27, 1995 114
9.29 Number of Satellites Available in Tree Canopy, May 27, 1995 114
9.30 Difference in Northing Between Map Aided GPS and Precise Fix in Tree Canopy, May 27, 1995 115
9.31 Difference in Northing Between Best DOP Fix and Precise Fix in Tree Canopy, May 27, 1995 115
9.32 Difference in Easting Between Map Aided GPS and Precise Fix in Tree Canopy, May 27, 1995 116
9.33 Difference in Easting Between Best DOP Fix and Precise Fix in Tree Canopy, May 27, 1995 116

9.34 Difference in Height Between Map Aided GPS and Precise Fix in Tree Canopy, May 27, 1995 117
9.35 Difference in Height Between Best DOP Fix and Precise Fix in Tree Canopy, May 27, 1995 117
9.36 Map Aided GPS in Tree Canopy 119
9.37 Best DOP Fix in Tree Canopy 119
9.38 Least Squares Fix in Tree Canopy 120
9.39 Precise Fix in Tree Canopy 120
9.40 HDOP in Tree Canopy, May 30, 1995 121
9.41 Number of Satellites Available in Tree Canopy, May 30, 1995 121
9.42 Map Aided GPS in Tree Canopy 123
9.43 Best DOP Fix in Tree Canopy 123
9.44 Number of Satellites Available in Tree Canopy, June 2, 1995 124
9.45 Map Aided GPS in Urban Canyon 126
9.46 Best DOP Fix in Urban Canyon 126
9.47 Least Squares Fix in Urban Canyon 127
9.48 Precise Fix in Urban Canyon 127
9.49 HDOP in Urban Canyon, May 30, 1995 128
9.50 Number of Satellites Available in Urban Canyon, May 30, 1995 128
9.51 Difference in Northing Between Map Aided GPS and Precise Fix in Urban Canyon, May 30, 1995 129

9.52 Difference in Northing Between Best DOP Fix and Precise Fix in Urban Canyon, May 30, 1995 129
9.53 Difference in Easting Between Map Aided GPS and Precise Fix in Urban Canyon, May 30, 1995 130
9.54 Difference in Easting Between Best DOP Fix and Precise Fix in Urban Canyon, May 30, 1995 130
9.55 Difference in Height Between Map Aided GPS and Precise Fix in Urban Canyon, May 30, 1995 131
9.56 Difference in Height Between Best DOP Fix and Precise Fix in Urban Canyon, May 30, 1995 131
9.57 Map Aided GPS in Urban Canyon 133
9.58 Best DOP Fix in Urban Canyon 133
9.59 Number of Satellites Available in Urban Canyon, May 31, 1995 134
9.60 Map Aided GPS in Urban Canyon 136
9.61 Best DOP Fix in Urban Canyon 136
9.62 Number of Satellites Available in Urban Canyon, June 2, 1995 137
9.63 Map Aided GPS in Urban Canyon 138

NOTATION

Symbols:

^	denotes estimated quantity
°	denotes an approximated quantity
a, b	semi-major and semi-minor axes of 2D confidence ellipse
a_e, b_e	semi-major and semi-minor axes of earth ellipsoid
$\mathbf{a}$	vector representing road link
$\mathbf{A}$	first design matrix (n x u)
b	Y-intercept of straight line
$\mathbf{b}$	vector representing search point
$\mathbf{B}$	second design matrix (m x u)
$\mathbf{c}$	vector component of **b** along **a**
$\mathbf{C}_l$	variance-covariance matrix of observations (n x n)
$\mathbf{C}_{\hat{r}}$	variance-covariance matrix of estimated residuals (n x n)
$\mathbf{C}_{\hat{x}}$	variance-covariance matrix of estimated parameters (n x n)
$\mathbf{C}_{\hat{\delta}_i}$	variance-covariance matrix of error states at time index i (u x u)
d	distance
d_{ion}	ionospheric delay
$\dot{d}_{ion}$	rate of change of ionospheric delay
dt	satellite clock offset
$\dot{dt}$	satellite clock drift rate
dT	receiver clock offset
$\dot{dT}$	receiver clock drift rate
d_{trop}	tropospheric delay
$\dot{d}_{trop}$	rate of change of tropospheric delay
d_ρ	radial orbit error
$\dot{d}_\rho$	rate of change of radial orbit error
e	ellipsoid eccentricity
$f(x)$	measurement model

$g(x)$	dynamics model
h	ellipsoidal height
K	Kalman gain matrix (u x u)
$\mathbf{l}^{obs}$	vector of observations (n x 1)
lat	latitude in Etak coordinate system
lon	longitude in Etak coordinate system
m	number of equations
m	slope of straight line
n	number of observations
N	normal equations matrix (u x u)
N	prime vertical radius of curvature
P	observed pseudorange
$\dot{P}$	pseudorange rate
q	spectral density
$\hat{\mathbf{r}}$	vector of residuals (n x 1)
r	standardized residual
t	time
u	number of unknown parameters
u	normal equations vector (u x 1)
v_n, v_e, v_h	3D local geodetic components of receiver velocity
v_x, v_y, v_z	3D Cartesian components of satellite velocity
v_X, v_Y, v_Z	3D Cartesian components of receiver velocity
w	vector of misclosures (m x 1)
x	vector of unknown parameters (u x 1)
x, y	2D Cartesian coordinates
x, y, z	3D Cartesian coordinates of receiver
X, Y, Z	3D Cartesian coordinates of satellite
y	vector of process noise (u x 1)
1-α	confidence level of test

α	significance level of test
β	inverse of correlation time
δt	difference between measurement time and epoch time
$\hat{\boldsymbol{\delta}}$	vector of corrections to the unknown parameters (u x 1)
$\hat{\boldsymbol{\delta}}_i$	vector of error states at time index *i* (u x 1)
Δt	measured time of signal travel
ε_P	pseudorange measurement noise
$\varepsilon_{\dot{P}}$	range rate measurement noise
ϕ	geodetic latitude of receiver
ϕ_m	geodetic latitude of map point
$\boldsymbol{\Phi}$	transition matrix (u x u)
$\dot{\Phi}$	doppler observable
λ	geodetic longitude of receiver
λ_m	geodetic longitude of map point
θ	orientation of semi-major axis in 2D confidence ellipse
θ	angle between vectors **a** and **b**
ρ	geometric range between receiver and satellite
$\dot{\rho}$	geometric range rate
σ_i	standard deviation of *i*
σ_{ij}	covariance between *i* and *j*
σ_i^2	variance of *i*
$\hat{\sigma}_o^2$	*a posteriori* variance factor

Constants:

C	speed of light in a vacuum - 299 792 458.0 m/s
C_e	approximate circumference of Earth - 40 030 000 m
E_{MAX}	maximum value of an Etak coordinate - 4 294 967 295
R_e	approximate radius of Earth - 6 371 000 m
λ	wavelength of L1 carrier signal - 19.0293672798 cm

Operators:

$\mathbf{A}^T$	matrix transpose
$\mathbf{N}^{-1}$	matrix inverse
$\|\mathbf{a}\|$	length of the vector **a**
$\|\mathbf{a} \bullet \mathbf{b}\|$	dot product of vectors **a** and **b**
$\|\mathbf{a} \times \mathbf{b}\|$	cross product of vectors **a** and **b**
$(\cdot)^-$	Kalman prediction
$(\cdot)^+$	Kalman update
$\frac{\partial f}{\partial x}$	partial derivative of the function f with respect to the variate x

Acronyms:

2D	two dimensional
3D	three dimensional
AAA	American Automobile Association
AM	amplitude modulation
AMF	area master file
AS	Anti-Spoofing
AVLN	automatic vehicle location and navigation
C/A-code	coarse/acquisition code
CACS	Canadian Active Control System
CD-ROM	compact disc read only memory
COG	course over ground
CPU	central processing unit
CRT	cathode ray tube
DEMETER	Digital Electronic Mapping of European Territory
DGPS	differential GPS
DoD	Department of Defense (U.S.)
DOP	dilution of precision
DOS	disk operating system

DRIVE	Dedicated Road Infrastructure for Vehicle Safety in Europe
DRM	digital road map
DTM	digital terrain model
ECDIS	Electronic Chart Display and Information System
ECS	Electronic Chart System
ECS	Etak coordinate system
EDP	European Data Pool
EDRA	European Digital Road Map Association
EGT	European Geographic Technologies
FOC	Full Operational Capability
FM	frequency modulation
FMS	Flight Mananagement System
GDF	Geographic Data File
GDOP	geometric dilution of precision
GIS	Geographic Information System
GPS	Global Positioning System
HDOP	horizontal dilution of precision
IOC	Initial Operational Capability
ITS	Intelligent Transportation Systems
IVHS	Intelligent Vehicle Highway Systems
JDRMA	Japan Digital Road Map Association
JPO	Joint Program Office (U.S.)
LAN	local area network
LCD	liquid crystal display
MB	megabyte
NAD-27	North American Datum, 1927
NAVSTAR	NAVigation Satellite Timing And Ranging
MHz	megahertz
NRCan	Natural Resources Canada

NSRA	Navigation System Research Association
OEM	original equipment manufacturer
PC	personal computer
P-code	precise code
PCMCIA	Personal Computer Memory Card International Association
PDA	personal digital assistant
PDOP	position dilution of precision
PNA	personal navigation assistant
PortaNav	Portable Navigation
ppm	parts per million
PRN	pseudorandom noise
RAM	random access memory
RINEX	Receiver INdependant EXchange format
RMS	root mean square
SA	Selective Availability
SCSI	small computer systems interface
SDK	software development kit
SOG	speed over ground
TDOP	time dilution of precision
TFEDRM	Task Force European Digital Road Map
UHF	upper high frequency
USGS	United States Geological Survey
UTM	Universal Transverse Mercator
VAR	Value Added Reseller
VDOP	vertical dilution of precision
WGS-84	World Geodetic System, 1984

CHAPTER ONE

INTRODUCTION

1.1 Vehicle Navigation Systems

The field of vehicle navigation has advanced significantly over the past ten years. This has been due largely to the Global Positioning System (GPS) and the advancement of computer related technologies. During this time, land vehicle navigation has been known as, or associated with, Automatic Vehicle Location and Navigation (AVLN), Intelligent Vehicle Highway Systems (IVHS), and more recently, Intelligent Transportation Systems (ITS). Similarly, marine vehicle navigation terms include Electronic Chart Display and Information Systems (ECDIS), Electronic Chart Systems (ECS), and Smart Ships. Air navigation terms include Flight Management Systems (FMS) and En Route Navigation Receivers. Regardless of the name, vehicle navigation is the applied science of positioning and locating a vehicle in order to aid the driver and/or dispatcher in guiding the vehicle [French, 1987; Krakiwsky et al., 1987].

Positioning and locating are distinct processes in vehicle navigation (Figure 1.1). Positioning is determining coordinates in a fixed reference frame. The coordinates may be geodetic, Cartesian, or on a mapping plane. Reference frames may be earth fixed or fixed in inertial space, earth centred or topocentric [Krakiwsky and Wells, 1971; Vanicek and Krakiwsky, 1982]. Coordinates by themselves do little to tell the average person where they are. Locating is the process of putting coordinates into a frame of reference that is more useful. Typically, a map with topographical features, navigational aids, roads, street addresses, etc. is used to determine a location. Navigation is accomplished by informing the user how to proceed in order to arrive at the desired destination.

1.2 Historical Review

Vehicle navigation dates back to ancient days in China and Egypt. The Chinese had a system now known as the south pointing chariot [Harris, 1989]. This was a modified

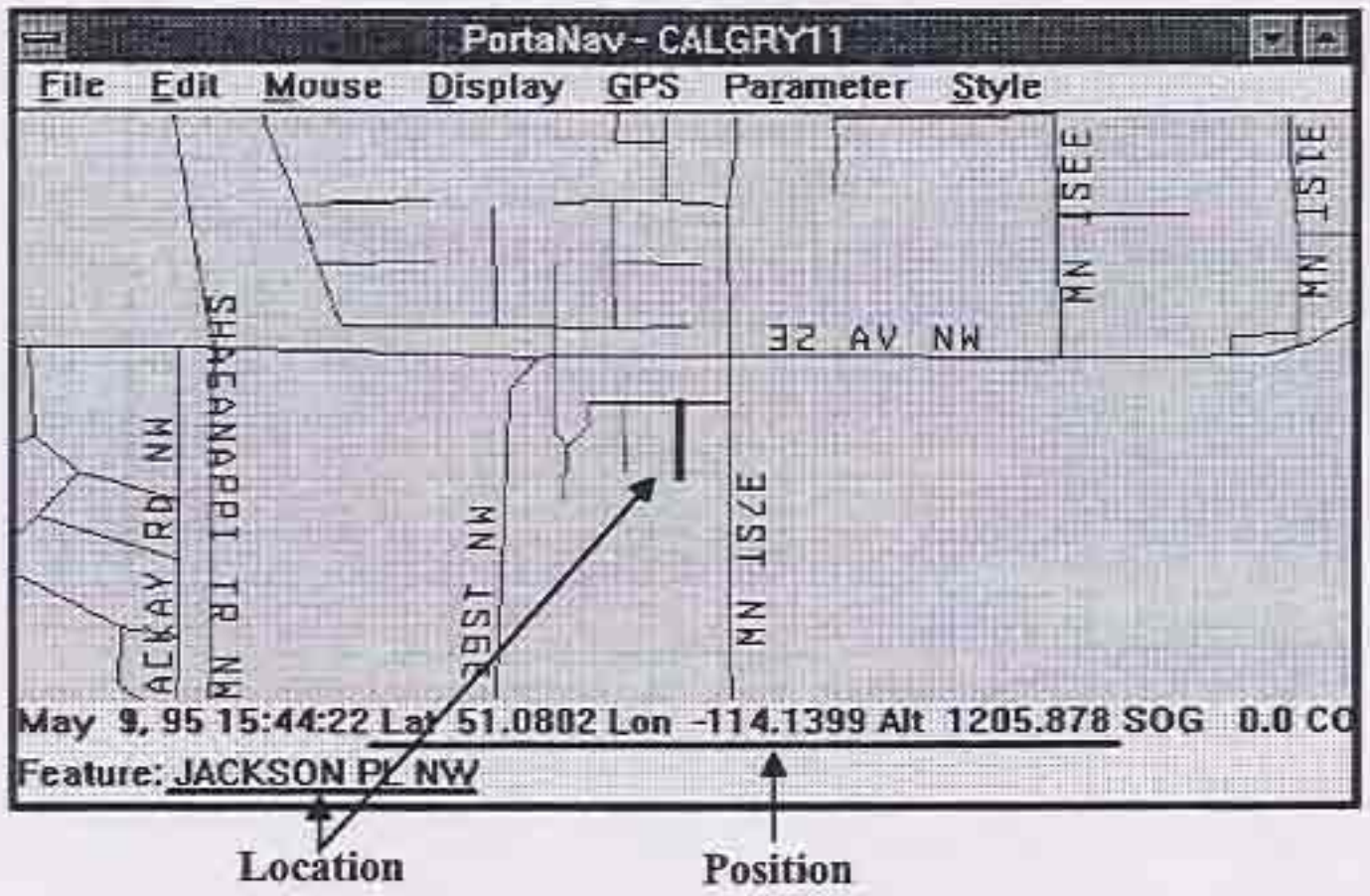

Figure 1.1 Position versus Location

chariot that used mechanical gears and the principle of differential odometry to keep track of an important direction (usually south, the ancient Chinese cardinal direction). The chariot had a personage on the top that rotated and pointed in the direction of concern. Used in battles, the system would initially be set to point towards the home base. As the army travelled, the figure would continue to point towards home. At the end of the battle, the army would simply follow the pointer home as they were fleeing or perhaps marching in glory.

Differential odometry can be used with a vehicle that has at least one axle and two wheels. As the vehicle turns, one wheel will travel a longer distance than the other. This difference in distance travelled is translated into a change in heading by the use of a set of gears. The principle of differential odometry has still been used in the late twentieth century in land vehicles to measure changes in heading [French and Lang, 1973; Kao, 1991].

The ancient Egyptians were also early entrants into the era of vehicle navigation; they had several methods of recording distance travelled. One such method involved dropping

stones into a bucket at a set interval, determined by a fixed number of paces. They would start with a fixed quantity of stones, so when they ran out, they would know that they had travelled the corresponding distance. Of course, odometers are used in all land vehicles today to record distance travelled. The actual methods of recording distance have advanced beyond stone dropping, however, the principles remain the same.

Sextants and time keeping devices were both developed specifically for navigation purposes. Other than the development of more sophisticated compasses, odometers, and clocks, little happened on the front of vehicle navigation until the twentieth century. In the 1970s, a few unique systems were developed for special purposes. One such system was developed to automatically throw papers to the doorsteps of customers. The system recorded distances and had a record of where the papers needed to be thrown [French and Lang, 1973]. Other early systems were intended to track police vehicles and other service fleets [Lezniak et al., 1977].

A significant development was the invention of the Etak Navigator in 1984 [New Scientist, 1984]. This system was intended for use as a land navigation aid to the individual driver. The Navigator consisted of a cassette tape player, an 8086-based computer, dual odometers, a compass, and a small CRT (Figure 1.2). A digital road map was stored on the cassette tape. The system used the compass, differential odometry and map matching to position the vehicle [Zavoli and Honey, 1986]. Map matching is the process of correlating the vehicle path with a path in the digital road map [French, 1989]. The map and the vehicle position were displayed, and as the vehicle moved, the map would move, keeping the vehicle symbol in the centre of the screen [Alegiani et al., 1989; Shuldiner, 1985].

With the coming of the Etak Navigator, the current explosion of vehicle navigation systems began. Fuelled by the advancement of positioning and computing technologies, this explosion continues today.

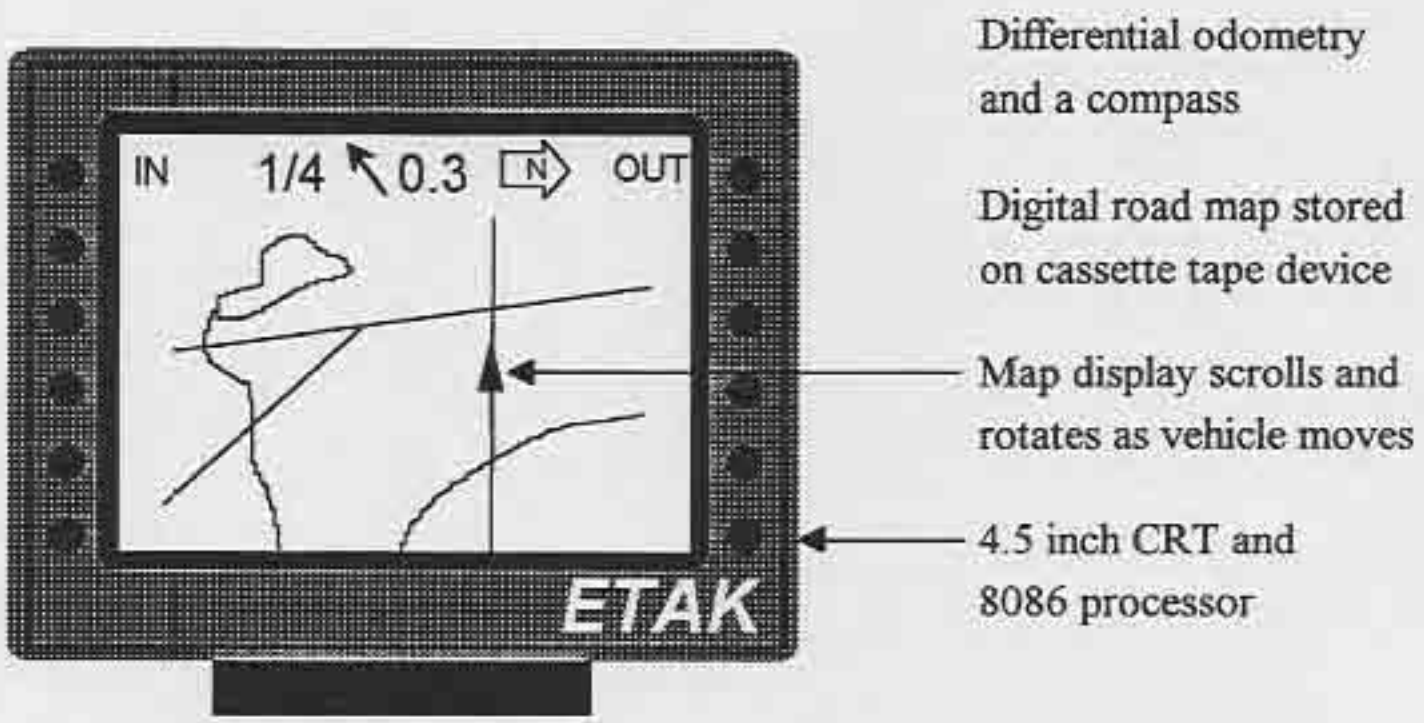

Figure 1.2 The Etak Navigator

1.3 Recent Technological Advances

During the eighties, computer technologies advanced rapidly. Performance increased, price decreased, and size decreased, making portable computing a reality. Several different technologies have contributed to the development of portable computing over the past five years.

Computer processors become faster every year, from 8 MHz in the early eighties to 133 MHz today. Single computer chips now have millions of transistors. Digital storage techniques improved so that large quantities of digital information could be readily stored and accessed at a low cost. The cost per megabyte of data storage continues to decrease; fixed disk storage is now available at under $1 per megabyte. In addition to the tremendous gains in price and performance, the chips and data storage devices have become smaller and more suited to portable computing devices in terms of both power draw and shock resistance [Phail, 1991].

Display technologies, in particular, liquid crystal displays (LCDs), have also improved in the past few years. Active matrix colour LCDs are commonplace now in notebook computers. These displays are faster, larger, and brighter than their predecessors. Again, costs are continuing to decrease each year.

A more recent development in portable computing has been in credit card-sized peripherals [Reimer, 1994]. A standard form factor and protocol for these devices has been adopted by most of the major companies involved in the computer industry. The standard was developed and is now maintained by the Personal Computer Memory Card International Association (PCMCIA). The cards themselves are called either PCMCIA cards or simply PC cards. Specifications for PC cards include various storage devices, interfaces, and communications devices. PC cards with miniature hard drives or RAM have emerged for data storage; modems, ethernet, and LAN cards are available for communications; and SCSI cards allow connection to external hard drives or CD-ROM drives. These expansion cards greatly enhance the flexibility and power of portable computing devices. The key factor with PCMCIA cards is their compatibility; cards made by any company will work with computers made by any manufacturer.

It has been said that if the automobile industry had advanced as rapidly as the computer industry, cars today would break the sound barrier, cost under $100, and go 1 000 km on a litre of gasoline. There are no signs of the pace of computer development slowing down.

On the positioning and navigation front, the key technological advancement has been GPS. NAVigation Satellite Timing And Ranging (NAVSTAR) GPS dates back to 1973, when the U.S. Department of Defence (DoD) directed the Joint Program Office (JPO) to develop and deploy a satellite-based radio navigation system [Hofmann-Wellenhof et al., 1994]. The result is a US $15 billion military positioning and navigation system that has been authorized for civilian use. The constellation design consists of 24 satellites in six orbital planes inclined at 55 degrees. Users can obtain instantaneous position and velocity information anywhere in the world, 24 hours a day, in virtually any weather. An important feature of GPS is its capacity for an unlimited number of users due to the one-way ranging. GPS is much like AM or FM radio or broadcast television; users buy the reception equipment, then use the signals at no cost.

The first GPS satellites were deployed in the late seventies. The constellation grew throughout the eighties, slowing somewhat in 1986 after the space shuttle Challenger explosion. The Initial Operational Capability (IOC) of GPS was declared in December 1993 [Leick, 1995], followed by the Full Operational Capability (FOC) in April 1995, guaranteeing continuous global coverage.

Early GPS receiver equipment was bulky and very expensive. The first system used in Canada was a rack mount unit that cost $300,000 in 1979. Today, low-end hand-held GPS receivers for consumer use are available for under $500. In bulk, GPS boards for system integrators cost under $200 and are the size of a credit card. In fact, there are now PCMCIA card GPS receivers for use with portable computing devices.

Each of these technologies has contributed significantly to the advancement of the science and use of modern vehicle navigation.

1.4 Current Navigation Trends

Navigation is done on land, at sea, in the air, and in space. GPS has been used in each of these modes of navigation. A total of 280 distinct land navigation systems have been documented in Krakiwsky et al. [1995]. Of these, 171, or 61% use or can use GPS as a source of positioning input. Of the land systems, 174 are built in North America, of which 125, or 72% use or can use GPS. Of 122 marine navigation systems identified in Bullock and Krakiwsky [1995a], 109, or 89% use or can use GPS. Similarly, of 50 air navigation systems identified in Bullock and Krakiwsky [1995b], 47, or 96% use or can use GPS. Clearly, GPS is the dominant positioning tool used in navigation (Figure 1.3).

Due to the degradation of civilian GPS signals known as Selective Availability (SA), many techniques have been developed to augment GPS in order to improve accuracy and reliability. One of the best ways of improving the accuracy of GPS is by using differential GPS (DGPS) techniques to reduce or eliminate error sources. This involves placing a GPS receiver at a known position to solve for errors and biases (including SA) that are

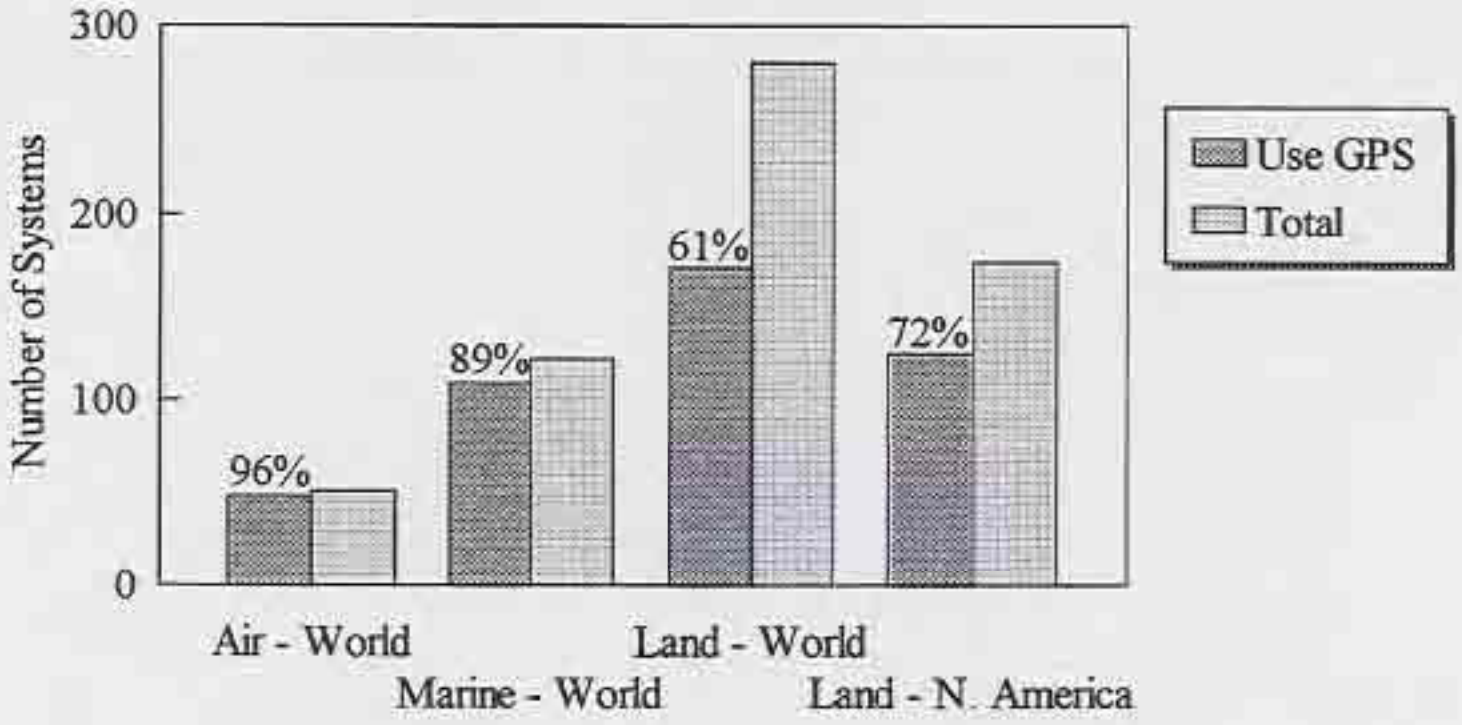

Figure 1.3 GPS Usage in Various Types of Vehicle Navigation Systems

common to both receivers. To use DGPS in real time, a communications infrastructure is required.

Another popular method for augmenting GPS is dead-reckoning, which is the use of direction and distance measuring sensors to record relative changes in position [McLellan, 1992; Cannon et al., 1992]. With the absolute positions determined by GPS, dead-reckoning can be used to extend positioning into areas where GPS is unavailable, such as downtown cores (urban canyon), tree covered areas, and tunnels [Kao, 1991].

Map matching is another technique commonly used with GPS, typically with dead-reckoning as well. Map matching is sometimes based on the assumption that the vehicle is on a road in the road network. This assumption becomes invalid if the vehicle enters a parking lot or leaves the road for some other reason. Another approach is to work on the knowledge that the vehicle is most likely on a road in the road network. As the vehicle travels, a trace of the track is created. This trace is compared with the digital road map in order to find the most probable location of the vehicle [Harris, 1989]. Map matching can be used to aid the positioning system or it can be used simply to display the vehicle on a road in the road map rather than in the middle of a block.

Land navigation can be broken down into five basic categories [Krakiwsky et al., 1995]. Autonomous navigation systems are for a single user, and consist of positioning, location, and navigation within the vehicle. Advisory systems add the component of real-time traffic information to autonomous systems. Fleet management systems involve vehicle positioning and position reporting to a dispatcher, but not necessarily location nor navigation within the vehicle. Inventory systems have a positioning system on board and some sort of data collection device. The positioning system is used to record coordinate tags for the information collected. Finally, portable systems are autonomous systems that are not permanently installed in a vehicle.

In Japan, autonomous navigation systems have flourished; following Dennehy [1994], Azuma et al. [1994], and Collier and Weiland [1994] it is estimated that there are over 600 000 systems now in use in Japan. In Europe, autonomous, advisory, and fleet management systems have all seen moderate success. In North America, fleet management systems have been the most predominant. It was only last year that the first OEM car navigation system, the Oldsmobile Guidestar, was released in the United States [Tapscott, 1994].

1.5 Market for Portable Navigation

In the last three years, over forty portable vehicle navigation systems have emerged. Some of these are hand-held GPS receivers that store waypoints (destinations). Others are based on notebook computers or other portable computing devices. Prices range from under US $300 to a few thousand dollars. The great advantage of any portable system is the autonomy from any one particular vehicle. A user is free to use them in any vehicle, including rented or borrowed vehicles, making them well suited for travellers.

Portable navigation devices are being used by hikers, tourists, real estate agents, hunters, travelling salespeople, business travellers, and others. The mission planning function of a navigation system allows the user to prepare a route while in the hotel or airport. Having

a prior knowledge of the route provides security and peace of mind, even if travelling by cab, bus, or train.

Many people already have portable computing devices that have the resources to display maps and plot positions. The incremental cost to add navigation software can be very low, particularly now that GPS receivers have become more affordable.

1.6 Definition of Research Project

The main goal of this research was to develop a prototype portable land vehicle navigation system (PortaNav). Since dead-reckoning sensors cannot be used in a portable system, PortaNav relies on GPS and a digital road map. The secondary goal of the project was to determine how much improvement can be realized by using map aiding with GPS. Several ideas for aiding GPS using map derived information are explored.

PortaNav is based on a colour notebook personal computer. The positioning module consists of a Trimble MobileGPS receiver that connects to the computer's PCMCIA port. The location module is based on an Etak digital road map developed specifically for the purpose of land vehicle navigation. A Kalman filter is used to filter the GPS pseudorange and Doppler observations. The filter is also used to introduce constraint equations based on roads in the digital road map database. The constraints are based on the assumption that the vehicle is most likely travelling on a road. When a probable road of travel is found, the azimuth of the road, a line of position, or a point on the road may be taken from the map and used as an observation in the Kalman filter.

It is hypothesized that the map aided constraining filter will result in a real-time position determination that is more accurate, more reliable, and smoother than an instantaneous stand-alone GPS fix. Augmenting GPS using map aiding has a low implementation cost compared to dead-reckoning or DGPS, as no additional hardware is necessary. The only requirements are a digital road map, which is already necessary for locating, and some additional software. In designing a vehicle navigation system, the major constraints are

cost, size, and power consumption. Map aided GPS adds no size, no power consumption, and very little cost to the system. Even if a marginal improvement over GPS alone is realized, it may be worth the expense.

To evaluate the performance of the map aiding algorithm, several parallel solutions will be computed and/or logged. The Trimble MobileGPS receiver computes a best DOP unique fix, which is logged by PortaNav. Using the raw measurements from the receiver, a least squares solution and a Kalman filtering solution are computed in real time by PortaNav and logged. Finally, the raw pseudorange data is recorded for further post-mission processing using precise satellite orbits and clocks. This final solution serves as a baseline against which the other solutions are compared.

This thesis documents the issues involved in the design and testing of PortaNav. Chapters 2, 3, and 4, contain background information on portable computing and navigation devices, GPS positioning issues, and digital road maps used in vehicle navigation, respectively. This information forms the basis of the design decisions outlined in Chapter 5, where the design objectives are stated, and the chosen solution is described in detail. A detailed description of the positioning and map database engine modules follows in Chapters 6 and 7. User interface issues are addressed in Chapter 8. Finally, the finished system was tested in various scenarios, and the results of these tests are presented in Chapter 9. Conclusions and recommendations for further research are then stated in Chapter 10.

CHAPTER TWO

PORTABLE NAVIGATION DEVICES

The first decision to make in the design and development of PortaNav is what platform to use. Various computing platforms, including the one chosen for PortaNav, will be described in this chapter.

2.1 Personal Digital Assistants (PDAs)

Computers are natural tools for managing information. As people started to use computers to plan their schedules and keep track of contacts and phone numbers, they had a desire to take them wherever they went so as to always have the information at their fingertips. This has not always been possible due to the size and weight of computer components. As the components became lighter and smaller, computers became more and more portable. It eventually became possible for people to use computers as personal digital assistants (PDAs) [Soviero, 1992]. Some typical PDAs are pictured in Figure 2.1.

Figure 2.1 Typical Personal Digital Assistant (PDA) Form Factors

The first portable computers were actually better named luggable. They were the size of a suitcase and very heavy. These soon became laptop computers the size of a briefcase. Laptop computers evolved further into notebook computers which have a footprint the size of a typical notebook and weigh under ten pounds [White, 1993]. These notebook computers were the first truly portable computers and are now very popular, selling in the millions.

Many people incorrectly thought that notebook-sized computers were at the size limit for a computer. Palmtop computers compromised on keyboard size and were able to break the notebook barrier. Typical palmtop computers are the HP 95 LX, the Zeos Contenda, and the Gateway HandBook. These computers are about half the size of a notebook and weigh three to five pounds.

Going one step smaller required eliminating the keyboard altogether. Without the keyboard, an alternative method of data entry is required. Pen computing has stepped in with touch screens and handwriting recognition to provide an interface to the user. Several pen-based devices have emerged in the past two years. These include the Apple Newton, the Casio Zoomer, the BellSouth Simon, and more recently, the Motorola Envoy [Ballard, 1994]. Each of these computing devices is the size of a large calculator and is operated with a touch pen. The primary function of a PDA is to keep track of personal data. Many PDAs also provide wireless communications such as e-mail or paging, or in the case of the Simon a cellular phone.

As seen in Figure 2.2, the common elements in all PDAs are a processor, a display, a user interface, and a mass storage device. In addition to built-in communications devices, most PDAs now include one or more interfaces for integration with various peripheral devices. The most common interface found on PDAs today is one or more PCMCIA slots. Other interfaces include infrared data transfer devices, serial ports, or a direct port for connection with a desktop computer.

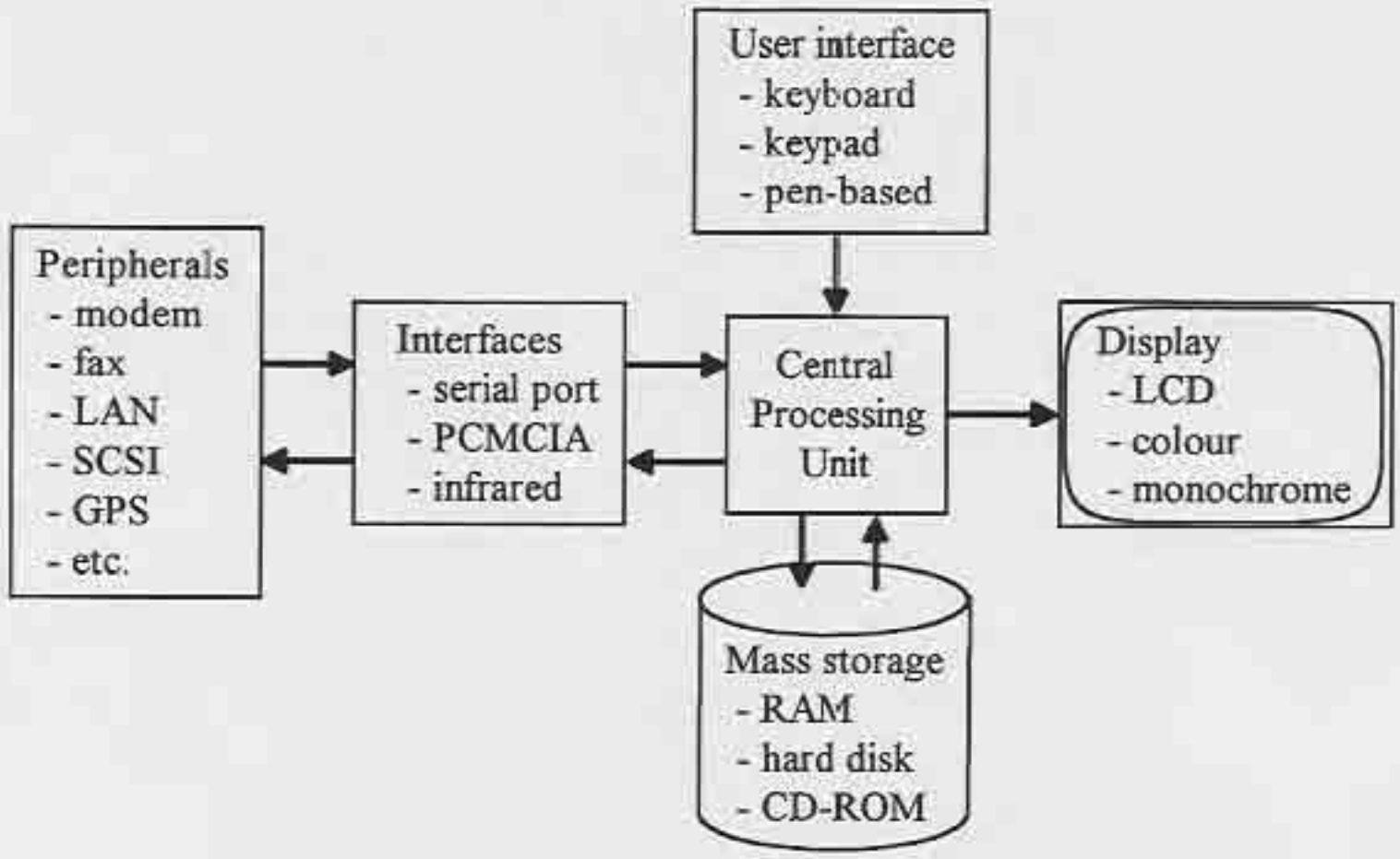

Figure 2.2 Basic Elements of a PDA

2.2 Personal Navigation Assistants (PNAs)

Akin to PDAs are personal navigation assistants (PNAs), which incorporate positioning and navigation. The majority of PNAs use small GPS receivers to provide positioning information. Like the PDAs, PNAs typically cost under US $1,000. The GARMIN GPS 45 and the Lowrance Global Map Sport are two hand-held PNAs with built-in GPS receivers (Figure 2.3). Both these systems have a small navigation display and waypoint storage.

Many PDAs have one or two PCMCIA slots for expansion devices. With a PCMCIA GPS receiver, a PDA can become a PNA. Several companies have developed custom software for hand-held PDAs such as the Newton to make use of a GPS receiver for data logging in the field. Hand-held PNAs have severe limitations on power consumption and data storage for digital maps. Notebook computers typically have larger batteries and larger hard drives, so they are better suited for navigation.

Lowrance Global Map Sport GARMIN GPS 45

Figure 2.3 Typical Personal Navigation Assistants (PNAs)

2.3 Notebook Computer Based PNAs

Today's notebook computers have hard drives with capacities of a few hundred megabytes and batteries that last several hours. Notebook computers are a natural platform for a PNA because they have the capability of storing extensive digital road maps and other information. Also, most notebook computers on the market today have PCMCIA slots and serial ports, both of which can be used for interfacing to a GPS receiver.

There are at least three companies that have developed navigation software for notebook computers. Retki from Liikkuva Systems International, City Streets from Road Scholar Software, and DeLorme MapExpert are all software packages that allow a user to plot a GPS-derived position on a digital road map. An advantage to a PNA of this type is that the computer is not dedicated to the navigation function. This allows the cost of the computer to be rationalized over several functions. Each of these three software packages costs a few to several hundred dollars. The software together with a GPS receiver typically costs around US $1,000. These systems are used in land vehicles of all types and are also used in homes or offices for mission planning. PortaNav is a PNA similar to these systems, based on the portable notebook computer platform.

CHAPTER THREE

GPS TECHNOLOGIES

Satellite navigation systems, such as GPS, have become the positioning method of choice in many navigation applications. The main reasons for this are the continuous worldwide coverage and high accuracy. GPS was chosen for PortaNav for these reasons and because of the availability of low-cost receivers. There are many vendors and types of GPS receivers and many modes of operating GPS. The best receiver and configuration depend largely on the requirements of the navigation system, the infrastructure available, and the limitations on resources.

Positioning using GPS consists of measuring distances to four or more satellites in orbit. A position can be computed using trigonometry and the known positions of the satellites (Figure 3.1). Detailed descriptions of GPS theory, technology, and issues can be found in Hofmann-Wellenhof et al. [1994], Leick [1995], and Van Dierendonck [1995]. The discussion here is limited to the factors important in the design of PortaNav.

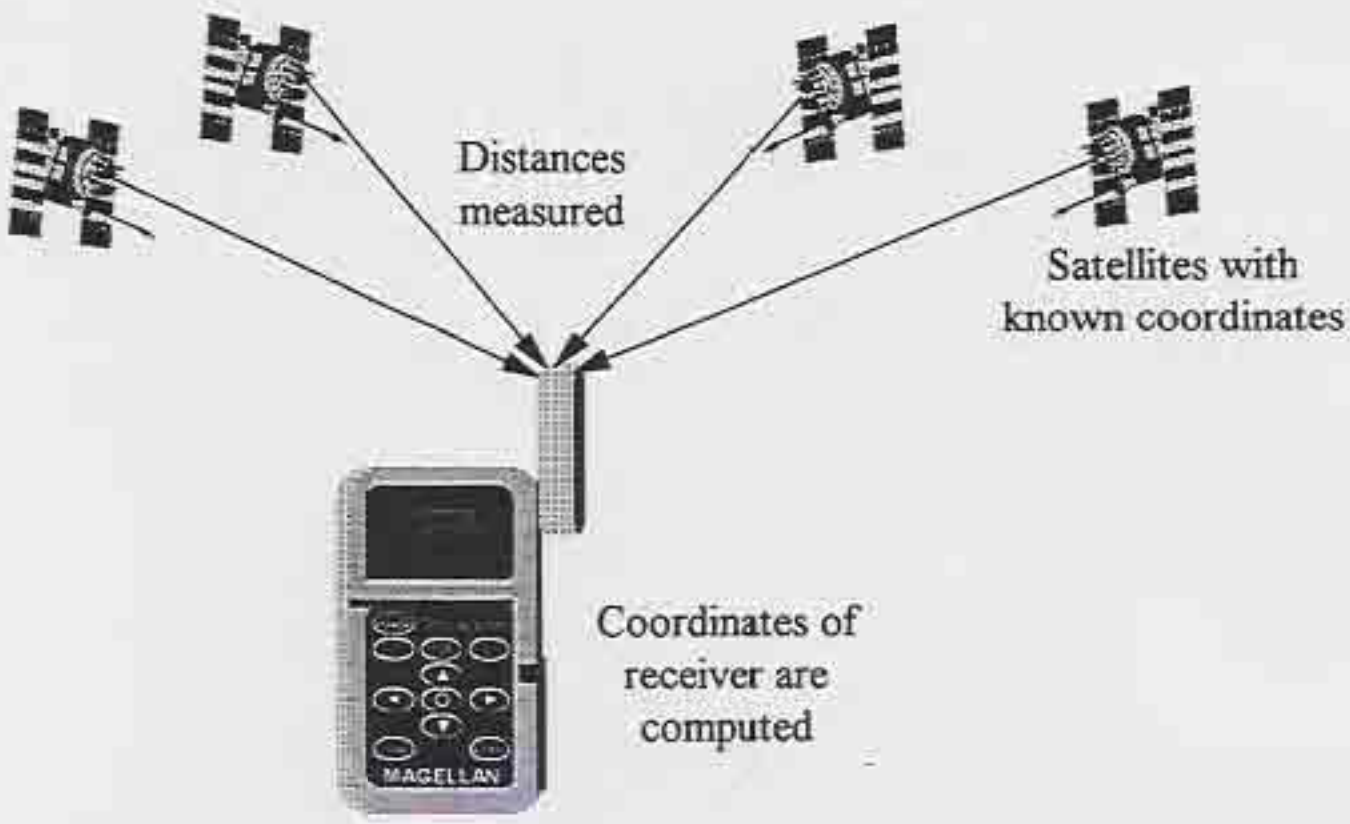

Figure 3.1 Concept of GPS Positioning

3.1 Single Point GPS versus Differential GPS (DGPS)

In single point mode, the autonomous GPS receiver is subject to errors from the atmosphere, multipath, satellite orbits, satellite clocks, and receiver noise [Greenspan and Donna, 1986]. Note that SA is effectuated by dithering the satellite clocks. A second GPS receiver operating in the same vicinity is subject to much the same error. Satellite orbit and clock errors (including the effects of SA), and atmospheric delays (ionospheric and tropospheric), are highly correlated over distances of up to a few hundred kilometres. Hence with two GPS receivers, a relative position can be computed with a much higher level of accuracy. This is the principle behind differential GPS positioning [Beser and Parkinson, 1981; Blackwell, 1985]. Typically, a GPS receiver is placed at a benchmark that has been surveyed very accurately. Corrections to the GPS measurements are computed using the known coordinates and applied to the measurements of the second GPS receiver. The remaining errors are primarily receiver noise and multipath. Table 3.1 lists typical GPS error budgets for single point positioning and differential positioning using code range corrections for baselines under 50 kms.

Differential GPS can be achieved in real time or post mission. For vehicle navigation, users are concerned about their position as they travel. Real-time differential GPS

Error source	Typical C/A-code range error	
	Single point mode	Differential mode
Tropospheric delay	2 - 15 m	0.3 - 3 ppm
Ionospheric delay	2 - 20 m	0.2 - 0.4 ppm
Satellite orbit errors (not including SA)	5 - 20 m	0.5 - 1 ppm
Selective Availability (SA)	20 - 30 m	1 - 2 ppm
Measurement noise	0.1 - 3 m	0.141 - 4.24 m
Multipath	0 - 10 m	0 - 10 m

Table 3.1 Summary of Single Point and Differential GPS Range Errors

requires that the differential range corrections be broadcast to the mobile receiver so that they can be applied to the measured ranges before being used in the position fix. Various communications systems have been used for broadcasting differential corrections, including UHF data radio, satellite, beacon, trunked radio, FM sub-carrier paging, and cellular telephone [Lanigan et al., 1990; Krakiwsky and Harris, 1994]. Regardless of the method, there is an additional cost for hardware and/or time used. This must be weighed with the benefit of improved accuracy. Single point users can expect a 95% 2D positional accuracy of 100 m, while differential users can achieve positional accuracies of one to fifteen metres, depending on the equipment used.

3.2 Single Frequency versus Dual Frequency Receivers

GPS satellites broadcast measurements on two frequencies, namely L1 and L2, which are at 1 575.42 MHz and 1 227.6 MHz respectively. Most GPS receivers receive signals on the L1 frequency while some receive on both. The primary advantage to using measurements on two frequencies is to solve for the ionospheric delay [Klobuchar, 1983]. In this frequency range, the ionosphere is dispersive, i.e. the delay is inversely proportional to the square of the frequency. Hence with measurements on two frequencies, the delay can be solved for and removed. This eliminates a fairly large source of error. With single frequency receivers there are various methods for modelling the ionosphere to reduce the error [Klobuchar, 1986; Qiu et al., 1994]. Dual frequency receivers cost more than single frequency receivers, so again the gains must be weighed with the costs.

3.3 Pseudorange versus Carrier Phase Measurements

Pseudorandom noise (PRN) codes are superimposed on the broadcast carrier waves. There are two codes, coarse/acquisition (C/A) and precise (P), differing primarily in their chipping rates and periods. Note that P-code is now Y-code under the implementation of Anti-Spoofing (AS); Y-code is encrypted P-code for authorized military use only. Both codes provide a time tag on the carrier wave so that the signal travel time can be determined. Navigation messages modulated on the carriers by each satellite provide the

satellite ephemerides so that the satellite positions can be computed. With a measured range to each known satellite position, the receiver coordinates can be computed. The time of travel, or range, is not directly measured because the satellite clock and the receiver clocks are both offset from GPS time. The satellite clock is modelled using broadcast parameters and the receiver clock offset is solved for since it is the same for all satellites. The observable is called a pseudorange since it is not the true geometric range.

Pseudorange measurements are obtained by measuring the difference in phase between the code received from the satellite and the code generated in the receiver. For this reason, pseudoranges are sometimes referred to as code phase measurements. There is an ambiguity involved in code phase measurements. The C/A-code has a chipping rate of 1.023 Mbps and the code consists of 1 023 bits, hence the code is one millisecond long, or 299 752.458 m. GPS satellites are at a nominal altitude of 20 200 km, so there is an unknown number of complete codes, or integer milliseconds, between the satellite and the receiver. This ambiguity is easily determined by knowing the receiver coordinates to within half the code length (150 km), which is usually not a problem.

Carrier beat phase measurements are obtained by measuring the phase of the difference between the received satellite signal and the frequency generated by the receiver oscillator. The wavelength of the L1 carrier is just over 19 cm, so the resolution of carrier phase measurements is much higher than code phase measurements. This is because receiver tracking loops can determine the phase to about 1% of the wavelength. The chip length of C/A-code is over 300 m, so it is much noisier than the carrier phase. The disadvantage with using carrier phase measurements is the unknown ambiguity. In order to resolve the ambiguity, the receiver position must be known to an accuracy of about nine centimetres, otherwise an ambiguity search must be performed. Once the initial ambiguities are solved, the full benefits of the higher measurement accuracy are realized. Carrier phase and P(Y)-code receivers are very expensive when compared to C/A-code receivers. So once again, cost-benefit analysis must be done.

3.4 PCMCIA GPS Receivers

Two companies have recently introduced low-cost single frequency C/A-code GPS receivers that interface with a computer via a PCMCIA card. The Rockwell NavCard and Trimble MobileGPS receivers both cost under US $1,000. Both of these receivers have been designed to draw power directly from their host, eliminating the need for a separate power supply. The Rockwell is a five channel design while the Trimble has six channels. Each has a magnetic mount antenna for use in any vehicle. PCMCIA GPS receivers are possibly the ideal form factor for use in a PNA. The only better alternative is to have the receiver built-in to the computer equipment.

Both Rockwell and Trimble offer a software development kit (SDK) with their GPS receivers. This SDK allows users to write their own software applications using high-level function calls to obtain information from the receivers. This relieves the programming burden by hiding all of the bit-level communications between the receiver and the host.

3.5 Design Implications for PortaNav

PortaNav uses a PCMCIA GPS receiver for three main reasons. Firstly, the low cost makes it potentially affordable even for casual users. Secondly, the small form factor is convenient for maintaining portability. Finally, power is drawn directly from the notebook computer, eliminating the need for a separate power supply.

Operating in stand-alone mode leaves SA as the single largest source of error. Reducing ionospheric error with a dual frequency GPS receiver would not have a large effect on the overall error. Similarly, reducing the receiver noise with a high performance C/A-code or a carrier phase receiver would have little or no effect on the total error. Therefore, a higher cost receiver is not justified for the PortaNav application. With the low-cost receiver, the expected positional accuracy of the system is about 50 to 100 m at the 95% confidence level due to SA.

CHAPTER FOUR

DIGITAL ROAD MAPPING TECHNOLOGIES

PortaNav requires a digital road map for various navigation functions. A digital road map must be able to support the required functionality in terms of feature content, accuracy and data coverage. In this chapter, the basic map-related functions are described and the suppliers of digital road map data are summarized. As will be seen, deciding on a set of functions and regions of operation for a navigation system limit the available choices of digital road map suppliers.

4.1 Digital Map-Related Functions

Geometric consistency and topological integrity are essential in any digital road map used for locating a position. Digital road maps are the basis for many other navigation related functions besides locating. Map display, address matching, map matching, pre-mission route planning and route calculation, and *en route* route guidance, are all functions that rely on the presence of certain features and attributes in digital road maps. These functions will each be described, and the requirements placed on the digital road maps will be outlined. These requirements have been described more fully in White [1987], Harris et al. [1988], Pulsearch [1992] and Bullock and Krakiwsky [1994].

4.1.1 *Map Display*

The first and most obvious function of a digital road map in a vehicle navigation system is map display. The navigation system will have a screen or display of some sort on which a portion of the map can be shown. Once the map is displayed and the current position is marked, the user can see their location with respect to other features on the map. As the vehicle moves, the position can be traced on the map or the map can be scrolled and rotated to keep the vehicle in the centre of the map, as in the Etak Navigator moving map display. For the driver of a vehicle, a complicated map display can be distracting. To avoid a potential hazard, the map should be simple to comprehend. There should also be

an instruction mode of operation where the guidance instructions are communicated in place of displaying the map.

For a digital road map to be displayed, the roads and road-related features can be stored in either a vector or raster image form. A vector map database stores each road link with the coordinates of the end points and any points required to give it shape (i.e. for curved roads). A raster map on the other hand, is best described as a picture of the map; the road links are not explicitly stored. In the case of a raster map, none of the following functions can be performed.

There are usually hardware limitations in a vehicle navigation system. Typically, data storage space and processors are limited. Consequently, the digital road map should be compact in terms of storage requirements. It is necessary for the map to be stored in a manner that is efficient to access and display. This is particularly true in the case of a moving map display where the map must be redrawn frequently. It is not efficient for the map display procedure to search the entire database for the roads that must be displayed.

4.1.2 *Address Matching*

Often called geocoding, address matching is the process of determining a street address given a set of coordinates (i.e. latitude and longitude), or vice versa. The algorithms in a vehicle navigation system operate in a position domain (mathematical coordinates). Users, however, operate in the location domain (real-world objects), as they know the street address of their destination rather than the coordinates. Therefore, to navigate to an address, the address must be converted to mathematically defined coordinates.

Address matching requires street names and address ranges as attributes of the roads in a digital road map. The roads and intersections in a digital road map must be stored using a coordinate system that can be related to the coordinates output from positioning systems, such as WGS-84 ellipsoidal or UTM mapping plane coordinates. Given a latitude and longitude then, the nearest road in the digital road map is found using a shortest distance

approach. The address ranges are most often stored for links (road segments) between two adjacent nodes (intersections). A given address is found by linear interpolation between the address numbers of two intersections. Note that different address ranges must be stored for each side of the road.

Ideally, an address match should give coordinates that are accurate to about fifteen metres so that the driver can identify the destination once at that position. This is difficult to achieve even with a perfect position. Since address numbers are not distributed evenly along a road link, linear interpolation will not always be very accurate. There is no simple method of properly modelling the irregular distributions of addresses along a link to overcome this problem. If storage space is not at a premium, each individual address can be stored as a point in the database at its true location.

A recent trend in digital road maps has been the inclusion of digital yellow pages. As the name implies, these are digital directories of service providers. Digital yellow pages in a navigation system might include hotels, restaurants, service stations, and other road-related services, as well as attractions, banks, etc. Digital yellow pages are intended to assist in destination selection by passing a street address to the geocoding routine for plotting.

4.1.3 *Map Matching*

The purpose of map matching is to determine the most probable location of the vehicle on the map. Some implementations of map matching assume that the vehicle is on a road in the digital road map. Other algorithms allow for the fact that the vehicle may not be on a road at every instant. For example, the vehicle may be in a parking lot or in an area where the map is not up to date. Map matching can be used as a positioning input, or just as a means of displaying the vehicle on a road. Figure 4.1 illustrates the use of map matching for display purposes. When a positioning system computes coordinates that are not exactly on a link in the digital road map, the map matching algorithm finds the nearest link

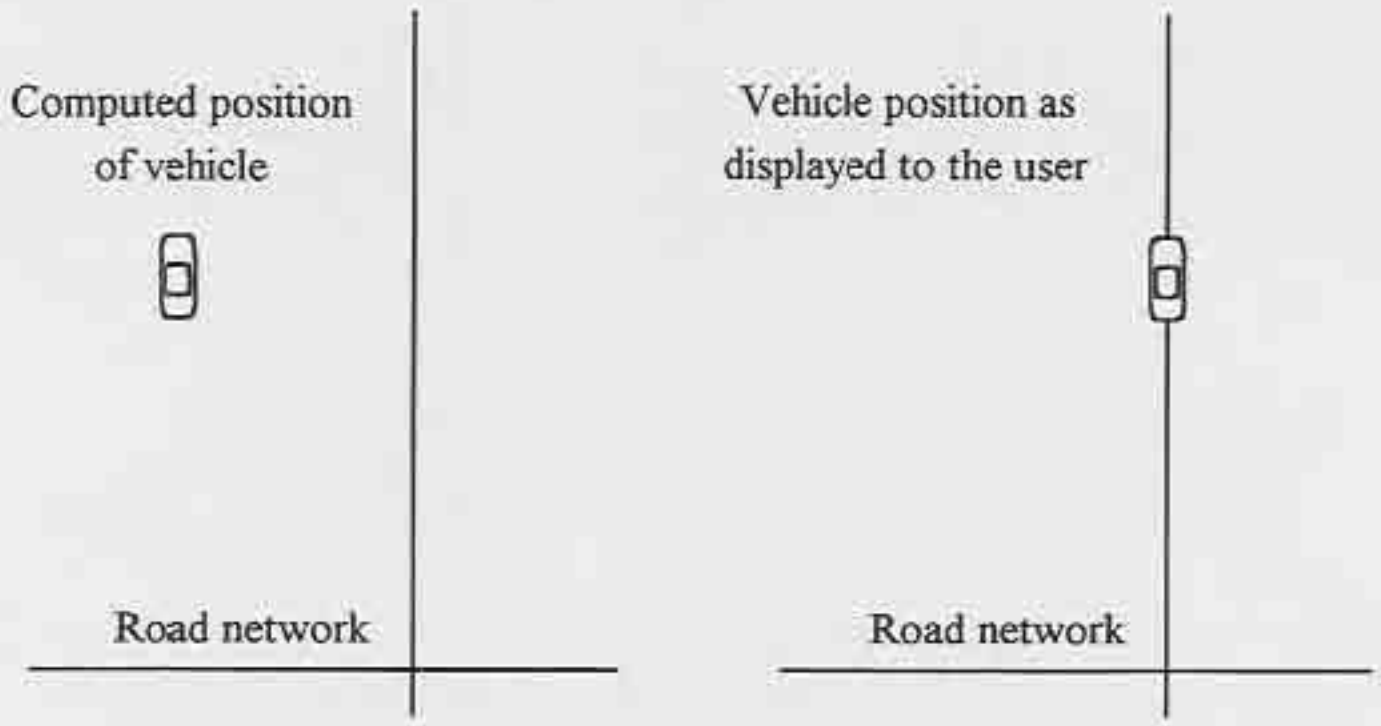

Figure 4.1 Map Matching for Display

and 'snaps' the vehicle onto that link. In this manner, the user is presented with an appealing view of the vehicle actually being on the road.

Using the map as a source of positioning information is usually based on correlating the traced path of the vehicle with potential routes in the digital road map. As the vehicle travels, distance travelled and changes in direction are used to continuously determine the shape of the route travelled; this shape is used to match the road network in the map through shape correlation.

A good map matching algorithm relies on maps with high positional accuracy, generally better than 30 m, ideally better than fifteen metres, to minimize incorrect road selections. Also, for map matching to be robust, the links in the map must be topologically correct so that they reflect the real world. If the road being travelled does not appear in the map database, the algorithm may get confused since it will not consider the route a valid path of travel.

Map matching is considered a pseudo-positioning system. This is because it can return a position based on the coordinates of an intersection or shape point (a node in a link that

represents a change in the road direction, but not an intersection), and the azimuth of the road being travelled upon. If the positional accuracy of the map is better than the positioning system accuracy, the position obtained by map matching can be used in the position determination algorithm, whether it be a filter or a weighted mean. For this to occur, the map should have an absolute positional accuracy in the order of ten metres. Map matching is critical to obtaining absolute vehicle positions in dead-reckoning. Dead-reckoning is a positioning method where various sensors are used to measure the distance travelled and the vehicle heading in order to compute relative changes in position. Map matching can also be also used to smooth the noise in positioning sensors or systems such as GPS, particularly under the effects of SA.

4.1.4 *Best Route Calculation*

In the pre-mission phase of vehicle navigation, a user may wish to select a destination and have assistance in determining the optimal route to travel [Guzolek and Koch, 1989]. A digital road map coupled with a best route calculation algorithm can provide an optimal route based on travel time, travel distance or some other specified criterion. This process is often referred to as pathfinding. The Dijkstra [Dijkstra, 1959] and A* [Nilsson, 1980; Winston, 1984] algorithms have both been used for best route calculation in vehicle navigation applications. The results of the best route calculation are turn-by-turn driving instructions from the initial location to the destination. Regardless of the algorithm used, best route calculation is a function that requires a high level of road-related map information.

First of all, the route selected must be valid. The route must not involve travelling the wrong way on one-way roads or consist of any impossible or illegal turns. To prevent this from happening, the digital road map must store turn restrictions and the directionality of each road link. Turn restrictions are considered 'hard' if it is impossible to turn there, such as from a freeway onto a side street where there is no ramp, or 'soft' if it is just illegal to turn there. In addition to constant 'soft' turn restrictions, there are also time variant turn

restrictions that must be accounted for. Some turns that are normally legal, are illegal during rush hours. There are also some cases of time variant directionality to be considered where rush hour lane reversals are implemented.

The criteria for a best route may vary depending on the situation. The most common criterion is to determine the shortest route according to time or distance travelled. Other criteria may be to avoid freeways, avoid certain areas of town, or select the most fuel efficient route. Each of these criteria require different data to be stored in the digital road map. To calculate the route of shortest distance requires only that the road map be of a consistent scale throughout. The route of shortest travel time would require speed limits or average travel times for each link; this criterion is not very effective if real-time data is not available. Routes that avoid freeways require that roads be classified. Routes that avoid certain areas require that these areas be stored in the map. And routes that are the most fuel efficient for trucks must have road grades stored in the map.

4.1.5 *Route Guidance*

Once a route has been determined by the driver or the best route algorithm, the navigation system must guide the driver along the route. Route guidance can be given pre-mission or in real time. Pre-mission route guidance consists of a printout of door-to-door turn-by-turn driving instructions that include street names, distances, turns, and landmarks.

Real-time route guidance is much more useful than pre-mission route guidance, and much more demanding in terms of software. As the vehicle travels, each position must be determined and geocoded to a location in the digital road map. In this manner, the route guidance algorithm knows where the vehicle is in the route and the direction of travel. As a turn or manoeuvre approaches, the algorithm must alert the driver, with audible or visual signals, and then indicate when the manoeuvre is to be performed. If all goes well, the vehicle will continue along the planned route. If the driver misses a turn or manoeuvre, the position reported will result in a location that is off of the planned route. If this occurs, the route guidance algorithm must invoke the pathfinding algorithm to compute a

new best route to get from the current location to the destination. Route guidance would then resume along the new route. In addition to digital road maps, real-time route guidance relies on positioning, address matching, and pathfinding. If a digital road map supports both pathfinding and route guidance, it is said to be navigable [Shields, 1994].

Each of the five functions discussed relies on specific features in the digital road map database. These database feature requirements are summarized for each of these map-related functions in Table 4.1.

Function	Database features required
Map display	links (roads), nodes (intersections), coordinates of nodes
Address matching	links, names of links, nodes, coordinates of nodes, address ranges between nodes
Map matching	links, nodes, coordinates of nodes, correct and complete topology
Pathfinding	link classification, connectivity between nodes, driving and turn restrictions, auxiliary attributes
Route guidance	all address matching and pathfinding features

Table 4.1 Digital Road Map Feature Content Requirements for Map-Related Functions

4.2 Digital Road Map Suppliers and Standards

There are several mapping companies and organizations that produce and maintain digital road maps specifically for vehicle navigation. Reviewed in this section are the major data formats/suppliers being used in vehicle navigation systems in the world, and the navigation functions that they support. When designing a navigation system, the choice of an appropriate digital road map is very important since the map is a foundation for several of the navigation functions.

There are five mapping suppliers that are predominant in vehicle navigation systems: Etak, NavTech, JDRMA, EGT, and EDRA. These five data suppliers, their origins, and their database formats will be discussed. The functions supported by each of the five main data suppliers are summarized in Table 4.2. It will be seen that the choice of a digital map format and supplier for a vehicle navigation system affects both the functionality and the potential market of the system.

Function	DRM	EtakMap	NavTech	GDF/EDP	EGT
Map display	Yes	Yes	Yes	Yes	Yes
Address matching	Yes	Yes	Yes	Yes	Yes
Map matching	Yes	Yes	Yes	Yes	Yes
Pathfinding	No[1]	No[2]	Yes	Yes	Yes
Route guidance	No[1]	No[2]	Yes	Yes	Yes

1 - The JDRMA does not include restrictions in the DRM data, however, many companies have included these functions by either ignoring restrictions, or adding them to the database themselves.

2 - Etak has produced maps with restrictions that support pathfinding, however, coverage is only available on a custom basis at this time.

Table 4.2 Map-Related Functions Supported by
Major Digital Road Map Formats/Suppliers

4.2.1 *Etak*

Etak Corporation of Menlo Park, California, is a digital map company that focuses on producing and distributing highly accurate digital road maps known as EtakMaps [Zavoli, 1989]. Etak has been producing digital road maps for over a decade, starting with the maps for the Etak Navigator vehicle navigation system in the early eighties.

EtakMaps are available in two formats: MapAccess and MapBase. MapAccess is a proprietary binary format that is optimized for storage space and display speed. MapBase

is a non-proprietary ASCII format that can be imported into most commercially available Geographic Information System (GIS) packages for use and modification. The MapAccess data requires less than one-tenth the storage space of MapBase. Although the MapAccess format is proprietary, Etak provides a library of software development tools for Value Added Resellers (VARs) that wish to develop applications using these EtakMaps. For example, VARs for Etak include Blaupunkt Werke GmbH. of Germany, Clarion Co. of Japan, and PacTel Teletrac Systems Inc., OCS Technologies, Radio Satellite Integrators Inc., and Trimble Navigation of California.

To produce digital road maps, Etak uses a heads-up digitizing method. Scanned images of source material are presented on the display of a computer, and an operator uses a cursor to digitize features directly. Etak maps incorporate TIGER files, ZIP + 4 data, low-level photography, field work, and U.S. Geological Survey (USGS) digital orthophotoquads.

The coverage for EtakMaps is extensive. The entire area of the United States is covered by one of the versions of EtakMaps. Over 100 major metropolitan areas are covered in EtakMap Versions 3 and 3.4, which have an accuracy equivalent to 1:24 000 scale topographic maps. All of the rural areas in between the cities are covered by EtakMap Version Connect, which has an accuracy equivalent to 1:100 000 scale maps. Additionally, Etak has coverage in France, Germany, Japan, Canada, Hong Kong, and The Netherlands. In France, all cities with populations of more than 100 000 plus the major interconnecting roads are covered. In Germany, the same applies, but for cities with populations of more than 50 000. For Japan, Etak has taken the DRM format (see JDRMA below), which meets Etak's standards of positional accuracy, and converted it into the EtakMap format. Etak has acquired the Statistics Canada area master files (AMF) for use as a starting base map in Canada. Varying levels of coverage are available for the other countries mentioned.

EtakMap Versions 3, 3.4, and Connect do not support pathfinding. Etak has developed Version 4 EtakMaps which do support pathfinding, however, coverage is only available in a few areas, or on a custom basis.

4.2.2 *NavTech*

Navigation Technologies Inc. (NavTech) of Sunnyvale, California, is a producer and provider of fully navigable digital road maps known as NavTech maps. NavTech has developed their databases from the beginning to support navigation functions such as map matching, pathfinding, and route guidance [Sweetman and Collier, 1993]. NavTech's strategic partners include Philips International B.V. and European Geographic Technologies B.V. (EGT) of The Netherlands (see Section 4.2.4), Motorola Inc. and SEI Information Technology of Chicago, Nippondenso Ltd. and Zexel Corporation of Japan, and the American Automobile Association (AAA). Philips, Motorola, Nippondenso, and Zexel are developing vehicle navigation systems, SEI develops software for creating and using NavTech databases, EGT is a mapping company in Europe, and the AAA provides driver information services.

The first NavTech databases were released in 1991. Currently, NavTech databases are available for about 60 major US cities. NavTech has an aggressive schedule for producing and releasing additional databases over the next two years. Software development tools that access NavTech proprietary maps are available through SEI.

Data sources used in NavTech databases include aerial photos, local base maps, AAA-collected data, and field work [Schiff, 1993]. The databases are cross-checked with other data sources such as ZIP + 4 files, state departments of transportation, and other Federal, state, county, and municipal sources. The completed NavTech databases are guaranteed to be 97% complete and accurate both in position (better than fifteen metres) and in the correctness of the restrictions and geometry of the road network.

NavTech maps have been used in the AAA DriverGuide kiosk system that provides users with written door-to-door turn-by-turn driving instructions. Vehicle navigation systems that use NavTech maps are the Zexel NAVMATE (offered as an option on the '95 Oldsmobile 88 LSS as the Guidestar System) and the Motorola Advanced Traveller

Information System (ATIS). Nippondenso has demonstrated their navigation system (normally based on DRM) with NavTech maps.

4.2.3 *JDRMA*

The Japan Digital Road Map Association (JDRMA) [Shibata and Fujita, 1989] is a consortium of Japanese companies involved in vehicle navigation. Member companies, over 82 in all, include Toyota Motor Corporation, Summitomo Electric Industries Ltd., Mazda Motor Corporation, Sanyo Electric Company Ltd., Mitsubishi Electric Corporation, Nissan Motor Co., Pioneer Electronics, Suzuki Motor Co., Sony Corporation, Nippondenso Co., and Toshiba. In 1988, the JDRMA released the first Digital Road Map (DRM) of Japan, which was derived from 1:50 000 and 1:25 000 topographical maps. Each member of the JDRMA has access to the DRM format and data. Typically, a company takes the DRM data and converts it into a proprietary structure for use in their own vehicle navigation system. At the end of 1994, it was estimated that more than 600 000 vehicles on the road in Japan had been equipped with a navigation system, most of which use DRM or some derivative digital map.

A specialized group called the Navigation Systems Research Association (NSRA) takes the DRM data and puts it onto a CD-ROM in a format known as Naviken. Most of the member companies of the NSRA are also members of the JDRMA. Each of these companies builds navigation systems that use the Naviken CD-ROM directly, so the CDs are interchangeable between systems.

As of March 1993, the two gigabyte DRM covered approximately 1.1 million kilometres of roads in Japan; virtually all of the urban and rural areas have complete coverage. Efforts continue to upgrade the detail of the DRM to the 1:25 000 level. Currently, all cities with a population greater than 100 000 are digitized at this higher level of detail. In addition to increasing the level of detail, the JDRMA maintains the DRM by adding newly constructed and modified roads. Updated versions of the DRM are released at the end of March each year.

The DRM does not contain any turn restriction information. Companies that wanted to add pathfinding to their navigation systems had to modify the DRM database. Often these companies would add the turn restriction data as well as traveller information in the form of digital yellow pages. Recently, legislation was introduced in Japan to prevent vehicle navigation systems from directing traffic away from the congested main roads to the side streets. This has resulted in an increased number of navigation systems that simply plot the vehicle position on the map display, and offer no route guidance.

4.2.4 *EGT and EDRA*

In Europe, the development of digital road maps has been driven by the requirements of vehicle navigation systems. Both Bosch and Philips were developing systems in the mid-eighties, namely the Blaupunkt Travelpilot and the CARIN, respectively. These systems were both based on map matching and relied on high quality digital road maps, of which there were none at the time. The Digital Electronic Mapping of European Territory (DEMETER) project was commenced jointly by Philips and Bosch to create common technical specifications for a digital road database for vehicle navigation purposes. The result was the Geographic Data File (GDF) Version 1.0, released in October 1988 [Philips and Bosch, 1988].

The Dedicated Road Infrastructure for Vehicle Safety in Europe (DRIVE), funded by the E.U. (European Union), formed the Task Force European Digital Road Map (TFEDRM) to oversee the subsequent development of the GDF. At this phase of development, Daimler-Benz GmbH. of Germany, Renault of France, Tele Atlas International B.V. of The Netherlands, and Intergraph Corp. of Alabama joined the consortium. Benz and Renault are car manufacturers, Tele Atlas is a map producer, and Intergraph is a major GIS vendor. The work by TFEDRM resulted in GDF Version 2.0, which was released in January 1992. Since then, GDF has been updated to Version 2.1.

Since GDF maps can contain extensive information, vehicle navigation system manufacturers generally use only a subset of the available data for their system. The

manufacturer takes the required data and puts it into a proprietary data format that has been optimized for use in their system. Rather than being a format for direct end use, GDF takes the role of being a data pool and exchange format. Bosch, Tele Atlas, and Etak have in fact signed a co-operative agreement to create a pool of digital road map data for all of Europe; this project is known as the European Digital Road Map Association (EDRA), and the European data pool [Claussen, 1993]. EGT has declined to join the data pool, opting to map all of Europe on their own [French and Querèe, 1993]. This rift is possibly due to the fact that EGT's partner NavTech and Bosch's partner Etak are competitors in the North America.

EGT maps currently cover all of Germany and France and parts of Italy. Austria, Switzerland, and Benelux are the next priorities, followed by the United Kingdom. Scandinavia and eastern Europe may eventually be mapped as well. EGT has licensed NavTech database management technology for mapping, and can supply maps in the GDF, NavTech and DRM formats. EGT supplies the databases for the Philips CARIN system, and has the potential to supply data for any system based on NavTech, DRM or GDF derived maps.

The European data pool's objective is to complete a digital road map of all of Europe within two years. A country is considered complete if a minimum 50% of the population is covered by the map. To date, Germany, France, The Netherlands, Belgium, Luxembourg, and much of Italy have been completed [De Taeye, 1994]. The United Kingdom, Switzerland, and Austria are the next priority. The data pool is looking for other partners to map Spain, Portugal, and the Scandinavian countries. The Blaupunkt Travelpilot is the first system on the market that will use the data pool maps. The data pool uses GDF as their storage and exchange format.

Both the data pool and EGT have focused on the vehicle navigation and GIS markets for their maps. Also, both map suppliers are including high-level route guidance support features, such as turn restrictions and one-way streets, in their maps.

4.3 Design Implications For PortaNav

PortaNav was designed and tested in Calgary, Alberta, Canada. To avoid creating the digital road map data, a supplier with coverage in Canada was sought. At the commencement of the PortaNav project, Etak was the only supplier with coverage in Calgary, so there was in fact no real choice in the matter. By using Etak digital road maps, PortaNav is limited in its functionality; best routes cannot be computed. The Etak maps do however, support address matching and map matching, which was the minimum requirement for PortaNav. Pathfinding was on the list of desired features, but simply is not possible in Calgary at this time. Etak plans to provide navigable digital road maps of Canadian cities in the future.

PortaNav provides locating and map display, automatic scrolling of the map as the vehicle moves, and address matching for destination selection and road identification. It is possible to implement map matching for displaying the vehicle on a road with the Etak map. For testing reasons, however, the display routine did not use map matching. The Etak map also forms the foundation for the map aiding process used in PortaNav. As will be seen in Chapter 7, the Etak digital road map became the engine behind map aiding.

CHAPTER FIVE

PROTOTYPE SYSTEM DESIGN

There were several objectives behind the development of PortaNav. First of all, PortaNav was to be a prototype portable vehicle navigation system, completely autonomous from any one vehicle. The system has to be relatively easy to carry from vehicle to home or office. Minimum functionality for the system was to include positioning, location, navigation, and map display. As this is a prototype system, testing flexibility is also an important consideration. This chapter describes and justifies the chosen design for PortaNav.

5.1 Hardware and Software Components

The constraints for this research project simplified the decision making process for hardware components. In order to avoid assembling raw electrical components, end-user products were sought for the processing, positioning, and database engine modules. The complete PortaNav system is pictured in Figure 5.1.

The choices for a portable processor platform were a notebook computer or a hand-held PDA. The size and cost disadvantage of the notebook computer was weighed against the capabilities of software development platforms. Two years ago when this research project began, pen-based operating systems were in their infancy. A notebook PC on the other hand, can use DOS with Windows as the operating system, development platform, and user interface. The other disadvantage to using a hand-held PDA is the size and resolution of the display. Notebook PCs are available with large colour LCDs.

The notebook computer chosen for this project was an NEC Ultralite Versa 25C. This computer has an Intel 80486 SLC CPU with a clock speed of 25 MHz. The screen is an active matrix colour LCD that measures 9.5" diagonally and has a resolution of 640 by 480 pixels. The 120 MB hard drive was more than sufficient to store the operating system, PortaNav software, and digital road maps. The computer was configured with

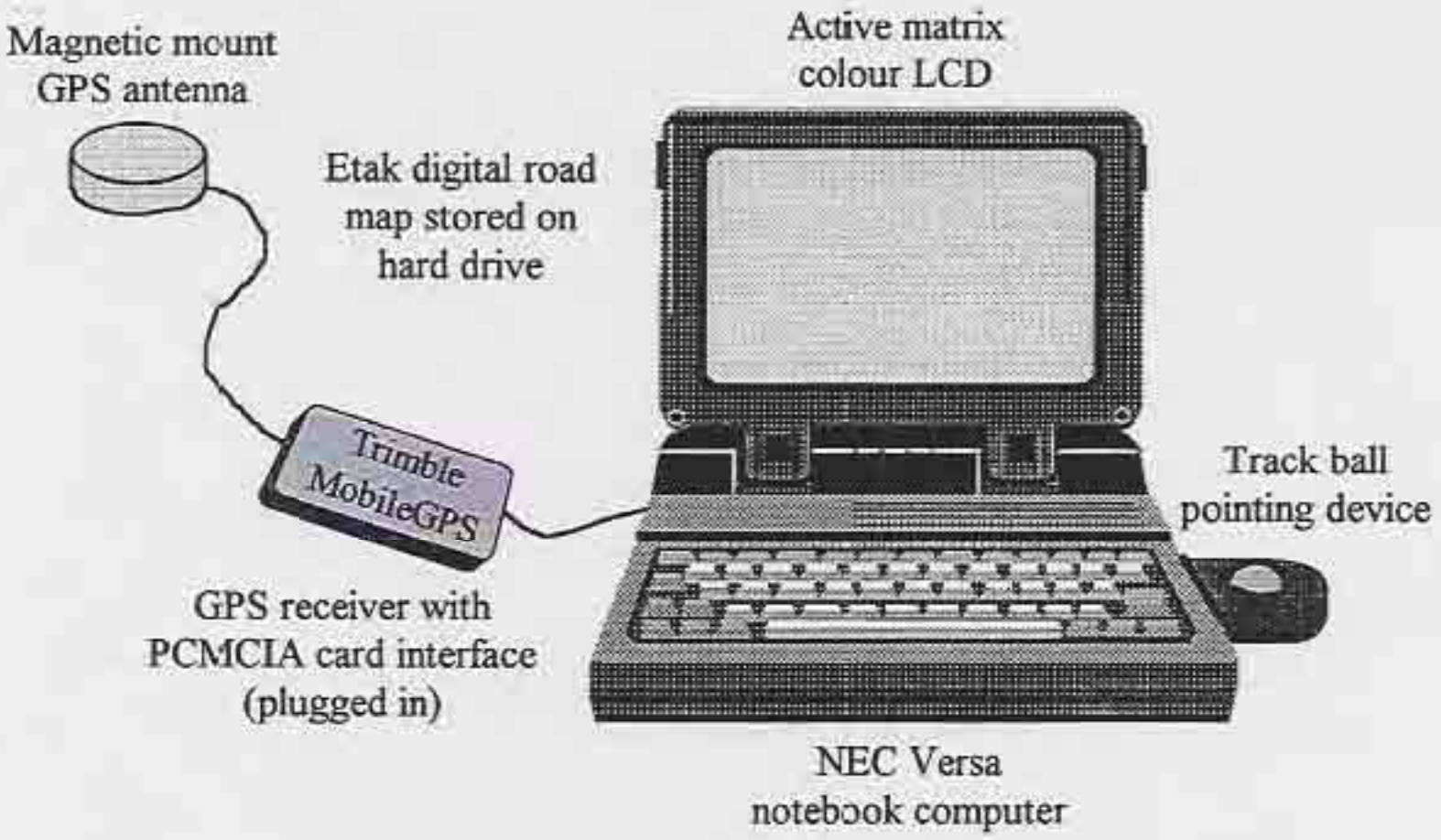

Figure 5.1 PortaNav System Components

eight megabytes of RAM for the memory intensive software, and dual NiMH batteries for longer battery life on the road. The second battery can be inserted in place of the removable floppy disk drive for up to six hours of continuous use. Finally, there is a Type III PCMCIA slot for expansion cards.

GPS formed the foundation of the positioning module. A compact, easily portable, low-cost receiver was a high priority. A serial port connection can be used to interface virtually any GPS receiver with a PC. Unfortunately, the GPS receiver would then require its own power source, adding bulk and clumsiness to the system. The two PCMCIA card GPS receivers available were the Trimble MobileGPS and the Rockwell NavCard. Both are single frequency (L1) C/A-code receivers that have a compact design and small microstrip magnetic mount antennas. Both draw power from the host notebook computer through the PCMCIA slot, and both cost under US $1,000. The main difference is the number of channels; the Trimble has six parallel channels and tracks eight satellites, while

the Rockwell has five parallel channels. The Trimble was chosen so that greater redundancy in the Kalman filter could be realized.

The Trimble MobileGPS receiver comes with a software development kit (SDK) for users who wish to develop their own software. The SDK is supported under DOS and Windows in either 'C' or visual basic. With the SDK, third party software can access all of the position, velocity, and raw measurement data directly from the receiver with high-level function calls. There is never a need to deal with the bit-level communications with the GPS receiver. This unloads the burden on the developer so that software can be developed more quickly.

As described in Chapter 4, the digital road map database is a limiting factor in the functionality of a vehicle navigation system. Geographic coverage is an even larger limiting factor. Etak was the only map supplier that had coverage available for the Calgary area, so there was really no choice in the matter. Fortunately, Etak also has an SDK that is available through a value-added reseller (VAR) agreement. The University of Calgary became an educational development site, and as such, was granted the appropriate licenses for the SDK. The Etak software libraries access the proprietary digital maps and allow third party software to display and manipulate the map data. Once again, the developer is unloaded of the burden to write low-level software for map drawing and is empowered with high-level function calls that can be used to perform various map-related tasks. The Etak SDK is available on the PC and Sun platforms under DOS, Windows and Unix in the 'C' programming language.

The common denominators between the Trimble and Etak SDKs were DOS, Windows, and 'C' on the PC platform. The first version of PortaNav was developed in the DOS environment, and the second version was developed in the Windows environment. The Borland C/C++ compiler was selected as it was also supported by both SDKs.

As discussed previously, the primary function of PortaNav is portable navigation. The portable descriptor implies that there are no components hard-wired to the vehicle, i.e. the

whole system can be removed and used in another location or vehicle. This eliminated the possibility of using dead-reckoning sensors such as an odometer or a compass.

Differential GPS was not used in PortaNav because the portability requirement impedes the use of differential GPS equipment. At the time this project was commenced, there were no compact differential GPS correction receivers available. Nor was there an infrastructure to support the dissemination of the corrections at a low cost. Consideration was given to the possibility of using a cellular phone to transmit the corrections, but the cost of air time was prohibitive. Now, there are small paging devices available that receive wide area differential corrections from FM radio stations via an FM sub-carrier [Abousalem et al., 1995]. The infrastructure for the broadcasting of the corrections is now coming on line. The paging receiver costs under $200 and there is a subscription cost for the service. This seems be the ideal method for consumers to receive differential corrections in a vehicle. If PortaNav were being developed now, it would most likely make use of an FM paging device to receive differential corrections.

5.2 Functionality

PortaNav is intended to aid a user in getting from one location to another. In order to do this, the user must first be able to select and plot the destination. Since users know their destinations in terms of an address, address matching is a necessity, and is implemented in PortaNav. Once the destination is plotted and the current position is computed, the user can inspect the map with panning and zooming functions to determine the optimum route. The map display procedure includes labelling the roads. The names of roads that are not labelled can be determined using the nearest feature search. Typical users of the navigation software will not necessarily be able to read a map, so best route calculation should be automated. This is naturally followed by route guidance. Unfortunately, the Etak map of Calgary is not navigable, hence best route calculation and route guidance cannot be implemented in PortaNav.

Position computation is done in real time using the GPS measurements. The MobileGPS receiver is capable of providing pseudorange and Doppler (phase rate) measurements, both of which are used in computing the position and velocities. The position is indicated on the map display with a small marker, and the track of the vehicle's path is traced out.

5.3 Performance

As described in Chapter 2, there are still unresolved error sources in GPS. When operating in single point mode, the GPS measurements are subject to Selective Availability and multipath errors, resulting in 2D positional accuracies as bad as 100 m at the 95% confidence level. In downtown areas, the urban canyon effect tends to block most satellite signals, making it very difficult for satellite signals to be received. This is also the case when the vehicle travels under dense tree cover or through a tunnel [Lachapelle and Henriksen, 1995]. Signal availability is a primary concern when navigating in urban areas.

As indicated, single point GPS position accuracies obtained by instantaneous fixes can be as poor as 100 m. Independent position fixes from epoch to epoch can also be very noisy if the constellations used do not remain the same. In vehicle navigation, this is not satisfactory for determining the vehicle's location in the street network and presenting it to the user. In areas with many streets close together, there is a high danger of misleading the driver. The secondary goal of the PortaNav project is to improve upon this level of accuracy and to compute a smooth trajectory. It is hypothesized that a higher level of accuracy and a smoother trajectory can be achieved by using a Kalman filter that integrates all of the available pseudorange and Doppler observations. It is further hypothesized that additional improvements can be realized by utilizing information derived from the digital road map. The map aided GPS algorithms implemented in PortaNav will be described in detail in the next two chapters, and the testing results are presented in Chapter 9.

5.4 Software Design Considerations

As a prototype system, PortaNav must demonstrate usability while providing a mechanism for testing. Each of these two issues will be discussed. A diagram illustrating the various software modules is shown in Figure 5.2. A screen capture of the PortaNav software interface is shown in Figure 5.3.

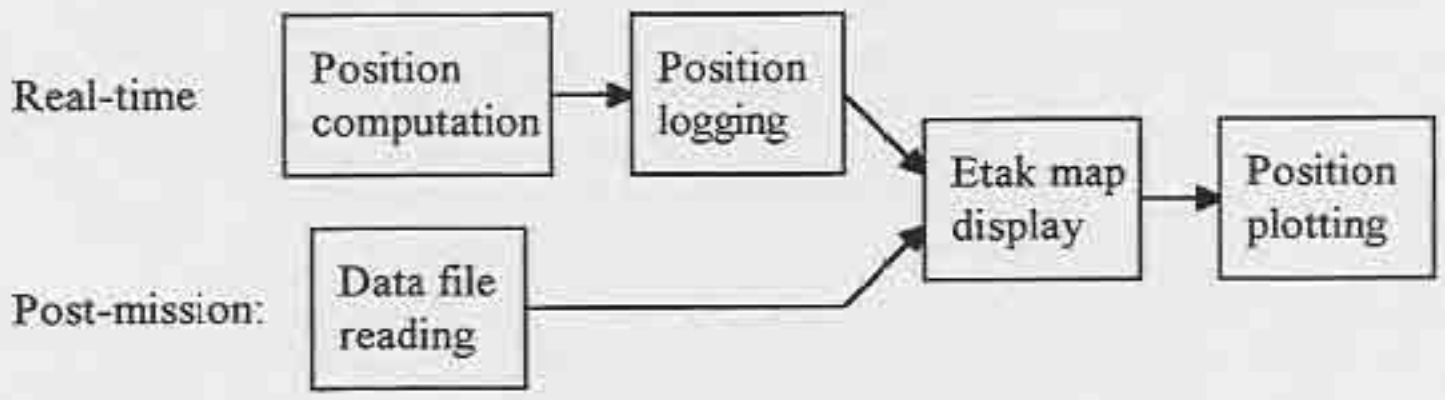

Figure 5.2 Main Software Modules in PortaNav

As an end-user product, ease of use, simplicity, and reliability are the driving forces behind the software design. By using the familiar Windows interface, users will instantly be able to perform basic functions such as opening maps and using the cursor to zoom and pan the map. A menu driven interface provides access to all of the functions of the software either by cursor control or by keyboard shortcuts. A help function can provide context sensitive assistance for the main functions of the software. The user should be able to start the program and be able to use it within minutes.

As a testing platform, various data streams must be processed and logged so that they can be analyzed. This is done by adding a command to start or stop the data logging when the GPS receiver is active. Any one or more of the three real-time computed solutions can be plotted on the screen, showing the results of the various algorithms in real time. The data files can be played back and plotted post mission for further analysis. The output of the post-mission precise processing can also be read and displayed on the map. Each of the

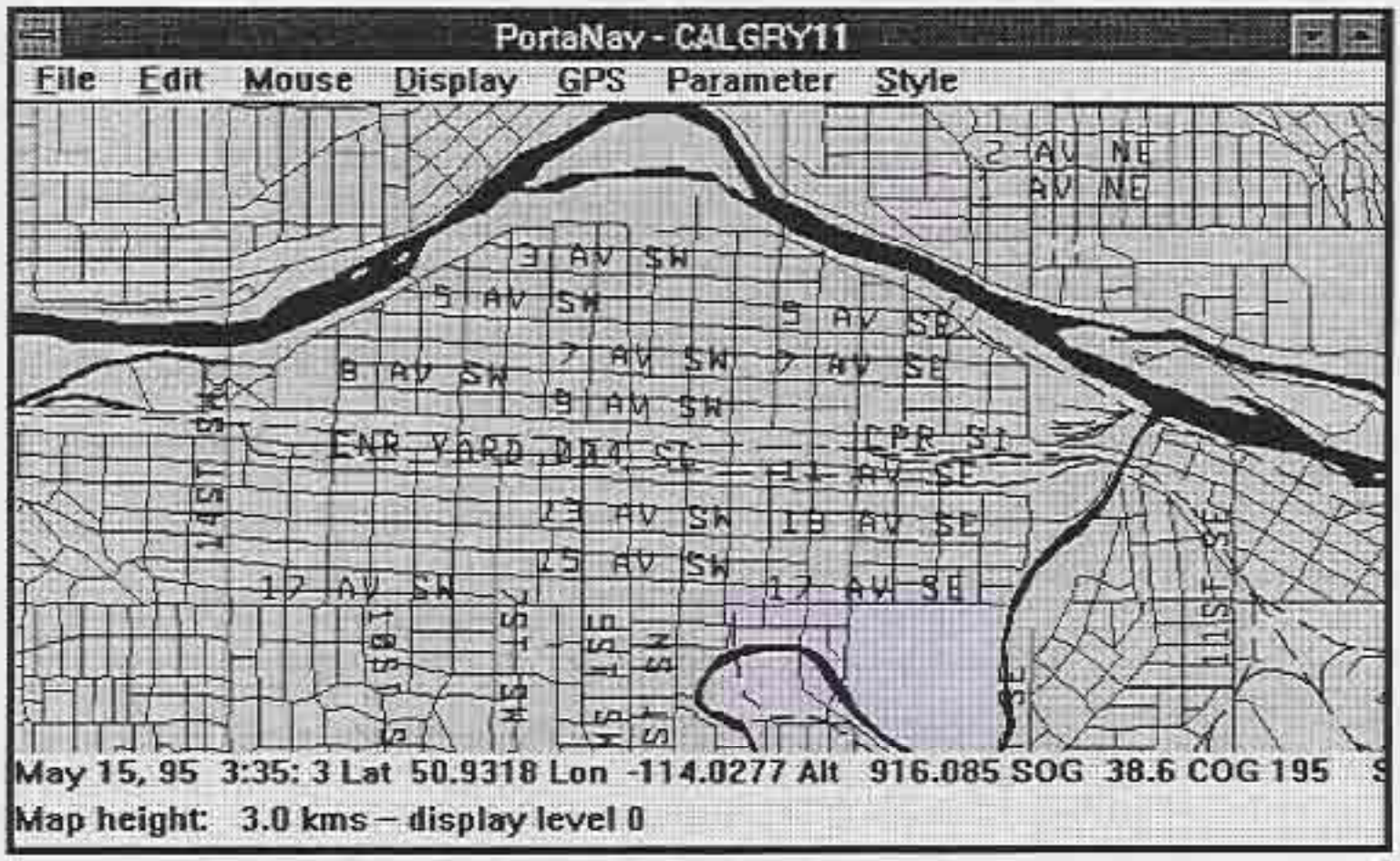

Figure 5.3 Screen Capture of the PortaNav User Interface

data files is in the same format, so that they can be analyzed quantitatively using spreadsheet software. Details on the various position data streams are found in Chapter 6, and the fundamentals behind the map database engine are presented in Chapter 7.

CHAPTER SIX

POSITIONING MODULE

The Trimble MobileGPS receiver forms the backbone of the positioning module in PortaNav. The only other source of positioning information is the digital road map. This chapter outlines the observation models and methodology used in the positioning module of PortaNav. Three GPS positioning solutions are presented (best DOP, least squares, and Kalman filtering) and implemented in PortaNav for testing purposes. These algorithms are largely redundant; in an end user system, only one would need to be used.

6.1 Global Positioning System

The Global Positioning System (GPS) is a satellite-based radionavigation system. The basic concept is to measure the distance to multiple known satellite locations to solve for the position of the receiver. The fundamental observables and the formation of the observation equations are described in this section. Formulations for computing solutions follow in Section 6.2. For a more in depth description of GPS, refer to Van Dierendonck [1995], Leick [1995] and Hofmann-Wellenhof [1994].

6.1.1 *GPS Pseudoranges*

In two dimensional space, measuring the distance to a known point gives a circle of position. By measuring distances to two known points, an ambiguous position can be determined. In a three dimensional frame, distances to three known points are required to solve for a position. In GPS, the known points are satellites, the unknown point is the position of the GPS receiver, and the distances are ranges (ρ) to the satellites. The ranges are obtained by multiplying the speed of light (C) by the measured time of travel (Δt) of the broadcast signal using

$$\rho = \Delta t \cdot C, \tag{6.1}$$

where $$C = 299\,792\,458.0\ m/s. \tag{6.2}$$

The pseudorange observation equation is formed in a three dimensional Cartesian coordinate frame as follows:

$$P = \rho + (dt - dT) \cdot C + d_{ion} + d_{trop} + d_\rho + \varepsilon_\rho, \tag{6.3}$$

where P is the observed pseudorange (m),

ρ is the geometric range between the receiver and satellite (m),

dt is the satellite clock offset from GPS system time (s),

dT is the receiver clock offset from GPS system time (s),

d_{ion} is the ionospheric delay (m),

d_{trop} is the tropospheric delay (m),

d_ρ is the radial orbit error (m), and

ε_P is the pseudorange measurement noise (m).

The satellite position and the receiver position are buried in the geometric range term

$$\rho = \sqrt{(X-x)^2 + (Y-y)^2 + (Z-z)^2}\,, \tag{6.4}$$

where X, Y, Z are the known satellite coordinates (m), and

x, y, z are the unknown receiver coordinates (m).

The term pseudorange is used because the measured quantity differs from the actual geometric range by the errors and time offsets.

The coordinates of a satellite at an instant in time are computed by using the ephemerides for that satellite. The ephemerides are based on Keplarian orbital parameters and terms to model the perturbances. The algorithm for computing a satellite position in the WGS-84 Cartesian coordinate frame using the broadcast ephemerides can be found in Leick [1995, pp. 75] and Rockwell [1987].

Both the ionospheric and tropospheric components of the atmosphere affect GPS signals. The free ions in the ionosphere and particles in the troposphere (mainly moisture) cause

the signal to be delayed. These atmospheric effects should be modelled and their effects removed. In PortaNav, the Goad and Goodman tropospheric model [Goad and Goodman, 1974; Leick, 1995, pp. 309] was applied, and the broadcast ionospheric model was used [Klobuchar, 1986; Hofmann-Wellenhof, 1994, pp. 105-106]. The tropospheric model removes up to 90% of the delay, while the ionospheric model only removes 50-60%. The magnitude of these corrections varies between two and twenty metres each.

Both the satellite and receiver clocks differ from true GPS system time. The ephemerides are based on GPS system time as a reference, so it must be determined. The cesium and rubidium clocks in the satellites are very stable and well behaved, so their deviations from true GPS time are modelled using a second order polynomial. The coefficients for the polynomial are broadcast as part of the navigation message. These clock parameters are dithered to degrade accuracy under the implementation of SA.

Modern GPS receivers use inexpensive quartz clocks to keep time. The offset between the receiver clock and GPS system time must be solved. Since this term is the same for all measurements, only one unknown offset is introduced at each epoch. This brings the number of unknowns to four, and hence, measurements to four satellites are required to solve for a three dimensional position. Additional measurements can be used to provide redundancy.

Residual orbit errors and the effects of SA are grouped together in one term. This error is not random, and it cannot be removed or modelled without using differential GPS techniques. The remaining term represents the receiver noise, which is random and relatively small.

Before proceeding to a solution, two other corrections to the pseudorange should be applied. The first is the relativity effect, being the perceived change in time due to the relative motion between the satellite and the receiver. A major portion of this effect is accounted for by shifting the fundamental frequency in the satellite before launch so that the observed frequency is near nominal. The remaining effects can be computed and

removed as given in Jorgensen [1986] and Hofmann-Wellenhof [1994, pp. 117-123]. The second correction is due to the rotation of the earth during the time the GPS signal travels to the receiver. This is accounted for by adding a term to the longitude of the ascending node equation in the ephemeris algorithm that effectively rotates the satellite position back in time with respect to the earth fixed coordinate frame.

An important issue to be addressed is the accuracy of the pseudorange observable. An error budget for C/A-code pseudoranges is given in Table 6.1 [Wells et al., 1986; Gao, 1992]. The dominant term in single point positioning is SA. This makes it difficult to determine the measurement accuracy of the pseudorange because SA is not random. Most C/A-code receivers have a measurement noise of a few metres, so without SA and in a low multipath environment, the observation accuracy could be at the ten metre level. It was determined empirically that the standard deviation of the pseudorange observable obtained from the Trimble MobileGPS is about fifteen metres.

Error source	Typical (m)	Maximum (m)	Typical after model (m)
Tropospheric delay	2 - 15	30	1 - 2
Ionospheric delay	2 - 20	150	1 - 10
Satellite orbit errors	5 - 20	30	
Selective Availability (SA)	20 - 30	100	
Code measurement noise	0.1 - 3	5	
Multipath	0 - 10	300	

Table 6.1 Typical Error Budget for Single Point C/A-Code GPS Pseudoranges

The solutions given in Section 6.2 require design matrices for each type of observation equation used in the model. The design matrix A for a set of n pseudorange observations and the four GPS unknowns is computed as follows:

$$\mathbf{A} = \begin{bmatrix} \frac{\partial P_1}{\partial x} & \frac{\partial P_1}{\partial y} & \frac{\partial P_1}{\partial z} & \frac{\partial P_1}{\partial CdT} \\ \frac{\partial P_2}{\partial x} & \frac{\partial P_2}{\partial y} & \frac{\partial P_2}{\partial z} & \frac{\partial P_2}{\partial CdT} \\ \cdots & \cdots & \cdots & \cdots \\ \frac{\partial P_n}{\partial x} & \frac{\partial P_n}{\partial y} & \frac{\partial P_n}{\partial z} & \frac{\partial P_n}{\partial CdT} \end{bmatrix}, \tag{6.5}$$

where $$\frac{\partial P_i}{\partial x} = \frac{-(X_i - x)}{\rho_i}, \tag{6.6}$$

$$\frac{\partial P_i}{\partial y} = \frac{-(Y_i - y)}{\rho_i}, \tag{6.7}$$

$$\frac{\partial P_i}{\partial z} = \frac{-(Z_i - z)}{\rho_i}, \text{ and} \tag{6.8}$$

$$\frac{\partial P_i}{\partial CdT} = 1. \tag{6.9}$$

Note that in Equation 6.9 the partial derivative is 1 rather than -1. This is because $-CdT$ is solved for in the model. In PortaNav, the design matrix was formulated in geodetic coordinate space. The partial derivatives are more complex, but the solution is given in geodetic coordinates, eliminating coordinate transformations after the solution is obtained. Using the chain rule,

$$\frac{\partial P_i}{\partial \phi} = \frac{\partial P_i}{\partial x}\frac{\partial x}{\partial \phi} + \frac{\partial P_i}{\partial y}\frac{\partial y}{\partial \phi} + \frac{\partial P_i}{\partial z}\frac{\partial z}{\partial \phi}, \tag{6.10}$$

$$\frac{\partial P_i}{\partial \lambda} = \frac{\partial P_i}{\partial x}\frac{\partial x}{\partial \lambda} + \frac{\partial P_i}{\partial y}\frac{\partial y}{\partial \lambda}, \text{ and} \tag{6.11}$$

$$\frac{\partial P_i}{\partial h} = \frac{\partial P_i}{\partial x}\frac{\partial x}{\partial h} + \frac{\partial P_i}{\partial y}\frac{\partial y}{\partial h} + \frac{\partial P_i}{\partial z}\frac{\partial z}{\partial h}. \tag{6.12}$$

The additional partial derivatives are

$$\frac{\partial x}{\partial \phi} = -(N+h)\cdot\sin(\phi)\cdot\cos(\lambda), \tag{6.13}$$

$$\frac{\partial x}{\partial \lambda} = -(N+h)\cdot\cos(\phi)\cdot\sin(\lambda), \tag{6.14}$$

$$\frac{\partial x}{\partial h} = \cos(\phi)\cdot\cos(\lambda), \tag{6.15}$$

$$\frac{\partial \nu}{\partial o} = -(N+h)\cdot \sin(\phi)\cdot \sin(\lambda), \tag{6.16}$$

$$\frac{\partial \nu}{\partial \lambda} = -(N+h)\cdot \cos(\phi)\cdot \cos(\lambda), \tag{6.17}$$

$$\frac{\partial \nu}{\partial u} = \cos(\phi)\cdot \sin(\lambda), \tag{6.18}$$

$$\frac{\partial \nu}{\partial o} = [(1-e^2)\cdot N+h]\cdot \cos(\phi), \text{ and} \tag{6.19}$$

$$\frac{\partial \nu}{\partial k} = \sin(\phi), \tag{6.20}$$

where $e = \sqrt{\frac{a_e^2 - b_e^2}{a_e^2}}$ is the eccentricity of the reference ellipsoid, (6.21)

$N = \frac{a_e}{\sqrt{1-e^2\cdot \sin^2(\phi)}}$ is the prime vertical radius of curvature (m), and (6.22)

a_e, b_e are the semi-major and semi-minor axes of the earth ellipsoid of rotation (m).

GPS is based on the WGS-84 reference ellipsoid. The vector of misclosures is formed by using the equation

$$\mathbf{w} = \rho + (-CdT) - P, \tag{6.23}$$

where ρ is the geometric range computed using Equation 6.4 and the approximate receiver coordinates.

Note the treatment of the clock offset in Equation 6.23 due to solving for *-CdT*. The observation variance-covariance matrix will be a diagonal matrix with the pseudorange variance on the diagonal.

6.1.2 *Code Phase Observable*

A pseudorange is obtained using the code phase observable and an approximate position. GPS receivers either provide the pseudorange, or the raw code phase measurements. The Trimble MobileGPS receiver provides raw code phase measurements, so the pseudoranges must be generated, or manufactured in software. A description of the code phase measurement and the procedure to manufacture a pseudorange are given in this section [Trimble, 1994b].

GPS satellites superimpose a pseudorandom noise (PRN) code on the broadcast carrier waves. Recall that the Trimble MobileGPS receiver observes the phase of the C/A-code on the L1 carrier. The C/A-code is composed of 1 023 bits superimposed on the carrier at a chipping rate of 1.023 Mbps, therefore, the code repeats every one millisecond. This code is generated in the receiver and correlated with the broadcast code. The code phase is the shift required to match the two codes together. This measurement is either expressed in time or phase of the code.

Typically, a GPS satellite is between 20 000 and 25 000 kms away from the receiver. These ranges translate into times of roughly 65 to 85 ms, hence there is an unknown number of full PRN code lengths between the satellite and the receiver. This integer ambiguity is easily determined given approximate receiver coordinates. The coordinates must only be good to half the wavelength, or about 150 km, to solve for this ambiguity. The procedure for this is to compute a satellite position and determine the geometric range from the receiver to the satellite. The integer portion of this computed range should be the ambiguous number of code lengths. The pseudorange is then manufactured by adding the observed code phase to the integer ambiguity.

Some GPS receivers (including the Trimble MobileGPS) provide code measurements as they are made. The time stamp of the measurement is given as part of the observation. While tracking satellites, these measurements come continuously at a rate of approximately one to each satellite per second. The measurements will not all have the same time stamp. In order to use multiple measurements in a solution, they must be synchronized to a common time. This is done using the Doppler shift observable. Most GPS receivers do this internally and provide an epoch of observations at a common time stamp. The raw observations from the Trimble MobileGPS have to be synchronized.

If the Doppler measurement ($\dot{\Phi}$) is expressed in hertz, a range rate ($\dot{P}$) can be computed by multiplying by the wavelength (λ) of the carrier using

$$\dot{P} = \dot{\Phi} \cdot \lambda, \tag{6.24}$$

where $\lambda \cong 19.0294$ cm for L1.

The range rate is the rate of change of the geometrical (and pseudo) range. Pseudorange measurements can be synchronized to a common time stamp by adding the product of the range rate and the time difference (δt) between the measurement time and the epoch time using

$$\text{new } P = \text{old } P + \delta t \cdot \dot{P}. \tag{6.25}$$

There is no appreciable loss in accuracy when this is done over short periods of time (less than half a second). Care must be taken in the sign of the correction; the definition of positive Doppler shift varies from receiver to receiver.

6.1.3 *Doppler Observable*

The Doppler shift used to synchronize the pseudoranges can also be used as an observable in a GPS solution. The Doppler, or phase rate, observation is provided by many of the low-cost GPS receivers, including the Trimble MobileGPS. Due to the relative motion between the satellite and the receiver, there is an apparent shift in the frequency of the signal. This shift is proportional to the relative radial velocity between the satellite and the receiver. As was shown in Equation 6.24, the Doppler shift can be converted into a range rate. The range rate observation equation is as follows:

$$\dot{P} = \dot{\rho} + (\dot{dt} - \dot{dT}) \cdot C - \dot{d}_{ion} + \dot{d}_{trop} + \dot{d}_{\rho} + \varepsilon_{\dot{P}}, \tag{6.26}$$

where $\dot{P}$ is the range rate (m/s), and

$\varepsilon_{\dot{P}}$ is the range rate measurement noise (m/s).

Each of the remaining terms is a time derivative of the corresponding term in the pseudorange equation. Doppler observables are not required to compute a GPS position solution, however, they are very useful in determining the velocity components in kinematic applications such as vehicle navigation. PortaNav makes use of the Doppler measurements in the Kalman filter solution.

The form of the design matrix for the Doppler observation model is as follows:

$$\mathbf{A} = \begin{bmatrix} \frac{\partial \dot{P}_1}{\partial \phi} & \frac{\partial \dot{P}_1}{\partial \lambda} & \frac{\partial \dot{P}_1}{\partial h} & \frac{\partial \dot{P}_1}{\partial v_n} & \frac{\partial \dot{P}_1}{\partial v_e} & \frac{\partial \dot{P}_1}{\partial v_h} & \frac{\partial \dot{P}_1}{\partial C\dot{d}T} & \frac{\partial \dot{P}_1}{\partial C\dot{d}T} \\ \frac{\partial \dot{P}_2}{\partial \phi} & \frac{\partial \dot{P}_2}{\partial \lambda} & \frac{\partial \dot{P}_2}{\partial h} & \frac{\partial \dot{P}_2}{\partial v_n} & \frac{\partial \dot{P}_2}{\partial v_e} & \frac{\partial \dot{P}_2}{\partial v_h} & \frac{\partial \dot{P}_1}{\partial C\dot{d}T} & \frac{\partial \dot{P}_2}{\partial C\dot{d}T} \\ \cdots & \cdots & \cdots & \cdots & \cdots & \cdots & \cdots & \cdots \\ \frac{\partial \dot{P}_n}{\partial \phi} & \frac{\partial \dot{P}_n}{\partial \lambda} & \frac{\partial \dot{P}_n}{\partial h} & \frac{\partial \dot{P}_n}{\partial v_n} & \frac{\partial \dot{P}_n}{\partial v_e} & \frac{\partial \dot{P}_n}{\partial v_h} & \frac{\partial \dot{P}_1}{\partial C\dot{d}T} & \frac{\partial \dot{P}_n}{\partial C\dot{d}T} \end{bmatrix}, \tag{6.27}$$

where

$$\frac{\partial \dot{P}_i}{\partial \phi} = \frac{\partial \dot{P}_i}{\partial x} \cdot \frac{\partial x}{\partial \phi} + \frac{\partial \dot{P}_i}{\partial y} \cdot \frac{\partial y}{\partial \phi} + \frac{\partial \dot{P}_i}{\partial z} \cdot \frac{\partial z}{\partial \phi}, \tag{6.28}$$

$$\frac{\partial \dot{P}_i}{\partial \lambda} = \frac{\partial \dot{P}_i}{\partial x} \cdot \frac{\partial x}{\partial \lambda} + \frac{\partial \dot{P}_i}{\partial y} \cdot \frac{\partial y}{\partial \lambda}, \tag{6.29}$$

$$\frac{\partial \dot{P}_i}{\partial h} = \frac{\partial \dot{P}_i}{\partial x} \cdot \frac{\partial x}{\partial h} + \frac{\partial \dot{P}_i}{\partial y} \cdot \frac{\partial y}{\partial h} + \frac{\partial \dot{P}_i}{\partial z} \cdot \frac{\partial z}{\partial h}, \tag{6.30}$$

$$\frac{\partial \dot{P}_i}{\partial v_n} = \left[\frac{\partial P_i}{\partial x} \cdot \frac{\partial x}{\partial \phi} + \frac{\partial P_i}{\partial y} \cdot \frac{\partial y}{\partial \phi} + \frac{\partial P_i}{\partial z} \cdot \frac{\partial z}{\partial \phi} \right] \cdot \frac{1}{N+h}, \tag{6.31}$$

$$\frac{\partial \dot{P}_i}{\partial v_e} = \left[\frac{\partial P_i}{\partial x} \cdot \frac{\partial x}{\partial \lambda} + \frac{\partial P_i}{\partial y} \cdot \frac{\partial y}{\partial \lambda} \right] \cdot \frac{1}{Re \cdot \cos(\phi)}, \tag{6.32}$$

$$\frac{\partial \dot{P}_i}{\partial v_n} = \frac{\partial P_i}{\partial x} \cdot \frac{\partial x}{\partial h} + \frac{\partial P_i}{\partial y} \cdot \frac{\partial y}{\partial h} + \frac{\partial P_i}{\partial z} \cdot \frac{\partial z}{\partial h}, \tag{6.33}$$

$$\frac{\partial \dot{P}_i}{\partial C\dot{d}T} = 0, \text{ and} \tag{6.34}$$

$$\frac{\partial \dot{P}_i}{\partial C\dot{d}T} = 1. \tag{6.35}$$

The geodetic partial derivatives in the above equations are listed in Equations 6.13 to 6.20. The equation for the range rate between a satellite and the receiver expressed in three dimensional Cartesian coordinate space is

$$\dot{P} = \frac{1}{\rho} \cdot [(X-x) \cdot (v_X - v_x) + (Y-y) \cdot (v_Y - v_y) + (Z-z) \cdot (v_Z - v_z)], \tag{6.36}$$

where v_X, v_Y, v_Z are the known satellite velocities (m/s), and

v_x, v_y, v_z are the unknown receiver velocities (m/s).

Before presenting the Cartesian partial derivates for the Doppler model, the following terms are defined for convenience:

$$\Delta x = X - x, \tag{6.37}$$

$$\Delta y = Y - y, \tag{6.38}$$

$$\Delta z = Z - z, \tag{6.39}$$

$$\Delta v_y = v_Y - v_y, \tag{6.40}$$

$$\Delta v_z = v_Z - v_z, \tag{6.41}$$

$$\Delta v_x = v_X - v_x, \tag{6.42}$$

$$v_x = \cos(\lambda) \cdot \sin(\phi) \cdot v_n - \sin(\lambda) \cdot v_e - \cos(\lambda) \cdot \cos(\phi) \cdot v_h, \tag{6.43}$$

$$v_y = -\sin(\lambda) \cdot \sin(\phi) \cdot v_n + \cos(\lambda) \cdot \cos(\phi) \cdot v_e + \sin(\lambda) \cdot \cos(\phi) \cdot v_h, \text{ and} \tag{6.44}$$

$$v_z = \cos(\phi) \cdot v_n + \sin(\phi) \cdot v_h, \tag{6.45}$$

where v_n, v_e, v_h are the local geodetic components of the receiver velocity.

Now, the Cartesian partial derivatives are as follows:

$$\frac{\partial \dot{P}}{\partial x} = -\frac{\Delta v_x}{\rho} + \frac{(\Delta x)^2 \cdot \Delta v_x}{\rho^3} + \frac{\Delta x \cdot \Delta y \cdot \Delta v_y}{\rho^3} + \frac{\Delta x \cdot \Delta z \cdot \Delta v_z}{\rho^3}, \tag{6.46}$$

$$\frac{\partial \dot{P}}{\partial y} = -\frac{\Delta v_y}{\rho} + \frac{\Delta y \cdot \Delta x \cdot \Delta v_x}{\rho^3} + \frac{(\Delta y)^2 \cdot \Delta v_y}{\rho^3} + \frac{\Delta y \cdot \Delta z \cdot \Delta v_z}{\rho^3}, \tag{6.47}$$

$$\frac{\partial \dot{P}}{\partial z} = -\frac{\Delta v_z}{\rho} + \frac{\Delta z \cdot \Delta x \cdot \Delta v_x}{\rho^3} + \frac{\Delta z \cdot \Delta y \cdot \Delta v_y}{\rho^3} + \frac{(\Delta z)^2 \cdot \Delta v_z}{\rho^3}, \tag{6.48}$$

$$\frac{\partial \dot{P}}{\partial v_x} = \frac{\partial P}{\partial x} = \frac{-(X-x)}{\rho}, \tag{6.49}$$

$$\frac{\partial \dot{P}}{\partial v_y} = \frac{\partial P}{\partial y} = \frac{-(Y-y)}{\rho}, \text{ and} \tag{6.50}$$

$$\frac{\partial \dot{P}}{\partial v_z} = \frac{\partial P}{\partial z} = \frac{-(Z-z)}{\rho}. \tag{6.51}$$

The misclosure vector is formed by using the following equation:

$$\mathbf{w} = \dot{\rho} + (-C\dot{d}T) - \dot{P}, \tag{6.52}$$

where $\dot{\rho}$ is the range rate computed using Equation 6.36 and the approximate receiver coordinates and velocities.

Again, the treatment of the clock drift rate is due to solving for $(-C\dot{d}T)$. As was the case with the pseudorange observable, the variance-covariance matrix of the Doppler observations is diagonal with the Doppler variances on the diagonal. The Doppler observable from the Trimble MobileGPS receiver has a standard deviation of about two tenths of a metre per second.

6.2 Positioning Solutions

There are various ways that the GPS observables can be used to compute a position solution. Three common GPS positioning methods are the best DOP unique solution, the least squares adjustment solution, and Kalman filtering. Each of these will be outlined in this section, and each of these is computed and/or logged in PortaNav for comparison and analysis (see Chapter 9).

6.2.1 *Unique Solution*

A solution can be computed with an epoch of at least four pseudoranges. With only four pseudoranges, the solution is unique. If five or more pseudoranges are available, a least-squares adjustment can be done to compute the best fit solution. Some receivers use a unique solution even when redundant observations are available. The receiver picks the best four satellites based on some criterion, usually a dilution of precision (DOP) measure, and computes a unique solution disregarding the other measurements. The Trimble MobileGPS uses this best DOP method for computing instantaneous position fixes. PortaNav logs these fixes for comparison with the other solutions.

A DOP is a measure of the geometric strength of a constellation of visible satellites. The DOP factor is a multiplier applied to the measurement error to determine the overall accuracy of the position fix using

$$\sigma = \sigma_o \cdot \mathrm{DOP}, \tag{6.53}$$

where σ is the solution accuracy, and

σ_o is the observational accuracy.

Various DOP measures are used, namely geometric (GDOP), position (PDOP), time (TDOP), horizontal (HDOP), and vertical (VDOP). A low DOP value represents good geometry, and is realized when satellites are spread out around the horizon, with one at the zenith. DOPs are computed from the inverse of the normal equation matrix ($\mathbf{N}^{-1}$) (see Equation 6.64) in the following manner:

$$\mathbf{N}^{-1} = \begin{bmatrix} \sigma_x^2 & \sigma_{xy} & \sigma_{xz} & \sigma_{xt} \\ \sigma_{yx} & \sigma_y^2 & \sigma_{yz} & \sigma_{yt} \\ \sigma_{zx} & \sigma_{zy} & \sigma_z^2 & \sigma_{zt} \\ \sigma_{tx} & \sigma_{ty} & \sigma_{tz} & \sigma_t^2 \end{bmatrix}, \text{ or } \mathbf{N}^{-1} = \begin{bmatrix} \sigma_n^2 & \sigma_{ne} & \sigma_{nh} & \sigma_{nt} \\ \sigma_{en} & \sigma_e^2 & \sigma_{eh} & \sigma_{et} \\ \sigma_{hn} & \sigma_{he} & \sigma_h^2 & \sigma_{ht} \\ \sigma_{tn} & \sigma_{te} & \sigma_{th} & \sigma_t^2 \end{bmatrix}, \tag{6.54}$$

$$\text{GDOP} = \sqrt{\sigma_x^2 + \sigma_y^2 + \sigma_z^2 + \sigma_t^2 \cdot C^2} = \sqrt{\sigma_n^2 + \sigma_e^2 + \sigma_h^2 + \sigma_t^2 \cdot C^2}, \tag{6.55}$$

$$\text{PDOP} = \sqrt{\sigma_x^2 + \sigma_y^2 + \sigma_z^2} = \sqrt{\sigma_n^2 + \sigma_e^2 + \sigma_h^2}, \tag{6.56}$$

$$\text{TDOP} = \sigma_t, \tag{6.57}$$

$$\text{HDOP} = \sqrt{\sigma_n^2 + \sigma_e^2}, \text{ and} \tag{6.58}$$

$$\text{VDOP} = \sigma_h. \tag{6.59}$$

Note that HDOP and VDOP are computed from variances in the local geodetic coordinate frame [Leick, 1995, pp. 254].

A receiver that computes a unique solution based on a best DOP criterion will monitor all of the satellites visible and then select the ones that yield the best DOP. When one satellite drops out of view, it is replaced by another if available. The advantage to the best DOP solution is a relatively stable constellation in areas where satellites are not coming in and going out of view. The disadvantage is the possibility of including blunders (bad measurements) in the solution.

6.2.2 *Least Squares Solution*

When four or more observations are available, a least squares adjustment can be performed to compute a best fit solution based on all of the information available. With a

least squares adjustment, each measurement has a residual that can be examined to see if it was a blunder. The procedure for a least squares adjustment with blunder detection is described in this section.

As the name implies, a least squares adjustment is a method of computing a solution that minimizes the weighted sum square of the residuals. Pseudorange equations are parametric in that the observable is expressed in terms of known and unknown quantities. The formulation for a parametric least squares adjustment is as follows:

$$\hat{\mathbf{l}} = f(\hat{\mathbf{x}}),\ \mathbf{C}_l, \text{ and} \tag{6.60}$$

$$\hat{\mathbf{r}} = \mathbf{A}\hat{\boldsymbol{\delta}} + \mathbf{w}, \tag{6.61}$$

where $\hat{\mathbf{x}}$ is the vector of adjusted unknowns (u x 1),

$\hat{\mathbf{l}}$ is the vector of adjusted observations (n x 1),

$\mathbf{C}_l$ is the variance-covariance matrix of the observations (n x n),

$\mathbf{A}$ is the design matrix (n x u),

$\hat{\boldsymbol{\delta}}$ is the vector of corrections to the unknowns (u x 1),

$\mathbf{w}$ is the vector of misclosures (n x 1),

n is the number of observations in the adjustment, and

u is the number of unknowns in the adjustment.

The model in Equation 6.60 is linearized in Equation 6.61. A (^) above a vector denotes an adjusted quantity. Bolded letters represent either vectors or matrices, the dimensions of which are given in brackets. The solution for the parametric model is obtained as follows:

$$\hat{\mathbf{x}} = \mathbf{x}^o + \hat{\boldsymbol{\delta}}, \tag{6.62}$$

$$\hat{\boldsymbol{\delta}} = -\mathbf{N}^{-1}\mathbf{u}, \tag{6.63}$$

$$\mathbf{N} = \mathbf{A}^T\mathbf{C}_l^{-1}\mathbf{A}, \tag{6.64}$$

$$\mathbf{u} = \mathbf{A}^T\mathbf{C}_l^{-1}\mathbf{w}, \text{ and} \tag{6.65}$$

$$\mathbf{w} = f(\mathbf{x}^o) - \mathbf{l}^{obs}, \tag{6.66}$$

where $\hat{\mathbf{x}}$ is the vector of adjusted unknowns (u x 1),

$\mathbf{x}^o$ is the vector of approximate unknowns (u x 1),

$\mathbf{N}$ is the normal equation matrix (u x u),

$\mathbf{u}$ is the normal equation vector (u x 1), and

$\mathbf{l}^{obs}$ is the vector of observed observations (n x 1).

The design matrix A has previously been defined for both pseudorange and Doppler observations (see Equations 6.5 and 6.27). The residuals of the observations and the variance-covariance matrix of the unknowns and the residuals are important for accuracy assessment and blunder detection. These quantities are computed as follows:

$$\hat{\mathbf{r}} = \mathbf{A}\hat{\boldsymbol{\delta}} + \mathbf{w} = \hat{\mathbf{l}} - \mathbf{l}^{obs}, \tag{6.67}$$

$$\hat{\mathbf{l}} = f(\hat{\mathbf{x}}) = \mathbf{l}^{obs} + \hat{\mathbf{r}}, \tag{6.68}$$

$$\mathbf{C}_{\hat{x}} = \mathbf{N}^{-1}, \text{ and} \tag{6.69}$$

$$\mathbf{C}_{\hat{r}} = \mathbf{C}_l - \mathbf{A}\mathbf{C}_{\hat{x}}\mathbf{A}^T, \tag{6.70}$$

where $\hat{\mathbf{r}}$ is the vector of residuals (n x 1),

$\mathbf{C}_{\hat{x}}$ is the variance-covariance matrix of the adjusted unknowns (u x u), and

$\mathbf{C}_{\hat{r}}$ is the variance-covariance matrix of the residuals (n x n).

Note that the residuals can be computed directly or by using the adjusted observations as computed from the adjusted unknowns in the model. Derivations of these least squares equations can be found in Krakiwsky [1992b] and Krakiwsky and Abousalem [1995].

For non-linear models, such as the pseudorange (6.3) and Doppler equations (6.26), iteration is required. This is because the model is linearized by using a Taylor series expansion around an approximate solution. Only the first order terms are used in the solution; the higher order terms are truncated. Iteration is performed by first using an

approximate solution as the expansion point. The corrections ($\hat{\delta}$) are applied, and the solution becomes the new approximate point of expansion. This procedure is repeated until successive corrections are sufficiently small. Usually two to four iterations are required for the pseudorange model. Once the solution is obtained, the variance-covariance matrices of the solution and the residuals should be computed. Residual testing and error analysis is then performed.

Each of the residuals is first examined for remaining millisecond offsets. If an incorrect ambiguity was used to manufacture the pseudorange, the residual will be about 299 792 m (one millisecond). The pseudoranges should be corrected for these offsets so that correct pseudoranges can be passed on to the Kalman filter. Any remaining residual amount can then be tested to detect blunders. If one of the measurements was bad, the residual will be much larger than the rest in a statistical sense. Of course, if only four satellites are used, the residuals will all be near zero and blunders go undetected (the millisecond offsets still show up). Using undetected blunders can cause large shifts in the computed solution.

After a redundant adjustment has been performed, the residuals are standardized using

$$\tilde{r}_i = \frac{\hat{r}_i}{\sigma_{\hat{r}_i}}, \tag{6.71}$$

where $\tilde{r}_i$ is the standardized residual, and

$\sigma_{\hat{r}_i}$ is the standard deviation of the adjusted residual.

For random measurements, the expected value of the residuals is zero, the standard deviation of the standardized residual is one, and the residuals should be distributed normally. A confidence interval can be constructed wherein all of the standardized residuals should lie. The following in-context interval accounts for testing all n residuals [Vanicek and Krakiwsky, 1982]:

$$\left[-\xi_{n(0,1),1-\frac{\alpha}{2\cdot n}} < \tilde{r}_i < \xi_{n(0,1),1-\frac{\alpha}{2\cdot n}}\right], \tag{6.72}$$

where α is the significance level of the test,

$1-\alpha$ is the confidence level of the test, and

$\xi_{*(0,1)}$ is the abscissa value of the standard normal for the given confidence.

Residuals that fall outside this confidence interval should be rejected and a new solution should be computed without the corresponding observation. Blunder detection and removal can go a long way towards improving the accuracy of the solution. In PortaNav, a confidence level of 95% was used for blunder detection.

Error analysis of the computed solution is based on the variance-covariance matrix of the adjusted parameters ($\mathbf{C}_x$). The equations for DOP measures were given in Equations 6.55 to 6.59. DOP measures alone are not sufficient for representing the errors in a GPS position fix. Due to the varying geometry, errors can be larger in certain directions and smaller in others. A confidence ellipse can be constructed from the variances and covariance of the horizontal components of the solution. This confidence ellipse shows the error in each direction (Figure 6.1). The ellipse is represented by the semi-major axis (a), the semi-minor axis (b), and the orientation of the semi-major axis (θ) with respect to north as follows [Krakiwsky and Abousalem, 1995]:

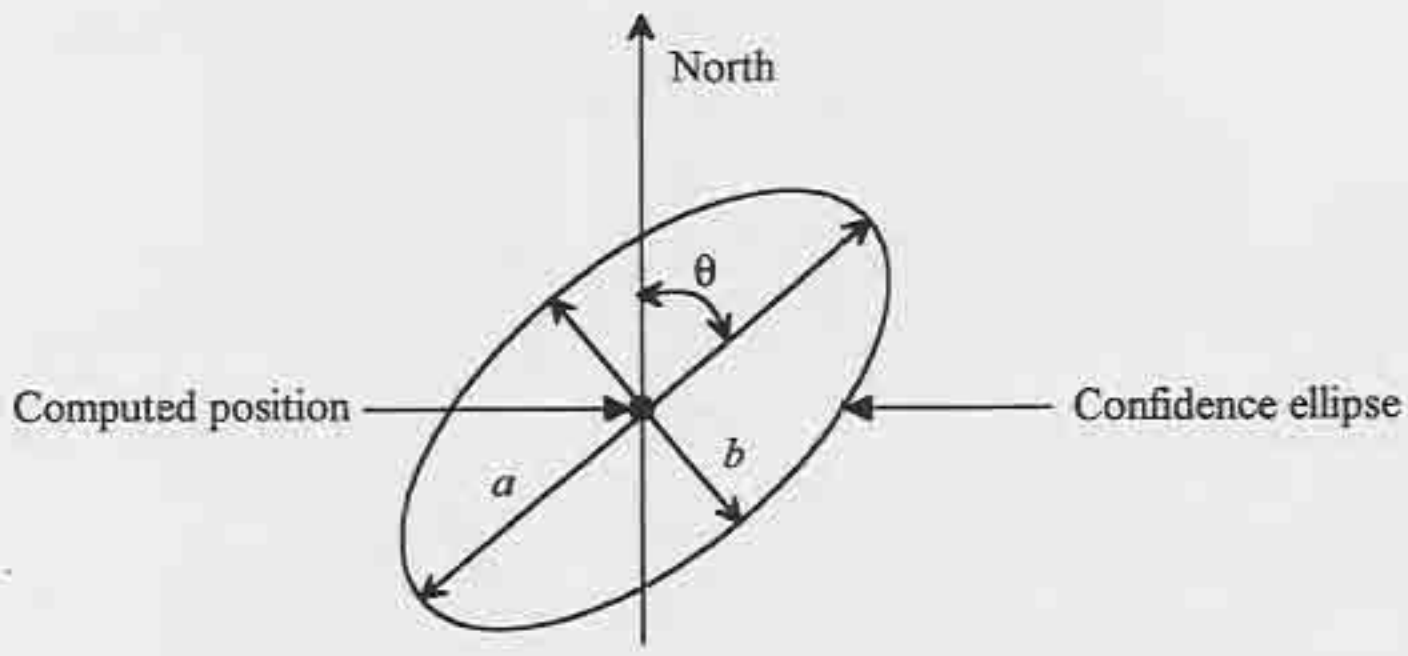

Figure 6.1 Confidence Ellipse for Computed Position

$$a = \left[\frac{1}{2}(\sigma_e^2 + \sigma_n^2) + \left(\frac{1}{4}(\sigma_e^2 - \sigma_n^2) + \sigma_{en}^2 \right)^{\frac{1}{2}} \right]^{\frac{1}{2}}, \tag{6.73}$$

$$b = \left[\frac{1}{2}(\sigma_e^2 + \sigma_n^2) - \left(\frac{1}{4}(\sigma_e^2 - \sigma_n^2) + \sigma_{en}^2 \right)^{\frac{1}{2}} \right]^{\frac{1}{2}}, \text{ and} \tag{6.74}$$

$$\theta = \frac{\pi}{2} - \frac{1}{2}\tan^{-1}\left(\frac{2 \cdot \sigma_{en}}{\sigma_e^2 - \sigma_n^2} \right). \tag{6.75}$$

This two dimensional confidence region represents the area of certainty at the one sigma (39% in 2D) confidence level. The semi-major and semi-minor axes can be scaled to increase the confidence level of the ellipse. In PortaNav, a 95% confidence ellipse is computed using a scale factor of 2.45. It can then be said with 95% certainty that the true position lies within the computed confidence region. This is used for determining the possible roads of travel.

In PortaNav, a least squares solution is computed for two reasons: to remove the millisecond offsets in the pseudorange for an initial solution, and to detect and remove blunders. An initial least squares solution is required in order to start the Kalman filter. For testing purposes, the least squares solution is computed for every epoch and logged to a data file for comparison to the other solutions. Once the filter is running, it can be used to detect and remove blunders [Abousalem, 1993]. The least squares method, however, was used in PortaNav for simplicity.

6.2.3 *Kalman Filtering*

An instantaneous least squares fix is an excellent method for blending all of the available pseudorange observations into one solution, thus capitalizing on redundancy if more than four satellites are visible. A least squares formulation does not take into account the fact that two sequential position fixes are correlated. In the case of a moving vehicle, the correlation follows from the dynamics of the vehicle. A Kalman filter [Kalman, 1960] combines the measurement models with a dynamic model to compute a series of position fixes that are spatially correlated. The position of the vehicle at each successive epoch

depends on the computed position at the previous epoch and on the current set of observations.

Kalman filters have been used extensively in vehicle navigation for several years. Typically, a Kalman filter is used to process observations from one or more positioning sources. In the case of land navigation, auxiliary sensors (e.g. odometer, compass, etc.) can be integrated with GPS through the use of a Kalman filter. In PortaNav, a centralized discrete Kalman filter with a constant velocity dynamics model is used to integrate GPS measurements with observational information derived from a digital road map, and to compute a smooth trajectory. The procedure used for integrating the map data will be outlined in Section 6.3. This section reviews the basic Kalman filter equations, derivations of which can be found in Kalman [1960], Morrison [1969], and Krakiwsky [1992b].

The basic Kalman filter algorithm solves the following system of equations:

$$f_k\left(\hat{\mathbf{x}}_k, \hat{\mathbf{l}}_k\right) = 0,\ t_k, \tag{6.76}$$

$$f_{k+1}\left(\hat{\mathbf{x}}_{k+1}, \hat{\mathbf{l}}_{k+1}\right) = 0,\ t_{k+1}, \text{ and} \tag{6.77}$$

$$g\left(\hat{\mathbf{x}}_k, \hat{\mathbf{x}}_{k+1}, \hat{\mathbf{y}}_{k,k+1}, t\right) = 0. \tag{6.78}$$

The first two equations are measurement models at two successive epochs t_k and t_{k+1}. The measurement models are precisely the same as in the least squares formulations. The third equation represents the dynamics model of the system. Process noise ($\hat{\mathbf{y}}_{k,k+1}$) and vehicle dynamics are introduced into the system via the dynamics model (g).

As in least squares, the unknown parameters of the model are not solved for directly. Corrections to the estimated unknown parameters are computed, then applied to the estimated parameters. In Kalman filtering, the unknown parameters are chosen to model the behaviour of the system, and are grouped into a state vector ($\hat{\mathbf{x}}$). In GPS it is common to model the position states (ϕ, λ, h), the velocity states (v_n, v_e, v_h), the receiver clock offset (CdT), and the receiver clock drift rate ($\dot{C}dT$). In situations where velocity

measurements are available, such as is the case with PortaNav, an eight state vector has been used quite successfully. The error state vector then takes the form

$$\hat{\boldsymbol{\delta}} = \left(\delta\phi, \delta\lambda, \delta h, \delta v_n, \delta v_e, \delta v_h, \delta CdT, \delta \dot{C}dT \right). \tag{6.79}$$

This state vector is not a complete parameterization of the problem at hand. In single point GPS, the solution is affected by SA, which is not random. Normally, this would cause problems in a Kalman filter unless parameters are introduced to model the bias effect of SA. In PortaNav, the filter parameters were chosen so that the filter would be lax enough to absorb the bulk of the effects of SA. The results presented in Chapter 9 demonstrate that this was effective.

The solution algorithm takes on a recursive form as illustrated in Figure 6.2. At each epoch, the vehicle's dynamics and the state vector ($\hat{\boldsymbol{\delta}}_k^{(-)}$) at time t_k, are used to predict the state vector ($\hat{\boldsymbol{\delta}}_{k+1}^{(-)}$) of the vehicle at time t_{k+1}. The associated variance-covariance matrix of the state vector ($\mathbf{C}_{\hat{\delta}_k}^{(-)}$) at time t_k is also projected to time t_{k+1} to arrive at the predicted variance-covariance matrix ($\mathbf{C}_{\hat{\delta}_{k+1}}^{(-)}$). All of the measurements ($\mathbf{l}_{k+1}^{obs}$) at time t_{k+1} are then

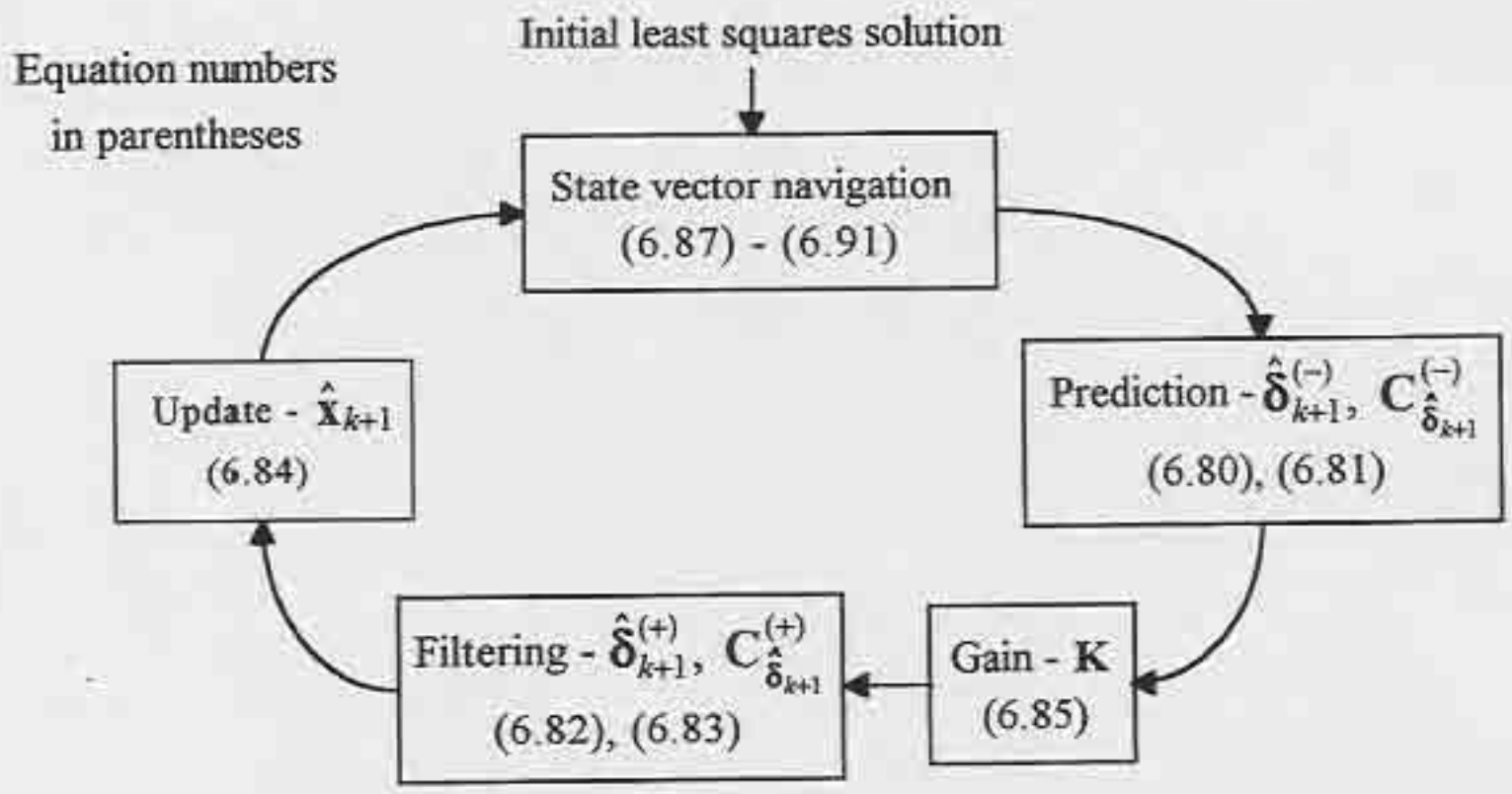

Figure 6.2 Recursive Kalman Filtering Algorithm

used to filter the predicted solution and the predicted variance-covariance matrix. The filtered error states ($\hat{\boldsymbol{\delta}}_{k+1}^{(+)}$) are then used to update the vehicle states ($\hat{\mathbf{x}}_{k+1}^{(+)}$) for time t_{k+1}. This process is then repeated for the next epoch. The subscripts of these vectors and matrices refer to the time index. The superscripts indicate whether the current set of measurements (at time t_{k+1}) have been incorporated ($^{(+)}$), or not ($^{(-)}$). The Kalman filter solution for the combination of models in Equations 6.76 to 6.78 proceeds as follows:

Prediction: $$\hat{\boldsymbol{\delta}}_{k+1}^{(-)} = \boldsymbol{\Phi}_{k,k+1}\,\hat{\boldsymbol{\delta}}_{k}^{(-)}, \text{ and} \tag{6.80}$$

$$\mathbf{C}_{\hat{\boldsymbol{\delta}}_{k+1}}^{(-)} = \boldsymbol{\Phi}_{k,k+1}\left(\mathbf{C}_{\hat{\boldsymbol{\delta}}_{k}}^{(-)}\right)^{-1}\boldsymbol{\Phi}_{k,k+1}^{\mathrm{T}} + \mathbf{C}_{k,k+1}, \tag{6.81}$$

Filtering: $$\hat{\boldsymbol{\delta}}_{k+1}^{(+)} = \hat{\boldsymbol{\delta}}_{k+1}^{(-)} - \mathbf{K}\left(\mathbf{A}_{k+1}\,\hat{\boldsymbol{\delta}}_{k+1}^{(-)} + \mathbf{w}_{k+1}\right), \text{ and} \tag{6.82}$$

$$\mathbf{C}_{\hat{\boldsymbol{\delta}}_{k+1}}^{(+)} = \mathbf{C}_{\hat{\boldsymbol{\delta}}_{k+1}}^{(-)} - \mathbf{K}\mathbf{A}_{k+1}\,\mathbf{C}_{\hat{\boldsymbol{\delta}}_{k+1}}^{(-)}, \tag{6.83}$$

Update: $$\hat{\mathbf{x}}_{k+1}^{(+)} = \mathbf{x}_{k+1}^{o} + \hat{\boldsymbol{\delta}}_{k+1}^{(+)}, \tag{6.84}$$

where $$\mathbf{K} = \mathbf{C}_{\hat{\boldsymbol{\delta}}_{k+1}}^{(-)}\mathbf{A}_{k+1}^{\mathrm{T}}\left[\mathbf{M}_{k+1} + \mathbf{A}_{k+1}\,\mathbf{C}_{\hat{\boldsymbol{\delta}}_{k+1}}^{(-)}\mathbf{A}_{k+1}^{\mathrm{T}}\right]^{-1}, \tag{6.85}$$

$$\mathbf{M}_{k+1} = \mathbf{B}_{k+1}\mathbf{C}_{\mathbf{l}_{k+1}}\mathbf{B}_{k+1}^{\mathrm{T}}, \tag{6.86}$$

$\boldsymbol{\Phi}_{k,k+1}$ is the transition matrix (u x u),

$\mathbf{C}_{k,k+1}$ is the process noise (u x u),

$\mathbf{K}$ is the Kalman gain matrix (u x n),

$\mathbf{B}_{k+1}$ is the second design matrix (m x n), and

$\hat{\mathbf{x}}_{k+1}^{o}$ is the vector of estimated states (u x 1).

All of the other parameters are as defined previously for the least squares model. As the filter is solving for errors rather than corrections, the misclosures as computed in Equations 6.23 and 6.52 must be negated for use in the filter. The **M** and **B** matrices refer to an implicit model. For the parametric formulation of the pseudorange and Doppler observations, **B** is an identity matrix, so **M** becomes $\mathbf{C}_{\mathbf{l}}$. The dimension m is the number of equations in the implicit model, which is equal to n for the parametric case. All of the

$\mathbf{C}_{\hat{\delta}}$ matrices have a dimension of (u x u), and all of the $\hat{\boldsymbol{\delta}}$ and $\mathbf{x}$ vectors are of the dimension (u x 1).

In land vehicle navigation, a constant velocity dynamics model has proven to be suitable [Schwarz et al., 1989; Brown and Hwang, 1992]. The following navigation equations are used to predict the position at the new epoch t_{k+1}:

$$\phi^{\circ}_{k+1} = \hat{\phi}_k + \frac{\hat{v}_{n_k} \cdot \Delta t}{R_e}, \tag{6.87}$$

$$\lambda^{\circ}_{k+1} = \hat{\lambda}_k + \frac{\hat{v}_{e_k} \cdot \Delta t}{R_e \cdot \cos(\hat{\phi}_k)}, \tag{6.88}$$

$$h^{\circ}_{k+1} = \hat{h}_k + \hat{v}_{h_k} \cdot \Delta t, \text{ and} \tag{6.89}$$

$$CdT^{\circ}_{k+1} = \hat{CdT}_k + \dot{CdT}_k \cdot \Delta t, \tag{6.90}$$

where $$\Delta t = t_{k+1} - t_k. \tag{6.91}$$

Again, the (^) represents an adjusted quantity and the (°) represents an estimated quantity. These estimated states are used in the evaluation of the design matrices.

In land vehicle navigation, a first order Gauss-Markov process is commonly used to characterize the system dynamics noise [Wong, 1988; Cannon, 1991]. The Gauss-Markov process is based on the spectral densities (q) and the correlation times ($\frac{1}{\beta}$) of the system dynamics. The relationship between the variance of the process noise (σ^2), the spectral density, and the correlation time is

$$q = 2 \cdot \beta \cdot \sigma^2. \tag{6.92}$$

The non-zero elements of the (8 x 8) transition matrix [Gao, 1992] are

$$\mathbf{\Phi}_{11} = \mathbf{\Phi}_{22} = \mathbf{\Phi}_{33} = \mathbf{\Phi}_{77} = 1, \tag{6.93}$$

$$\mathbf{\Phi}_{44} = e^{-\beta_{v_n} \cdot \Delta t}, \tag{6.94}$$

$$\mathbf{\Phi}_{55} = e^{-\beta_{v_e} \cdot \Delta t}, \tag{6.95}$$

$$\mathbf{\Phi}_{66} = e^{-\beta_{v_h}\cdot\Delta t}, \tag{6.96}$$

$$\mathbf{\Phi}_{88} = e^{-\beta_{C\dot{d}T}\cdot\Delta t}, \tag{6.97}$$

$$\mathbf{\Phi}_{14} = \frac{1-e^{-\beta_{v_n}\cdot\Delta t}}{\beta_{v_n}\cdot R_e}, \tag{6.98}$$

$$\mathbf{\Phi}_{25} = \frac{1-e^{-\beta_{v_e}\cdot\Delta t}}{\beta_{v_e}\cdot R_e\cdot\cos(\phi)}, \tag{6.99}$$

$$\mathbf{\Phi}_{36} = \frac{1-e^{-\beta_{v_h}\cdot\Delta t}}{\beta_{v_h}}, \text{ and} \tag{6.100}$$

$$\mathbf{\Phi}_{78} = \frac{1-e^{-\beta_{C\dot{d}T}\cdot\Delta t}}{\beta_{C\dot{d}T}}. \tag{6.101}$$

The non-zero elements of the variance-covariance matrix of the system noise ($\mathbf{C}_{k,k+1}$) are

$$\mathbf{C}_{11} = \frac{q_{v_n}}{\beta_{v_n}^2}\cdot\left[\Delta t - \frac{2}{\beta_{v_n}}\cdot(1-e^{-\beta_{v_n}\cdot\Delta t}) + \frac{1}{2\cdot\beta_{v_n}}\cdot(1-e^{-2\cdot\beta_{v_n}\cdot\Delta t})\right], \tag{6.102}$$

$$\mathbf{C}_{22} = \frac{q_{v_e}}{\beta_{v_e}^2}\cdot\left[\Delta t - \frac{2}{\beta_{v_e}}\cdot(1-e^{-\beta_{v_e}\cdot\Delta t}) + \frac{1}{2\cdot\beta_{v_e}}\cdot(1-e^{-2\cdot\beta_{v_e}\cdot\Delta t})\right], \tag{6.103}$$

$$\mathbf{C}_{33} = \frac{q_{v_h}}{\beta_{v_h}^2}\cdot\left[\Delta t - \frac{2}{\beta_{v_h}}\cdot(1-e^{-\beta_{v_h}\cdot\Delta t}) + \frac{1}{2\cdot\beta_{v_h}}\cdot(1-e^{-2\cdot\beta_{v_h}\cdot\Delta t})\right], \tag{6.104}$$

$$\mathbf{C}_{44} = \frac{q_{v_n}}{2\cdot\beta_{v_n}}\cdot[1-e^{-2\cdot\beta_{v_n}\cdot\Delta t}], \tag{6.105}$$

$$\mathbf{C}_{55} = \frac{q_{v_e}}{2\cdot\beta_{v_e}}\cdot[1-e^{-2\cdot\beta_{v_e}\cdot\Delta t}], \tag{6.106}$$

$$\mathbf{C}_{66} = \frac{q_{v_h}}{2\cdot\beta_{v_h}}\cdot[1-e^{-2\cdot\beta_{v_h}\cdot\Delta t}], \tag{6.107}$$

$$\mathbf{C}_{77} = \frac{q_{C\dot{d}T}}{\beta_{C\dot{d}T}^2}\cdot\left[\Delta t - \frac{2}{\beta_{C\dot{d}T}}\cdot(1-e^{-\beta_{C\dot{d}T}\cdot\Delta t}) + \frac{1}{2\cdot\beta_{C\dot{d}T}}\cdot(1-e^{-2\cdot\beta_{C\dot{d}T}\cdot\Delta t})\right], \tag{6.108}$$

$$\mathbf{C}_{88} = \frac{q_{C\dot{d}T}}{2\cdot\beta_{C\dot{d}T}}\cdot[1-e^{-2\cdot\beta_{C\dot{d}T}\cdot\Delta t}], \tag{6.109}$$

$$\mathbf{C}_{14} = \mathbf{C}_{41} = \frac{q_{v_n}}{\beta_{v_n}}\cdot\left[\frac{1}{\beta_{v_n}}\cdot(1-e^{-\beta_{v_n}\cdot\Delta t}) - \frac{1}{2\cdot\beta_{v_n}}\cdot(1-e^{-2\cdot\beta_{v_n}\cdot\Delta t})\right], \tag{6.110}$$

$$\mathbf{C}_{25} = \mathbf{C}_{52} = \frac{q_{v_e}}{\beta_{v_e}}\cdot\left[\frac{1}{\beta_{v_e}}\cdot(1-e^{-\beta_{v_e}\cdot\Delta t}) - \frac{1}{2\cdot\beta_{v_e}}\cdot(1-e^{-2\cdot\beta_{v_e}\cdot\Delta t})\right], \tag{6.111}$$

$$\mathbf{C}_{36} = \mathbf{C}_{63} = \frac{q_{v_h}}{\beta_{v_h}}\cdot\left[\frac{1}{\beta_{v_h}}\cdot(1-e^{-\beta_{v_h}\cdot\Delta t}) - \frac{1}{2\cdot\beta_{v_h}}\cdot(1-e^{-2\cdot\beta_{v_h}\cdot\Delta t})\right], \text{ and} \tag{6.112}$$

$$\mathbf{C}_{78} = \mathbf{C}_{87} = \frac{q_{C\dot{d}T}}{\beta_{C\dot{d}T}}\cdot\left[\frac{1}{\beta_{C\dot{d}T}}\cdot(1-e^{-\beta_{C\dot{d}T}\cdot\Delta t}) - \frac{1}{2\cdot\beta_{C\dot{d}T}}\cdot(1-e^{-2\cdot\beta_{C\dot{d}T}\cdot\Delta t})\right]. \tag{6.113}$$

As previously mentioned, both the pseudorange and the Doppler measurement data from the Trimble MobileGPS receiver are used in the Kalman filter in PortaNav. The design matrices presented in Equations 6.5 and 6.27 are used, with one minor change: The design matrix for the pseudoranges is expanded to include columns for the velocities and the clock drift rate. The partial derivatives for these four new columns are all zero.

The two distinct sets of observations are combined in a sequential manner. After the prediction is performed, the pseudorange observations are used to filter the state vector. The state vector filtered by the pseudorange observations becomes the predicted state vector for the Doppler observations. Finally, the Doppler observations are used to filter the state vector. The sequential filtering portion of the procedure is pictured in Figure 6.3. The sequential filtering expressions are as follows, where the numerical superscripts refer to the set of observations being added:

First set: $$\hat{\boldsymbol{\delta}}_{k+1}^{1(+)} = \hat{\boldsymbol{\delta}}_{k+1}^{(-)} - \mathbf{K}^{1}\left(\mathbf{A}_{k+1}^{1}\,\hat{\boldsymbol{\delta}}_{k+1}^{(-)} + \mathbf{w}_{k+1}^{1}\right), \tag{6.114}$$

$$\mathbf{C}_{\hat{\delta}_{k+1}}^{1(+)} = \mathbf{C}_{\hat{\delta}_{k+1}}^{(-)} - \mathbf{K}^{1}\,\mathbf{A}_{k+1}^{1}\,\mathbf{C}_{\hat{\delta}_{k+1}}^{(-)}, \text{ and} \tag{6.115}$$

$$\mathbf{K}^{1} = \mathbf{C}_{\hat{\delta}_{k+1}}^{(-)}\mathbf{A}_{k+1}^{1\mathrm{T}}\left[\mathbf{M}_{k+1}^{1} + \mathbf{A}_{k+1}^{1}\,\mathbf{C}_{\hat{\delta}_{k+1}}^{(-)}\mathbf{A}_{k+1}^{1\mathrm{T}}\right]^{-1}. \tag{6.116}$$

Second set: $$\hat{\boldsymbol{\delta}}_{k+1}^{2(+)} = \hat{\boldsymbol{\delta}}_{k+1}^{1(+)} - \mathbf{K}^{2}\left(\mathbf{A}_{k+1}^{2}\,\hat{\boldsymbol{\delta}}_{k+1}^{1(+)} + \mathbf{w}_{k+1}^{2}\right), \tag{6.117}$$

$$\mathbf{C}_{\hat{\delta}_{k+1}}^{2(+)} = \mathbf{C}_{\hat{\delta}_{k+1}}^{1(+)} - \mathbf{K}^{2}\,\mathbf{A}_{k+1}^{2}\,\mathbf{C}_{\hat{\delta}_{k+1}}^{1(+)}, \text{ and} \tag{6.118}$$

$$\mathbf{K}^{2} = \mathbf{C}_{\hat{\delta}_{k+1}}^{1(+)}\mathbf{A}_{k+1}^{2\mathrm{T}}\left[\mathbf{M}_{k+1}^{2} + \mathbf{A}_{k+1}^{2}\,\mathbf{C}_{\hat{\delta}_{k+1}}^{1(+)}\mathbf{A}_{k+1}^{2\mathrm{T}}\right]^{-1}. \tag{6.119}$$

This procedure is numerically equivalent to combining all of the observations and performing only one update [Abousalem, 1993]. The advantage to the sequential approach is that the effect of each set of measurements can be monitored. The sequential approach also lends itself to the addition of map-derived observations when available as will be seen in Section 6.3.

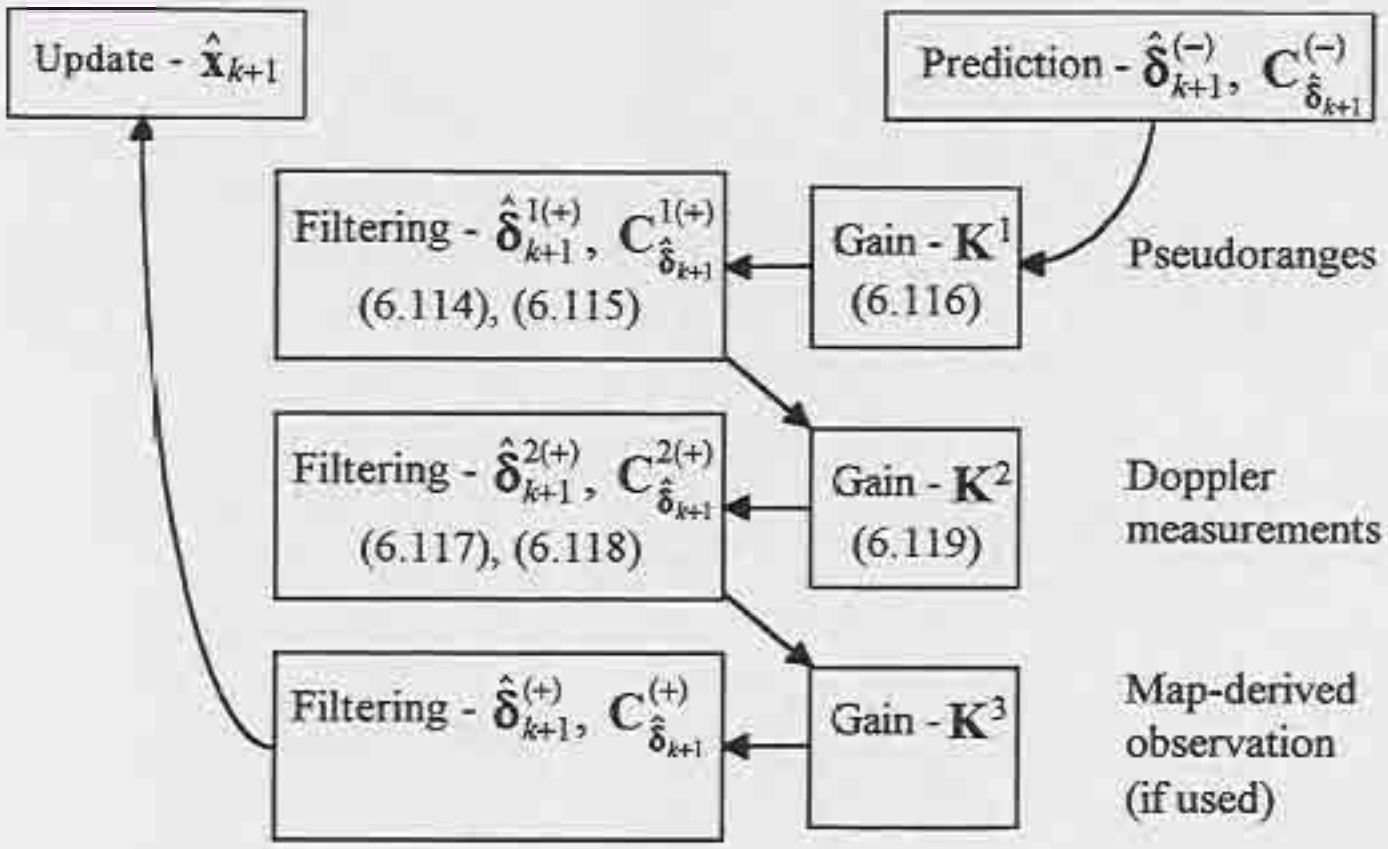

Figure 6.3 Sequential Updates in a Kalman Filter

6.3 Map Aiding

The positioning algorithms discussed to this point are common and have also been implemented in hundreds of other positioning and navigation systems. The idea of using information from a digital road map in a navigation system is not new either. The fundamental assumption behind map aiding is that the vehicle is most likely on a road in the road network. When a position is computed, it is compared with the map. If a road is identified as the only probable road of travel, one of two methods can be used to add a map-derived observation to the filter. The first is to introduce a weighted point into the positioning algorithm. The second is to compute a slope-intercept model of the road link and apply this equation as a constraint. The map-derived observation will help the filter maintain a smooth trajectory. In the following sections, each of these two models is presented. The algorithm for deciding when to use these models is described in Chapter 7.

6.3.1 *Weighted Point Model*

Given a computed position, a search is performed in the digital road map database to determine the nearest road (Section 7.2.1). The coordinates of the point on that road that

are nearest to the computed position are then obtained (Figure 6.4). These coordinates can be applied to the solution as a weighted point. In least squares, this would be similar to using *a priori* information on the unknown coordinates. The effect is that the coordinates are treated as observations with some weight. If the weight is the same order of magnitude as the weights of other observations in the adjustment, then the coordinates will affect the solution significantly.

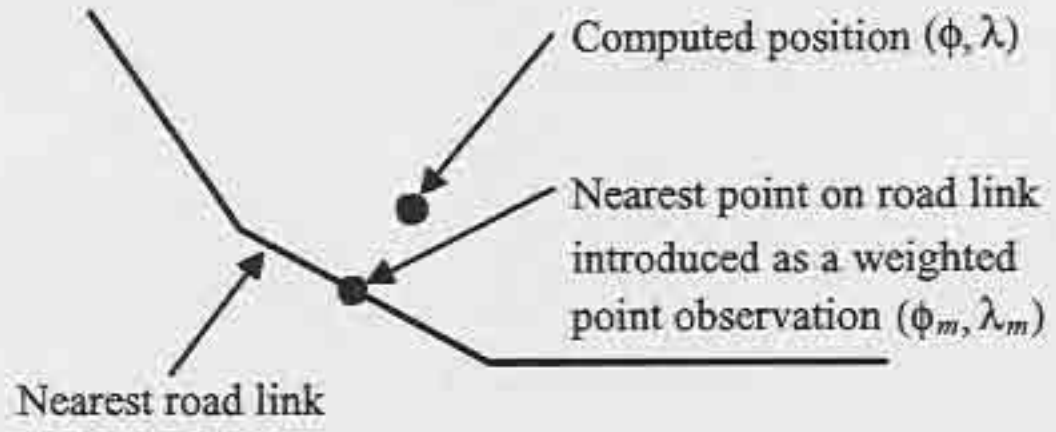

Figure 6.4 A Weighted Point Observation

To evaluate the potential effect of using the weighted point, one must compare the accuracies of the conventional observations with those of the map observations. In PortaNav, the positioning information for the solution is coming primarily from the GPS pseudoranges. As discussed, a horizontal accuracy of about 100 m can be expected for single point GPS solutions. If the coordinates derived from the digital road map have a better accuracy than this, then it may be beneficial to use a weighted point model.

Assuming the coordinates of the point to be weighted are given in the same geodetic reference frame as the computed GPS solution, the observation equations are

$$\phi_m = \phi, \ \sigma_{\phi_m}, \text{ and} \tag{6.120}$$

$$\lambda_m = \lambda, \ \sigma_{\lambda_m}, \tag{6.121}$$

where ϕ_m, λ_m are the map derived coordinates to be weighted,

ϕ, λ are the unknown geodetic coordinates, and

σ_{ϕ_m}, σ_{λ_m} are the standard deviations of the map coordinates.

At any epoch, only one weighted point will be added, so the design matrix will always have two rows. Only the first two columns will be populated as follows:

$$\mathbf{A} = \begin{bmatrix} \frac{\partial \phi}{\partial \phi} & \frac{\partial \phi}{\partial \lambda} & \frac{\partial \phi}{\partial h} & \frac{\partial \phi}{\partial v_n} & \frac{\partial \phi}{\partial v_e} & \frac{\partial \phi}{\partial v_h} & \frac{\partial \phi}{\partial CdT} & \frac{\partial \phi}{\partial \dot{C}dT} \\ \frac{\partial \lambda}{\partial \phi} & \frac{\partial \lambda}{\partial \lambda} & \frac{\partial \lambda}{\partial h} & \frac{\partial \lambda}{\partial v_n} & \frac{\partial \lambda}{\partial v_e} & \frac{\partial \lambda}{\partial v_h} & \frac{\partial \lambda}{\partial CdT} & \frac{\partial \lambda}{\partial \dot{C}dT} \end{bmatrix} = \begin{bmatrix} 1 & 0 & 0 & 0 & 0 & 0 & 0 & 0 \\ 0 & 1 & 0 & 0 & 0 & 0 & 0 & 0 \end{bmatrix}. \quad (6.122)$$

The associated variance-covariance matrix is simply

$$\mathbf{C_I} = \begin{bmatrix} \sigma_\phi^2 & \sigma_{\phi\lambda} \\ \sigma_{\lambda\phi} & \sigma_\lambda^2 \end{bmatrix}, \quad (6.123)$$

and the (2 x 1) misclosure vector is

$$\mathbf{w} = \begin{bmatrix} \phi - \phi_m \\ \lambda - \lambda_m \end{bmatrix}. \quad (6.124)$$

This type of an observation set can be applied to the least squares model or the Kalman filter. For the least squares model, the extra columns in the design matrix need to be eliminated; for the filter, the misclosure must be negated. In PortaNav, when a weighted point update is applied, it is added to the filter after the Doppler update.

6.3.2 *Slope-Intercept Model*

The second type of map aiding model used in PortaNav is based on the equation of a straight line. Each road in the digital road map database, whether straight or curved, is broken down into straight line segments. The coordinates of the end points of these line segments can be obtained from the database (Figure 6.5). With the two sets of coordinates, a straight line equation with a slope and Y-intercept is formed. The equation of the line is then added as an observation to the positioning algorithm. The solution is effectively constrained to a point somewhere on the line rather than to a single point, as was the case in the weighted point algorithm. Decisions on when to use this model are again made by the road finding algorithm (see Section 7.2).

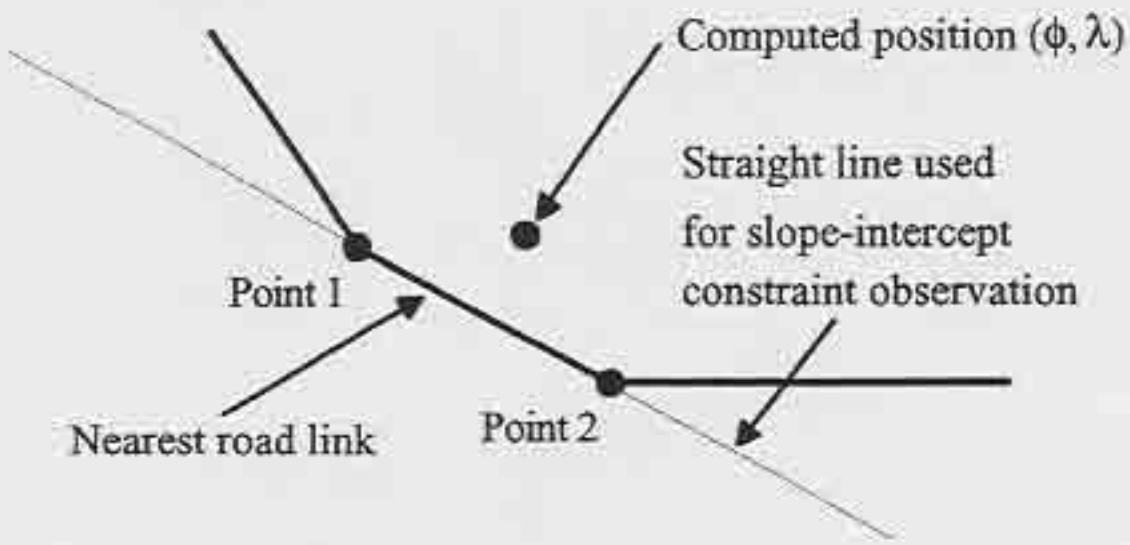

Figure 6.5 A Straight Line Slope-Intercept Observation

The straight line model is formed in a two dimensional planar coordinate system. Given the pairs of coordinates (x_1,y_1), and (y_1,y_2), the equations for the slope (m) and Y-intercept (b) of the line through them are

$$m=\frac{y_2-y_1}{x_2-x_1}, \text{ and} \tag{6.125}$$

$$b=y_1-m\cdot x_1. \tag{6.126}$$

Assuming the standard deviations of the two points are equal ($\sigma_{x_1}=\sigma_{x_2}$ and $\sigma_{y_1}=\sigma_{y_2}$), the error can be propagated through the above model to arrive at

$$\sigma_m^2=\frac{2\cdot k1}{k2}, \tag{6.127}$$

$$\sigma_b^2=\frac{(x_1^2+x_2^2)\cdot k1}{k2}, \text{ and} \tag{6.128}$$

$$\sigma_{mb}=\frac{-(x_1+x_2)\cdot k1}{k2}, \tag{6.129}$$

where $$k1=\sigma_x^2\cdot m^2+\sigma_y^2, \text{ and} \tag{6.130}$$

$$k2=2\cdot(x_1^2+x_2^2)-(x_1+x_2)^2. \tag{6.131}$$

Now with the slope, intercept, and associated errors of the line, the implicit straight line model can be formed as

$$f(\mathbf{x},\mathbf{l})=m\cdot x+b-y,\ \mathbf{C}_l, \tag{6.132}$$

where $$\mathbf{C}_l = \begin{bmatrix} \sigma_m^2 & \sigma_{mb} \\ \sigma_{bm} & \sigma_b^2 \end{bmatrix}. \quad (6.133)$$

In this equation, x and y are the unknown coordinates of the vehicle expressed in the two dimensional coordinate system, and m and b are the observations. At any epoch, only one road link will be used as a constraint, so there will only be one equation in this model. The implicit model has two design matrices as follows:

$$\mathbf{A} = \begin{bmatrix} \frac{\partial f}{\partial \phi} & \frac{\partial f}{\partial \lambda} & \frac{\partial f}{\partial h} & \frac{\partial f}{\partial v_n} & \frac{\partial f}{\partial v_e} & \frac{\partial f}{\partial v_h} & \frac{\partial f}{\partial CdT} & \frac{\partial f}{\partial C\dot{d}T} \end{bmatrix} \quad (6.134)$$

$$= \begin{bmatrix} \frac{\partial f}{\partial \phi} & \frac{\partial f}{\partial \lambda} & 0 & 0 & 0 & 0 & 0 & 0 \end{bmatrix}, \text{ and}$$

$$\mathbf{B} = \begin{bmatrix} \frac{\partial f}{\partial m} & \frac{\partial f}{\partial b} \end{bmatrix} = \begin{bmatrix} x & 1 \end{bmatrix}, \quad (6.135)$$

where $$\frac{\partial f}{\partial \phi} = \frac{\partial f}{\partial x} \cdot \frac{\partial x}{\partial \phi} + \frac{\partial f}{\partial y} \cdot \frac{\partial y}{\partial \phi}, \quad (6.136)$$

$$\frac{\partial f}{\partial \lambda} = \frac{\partial f}{\partial x} \cdot \frac{\partial x}{\partial \lambda} + \frac{\partial f}{\partial y} \cdot \frac{\partial y}{\partial \lambda}, \quad (6.137)$$

$$\frac{\partial f}{\partial x} = m, \text{ and} \quad (6.138)$$

$$\frac{\partial f}{\partial y} = -1. \quad (6.139)$$

The partial derivatives $\frac{\partial x}{\partial \phi}$, $\frac{\partial y}{\partial \phi}$, $\frac{\partial x}{\partial \lambda}$, and $\frac{\partial y}{\partial \lambda}$, and the misclosure equation will be derived when the coordinate frame for the slope-intercept model is developed in Chapter 7.

The slope-intercept model and the weighted point model are not both used in the same epoch. If the slope-intercept model is chosen, it is applied after the Doppler update in the Kalman filter.

6.4 Post-Mission Precise Orbit Processing

Post-mission processing is not of much use in a non-survey vehicle navigation system, since the primary goal of most systems is to aid the driver *en route*. Testing a vehicle navigation system is another matter, where a close to truth baseline is desired for

comparing the solutions obtained. To serve this purpose, precise GPS orbits and clocks will be used to process the pseudoranges post mission.

Precise orbits and clocks are computed by various organizations using networks of GPS observation stations. By observing the satellites from the network of known stations, the satellite orbits and clocks can be solved for to an accuracy of 15 to 20 cm. Using the precise orbits and clocks in place of the broadcast ephemerides and clock parameters eliminates large sources of error, particularly SA. It has been shown by Lachapelle et al. [1994] that single point GPS data processed with precise orbits and clocks can reach the metre level in accuracy with a high performance C/A-code receiver. This is with ephemerides spaced at fifteen minutes and clocks at 30 s. With SA, orbital and atmospheric errors removed or reduced, the receiver noise becomes a large part of the error budget. Hence the attainable accuracy depends largely on the quality of the receiver used.

In Canada, Natural Resources Canada (NRCan) uses the Canadian Active Control System (CACS) and other international GPS networks to provide precise orbits and clocks. The precise orbit and clock data files are available within a couple of days of the survey. NRCan has also produced a software package (GPSPACE) for performing the post-mission processing [Geomatics Canada, 1994]. GPSPACE requires the measurement data to be in the RINEX (Receiver INdependant EXchange) format [Gurtner, 1994]. With the measurement file and the precise orbit and clock files, GPSPACE computes either static or kinematic positions.

To test PortaNav, a RINEX file consisting of the pseudorange and Doppler measurements is logged. Processing this data results in a trajectory that can be taken as the best solution. By plotting this solution, the map accuracy can be evaluated. The precise file can be compared with the other three files logged to evaluate the performance of the three different solutions. Results of the testing are presented in Chapter 9.

6.5 Positioning Module Overview

Each of the four positioning solutions described in this chapter is logged by PortaNav for testing and evaluation. The flow of GPS data and positioning solutions is detailed in Figure 6.6. Recall that the Trimble MobileGPS receiver provides the raw observations and ephemeris data as well as a best DOP unique solution position fix. The best DOP fix is recorded directly by PortaNav. The raw GPS data is processed to synchronize, build, and correct the pseudorange observations for use in the least squares adjustment and Kalman filter. The constructed observations are logged in a RINEX file for use in post-mission precise orbit processing. Finally, the results of the least squares and Kalman filtering solutions are logged.

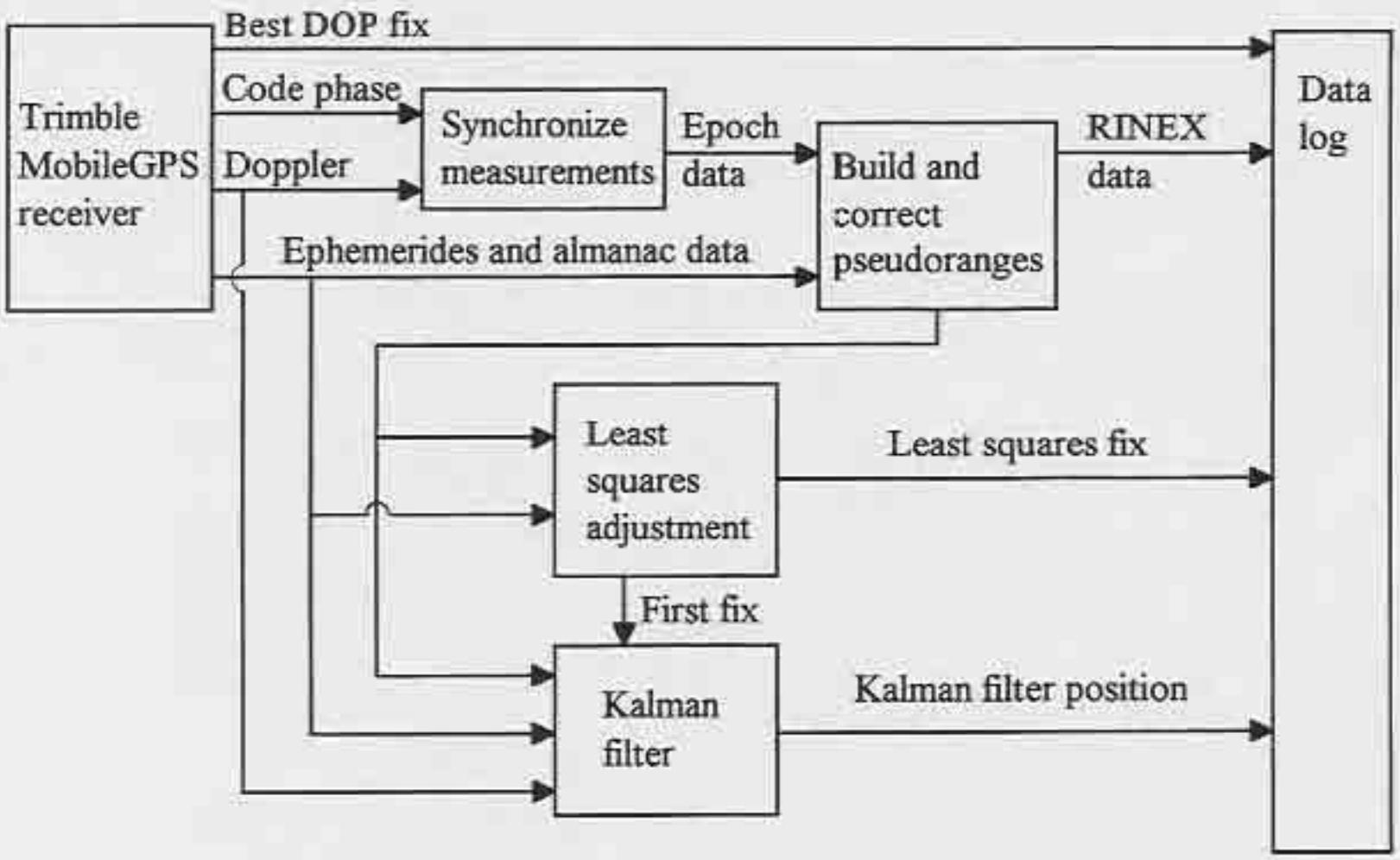

Figure 6.6 PortaNav Positioning Module Block Diagram

CHAPTER SEVEN

DATABASE ENGINE MODULE

The second component of navigation is location. Once a position is computed, it must be located in a frame of reference familiar to the user. A digital road map database forms the backbone of the location process. In PortaNav, the digital road map also plays a role in the positioning module. As described in Chapter 6, PortaNav uses two types of filter updates that hinge on map-derived information. This chapter describes the digital road map coordinate space and outlines the procedure used to find the most probable road of travel for use in the filter.

7.1 Digital Road Map Coordinate Frame

Throughout the ages of mapping, the world has been represented by using a flat surface. A paper map is based on some map projection that transforms the curvilinear real world to a planar map representation. Digital road maps are constructed in the same way. Knowledge of the transformation algorithm allows one to use the map space coordinates in a curvilinear model space. The positioning solution algorithms described in Section 6.2 are all formed in a geodetic coordinate frame, specifically, the WGS-84 reference ellipsoid. Etak maps are based on a unique map projection designed to suit the needs of storing and accessing a digital road map.

The Etak coordinate system (ECS) is based on the Etak-32 unit, which is an integer value that subtends an angle of $\frac{1}{2^{32}}$ of a great circle. Longitudes have a range of -2^{31} to $+2^{31}$, zero being at the Greenwich meridian and positive being east. Latitudes range from -2^{30} to $+2^{30}$, zero being at the equator, and positive being north. The reason for using this representation is so that coordinate values can be represented by 32-bit integers, thereby reducing the amount of storage space required for the map. The disadvantage to Etak-32 units is the limited resolution. At the equator, the length (d_{ECU}) of an Etak-32 unit is computed as

$$d_{ECU} = \frac{C_e}{2^{32}} \equiv 0.932\,cm, \tag{7.1}$$

where $C_e = 40\,030\,173$ is the approximate circumference of the Earth (m).

Due to meridian convergence, the length of an Etak-32 unit varies. In a north-south direction (dy), the Etak-32 unit is constant, and in an east-west direction (dx) it is scaled by the cosine of the average latitude. In all other directions the length varies according to the azimuth. The distance can be calculated by

$$dy = lat_2 - lat_1, \tag{7.2}$$

$$dx = \cos(\tfrac{lat_1 + lat_2}{2}) \cdot (lon_2 - lon_1), \text{ and} \tag{7.3}$$

$$d = \sqrt{dy^2 + dx^2}\,, \tag{7.4}$$

where lat_1, lat_2 are the latitudes of points 1 and 2 in ECUs, and

lon_1, lon_2 are the longitudes of points 1 and 2 in ECUs.

This approximation is valid for short distances relative to the Earth's circumference. For computing long distances accurately, one would need to resort to the spherical distance formula

$$d = \arccos(\sin(lat_1) \cdot \sin(lat_2) + \cos(lat_1) \cdot \cos(lat_2) \cdot \cos(lon_1 - lon_2)). \tag{7.5}$$

The coordinate system used for forming the straight line slope-intercept model (Section 6.3.2) is based on a modified local ECS. To form the model, it is best to have a coordinate system where distances are equal in every direction. This is accomplished by multiplying the longitudes by the cosine of latitude. Second, to preserve numerical accuracy, the origin should be shifted nearer to the area of interest. The first computed position is used as the origin for the local ECS. The transformation equations between geodetic coordinates and the local ECS can now be defined as follows:

$$y = \phi \cdot \frac{E_{MAX}}{\pi} - y_{off}, \tag{7.6}$$

$$x = (\lambda \cdot \frac{E_{MAX}}{\pi} - x_{off}) \cdot \cos(\phi), \tag{7.7}$$

$$\phi = (y + y_{off}) \cdot \frac{\pi}{E_{MAX}}, \text{ and} \tag{7.8}$$

$$\lambda = \left(\frac{x}{\cos(\phi)} + x_{off} \right) \cdot \frac{\pi}{E_{MAX}}, \tag{7.9}$$

where x_{off}, y_{off} are the offsets from the origin (m), and
E_{MAX} is the maximum Etak-32 value $(\frac{1}{2^{31}} - 1)$.

The extent of a road link rarely exceeds a few hundred metres, so this coordinate system will serve well to form the straight line slope-intercept model.

In Section 6.3.2, the partial derivatives for the straight line model were given with respect to the local coordinate system (Equation 6.134). Now the derivatives with respect to the geodetic coordinate system can be defined. Using Equations 7.6 and 7.7,

$$\frac{\partial y}{\partial \phi} = \frac{E_{MAX}}{\pi}, \tag{7.10}$$

$$\frac{\partial y}{\partial \lambda} = 0, \tag{7.11}$$

$$\frac{\partial x}{\partial \phi} = -\sin(\phi) \cdot \left(\frac{E_{MAX}}{\pi} - x_{off} \right), \text{ and} \tag{7.12}$$

$$\frac{\partial x}{\partial \lambda} = \cos(\phi) \cdot \frac{E_{MAX}}{\pi}. \tag{7.13}$$

The (1 x 1) misclosure vector then becomes

$$\mathbf{w} = \left[m \cdot \left(\lambda \cdot \frac{E_{MAX}}{\pi} - x_{off} \right) \cdot \cos(\phi) + b - (\phi \cdot \frac{E_{MAX}}{\pi} - y_{off}) \right], \tag{7.14}$$

where m, b were defined in Equations 6.125 and 6.126.

Note that the straight line slope-intercept model is formed in the local ECS, so the misclosure and the variance-covariance matrix of the observations (m, b) must be expressed in compatible units.

The weighted point model in Section 6.3.1 was formed in geodetic space. The observations are map points taken from the digital road map and converted into geodetic coordinates using Equations 7.8 and 7.9. The misclosure vector and the variance-covariance matrix of these points are also expressed in geodetic space.

7.2 Road Finding Algorithm

Before either one of the map aiding algorithms can be used, a road must be selected. If an incorrect constraint is introduced into the Kalman filter, the solution can be pulled off course. An algorithm must be designed to find roads and ascertain their validity. If it is not possible to determine which of a number of roads is the correct one at a certain epoch, no map constraints will be applied during that epoch and the filter will rely solely on the GPS measurements available.

7.2.1 *Nearest Feature Search*

The fundamental task behind selecting a road to use as a constraint is to do a nearest feature search. Given the coordinates of a point, a search is performed on the digital road map database to determine the feature that is closest to that point. The orthogonal distance (d) between a search point and a road link (see Figure 7.1) can be found using

$$d = \frac{|\mathbf{a} \times \mathbf{b}|}{|\mathbf{a}|}, \tag{7.15}$$

where $\mathbf{a}$ is a vector representing the road link,

$\mathbf{b}$ is a vector representing the point, and

$|\times|$ is the cross product operator.

The vectors $\mathbf{a}$ and $\mathbf{b}$ are defined as follows:

$$\mathbf{a} = (y_2 - y_1, x_2 - x_1), \text{ and} \tag{7.16}$$

$$\mathbf{b} = (y - y_1, x - x_1), \tag{7.17}$$

where x_1, y_1 are the coordinates of the start point of the road link,

x_2, y_2 are the coordinates of the end point of the road link, and

x, y are the coordinates of the search point.

The point on the road link that is nearest to the search point can be determined using the dot product operator ($\bullet$). Defining the vector $\mathbf{c}$ to be the component of vector $\mathbf{a}$ to the nearest point,

$$|\mathbf{c}| = |\mathbf{b}| \cdot \cos(\theta) = \frac{|\mathbf{a} \bullet \mathbf{b}|}{|\mathbf{a}|}, \tag{7.18}$$

where θ is the angle between the vectors **a** and **b**.

Now the vector **c** is determined by

$$\mathbf{c} = \mathbf{a} \cdot \frac{|\mathbf{c}|}{|\mathbf{a}|} = \mathbf{a} \cdot \frac{|\mathbf{a} \bullet \mathbf{b}|}{|\mathbf{a}|^2}. \tag{7.19}$$

Note that a singularity is possible if the road link represented by vector **a** is too short. Finally, the coordinates of the nearest point (x_n, y_n) are

$$x_n = x_c + x_1, \text{ and} \tag{7.20}$$

$$y_n = y_c + y_1, \tag{7.21}$$

where x_c, y_c are the components of the vector **c**.

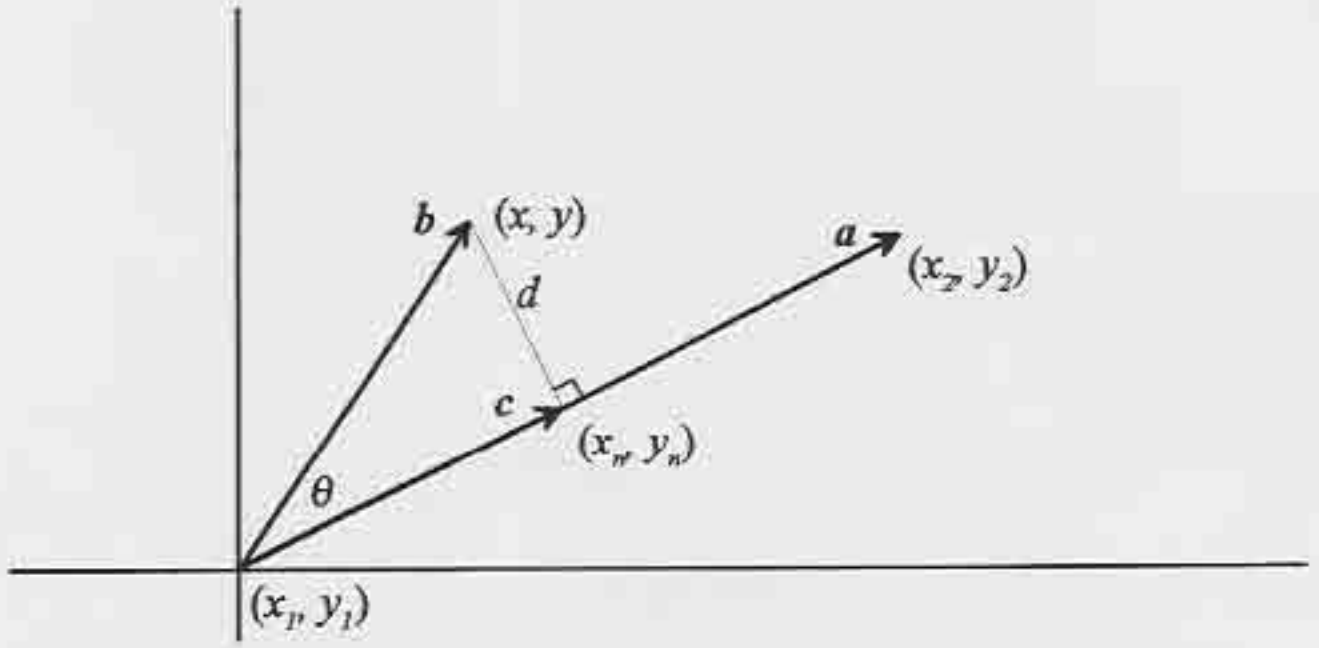

Figure 7.1 Geometry of a Nearest Feature Search

It is not necessary to search the entire database for the feature nearest to the search point. A search window is defined and used as a mask to limit the search to a small portion of the digital road map. It is convenient to use the display window as the starting point for the search window. As each road is called up from the database and displayed in graphics space, a record of the road is kept. Only the displayed features are searched, thereby dramatically reducing the computation time required to perform the road finding

algorithm. This is crucial in the operation of PortaNav, as multiple searches are performed at each epoch.

7.2.2 *Confidence Regions*

A confidence region is bounded by a line of constant certainty. If the vehicle is travelling on a road link in the digital road map, then at least one road should fall within the confidence region. Equations 6.73 to 6.75 give the parameters of a two dimensional confidence region that when scaled, represents an area of 95% certainty. The resulting error ellipse is the uncertainty of the position computed in the geodetic coordinate frame. This ellipse does not account for any uncertainty in the coordinates of the roads in the digital road map.

The uncertainty level in the digital road map is not homogeneous. There is no information stored in the Etak digital road map to quantify the uncertainty, so a global uncertainty level must be chosen. Etak claims a positional accuracy of fifteen metres on average. In Chapter 9 some of the tests indicate that the accuracies in the digital road map are at the fifteen metre level, thereby verifying the map specifications. The chosen standard deviation for the coordinates in the road map is then fifteen metres.

A good representation of the map uncertainty is a circle of error since the error is not direction dependant. To arrive at a 95% circle of error, the radius is scaled by 2.45. Combining the circle of error of the map with the error ellipse of the computed solution yields an ellipse that is extended by the radius of the circle. Hence the semi-major and semi-minor axes (Equations 6.73 and 6.74) of the error ellipse are expanded by the diameter (d_m) of the error circle as follows:

$$d_m = 2 \cdot \sigma_m \cdot 2.45, \tag{7.22}$$

$$a_m = a + d_m, \text{ and} \tag{7.23}$$

$$b_m = b + d_m. \tag{7.24}$$

where a_m, b_m are the semi-major and semi-minor axes of the combined position and map error ellipse.

The combined confidence region is pictured in Figure 7.2. Note that it is the uncertainty of all of the points in the digital road map that is being accounted for. If a road passed near the bottom of the confidence ellipse of the computed solution (as shown in Figure 7.2), its error circle would cause an overlap, and hence the road would be a potential hit; this is the reason for expanding the confidence ellipse in all of the directions.

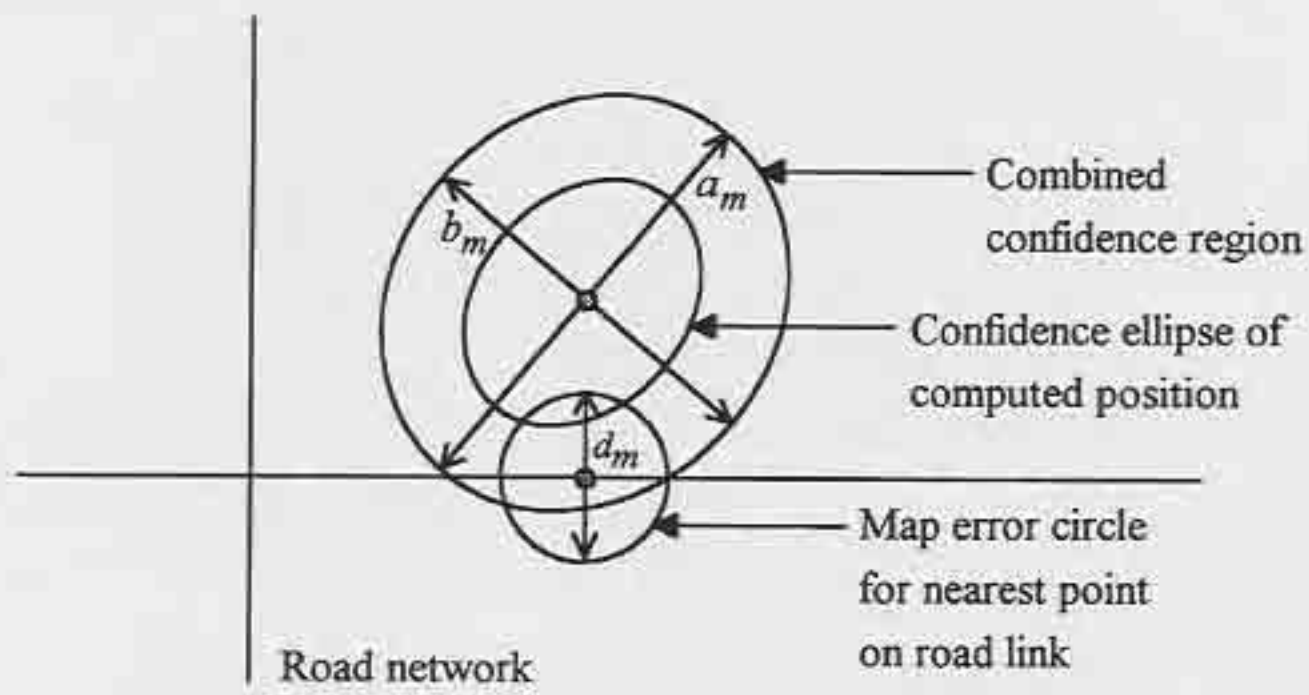

Figure 7.2 Combined GPS and Map Confidence Region

Now to find all of the possible roads of travel, a nearest road search should be performed using each of the points of the boundary of the combined confidence ellipse. This is not feasible for a real-time solution due to the excessive processing burden, so a simplification is in order. PortaNav uses the centre of the ellipse and four points on the boundary of the ellipse as defined by the end points of the semi-major and semi-minor axes. There are five points of interest, so five nearest feature searches are performed. This does not delay the processing significantly, while most of the possible roads are found. Once the nearest feature search is complete, a list of five possible roads is generated.

7.2.3 *Road Selection and Elimination*

It is possible that the list of five nearest roads may consist of one to five different roads. If two or more different roads are listed, then further processing is necessary to narrow down the possibilities. A procedure was devised to eliminate unlikely roads based on the azimuths of the road, the direction of travel, and the distance to the nearest point on the identified road.

In order to be considered plausible, a road link must conform to the following two conditions: the azimuth must be near the computed direction of travel (Figure 7.3), and the road must be within a certain distance from the current point. The first criterion only applies if the vehicle is moving; any road azimuth is valid if the vehicle is stationary. The tolerances chosen for the two conditions were based on the layouts of typical road networks.

The tolerance for the azimuth condition must be large enough to allow for noise in the computed position, and small enough to reject roads that are not in the general direction of travel. A threshold of twenty degrees was empirically chosen for this condition. At

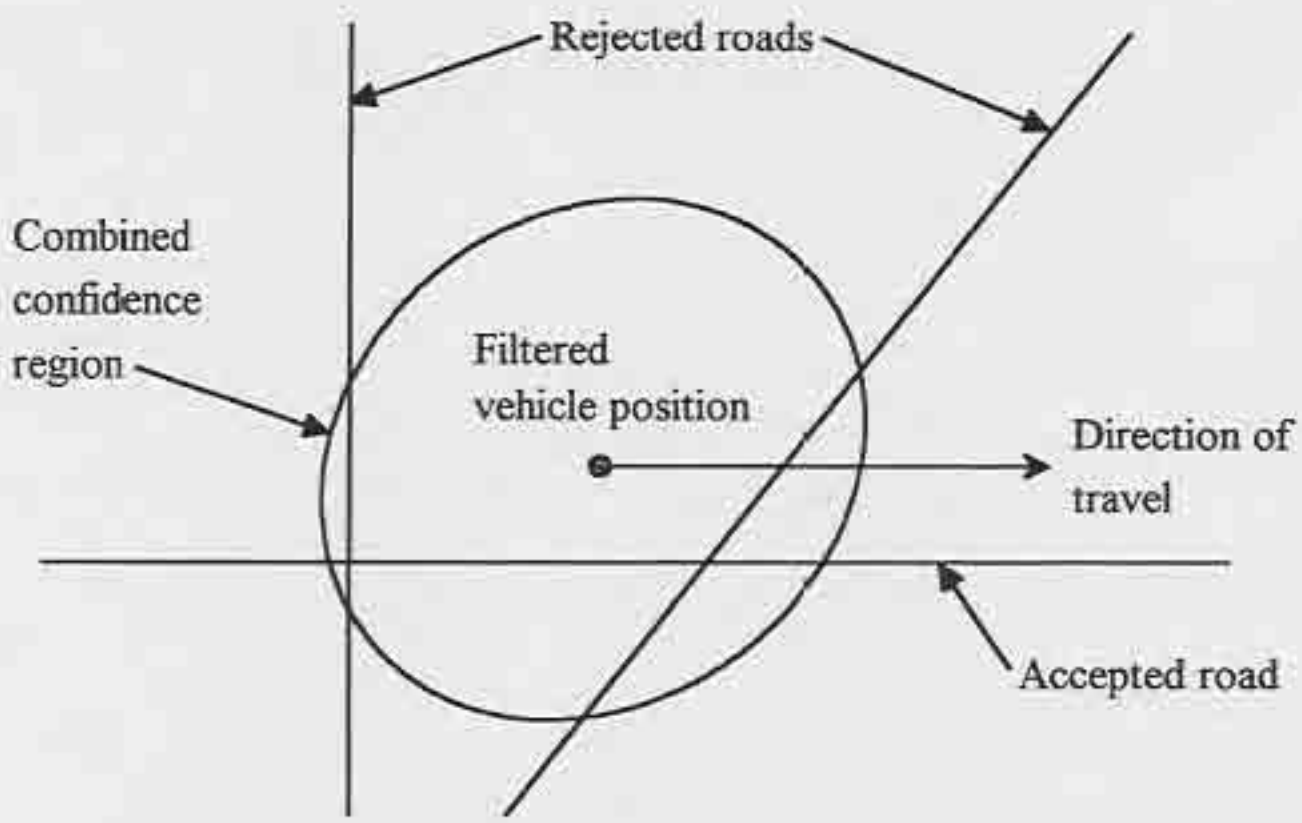

Figure 7.3 Road Acceptance and Rejection

most intersections, the intersecting roads are at an angle of 90°. In residential areas or hilly areas, the intersections may be at angles as low as 45° or 50°. The only time where intersections have a smaller angle is in the case of off-ramps.

The tolerance for distance is required to account for the fact that the vehicle may not be on a road in the database. This occurs when the vehicle is in a parking lot or in an area of the map that is not up to date or complete. Most urban areas have roads spaced at about 100 m. This is the case in most areas of Calgary including both the areas of gridded streets and avenues and residential areas. Some of the commercial areas of the city have roads that are spaced further apart.

In order to accept a road, it must be the only road found with an azimuth that agrees with the direction of travel within twenty degrees either way. Secondly, the nearest point on the road must be within 100 m of the computed position of the vehicle. If more than one road fits the first criterion, no map update will be performed for that epoch. If no roads meet the two conditions, no map update will be performed. If only one road passes the two conditions, one of the two map updates will be performed. A decision must still be made on which update to use.

7.2.4 *Map Aided Updates*

There are two possible updates that can be performed using the map derived information. They are the weighted point update (Section 6.3.1) and the straight line slope-intercept model update (Section 6.3.2). There is only a small difference in the effect of the two different updates. The weighted point model tends to constrain the solution to that point, while the slope-intercept model only tends to constrain the solution to a point somewhere along the road link. Understanding the desired effect of the map update is necessary before deciding when one or the other should be applied.

Road vehicles are either stationary or they are moving. If the vehicle is stationary, the solution should be constrained to a point, otherwise, the solution may tend to drift up and

down the road link due to the noise in the GPS measurements. If the vehicle is moving, the solution should be allowed the freedom of moving to a different point along the road link. Experience showed that a slow moving vehicle should not be allowed the freedom to wander up and down the road link, but should be constrained using the weighted point model as was the static vehicle. Accordingly, a slow vehicle is distinguished from a fast vehicle by a threshold speed. In Calgary, the speed limit for residential areas is 50 km/h. It was decided that the threshold should be just below this level so that only solutions of vehicles proceeding at slower speeds are constrained using the weighted point algorithm. PortaNav uses a threshold of 45 km/h to distinguish between a slow velocity and a fast velocity.

Tests showing the performance of the map aided filter as compared to the other solutions are presented in Chapter 9.

CHAPTER EIGHT

USER INTERFACE

There are two issues regarding the user interface in PortaNav. The first is the software control interface, and the second is the use of the hardware. The user will need to learn how to operate the equipment as with any other new piece of equipment.

8.1 Hardware Interface

In order to begin navigating in a road vehicle, the navigation system must be turned on and initialized. A user can not be expected to spend a great deal of time starting up the navigation system. The portable system must first be be secured inside the vehicle. The magnetic GPS antenna should be connected to the receiver and affixed to the roof of the vehicle to maximize signal reception. Once the computer is powered up, the software must be started and then the GPS receiver needs to be initialized. The whole start-up procedure takes at least one minute.

A notebook computer is an awkward piece of equipment to use in a car. There are special mounting racks that can be purchased, but they require a fair amount of space. Perhaps the optimum location for installing a notebook computer is on the passenger's lap. A permanently installed navigation system has an advantage in this area since the equipment remains in the vehicle connected and ready to go. Of course this again is a disadvantage because of the threat of theft.

8.2 Software Interface

Most software packages these days are designed with the end user in mind. Software developers realize that the customer must be able to use the software with minimum effort. Starting out with the familiar Windows interface will enable most users to intuitively know how to run the software. This is because all of the common commands in

the software will operate in the same fashion. For example, the procedure to open a map file is the same as for opening a word processing document.

All of the functions of PortaNav are accessed via the menu. The menu can be controlled by using the pointing device (a trackball for the NEC computer), or keystrokes. The menus are laid out so that the location of a certain command is intuitive. For example, all of the GPS related commands are under one menu item (GPS). Most of the commands bring up a dialogue box that is used for entering parameters for the software. The valid limits of the parameters are stated where possible. A detailed help system can and should be implemented for the end user product.

The pointing device is used for selecting menus and controlling the display of the map. In the 'mouse' pull down menu there are four items: zoom in, zoom out, centre map, and nearest feature. The zoom functions are controlled by clicking and dragging the mouse to create a box representing the region and scale of the new display. The centre map function is for panning across the map. The nearest feature function is for identifying roads and other features; when the mouse button is clicked, the nearest feature to the mouse pointer is found and highlighted, and its name is displayed in the view window.

While navigating, there are several quantities of interest to the navigator, primarily speed and course. In PortaNav, the position, height, time, and number of satellites being tracked are also displayed. Quantities such as distance and direction to the selected destination could also be displayed on this line. The bottom line on the screen is used for displaying error messages and various status messages.

A more sophisticated user interface would display speed and heading in a large easy to read font, or perhaps graphically in the form of a speedometer or compass display. Another enhancement to the user interface would be to include voice recognition and speech synthesis. The user would be able to control the unit by saying certain commands. The driving instructions for the best route could be communicated to the driver audibly rather than visually. This type of interface would be much less distracting, hence safer.

8.3 Capabilities

The PortaNav software was designed as a potential end user product, however the software had to support testing and evaluation. The features of these two functions are at times mutually exclusive.

For testing, several data files are computed and/or logged. A separate file for each solution type is recorded. These files can be played back, or they can be analyzed using other methods. An error file is also logged to keep track of the program flow. This file proved very useful for diagnostics and debugging. A menu was added for controlling which of the three solutions is displayed in real time. All three can be displayed simultaneously as well. In playback mode, the speed of the playback can be controlled and the playback can be paused for investigation.

A feature aimed more to an end user is the ability of the software to initialize itself and begin plotting automatically upon start-up. It is also possible to have the PortaNav software begin automatically when the computer is first turned on. This way, the user does not have to interact with the navigation system during start-up.

The Trimble software development kit includes a control panel interface to the receiver. The control panel is a separate window (Figure 8.1) that is created when the receiver is initialized. This window displays satellite related information so that the user can monitor signal strength, satellite elevations, etc. The control panel software eased the programming burden by presenting most of the essential GPS information so that it did not have to be presented within PortaNav. The control panel is not displayed continuously; the user can switch displays instantly between the map and the control panel.

In addition to panning and zooming, the map can be rotated manually through a menu operation. As the vehicle travels, the map automatically scrolls to keep the vehicle on the map. It is also possible to have the map rotate automatically to maintain a heading up display. Executing the moving and rotating map display requires a great deal of additional

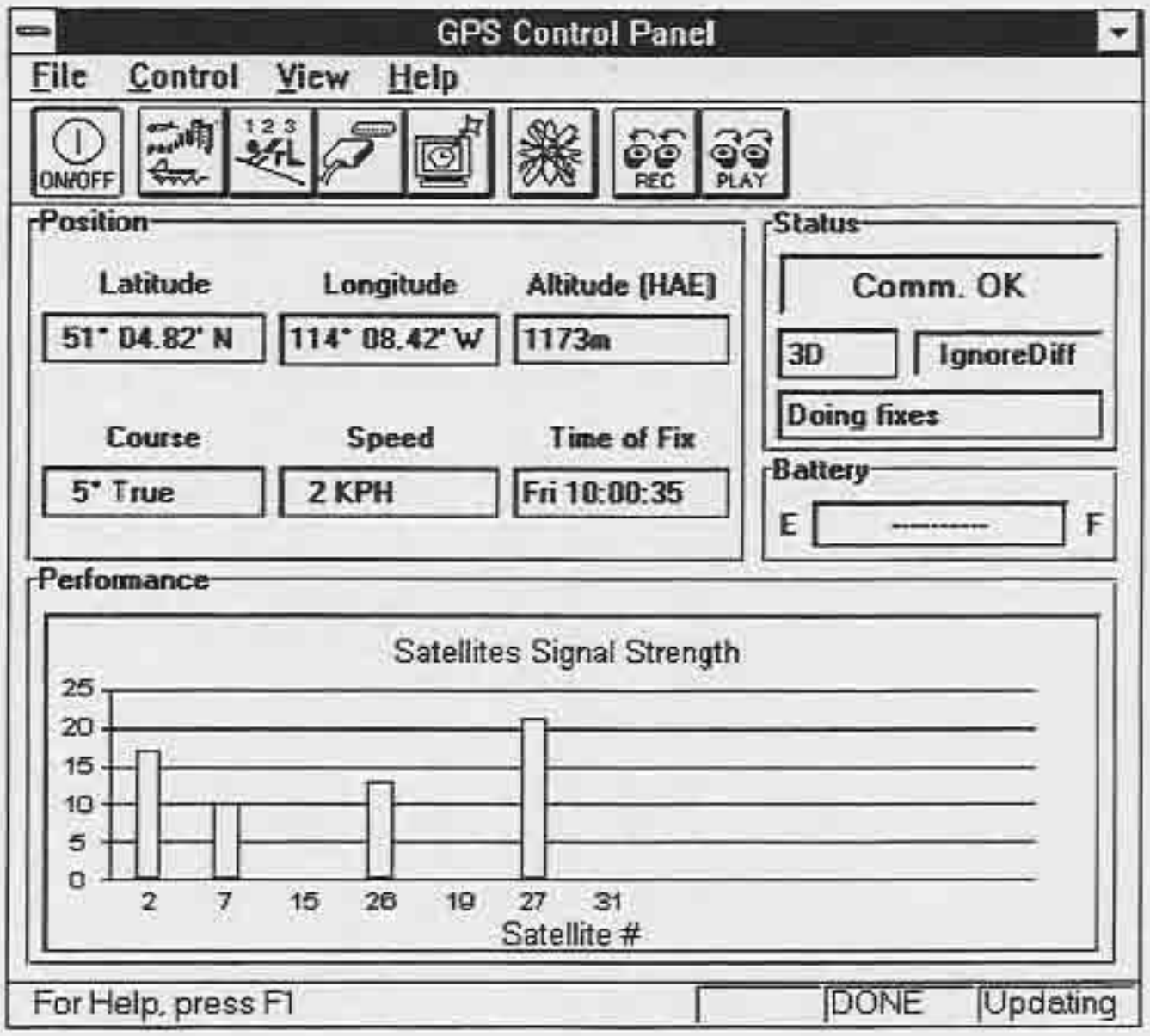

Figure 8.1 Trimble MobileGPS Control Panel

processing. For testing purposes, this feature was not implemented so that the map aided filter would not be unnecessarily hindered.

8.4 Limitations

As can be envisioned, many things will be happening in the software at once. This poses a problem as far as the operating system is concerned. Windows is not a multi-tasking platform, and as such, is not able to optimally share the CPU time between separate processes. This causes bottle necks in the processing and tends to slow down the overall performance of PortaNav. To the user, the effect is not significant. There is, however, an appreciable effect on the GPS interface. After each epoch of measurements, the processor has a heavy load as the filtering takes place. During this time, measurements reported by

the receiver are not recorded. By the time the CPU is free to process the raw data messages from the receiver, a few have been lost. The net effect is that a full epoch of raw observations is not available every second; the time between epochs varies from one to five seconds. This problem degraded the performance of the map aided filter, but did not prove to be fatal, as will be seen in Chapter 9. A faster processor or a multi-tasking operating system would aid in overcoming this problem.

8.5 Suitability for Use

No tests of using PortaNav as a system in typical applications were done. The conclusions drawn on the use of PortaNav are solely from experience testing the system personally.

The operation of the system proved simple, however, the externally mounted trackball pointing device was clumsy. A notebook computer with an integrated pointing device would be much better suited to operating in a constricted or mobile environment.

The vehicle used for testing had a relatively low and flat dashboard. Velcro strips were attached to the dashboard and the underside of the notebook computer. The notebook computer was then mounted right on the dash. The LCD screen was flipped around so that it could stand vertically. The reversible screen feature of the NEC proved to be useful for this mounting arrangement.

The biggest problem with using PortaNav is bright daylight; it is very difficult to see the screen in sunny conditions. Although the active matrix colour screen on the NEC computer is one of the brightest available, it was not bright enough. Display technologies still need to evolve further.

CHAPTER NINE

TESTING RESULTS

The objective of this chapter is to evaluate the positioning algorithms used in PortaNav. As described in Chapters 6 and 7, there are three solutions that will be compared with a baseline solution. First a review of the various solutions is in order. Second, the parameters and constraints used in the Kalman filter will be described. Then, results showing the performance of the solutions in various environments will be presented.

9.1 Solutions Compared

The first solution using GPS alone is the unique formulation as described in Section 6.2.1. This solution is arrived at by selecting the four satellites that give the best DOP, and using them in a unique solution to solve for the four unknowns. This solution is computed internally by the Trimble MobileGPS receiver and is logged by PortaNav.

The second solution uses all of the satellites in view above the cut-off elevation (10°) in a least squares adjustment (Section 6.2.2). Blunder detection and removal is performed if there is redundancy in the adjustment.

The third solution is the map aided GPS solution as outlined in Sections 6.3 and 7.2. This algorithm is based on a Kalman filter that uses pseudorange and Doppler measurements to filter a state vector with eight states. The digital road map is then used to find probable roads of travel, and if an acceptable road is found, map-derived information is used to update the filter with a spatial constraint. Both the least squares and Kalman filtering solutions are computed and logged by PortaNav.

Finally, the baseline solution against which the above three solutions are compared is described in Section 6.4. Precise GPS orbits and clocks and a RINEX observation file (logged by PortaNav) are used to compute a post-mission solution that will be considered the known track of the vehicle. The primary purpose for the precise solution is to

determine the accuracy of the digital road map so that an appropriate standard deviation for map coordinates can be used in the map aiding process.

9.2 Environments Tested

There are three main environments in urban land navigation: open road, tree canopy, and urban canyon. Each of these is described in brief, starting with the most treacherous. Section 9.4 describes the operational tests performed in each one of these three environments.

Urban canyons are areas where tall buildings line the streets, as in most downtown cores. GPS signals do not penetrate solid matter, so the buildings block visible satellites reducing the number of satellites available. Buildings are also highly reflective, so urban canyons tend to have a high level of multipath. As stated in Table 6.1, the maximum possible multipath error is about 300 m in a pseudorange. Multipath in the order of 150 m is common in urban canyon areas. The effects of multipath are large shifts in the computed positions from epoch to epoch. Multipath is unique for each position and time due to the motion of the satellites and the vehicle.

Tree canopy refers to areas where the trees are large, have heavy foliage, and possibly even cover the road overhead. GPS signals are attenuated by the foliage, so the heavier the foliage, the less likely the signal is to reach the receiver. In seasonal areas where the trees lose their leaves, tree canopy is not a concern for a portion of the year. Tree canopy areas tend to not have as bad multipath as the urban canyon areas, yet multipath is still apparent. In single point GPS, signal blockage is a large source of errors. This is because each satellite has a different range error due to SA. The result is that when a satellite drops out of or enters the constellation in view, the solution is shifted by up to a few tens of metres. Constellation changes occur frequently in both the tree canopy and the urban canyon environments, causing the solutions to appear quite noisy. This effect of constellation changes is not nearly so apparent in differential GPS mode or after precise processing because SA is removed.

The open road is anywhere that does not have obstructions to the satellite signals. Typically these areas are in residential areas with younger trees, major thoroughfares with large right-of-ways, and in areas where the buildings are only one to three stories tall.

9.3 Kalman Filter for Map Aided GPS

There are many parameters that are used to control the behaviour of a Kalman filter. In PortaNav, some constraints were also introduced to further improve the performance of the filter.

9.3.1 *Kalman Filter Parameters*

Recall that a first order Gauss-Markov process was used to model the dynamics of the vehicle. Different spectral densities and correlation times are used to control the noise along the trajectory of the solution. Long correlation times result in a trajectory that cannot vary significantly in short periods of time. To allow for abrupt changes in state, a relatively short correlation time is required. As shown in Equation 6.92, the spectral densities are a function of correlation times and variance. A small variance has the effect of tightening the model, or placing a high weight on the predicted solution. To allow for the measurements to have an effect on the filter, and in order for the vehicle dynamics model to filter out some of the measurement noise, the measurement variance and the spectral densities need to be properly balanced.

The characteristics of a slow moving vehicle are quite different than those of a fast vehicle. A slow vehicle can change heading quickly, while a fast vehicle can change position quickly. This knowledge was the basis behind selecting two sets of correlation times and spectral densities. The process variances remain the same regardless of the situation. Again, the threshold of 45 km/h was used to distinguish between fast and slow travel. The correlation times, spectral densities, and initial state variances used in PortaNav are listed in Table 9.1. The relatively high clock variances are due to the fact that the Trimble MobileGPS receiver makes use of a clock that is inexpensive but not very stable.

State parameters	Initial state variance	Spectral density of process noise (m^2/s^3)		Correlation time of process noise (s)	
		slow	fast	slow	fast
horizontal positions	2 500 m^2				
vertical position	2 500 m^2				
horizontal velocities	100 m^2/s^2	1 000	250	5	20
vertical velocity	100 m^2/s^2	250	125	20	40
clock offset	40 000 m^2				
clock drift	400 m^2/s^2	80	80	1 000	1 000

Table 9.1 Parameters Used in Kalman Filter

The measurement variances appear in Table 9.2. The errors in GPS pseudoranges vary largely from situation to situation, hence the error budget given in Table 6.1 does not always lead to a realistic value. A series of measurements was processed using least squares to determine an appropriate variance for the pseudorange observations. For each epoch, an *a posteriori* variance factor ($\hat{\sigma}_o^2$) can be computed:

$$\hat{\sigma}_o^2 = \frac{\hat{\mathbf{f}}^T \mathbf{C}_l^{-1} \hat{\mathbf{f}}}{n-u} \quad . \tag{9.1}$$

All of the terms in Equation 9.1 were previously defined in Section 6.2.2. This variance factor compares the standard deviations of the observations with the size of the residuals. A value of one indicates that the standard deviations and residuals agree globally. If the

Observation type	Variance
GPS pseudorange	225 m^2
GPS Doppler shift	0.04 m^2/s^2
map coordinates	225 m^2

Table 9.2 Variances of Observations Used

variance factor is larger than one, the residuals were too high, so the stated standard deviations were too optimistic [Vanicek and Krakiwsky, 1982]. By adjusting the standard deviations and performing several adjustments, a standard deviation of fifteen metres was selected as optimum. This standard deviation worked well except in the few cases where the multipath became very large. The error budget given in Table 6.1 would have led to a standard deviation in the order of 50 m to account for SA and the atmospheric errors. The standard deviation of 0.2 m/s for the Doppler measurement comes from the specifications for the Trimble MobileGPS receiver and some empirical testing.

Note that in a least squares adjustment of the pseudoranges, all of the observations are given equal weight. This means that the chosen standard deviation does not affect the outcome of the solution. The only effect is the scale of the variance-covariance matrices of the adjusted parameters and the residuals. The selected standard deviation does play a large role in the Kalman filter as the pseudorange weights are balanced with the weights of other sources of information.

The hypothesized map accuracy of fifteen metres was tested by plotting the precise solution on the digital road map in various areas of the city. Some of these plots appear in Section 9.4. The relative accuracy of the map over small distances seems to be quite good. However, in many areas there is a bias throughout the area, so the absolute accuracy of the coordinates is not as good. Unfortunately, the bias was not the same throughout the map. In some areas, the absolute accuracy of the coordinates is as bad as 25 to 30 m. An average map standard deviation of fifteen metres was chosen by testing the performance of the map aided filter in various regions. At this level, the map was never too tight for the pseudoranges and a proper balance was achieved.

9.3.2 *Kalman Filter Constraints*

Some of the weaknesses of the Kalman filter can be addressed by adding certain constraints to the state vector. Each of the constraints used in PortaNav will be briefly

described. Table 9.3 summarizes the constraints and their corresponding rules. Some of the tests presented in Section 9.4 illustrate the effectiveness of these constraints.

First of all, when the vehicle is stationary, the three velocity components are constrained to zero. This is implemented by observing the velocity as computed independently by the receiver. If the speed over ground (SOG) is less than 2 m/s (7.2 km/h), the vehicle is assumed to be stationary. The rationale behind this assumption is the fact that a road vehicle does not normally sustain speeds at this level. Once the static condition has been determined, the velocities are constrained to zero. This is done by setting the velocity states to zero when the states are updated at each epoch. Zeroing the velocities causes the predicted solution to remain unchanged for the next epoch, while the measurements at that epoch continue to affect the filtered position.

Due to the static constraint used, the Kalman filter experiences a lag when the vehicle begins to move again. To help compensate for this, the filter is 'kick started' when the vehicle starts moving after a static period. When the receiver determined SOG rises above

Rule	Action
Speed over ground is less than 2 m/s	Static constraint
Speed over ground is greater than 2 m/s after static period	Kick start filter
Only three satellites in view	Height constraint
Vertical velocity changes by more than 5 m/s over one epoch	Vertical velocity constraint
Road found after significant change in direction	Azimuth constraint

Table 9.3 Summary of Constraints Used in Kalman Filter

the static threshold, the horizontal velocity states in the Kalman filter are set using the receiver determined SOG and course over ground (COG).

The second major constraint comes into effect when measurements from only three satellites are available. This happens quite often in areas with tall buildings or trees. If an epoch with only three satellites is used, the height component of the position is constrained to the last known value. This allows the filter to remain stable, while making use of the information in the observations to determine the horizontal position and the velocities. This constraint is effectuated by leaving the height parameter unchanged when the state vector is updated.

In high multipath environments, such as urban canyon and tree canopy areas, the filtered solution is affected adversely. Test results have shown that the vertical position and velocity components are the states affected most. The reason for this seems to be that when a signal with a large multipath is observed, the vertical component of the velocity tends to become very large. The predicted solution for the next epoch then experiences a height change of a few hundred metres. To prevent this from happening, a constraint was placed on the vertical velocity. The physical rationale for this is the fact that road vehicles do not normally travel up faster than they are travelling forward. If the vertical component of the velocity changes by more than five metres per second over one epoch, it is held at the previous value to prevent large prediction errors in the next epoch. This allows for the fact that the vehicle may be travelling up a high grade at a fast, but stable, vertical velocity.

The final constraint placed on the filter is related to the road that is found. Kalman filters based on a constant velocity dynamics model tend to overshoot the turn when the direction of the vehicle changes. To assist the filter in finding the proper bearing after changing direction, a road azimuth is used to constrain the state vector. A change in azimuth of more than forty degrees over the span of a few epochs indicates that a significant change in direction has occurred. As soon as an acceptable road is found (see

Section 7.2) after a significant change in direction, the azimuth of the road is used to correct the ratio between the two horizontal velocity components. The absolute velocity (SOG) is projected into the easting and northing velocity components using the azimuth of the found road. Once again, this occurs during measurement update. This constraint causes the predicted position at the next epoch to be along the road, rather than having it overshoot the road laterally.

9.4 Test Descriptions

All of the kinematic tests were performed during the period May 27 to June 2, 1995. The static verification tests were performed in April, 1995. The date and the vertical height of each plot is shown on the bottom line of the screen captures. The other parameters visible are displayed during the run and as the file is played back post-mission. All of the trajectory plots are north-up unless otherwise indicated. The actual road of travel can be identified in most of the plots for the open road and tree canopy tests. The path in the urban canyon plots is usually not obvious, so descriptions of the actual path will be given when needed. The starting point of each run is indicated on the plot. Some general comments on each environment follow the test results (Section 9.5).

9.4.1 *Static Tests*

Static testing was performed throughout the software development stage to verify each new module of code for the GPS processing. Once completed, PortaNav was tested in static mode to determine the characteristics of the Trimble MobileGPS receiver. Shown in Figure 9.1 is the plot of a twenty minute static test after processing with the precise orbits and clocks. The dominant errors in this situation are the receiver noise and the remaining ionospheric error. A simultaneous test using an Ashtech Z-12 receiver was performed so that the difference in receiver noise levels could be determined. The Ashtech is a survey grade dual-frequency receiver that costs upwards of thirty thousand dollars. The RMS values for the Trimble and Ashtech static test results are listed in Table 9.4. Receiver noise is usually inversely proportional to receiver cost; this is the case in this test. Also

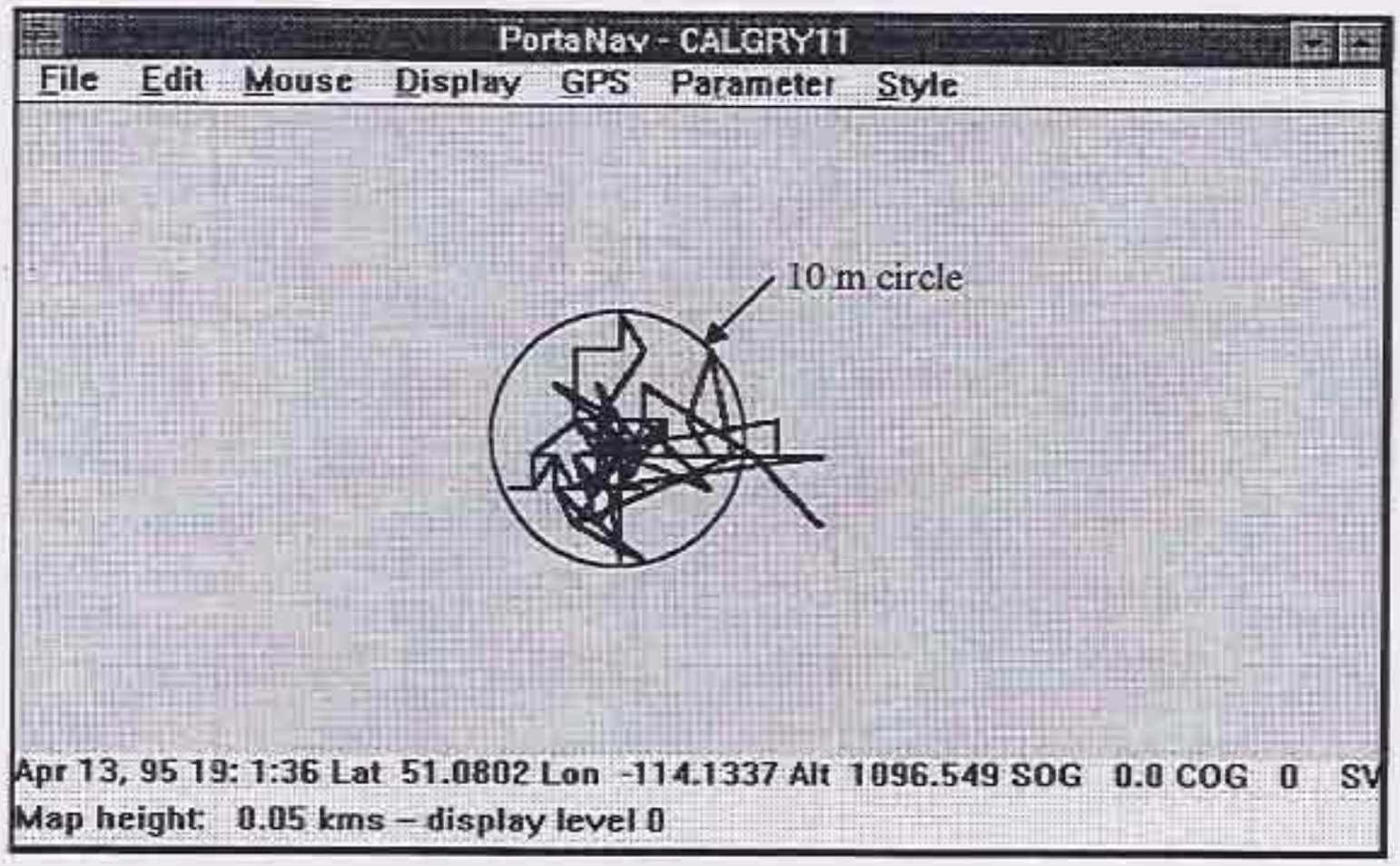

Figure 9.1 Precise Fix Static Test

listed are the coordinate differences of the averaged solution over the twenty minutes. There is a close agreement (2.02 m) between the absolute positions. The expected performance of the precise processing is then about five to ten metres of noise with the Trimble MobileGPS. The precise solution will be an adequate baseline for our purposes.

Before moving on to the kinematic tests, one example of the effect of static map aiding will be shown. Recall that when the velocity of the vehicle is below 2 m/s the velocity

	Northing (m)	Easting (m)	Height (m)
Trimble MobileGPS RMS	4.99	4.83	7.22
Ashtech Z-12 RMS	1.97	2.01	4.64
Coordinate difference	0.34	0.72	1.86

Table 9.4 Static Test Comparison Between Trimble MobileGPS and Ashtech Z-12

states of the filter are constrained to zero and a weighted point update is applied (Section 6.3.2). Figure 9.2 clearly shows the effect of the static weighted point update. The vehicle was heading south on Crowchild Trail and was stopped at an intersection for about twenty seconds. The advantage to using the map updates is readily apparent.

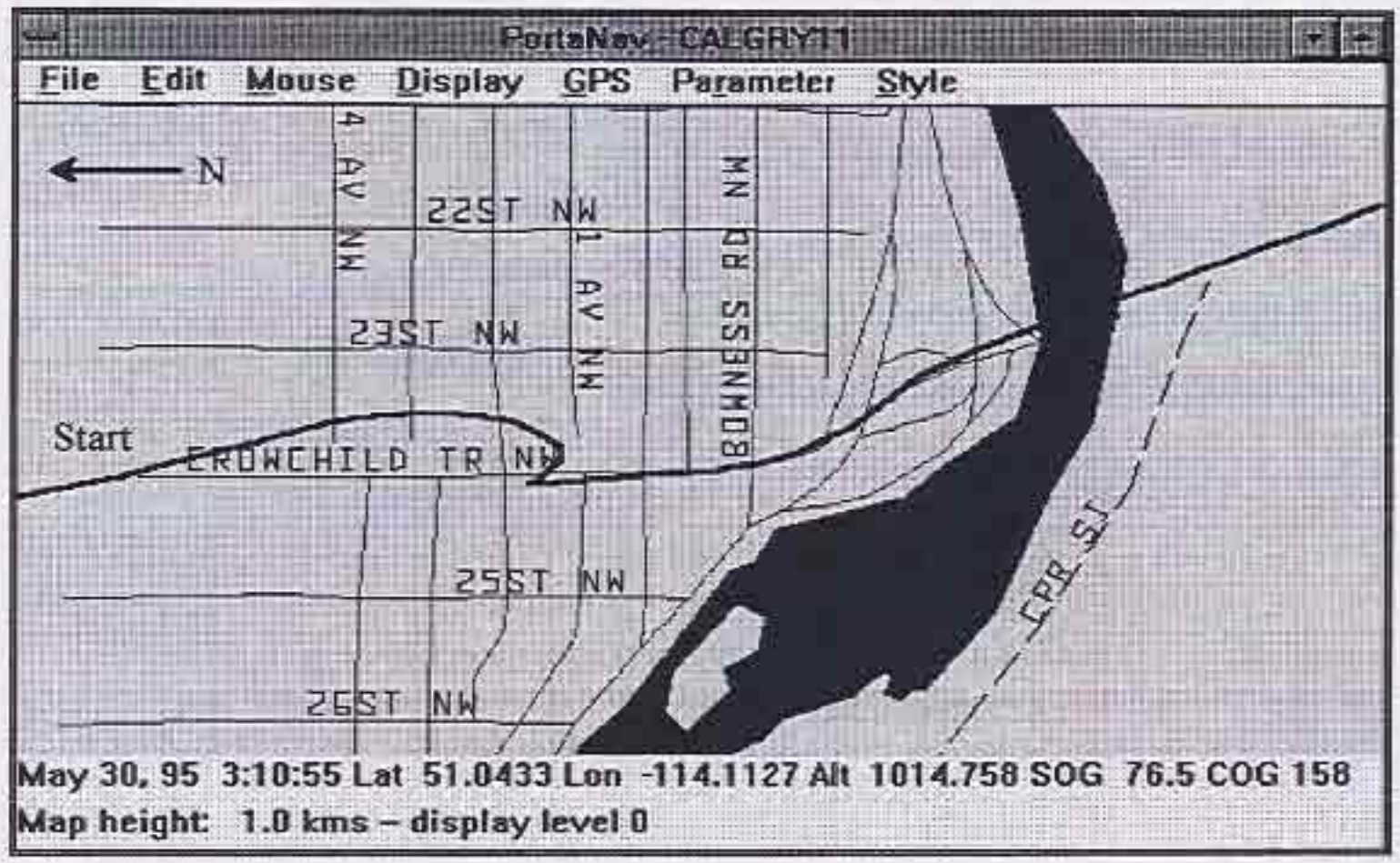

Figure 9.2 Effect of Static Map Constraint in Map Aided GPS

9.4.2 *Open Road Tests*

The open road is the most friendly environment to GPS and that fact is clear in all four of the positioning solutions. Note that trees lining the road may cause occasional blockages.

Test 1:

The first set of Figures is of a run taken on May 28, 1995. Plots of the map aided GPS, best DOP, least squares, and precise solutions appear in Figures 9.3 to 9.6. The total time of the run is 793 seconds. During this time, 541 best DOP fixes were reported by the receiver, which is one every 1.47 seconds on average. Only 243 epochs, or one every 3.26 seconds, were recorded by the other three solutions. The large discrepancy in the

data rate is due to the processing burden as described in Section 8.4. Figure 9.7 shows the HDOP for this time period, and Figure 9.8 shows the number of satellite measurements available. Note that these two plots are only for the epochs when a fix was computed; not for the epochs when a best DOP fix was reported by the receiver. Also, note that the available satellites is not the same as satellites in view; measurements for some satellites may not be available for every epoch.

The best DOP (Figure 9.4) and least squares (Figure 9.5) solutions experience spikes when a satellite is blocked momentarily, causing a change in the constellation used. This is due to SA having a different effect on each satellite; the overall effect of SA is constellation dependant. A constellation change occurs when the number of satellites changes or the combination of satellites used changes. For the least squares fix, this is quite frequent since all of the available satellites are used. The best DOP fix only experiences a constellation change if the geometry improves or if a satellite being used becomes unavailable. The result is much fewer constellation changes for the best DOP solution.

For the open road, the best DOP fix experiences a small number of constellation changes. Those that do occur are most likely due to switching to better constellations when new satellites becomes available or when a satellite being used drops out of view. The least squares fix experiences many more constellation changes than the best DOP fix, even on the open road. The reason for this has more to do with the GPS receiver and the software limitations as opposed to environmental conditions. This issue will be discussed further below.

The map aided solution in Figure 9.3 exhibits a common characteristic of constant velocity Kalman filter models, namely, overshooting the turns. When this happens, the map helps bring the solution into line again. This is evident at the point marked with arrow A in Figure 9.3. From the precise plot in Figure 9.6, there appears to be a bias in the map for this area to the south and west.

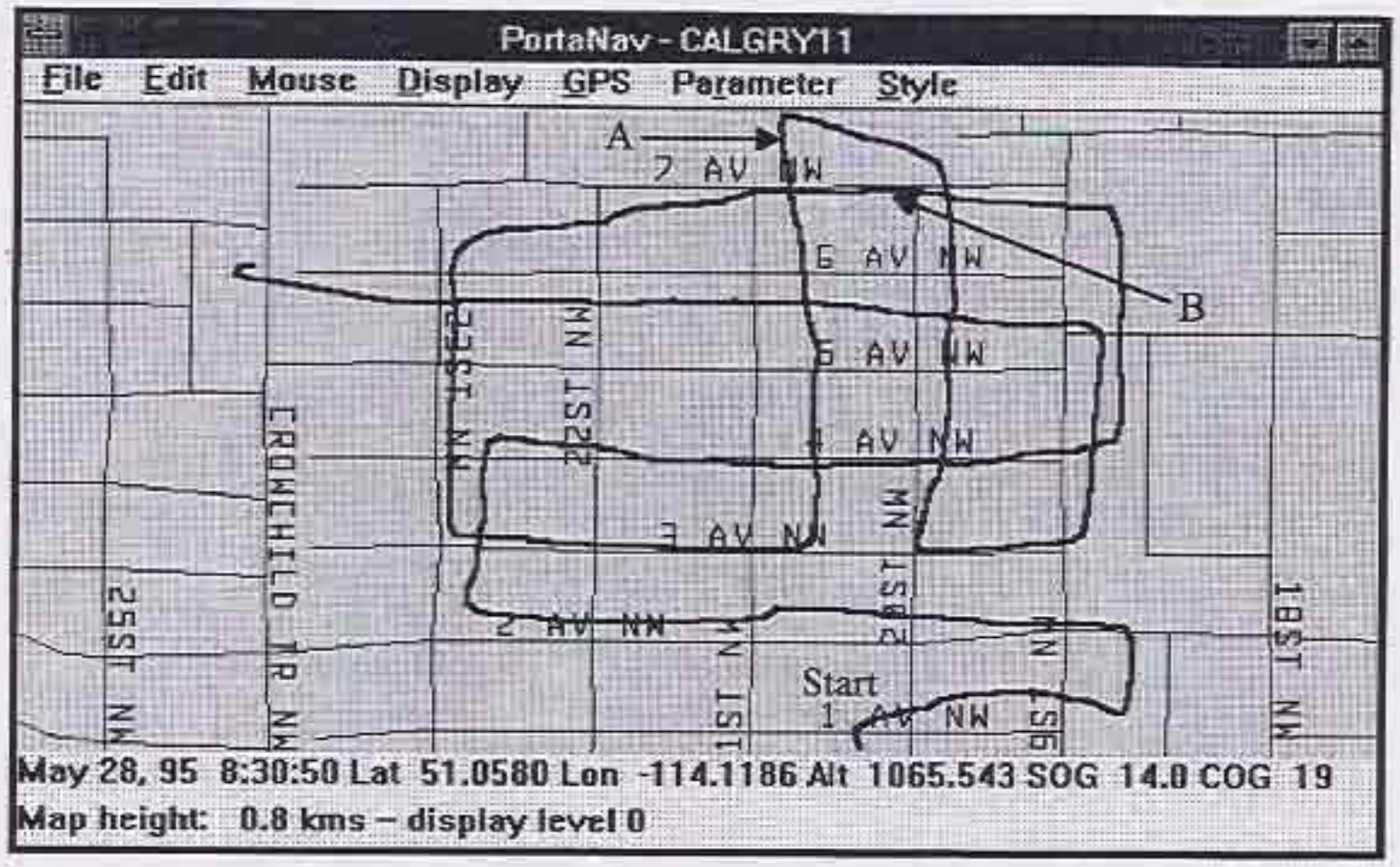

Figure 9.3 Map Aided GPS on Open Road

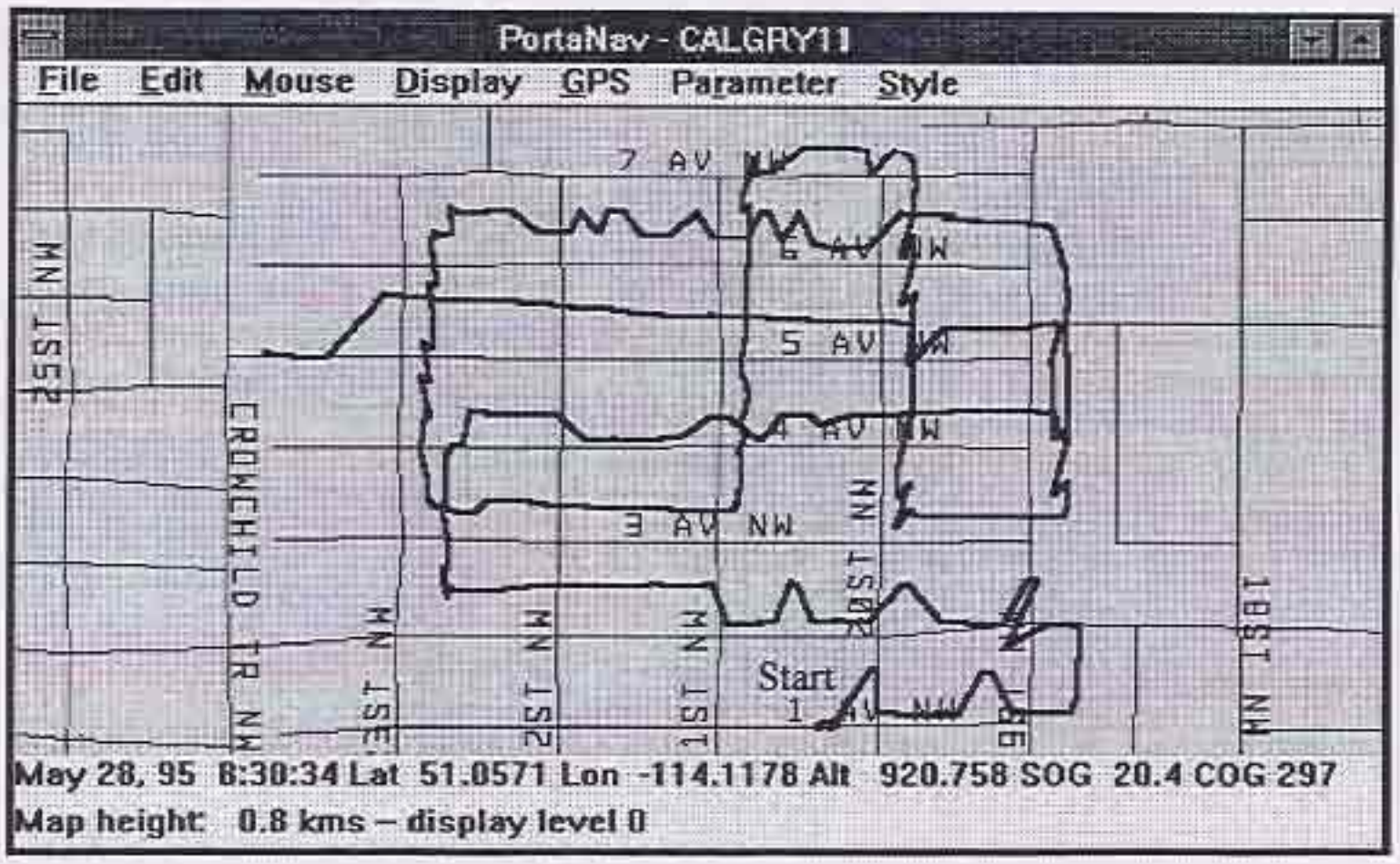

Figure 9.4 Best DOP Fix on Open Road

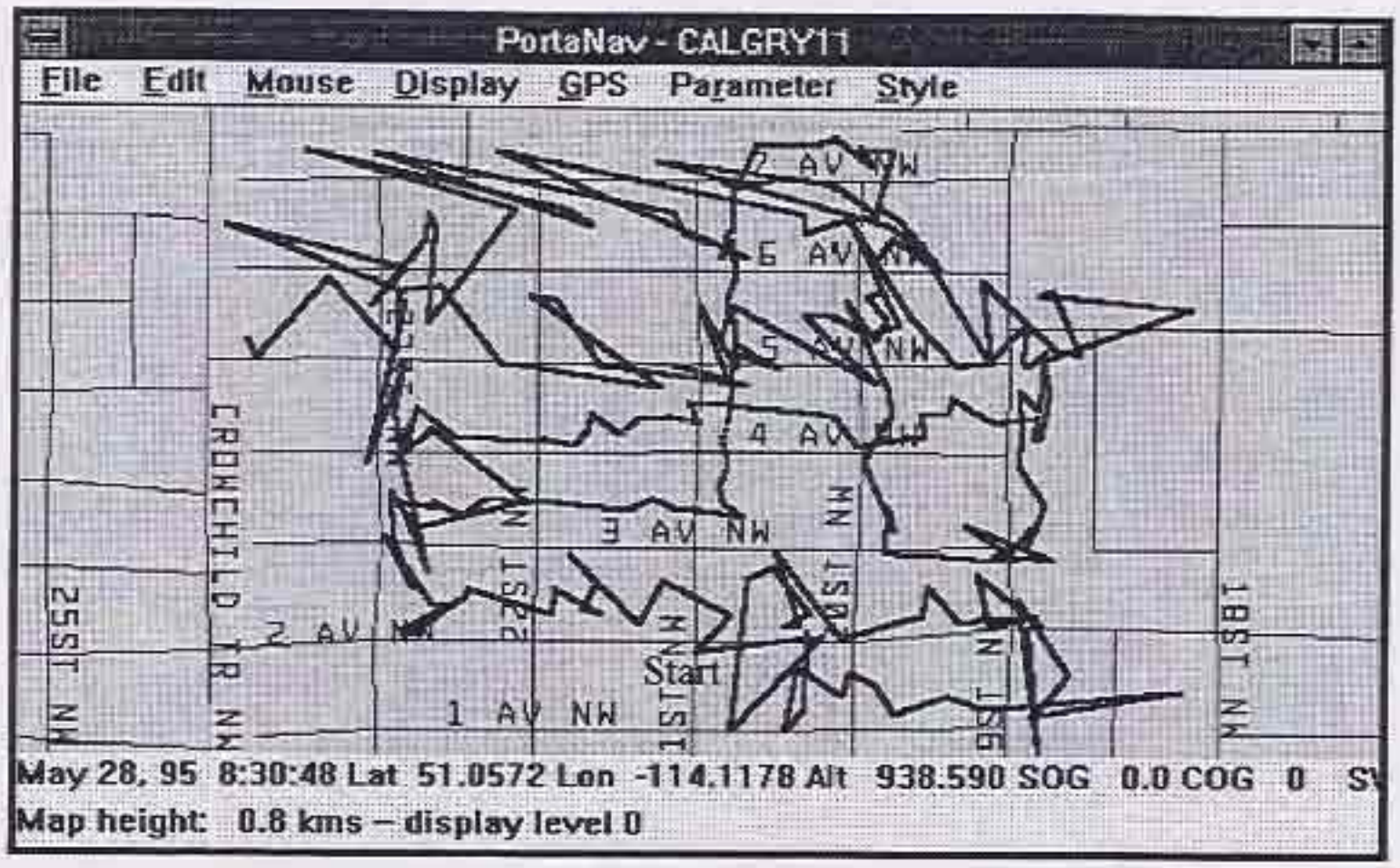

Figure 9.5 Least Squares Fix on Open Road

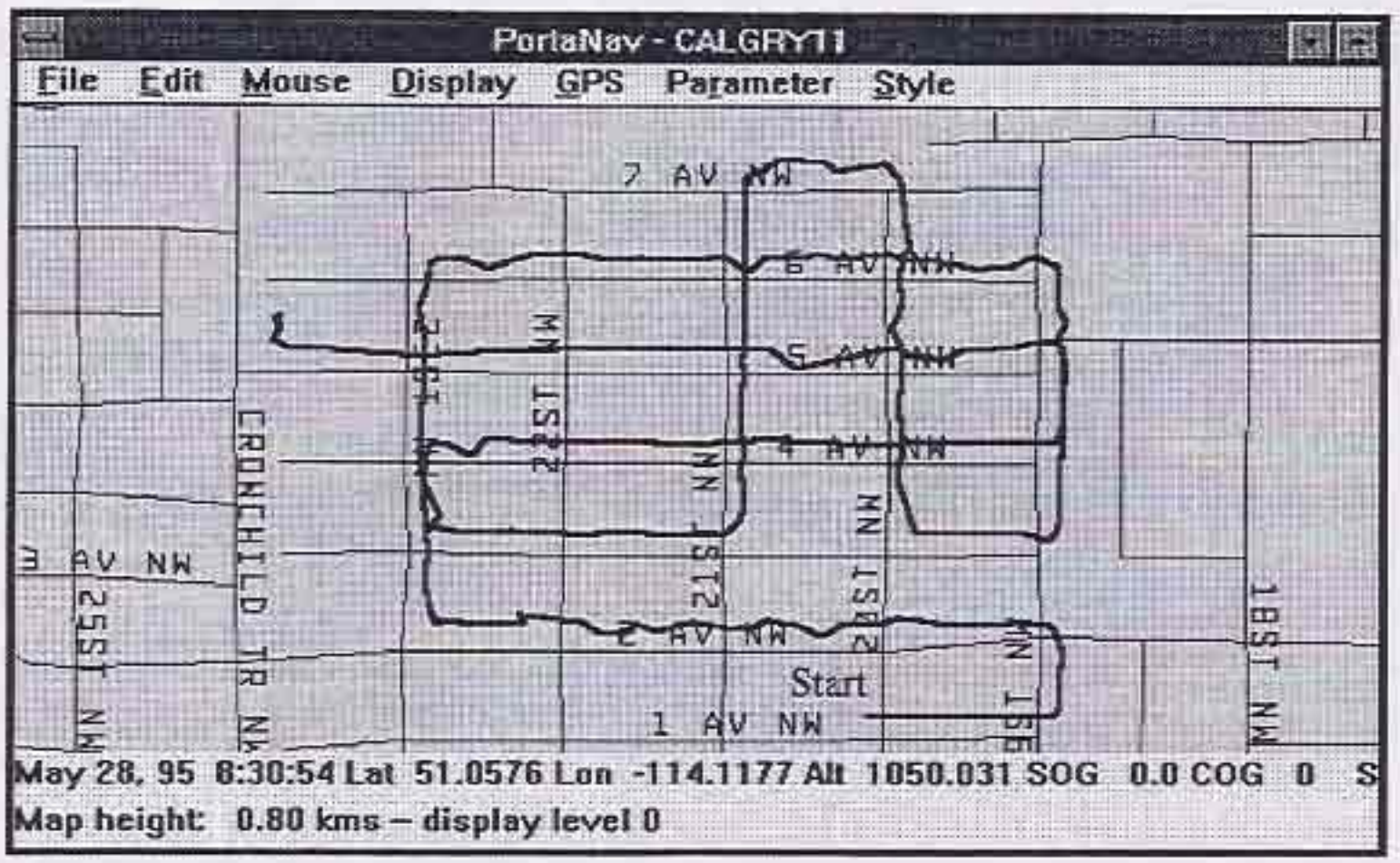

Figure 9.6 Precise Fix on Open Road

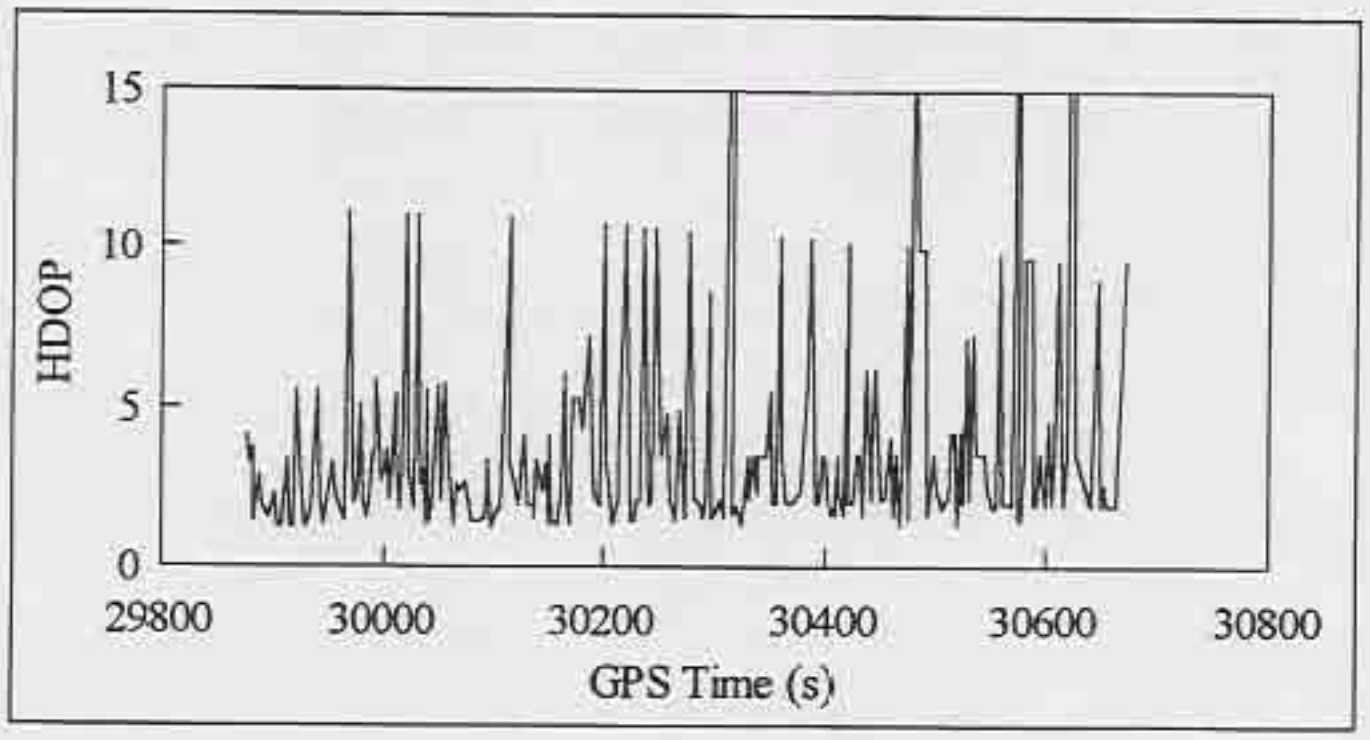

Figure 9.7 HDOP on Open Road, May 28, 1995

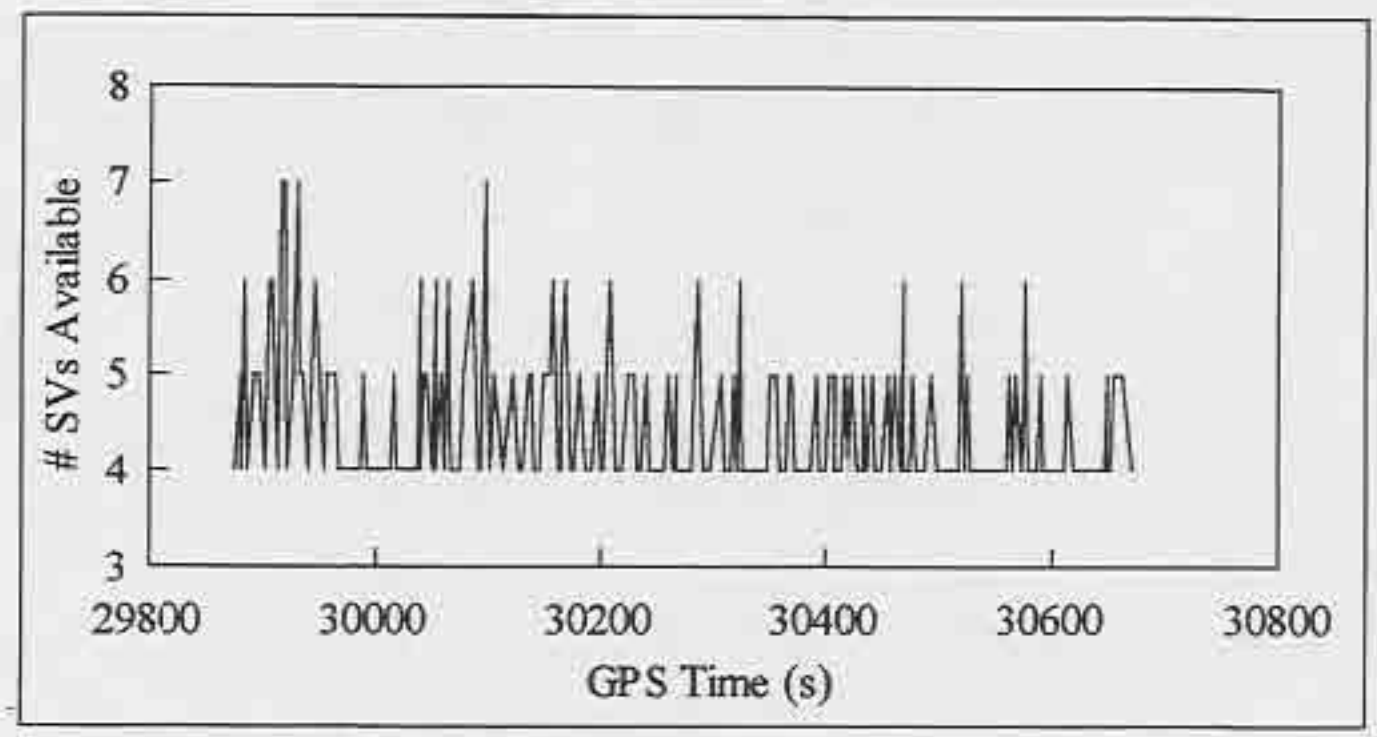

Figure 9.8 Number of Satellites Available on Open Road, May 28, 1995

Figure 9.9 shows the difference in northing between the map aided GPS solution and the precise solution. Near time 30 200 there is a large and fairly long bias to the north. The place where this occurred is marked in Figure 9.3 with arrow B. The correct road of travel was 6th Ave., as seen in the precise plot (Figure 9.6). It is apparent that as the vehicle turned onto this road heading west, the road finding algorithm incorrectly selected 7th Ave., and the solution was gradually shifted to the north, causing the large bias. Although the incorrect decision was made, we see that it was not entirely a failure as the solution soon left that road and headed south towards the correct road.

Figure 9.10 shows the difference in northing between the best DOP fix and the precise fix for the same period. The precise fixes are subject to multipath and receiver noise, so these errors appear in both sets of difference plots.

Figures 9.11 and 9.12 show the differences in eastings obtained from the map aiding and best DOP solutions. Figures 9.13 and 9.14 show the differences in heights. Comparing the performance of the map aided filter with the stand alone best DOP fix, we see that a significant improvement is achieved in the horizontal components, but nothing is gained in the vertical component. This is expected since the map aiding process only aids the horizontal components of the position.

Recall that the primary objective of this navigation system is to correctly identify what street the vehicle is travelling on. The software can then do a map match and snap the position onto the road for display purposes. For the open road case, the snapped position would be virtually equivalent for the map aided GPS and best DOP solutions.

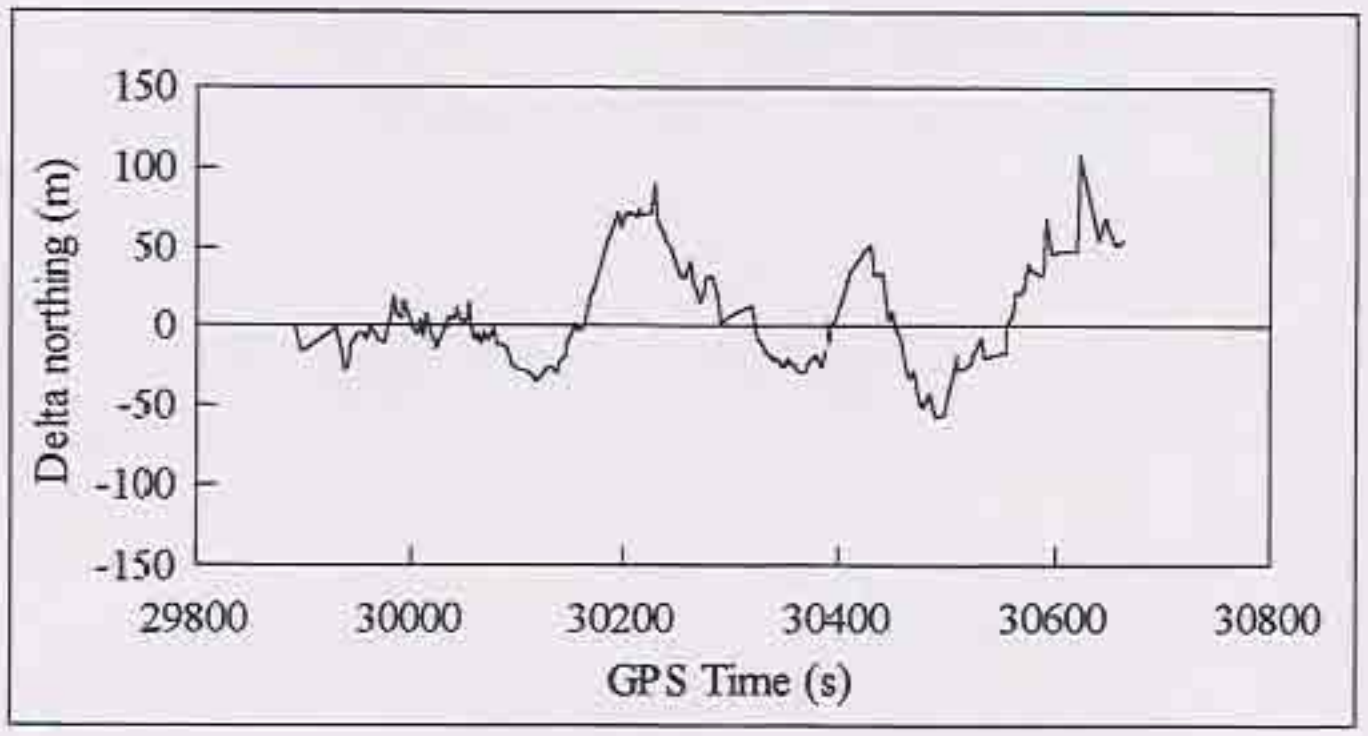

Figure 9.9 Difference in Northing Between Map Aided GPS and Precise Fix on Open Road, May 28, 1995

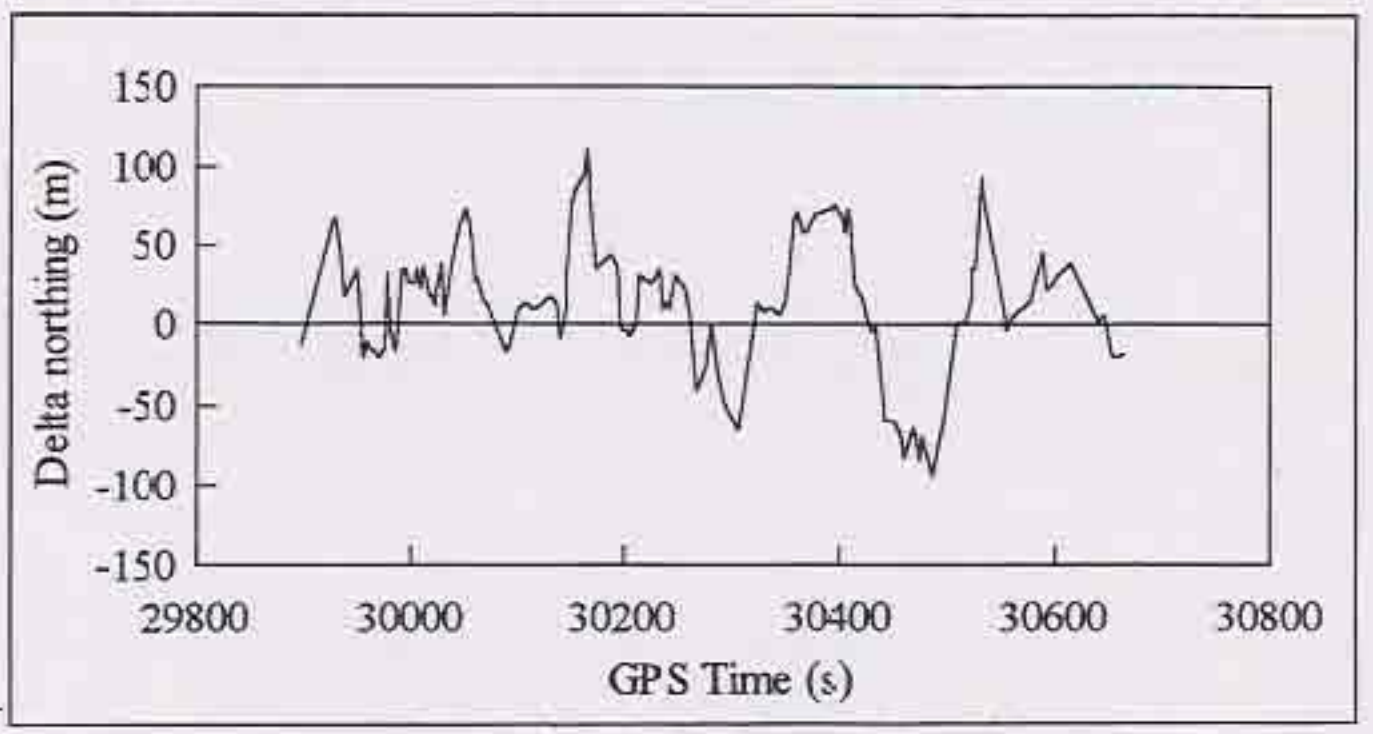

Figure 9.10 Difference in Northing Between Best DOP Fix and Precise Fix on Open Road, May 28, 1995

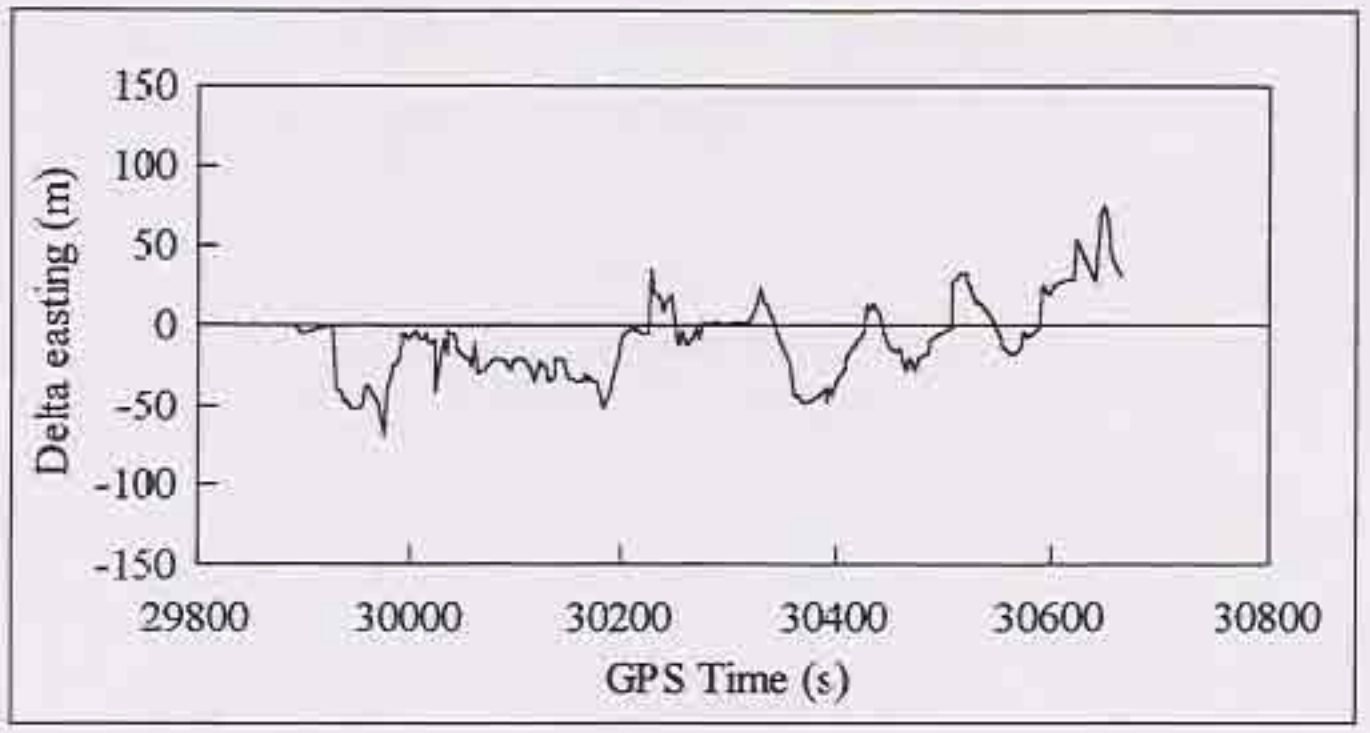

Figure 9.11 Difference in Easting Between Map Aided GPS and Precise Fix on Open Road, May 28, 1995

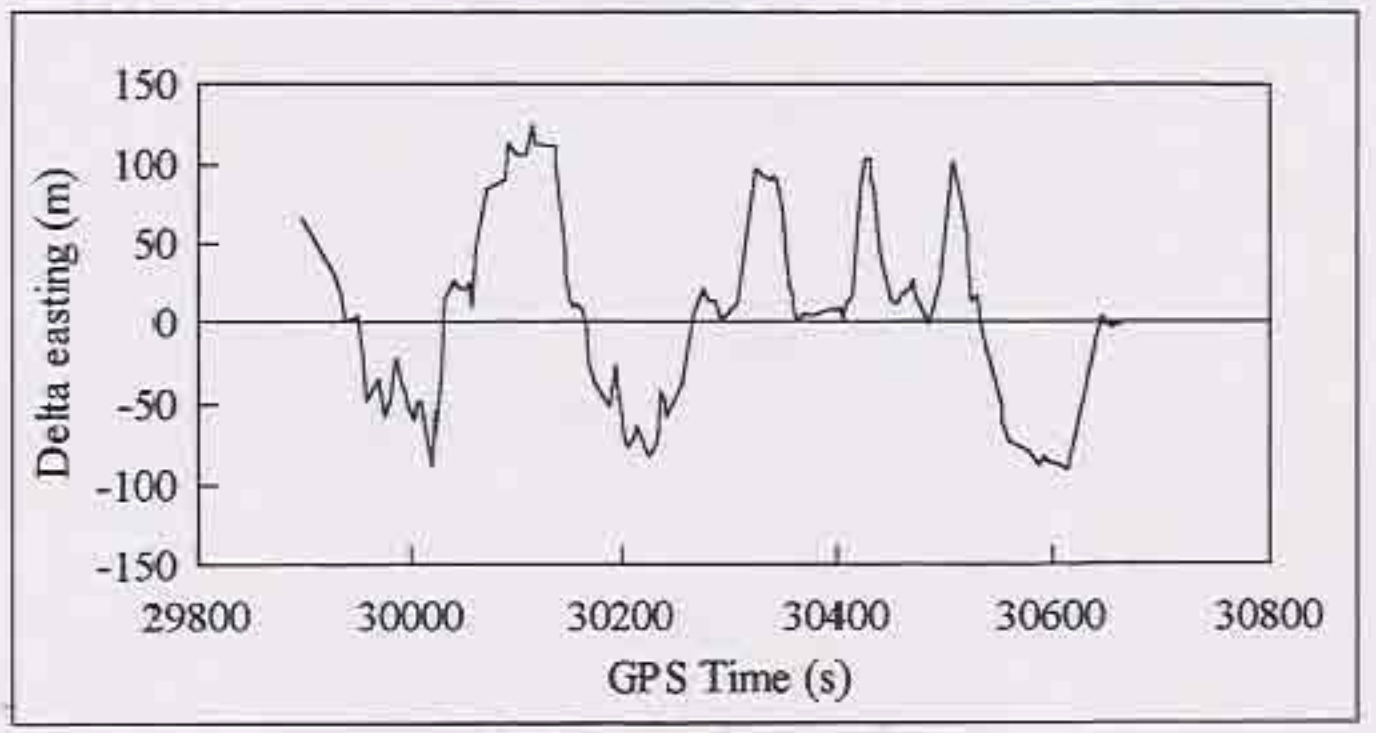

Figure 9.12 Difference in Easting Between Best DOP Fix and Precise Fix on Open Road, May 28, 1995

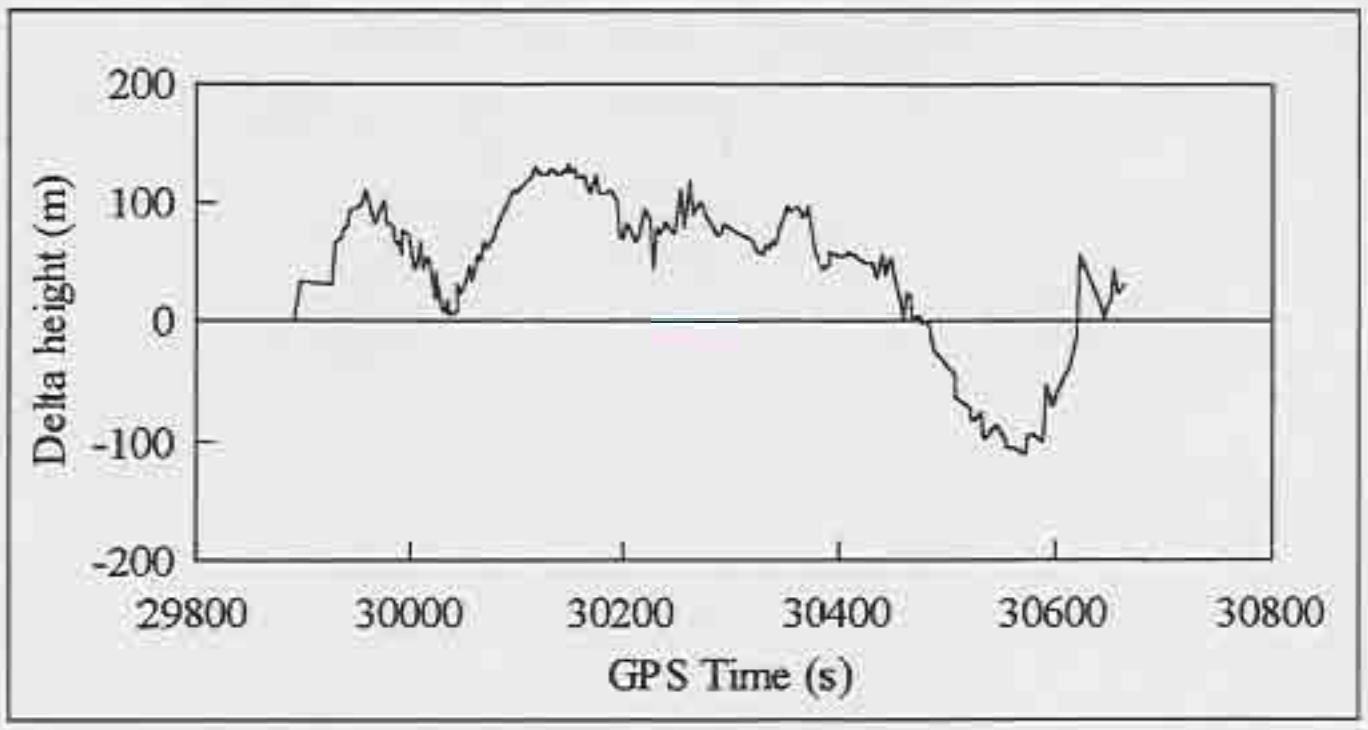

Figure 9.13 Difference in Height Between Map Aided GPS and Precise Fix on Open Road, May 28, 1995

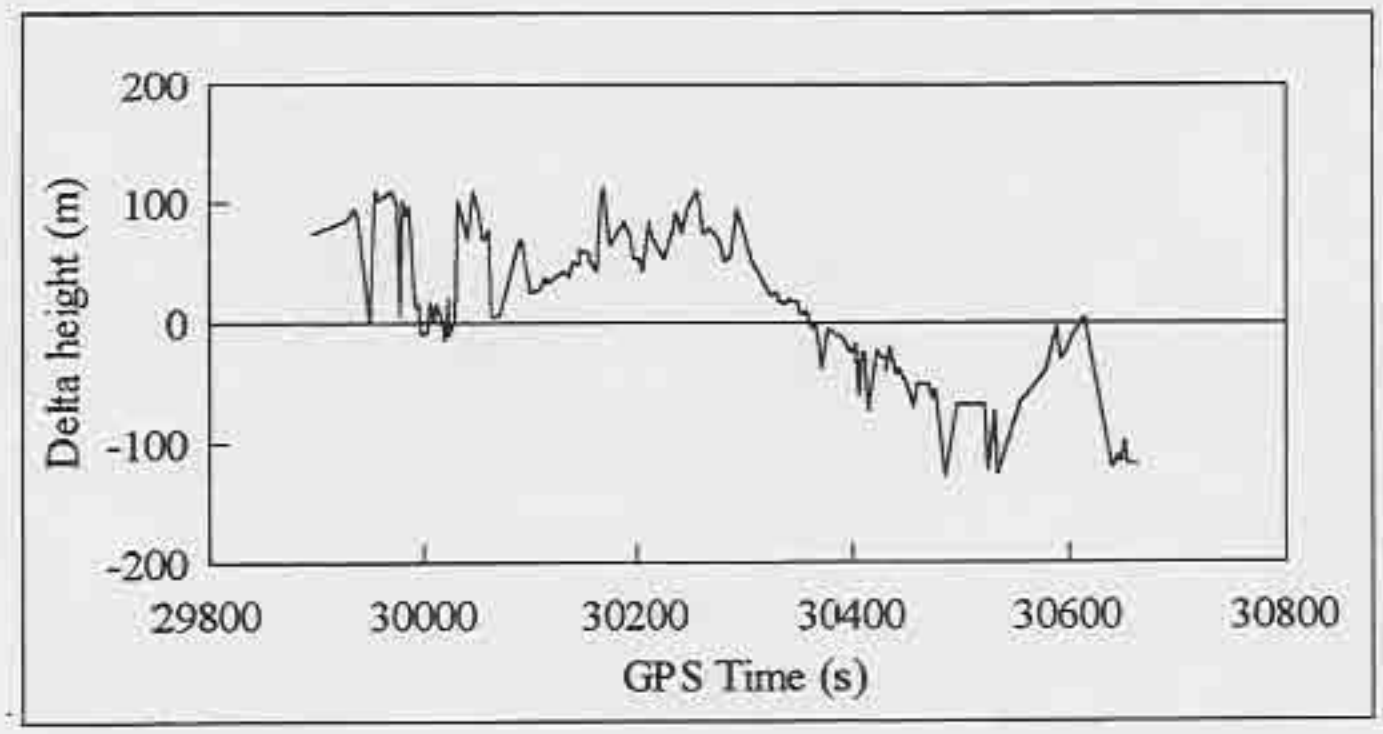

Figure 9.14 Difference in Height Between Best DOP Fix and Precise Fix on Open Road, May 28, 1995

Test 2:

The next test was done on May 29, 1995, on a major road with a speed limit of 80 km/h. Figures 9.15 to 9.18 show the plots of the four solutions of this run. The total time of the run was 379 seconds. A total of 241 best DOP fixes (one every 1.57 seconds) were recorded, while only 108 epochs (or one every 3.51 seconds) were computed.

The map aided GPS (Figure 9.15) and best DOP solutions (Figure 9.16) both performed well in this situation. The best DOP solution experienced fewer constellation changes due to a more stable HDOP (see Figure 9.19), hence was much smoother than in the previous test. The least squares solution still has a number of constellation changes because of the fact that it uses all of the measurements available in any one epoch (see Figure 9.20). The Trimble MobileGPS receiver has six channels; four are for continuously tracking the four satellites used in the best DOP fix, one is for monitoring all of the satellites and receiving updated ephemerides, and the sixth uses multiplexing to track up to four additional satellites. At each epoch, it may not be possible for the receiver to report measurements for all four of the multiplexed satellites, causing the number of available satellites (Figure 9.20) to change frequently. The end result of this situation is the noisy least squares solution.

When the best DOP solution is computed by the receiver with only three satellites, the height is held at the last known value. If this occurs at start-up, the last known value is zero. This results in a large bias in the horizontal position of the vehicle, as shown by arrow A in Figure 9.16.

In the precise solution, lane changes are sometimes apparent, as shown by arrow A in Figure 9.18. This is expected with the resolution of the precise fix being a few to several metres.

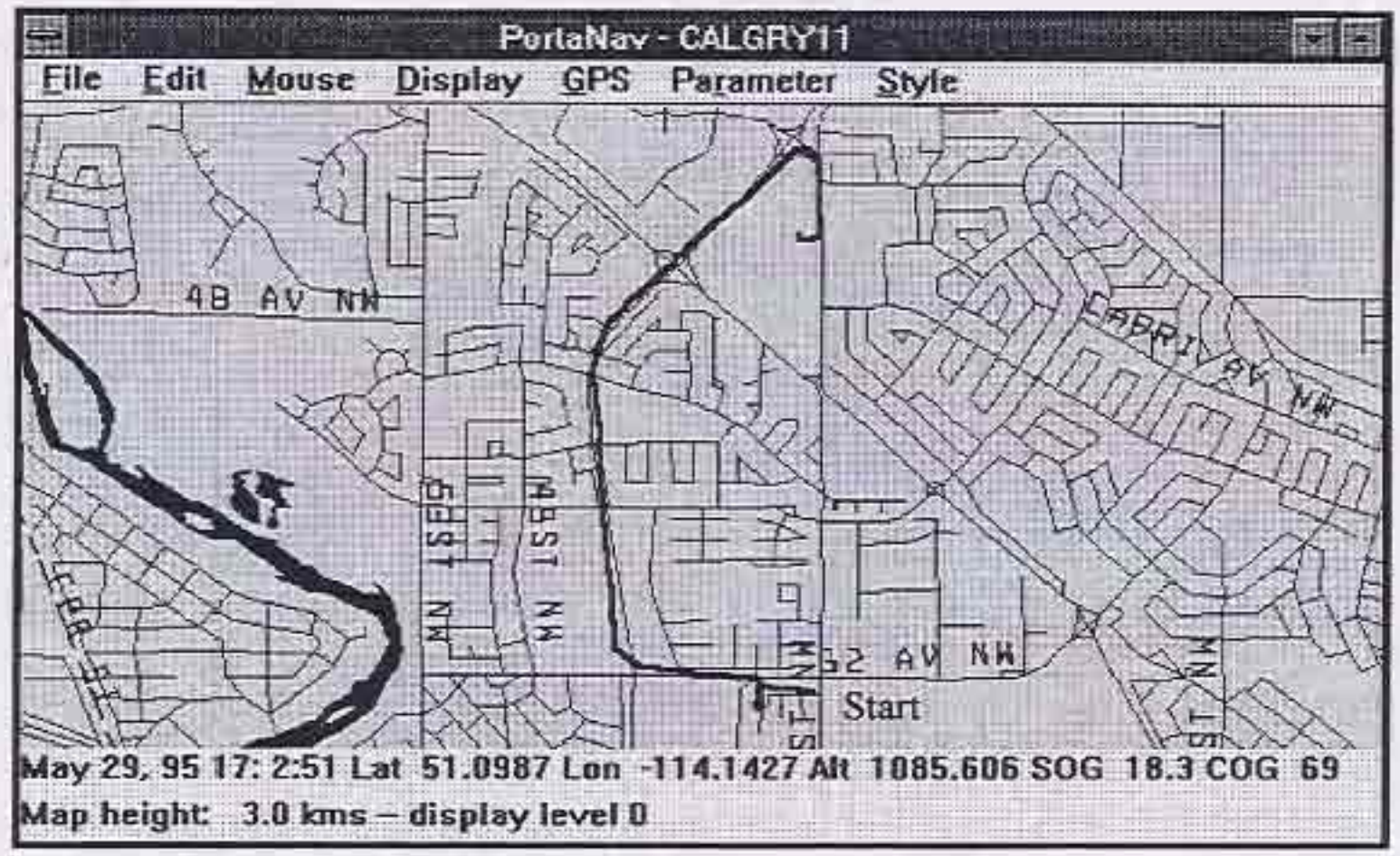

Figure 9.15 Map Aided GPS on Open Road

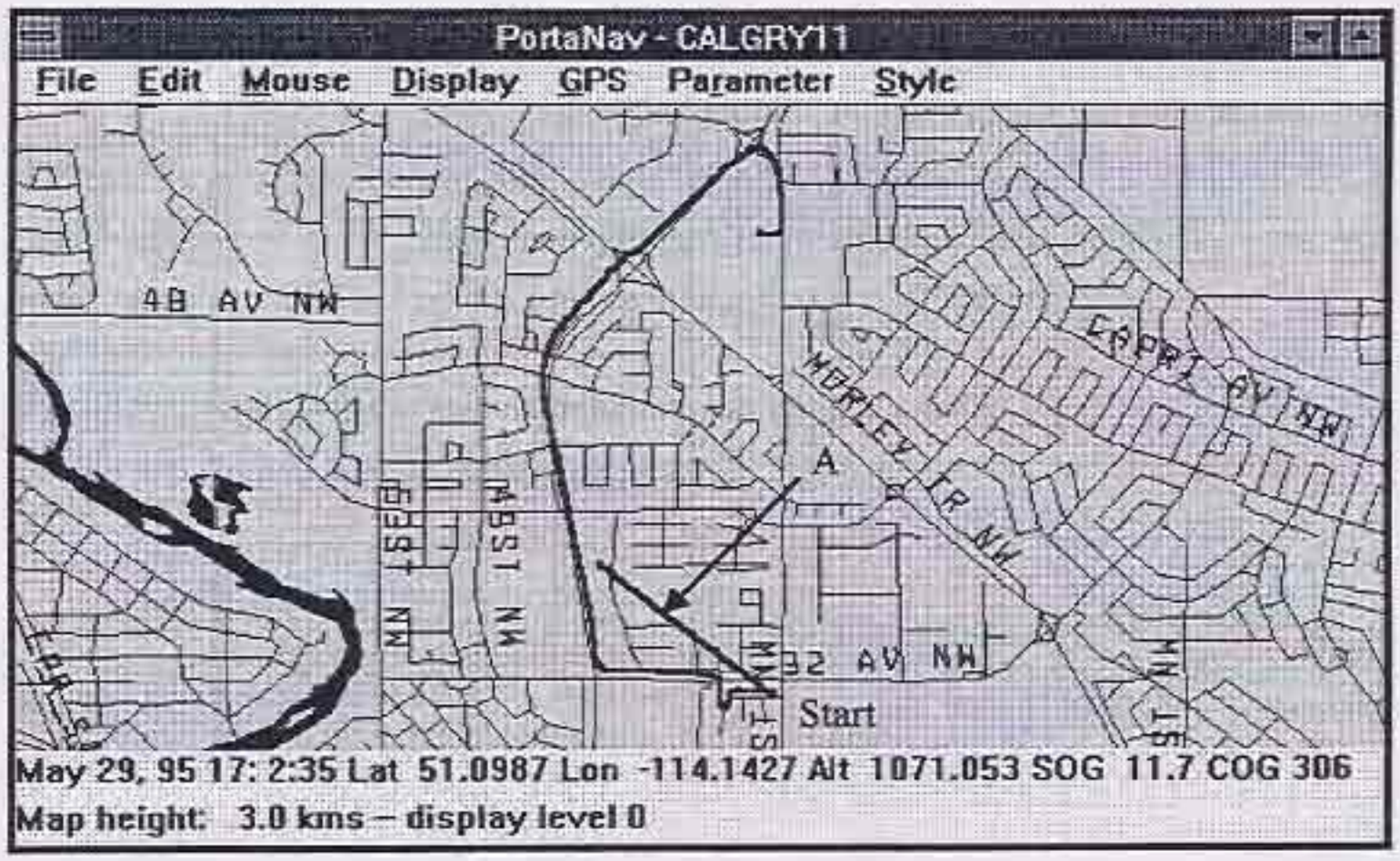

Figure 9.16 Best DOP Fix on Open Road

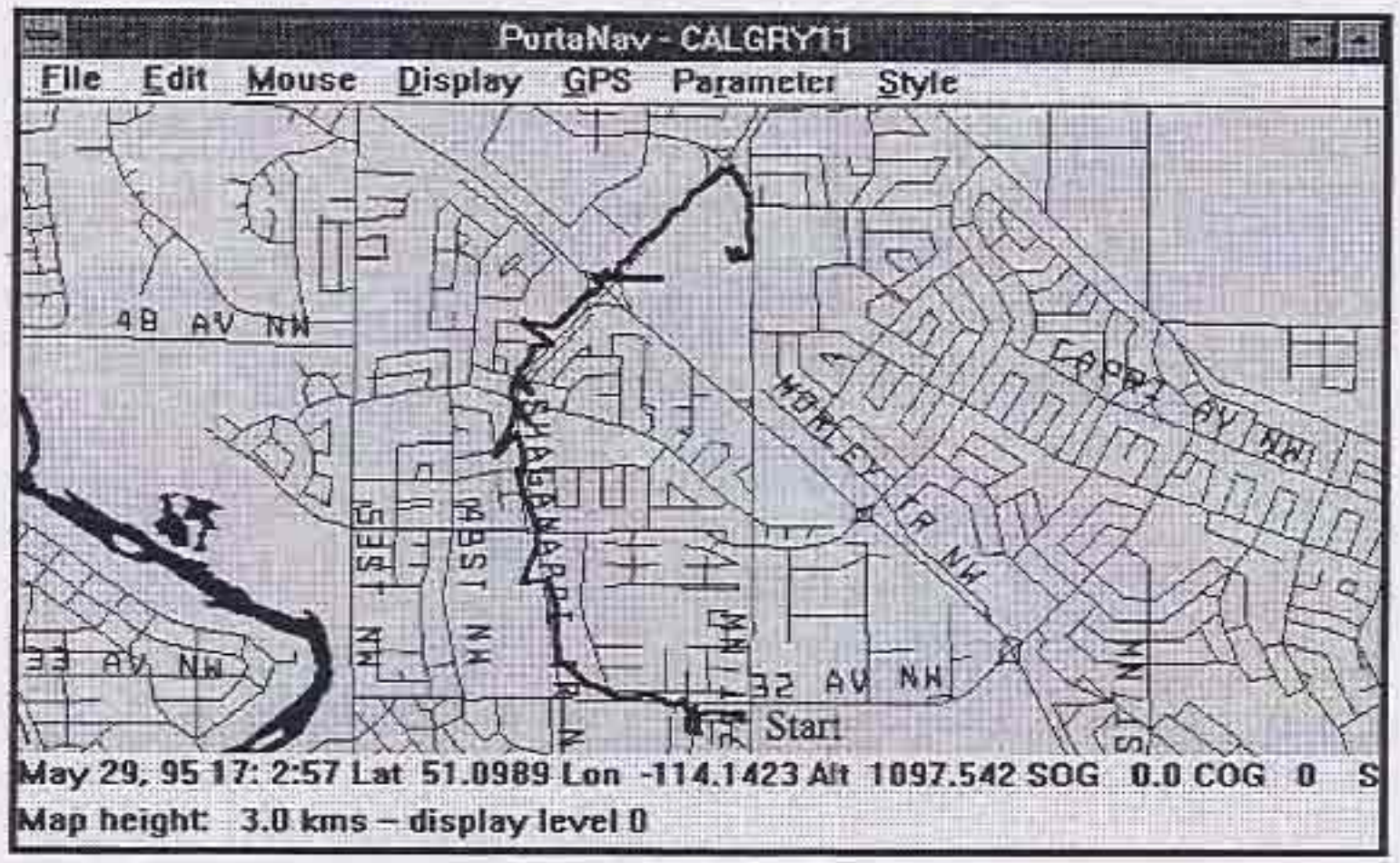

Figure 9.17 Least Squares Fix on Open Road

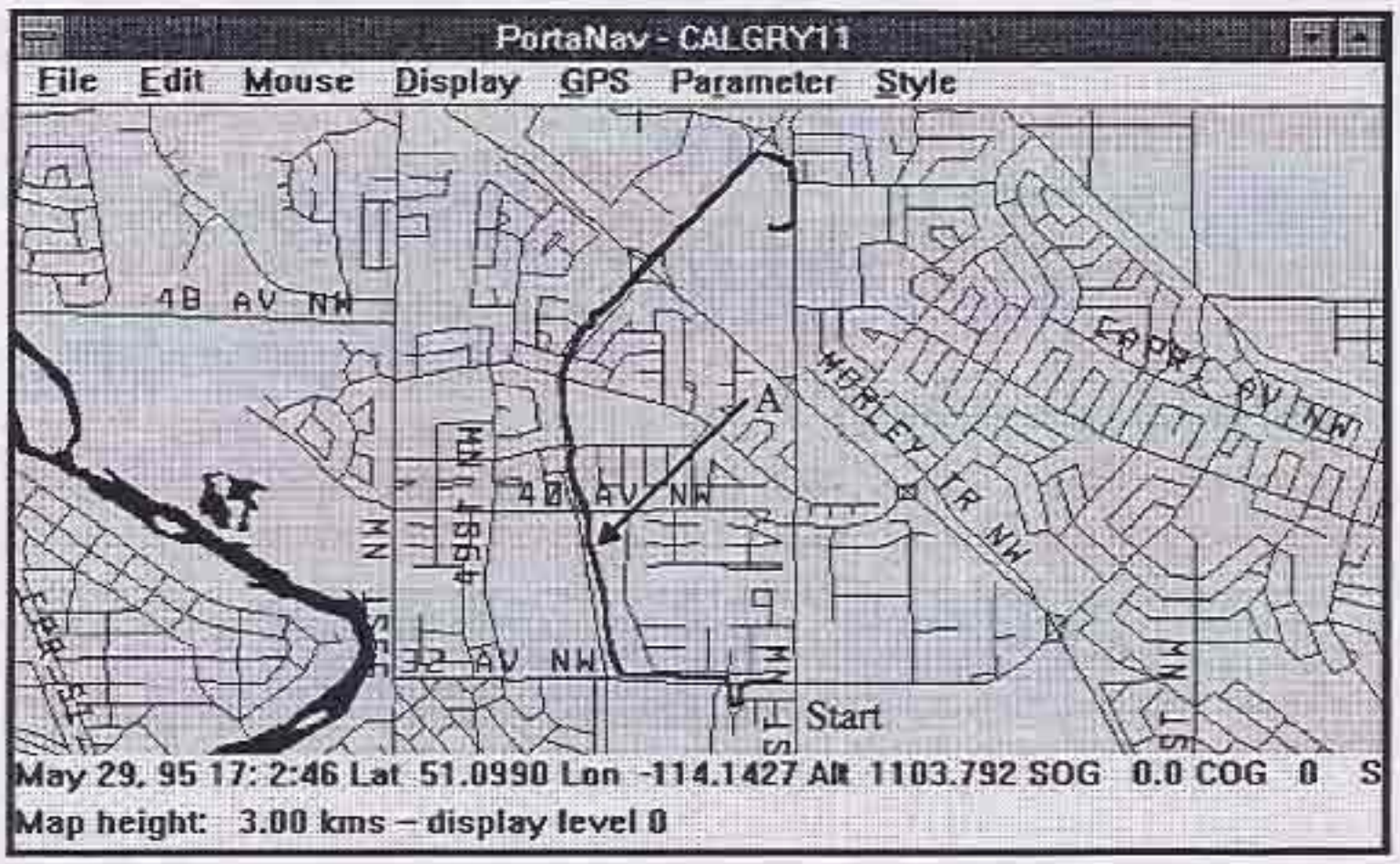

Figure 9.18 Precise Fix on Open Road

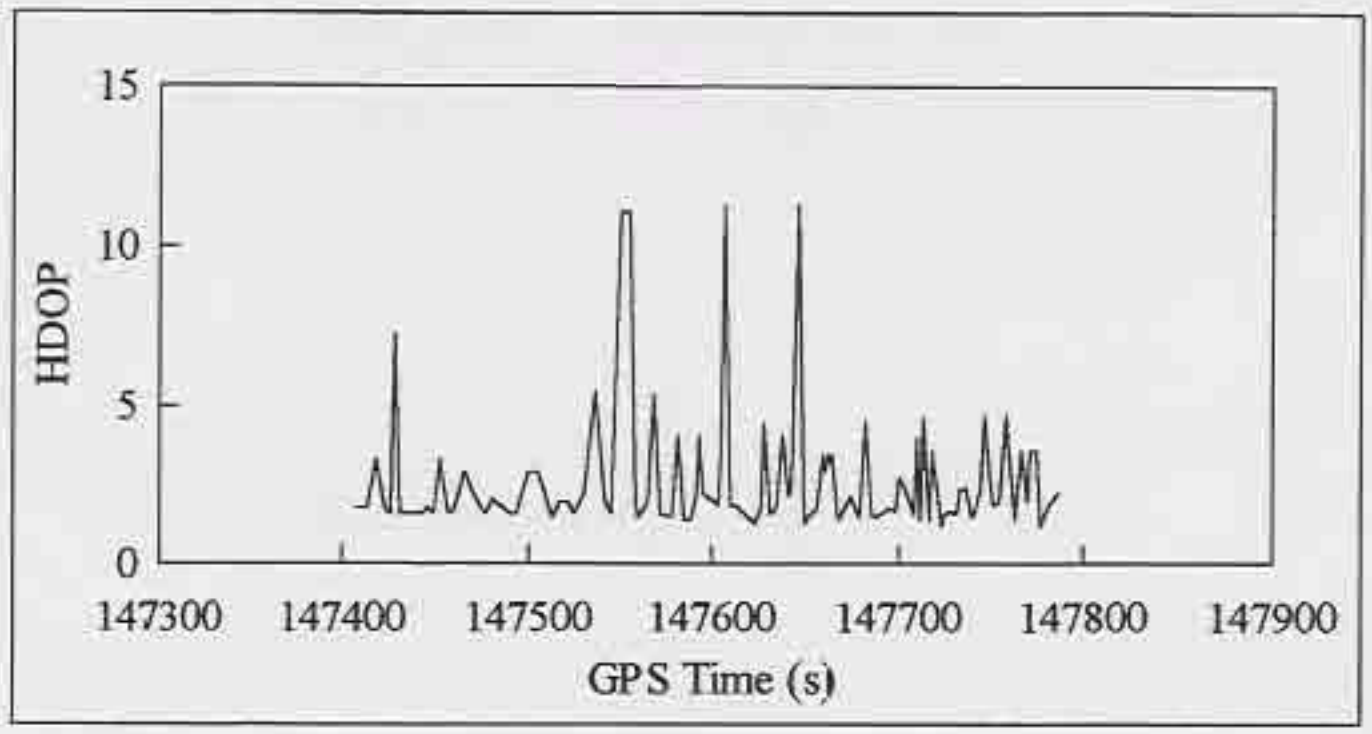

Figure 9.19 HDOP on Open Road, May 29, 1995

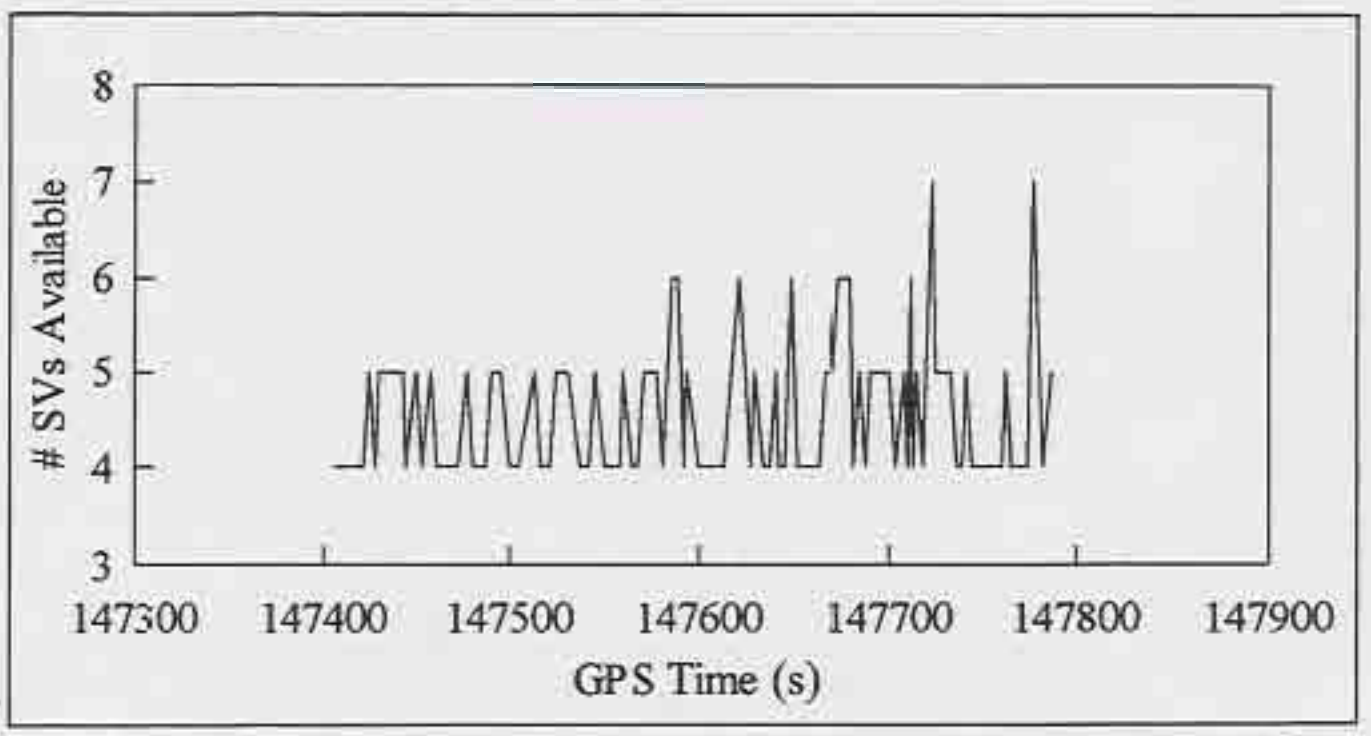

Figure 9.20 Number of Satellites Available on Open Road, May 29, 1995

Test 3:

The final open road test was done on June 2, 1995. For this test, the least squares solution was not computed in order to try and improve the data rate. Also, the constraints listed in Section 9.3 were implemented for the runs on this day. The total time of the test was 652 seconds. A total of 547 best DOP fixes (one every 1.19 seconds) were recorded, while 294 epochs (one every 2.22 seconds) were computed. The improvement in the data rate for the computed fixes is due to both the lower computational load and the use of the height aiding. As can be seen in Figure 9.23, there were a number of epochs (64) that used three satellites. If these epochs were not used, the data rate would have been about one epoch every 2.38 seconds.

Only the map aided GPS solution (Figure 9.21) and the best DOP fix (Figure 9.22) were plotted for this run. The three arrows in Figure 9.21 show cases where the azimuth was set in the filter after finding the first road after a turn occurred. Clearly the desired effect was achieved in that the roads were not overshot laterally after the map aiding. The kick starting aid helped the map aided filter avoid over and undershooting turns. Errant turns were not eliminated altogether.

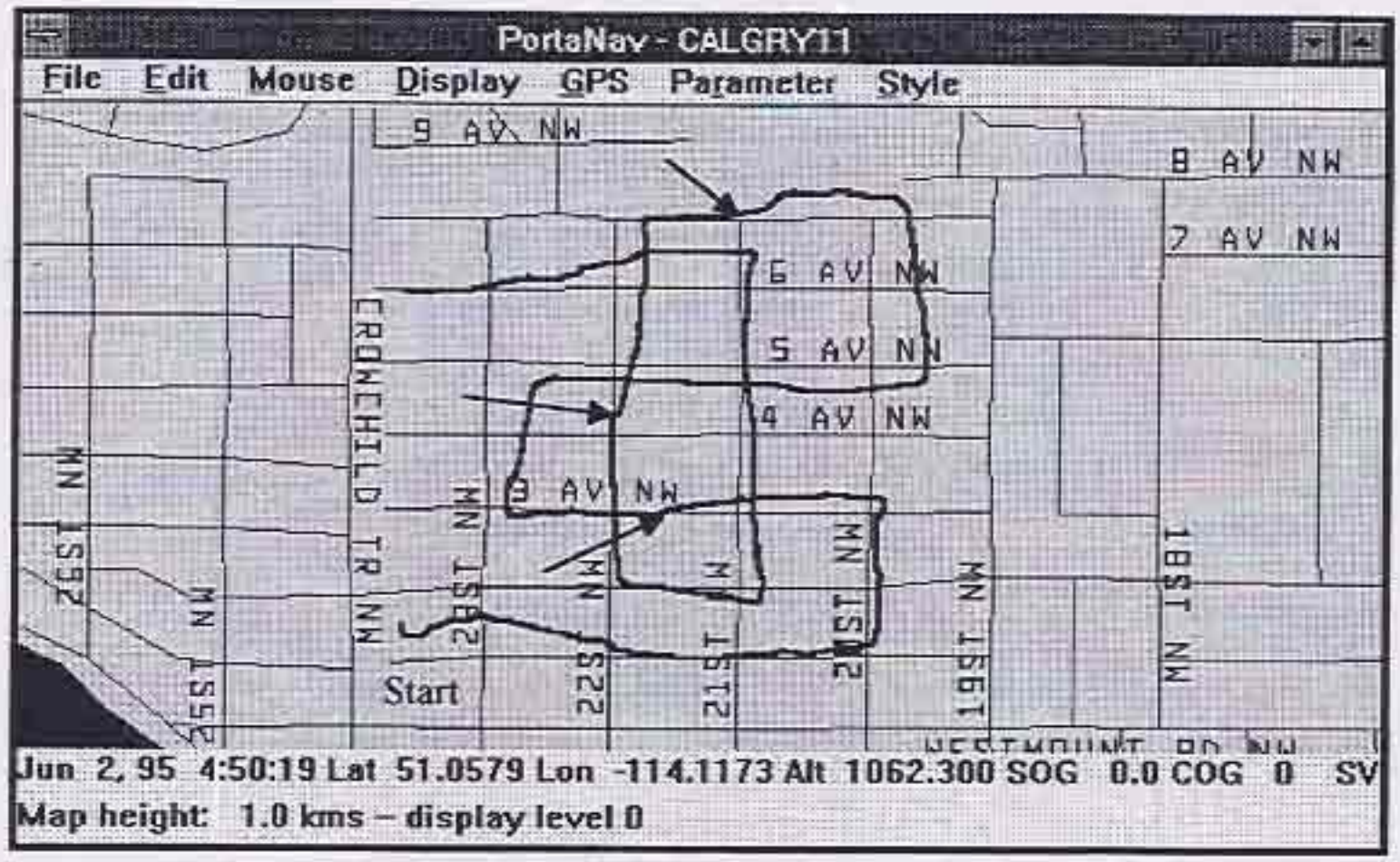

Figure 9.21 Map Aided GPS on Open Road

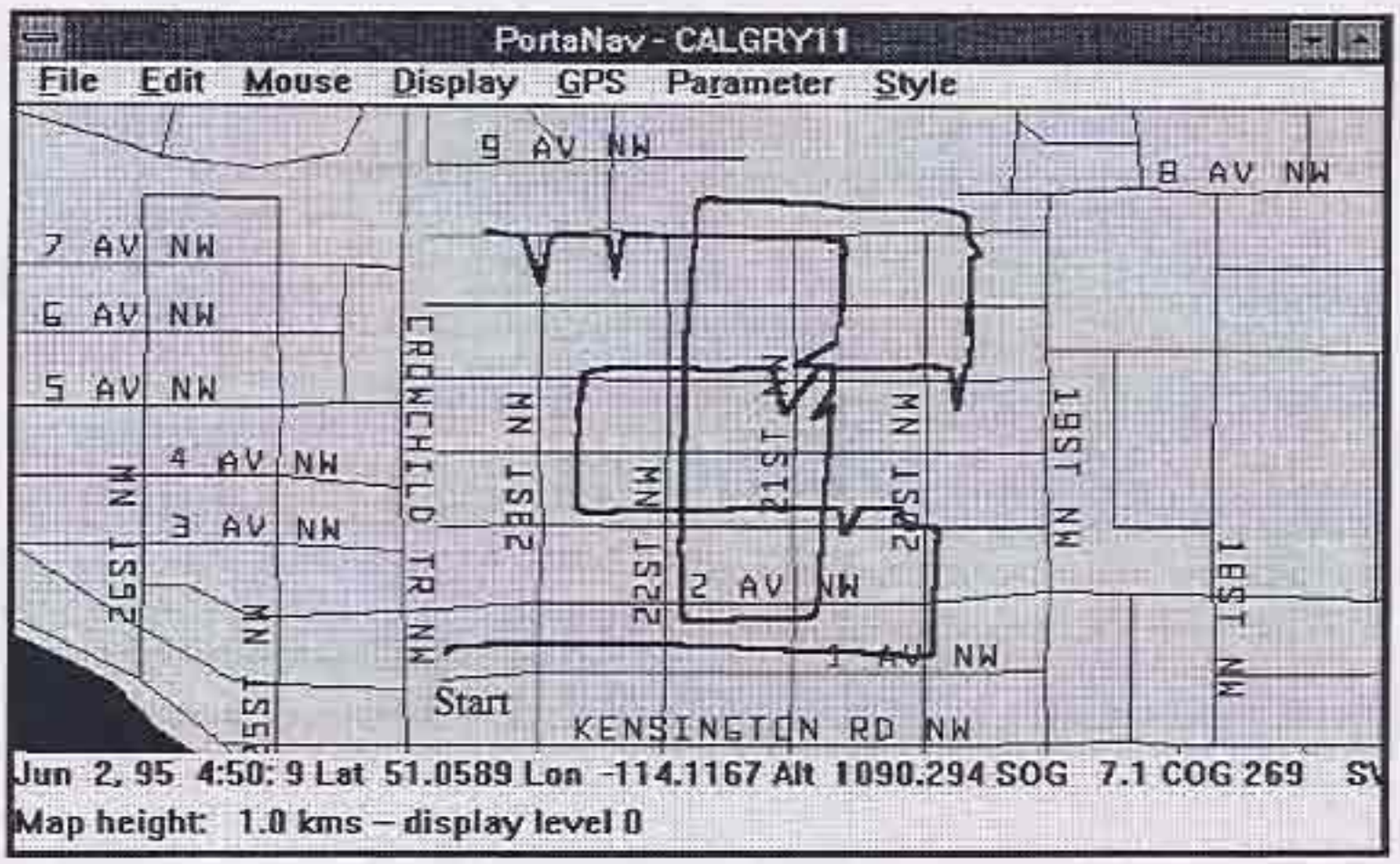

Figure 9.22 Best DOP Fix on Open Road

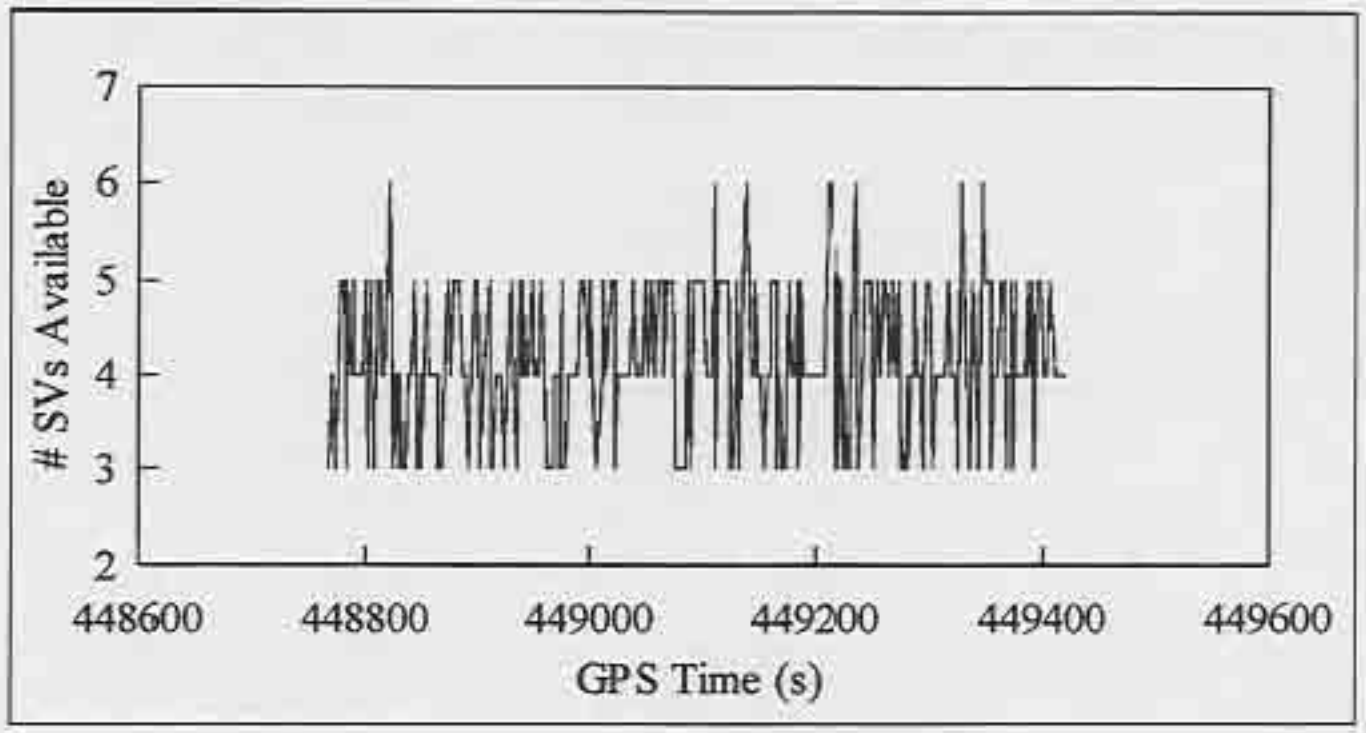

Figure 9.23 Number of Satellites Available on Open Road, June 2, 1995

9.4.3 *Tree Canopy Tests*

The area used for tree canopy testing has narrow roads, apartment buildings that are two to ten stories high, and large trees that occasionally cover the entire roadway. The effect of the trees and other obstacles is to block, reflect, and attenuate satellite signals, thereby decreasing GPS performance. The purpose of these tests was to see how much the map aided filter improved the situation as compared to stand-alone GPS.

Test 1:

The first test was done on May 27, 1995, and the plots of the four solutions appear in Figures 9.24 to 9.27. The duration of this run was 707 seconds. A total of 444 best DOP fixes (one every 1.59 seconds) were recorded, while only 205 epochs (one every 3.45 seconds) were computed. Plots of HDOP and number of satellites available are shown in Figures 9.28 and 9.29. There is a significant increase in the variation of the HDOP in this run over the second open road test.

The effect of the tree canopy on the best DOP and least squares fixes is an increased number of constellation changes, hence several large shifts in the position occur due to SA. The trajectory of the map aided solution is much smoother than the best DOP fix, and hence is much more pleasing to the end user. In this run, the correct road of travel was identified by the map aided GPS solution at all points along the trajectory. The best DOP and least squares solutions have a few ambiguous areas where there are large spikes in the trajectory.

In the map aided GPS solution (Figure 9.24), there are a few areas marked with arrows that show the lateral overcorrections of the filter when using map-derived updates. The software for this run did not have the constraints implemented as described in Section 9.3.2. Using the azimuth to set the velocity states when a road is found after a turn would have prevented these overcorrections.

The precise fix plot shown in Figure 9.27 reveals a map bias in the region to the south and the west. The spikes in this plot are due to the effects of mild multipath, while the remaining variation is due to the receiver noise.

Plots showing the difference in northing, easting, and height for map aided GPS and best DOP fix with respect to the precise solution are given in Figures 9.30 to 9.35. The map aided filter shows a large improvement again in both stability and absolute accuracy. Recall that multipath affects the precise fixes so both large spikes and small noise are introduced into the differenced plots for the map aided solution. Large spikes that appear in both of the difference plots are due to multipath in the precise solution. The smoothness of the trend curve and the magnitude of the variation of this trend curve are the traits that are attributed to the map aided solution itself.

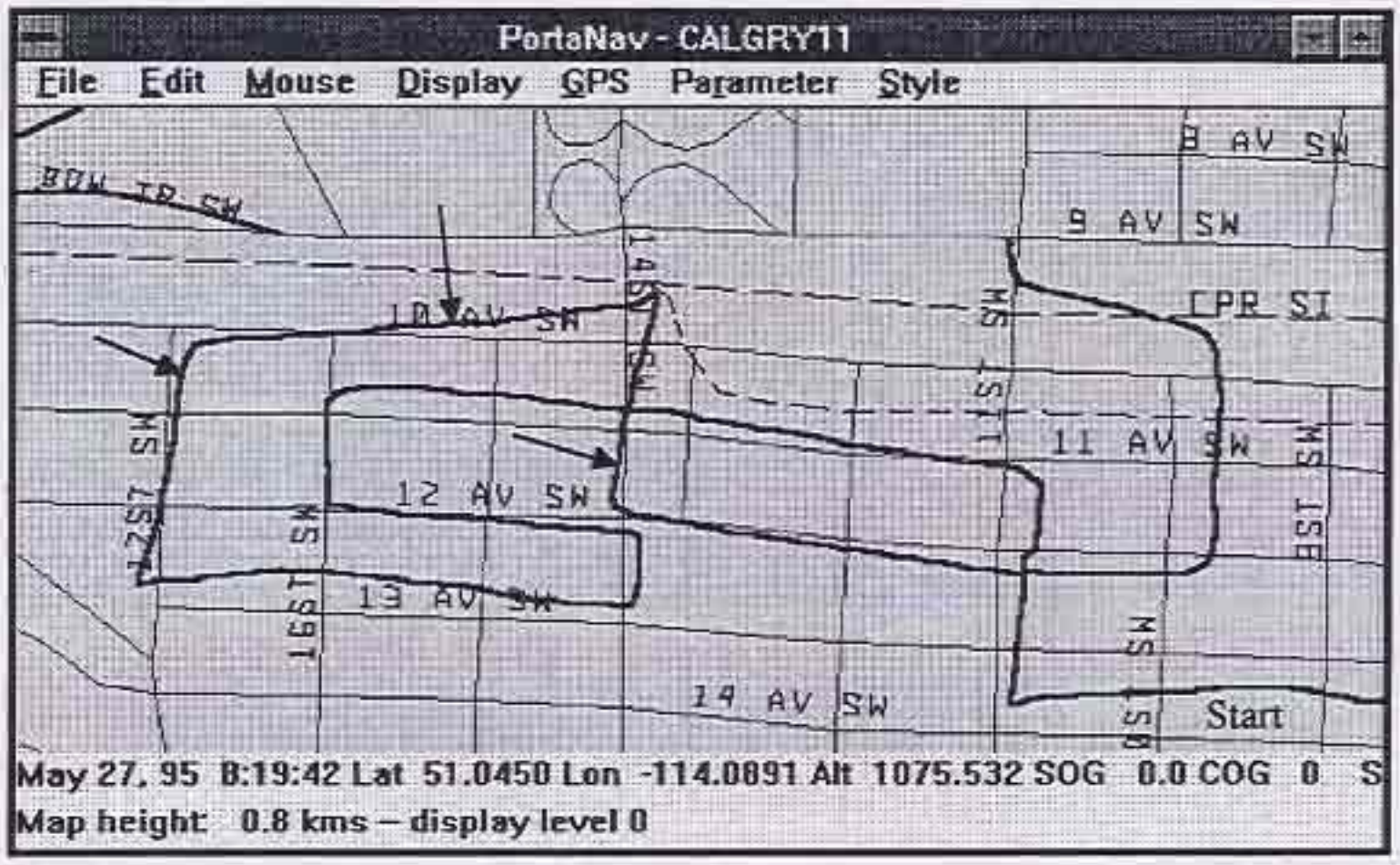

Figure 9.24 Map Aided GPS in Tree Canopy

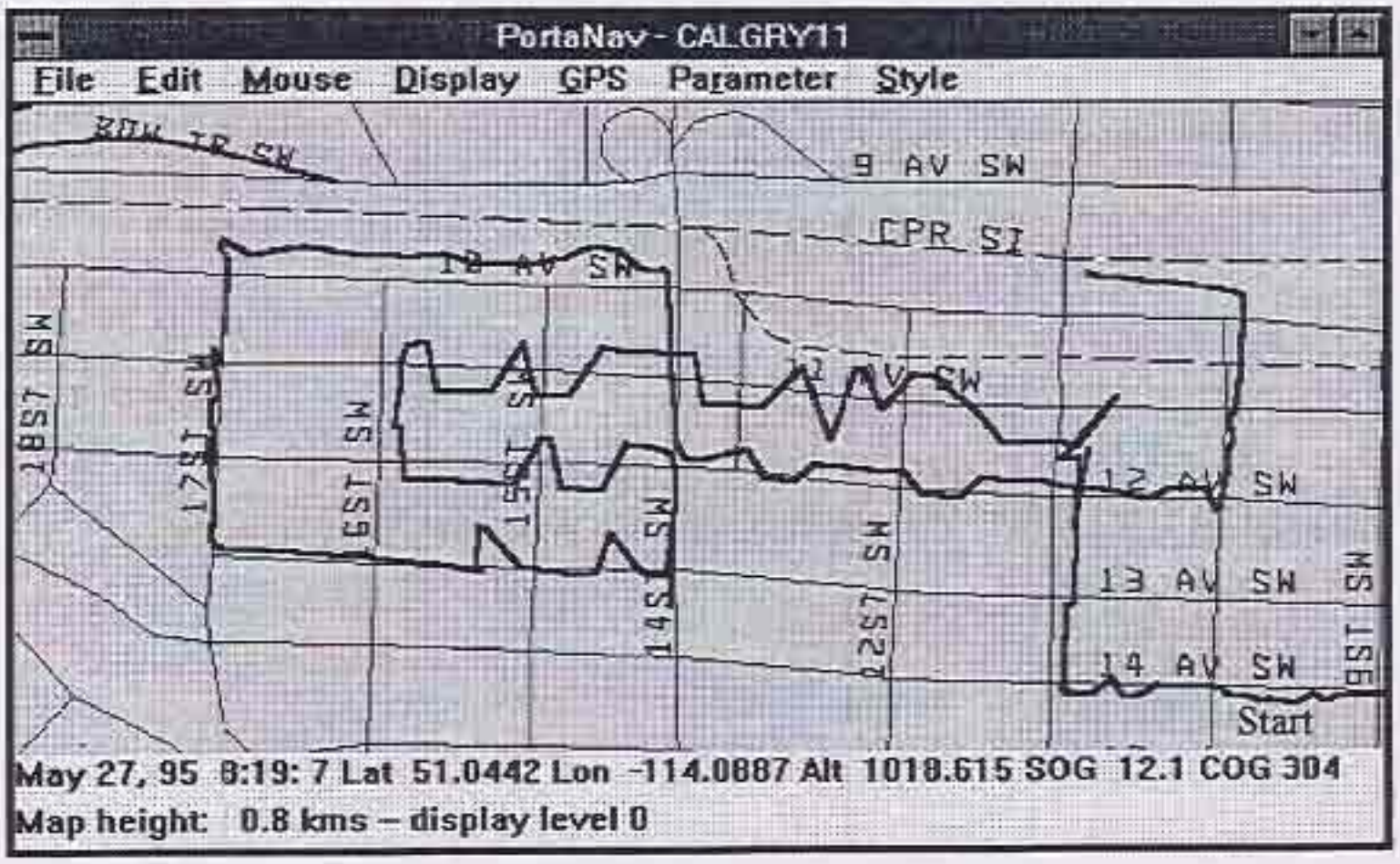

Figure 9.25 Best DOP Fix in Tree Canopy

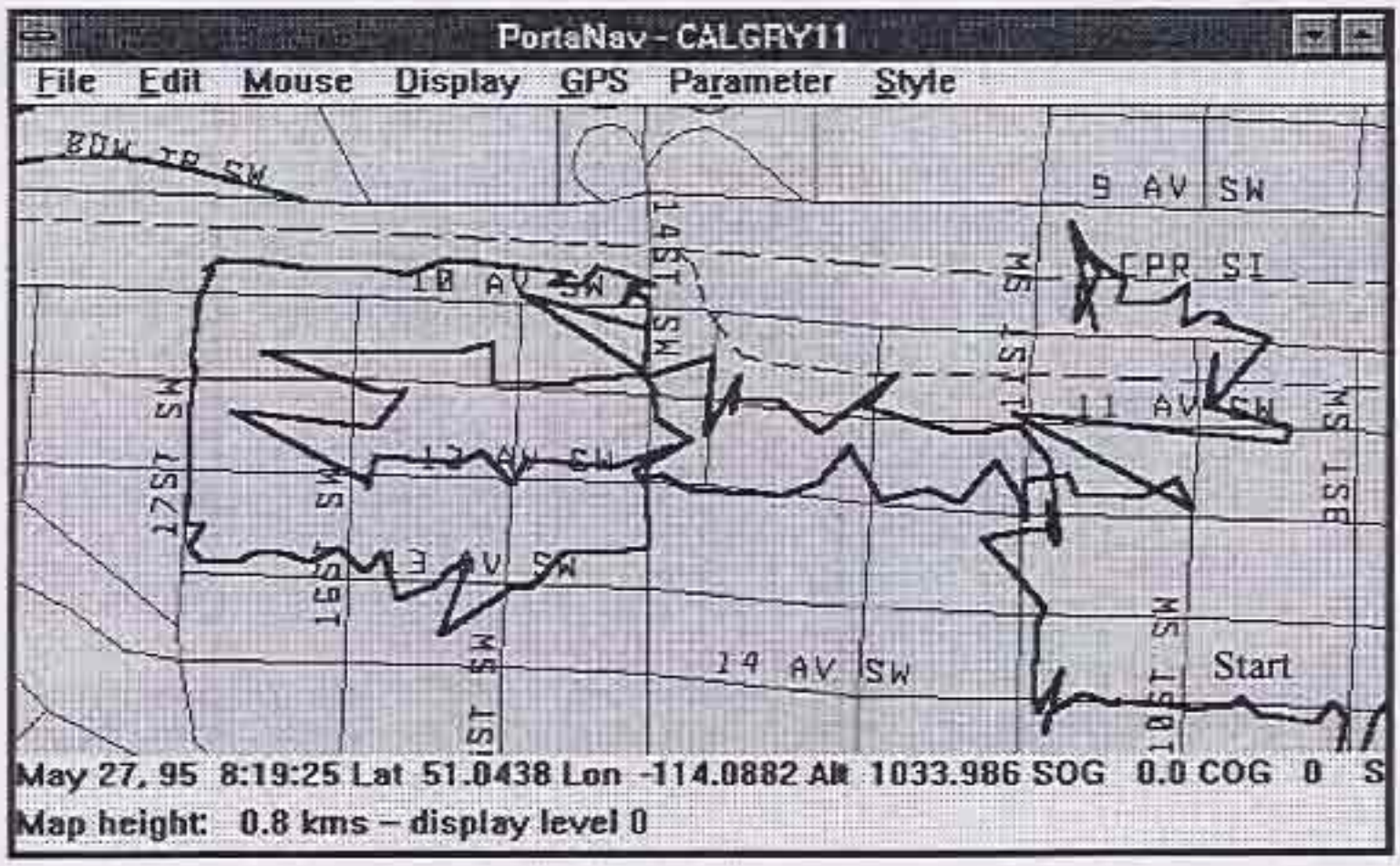

Figure 9.26 Least Squares Fix in Tree Canopy

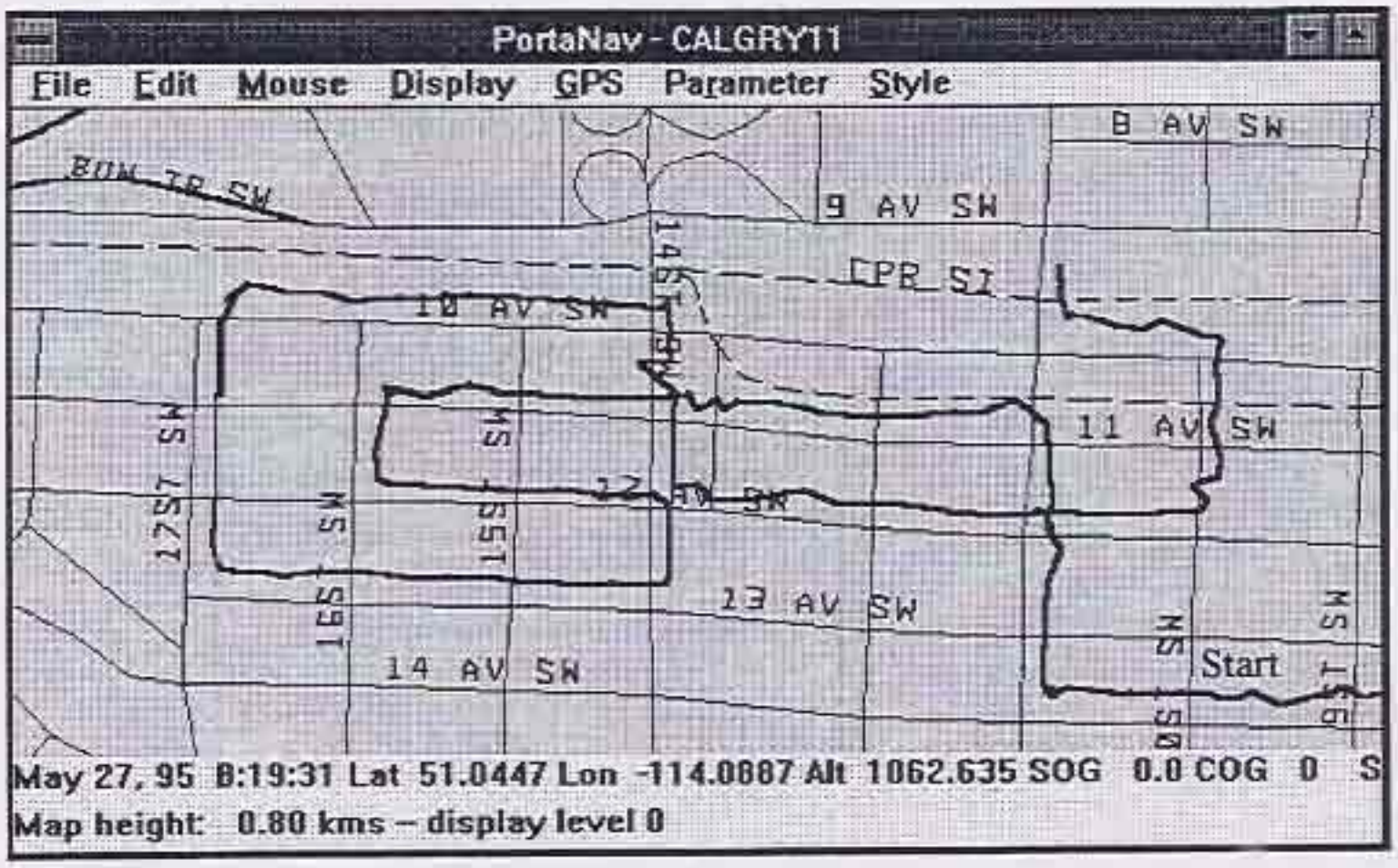

Figure 9.27 Precise Fix in Tree Canopy

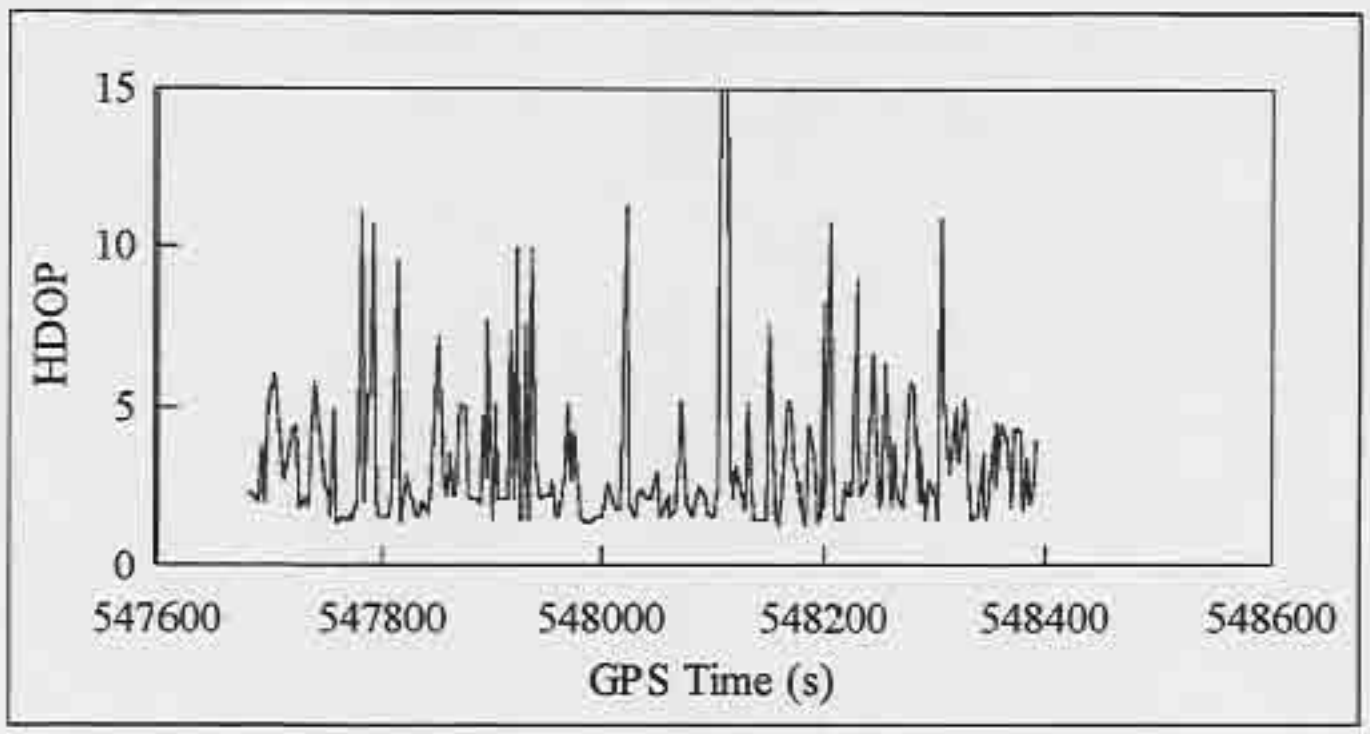

Figure 9.28 HDOP in Tree Canopy, May 27, 1995

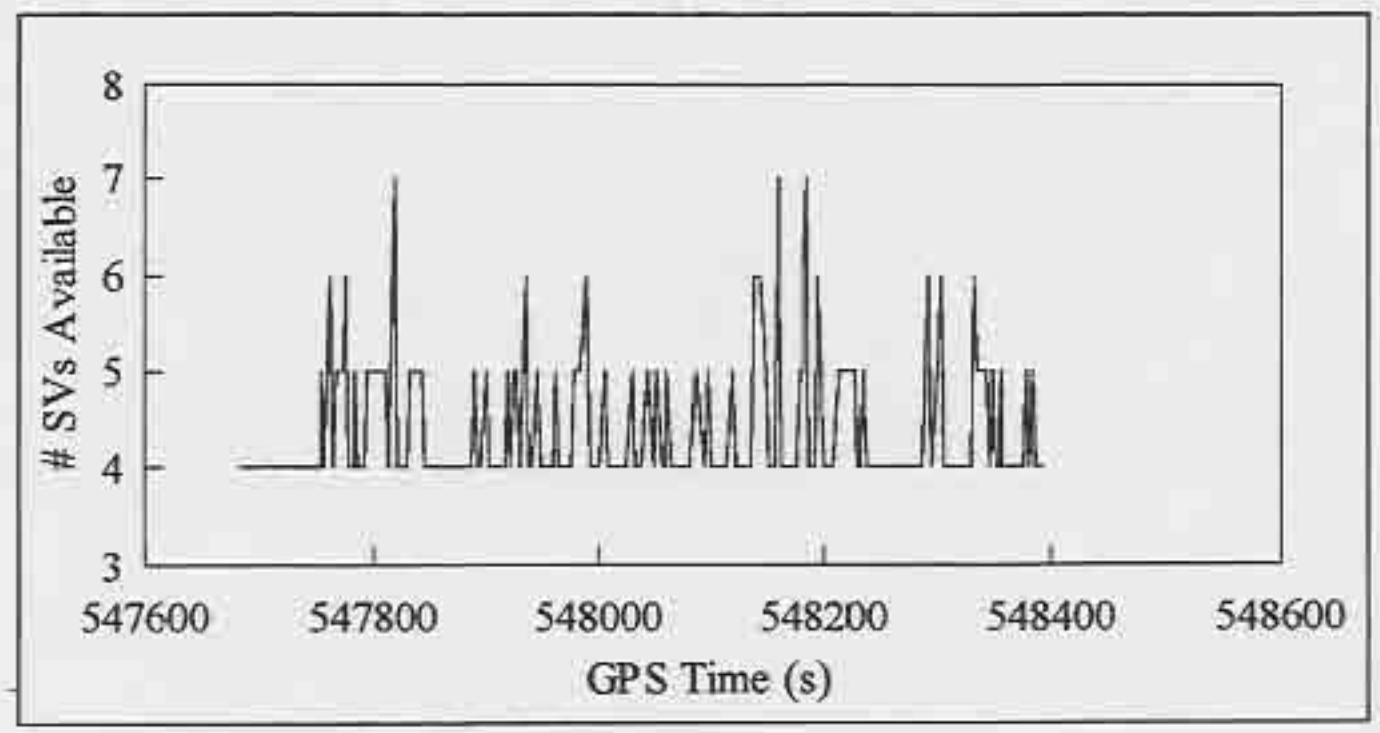

Figure 9.29 Number of Satellites Available in Tree Canopy, May 27, 1995

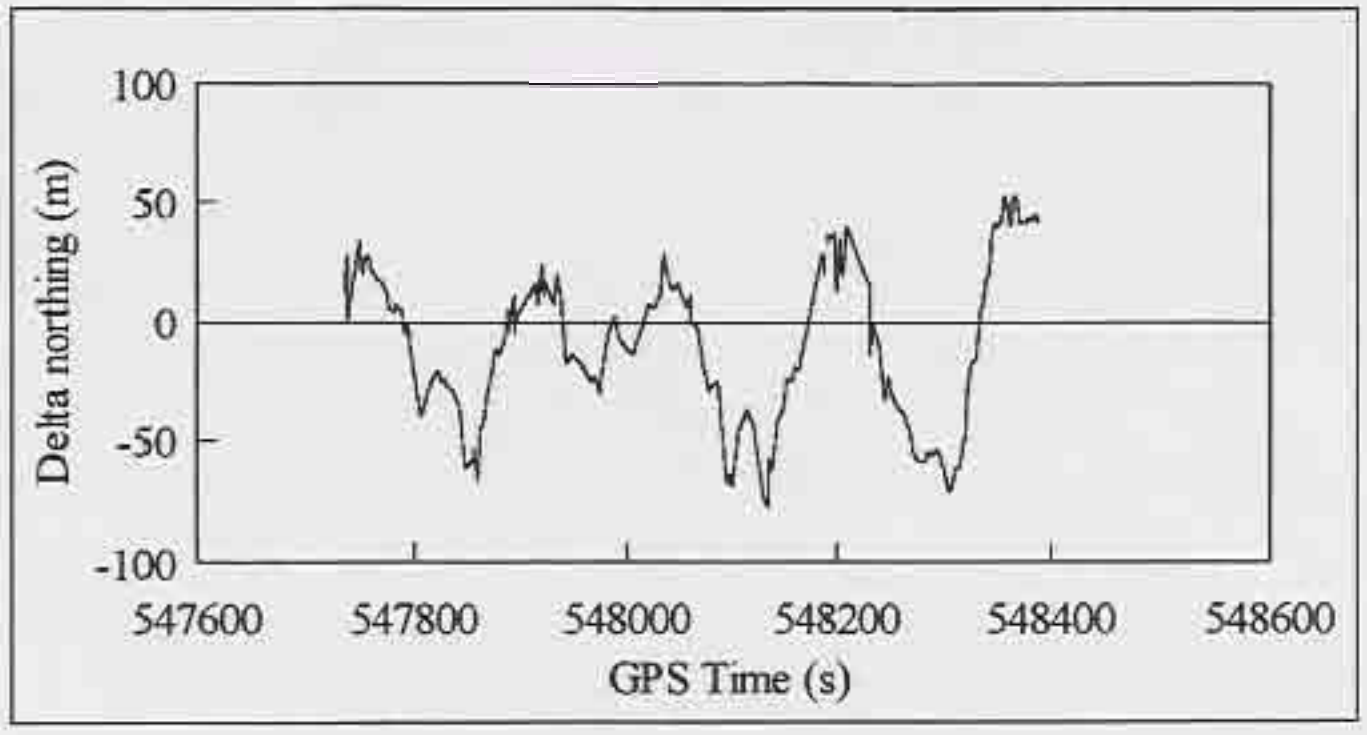

Figure 9.30 Difference in Northing Between Map Aided GPS and Precise Fix in Tree Canopy, May 27, 1995

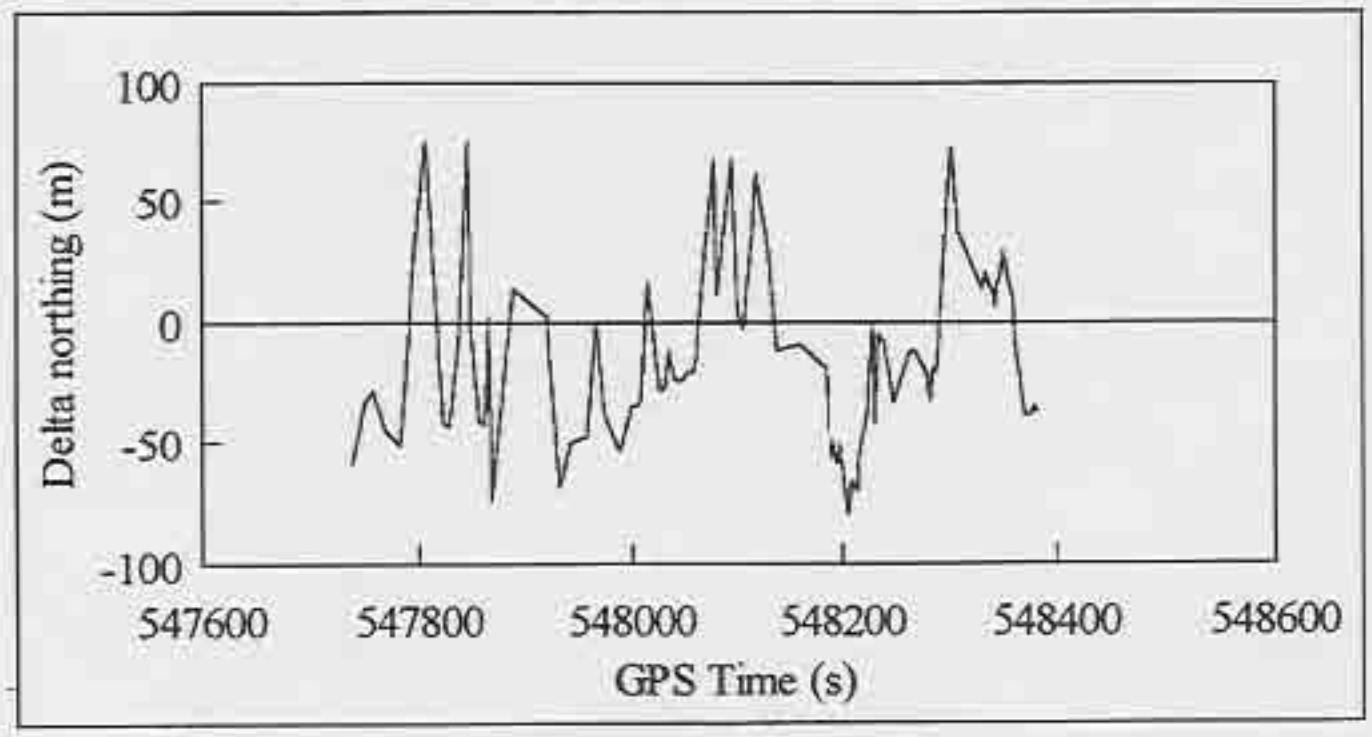

Figure 9.31 Difference in Northing Between Best DOP Fix and Precise Fix in Tree Canopy, May 27, 1995

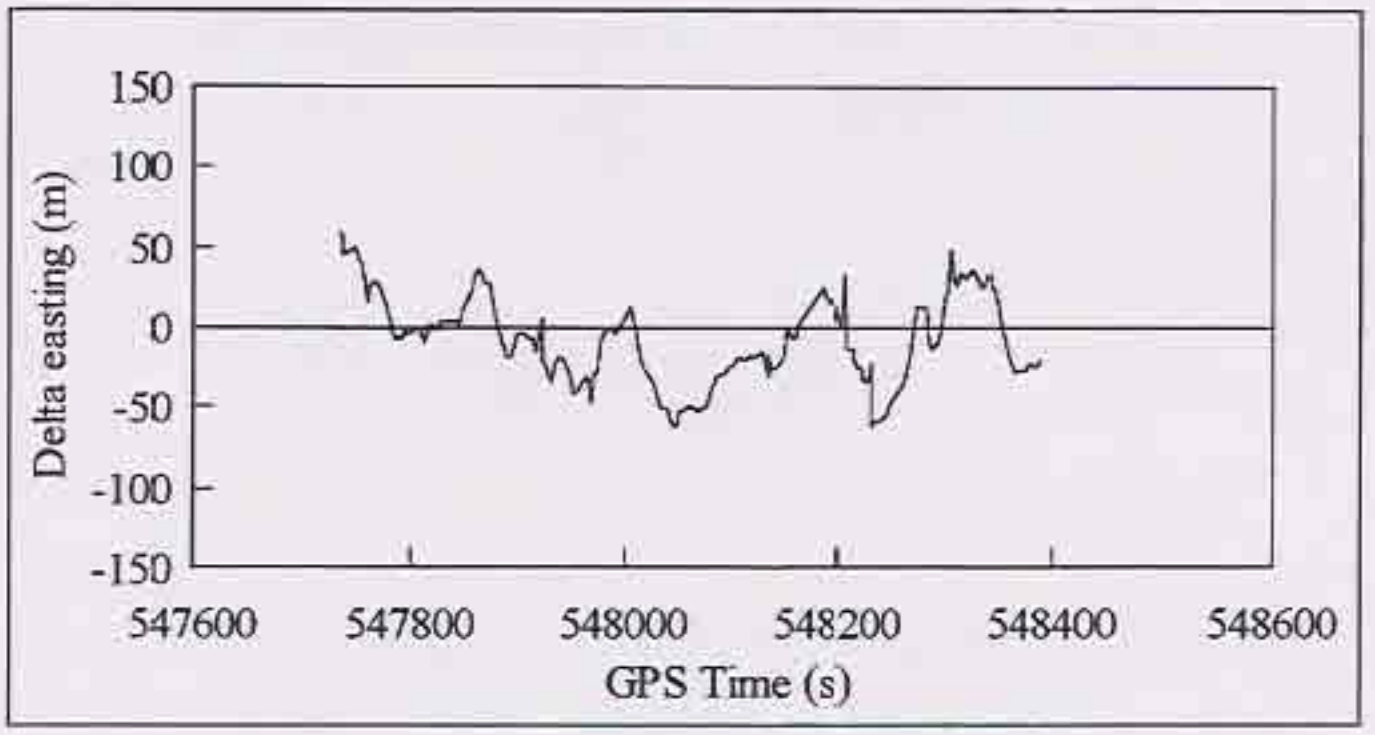

Figure 9.32 Difference in Easting Between Map Aided GPS and Precise Fix in Tree Canopy, May 27, 1995

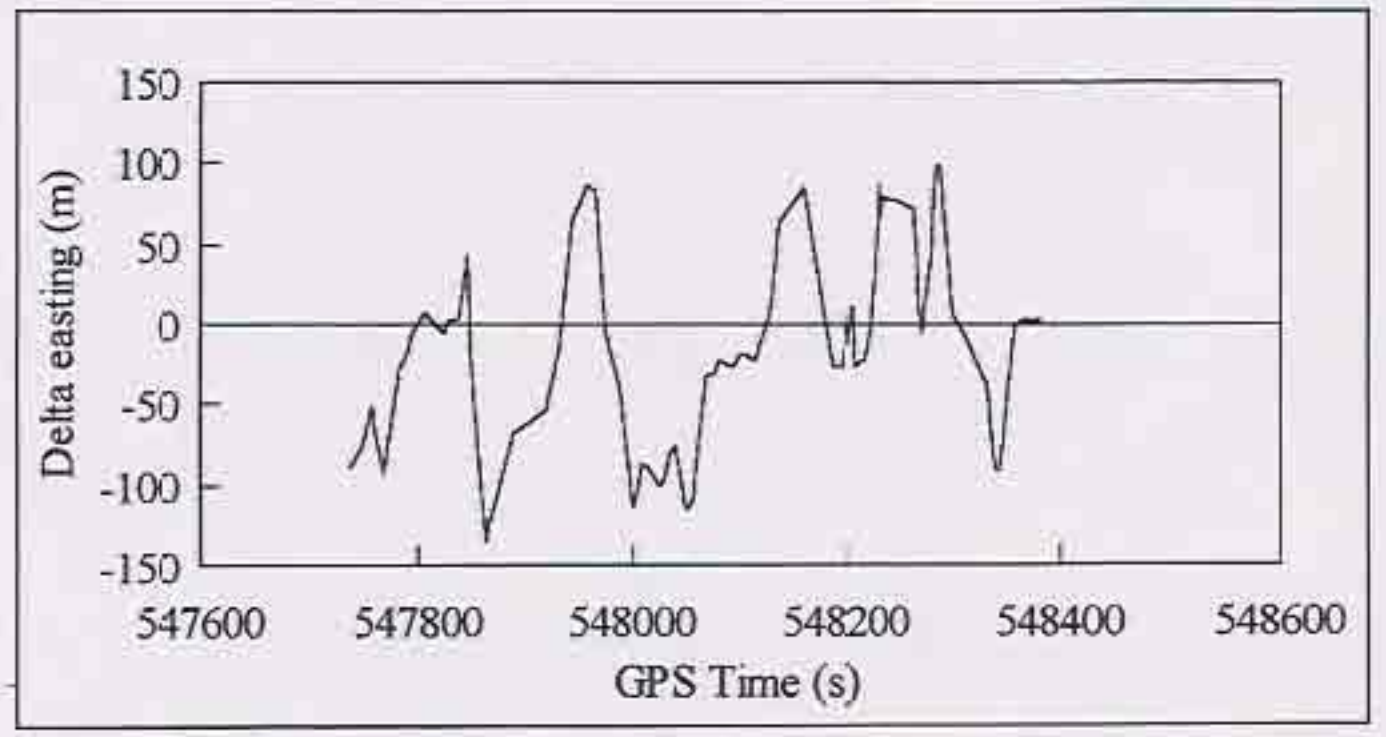

Figure 9.33 Difference in Easting Between Best DOP Fix and Precise Fix in Tree Canopy, May 27, 1995

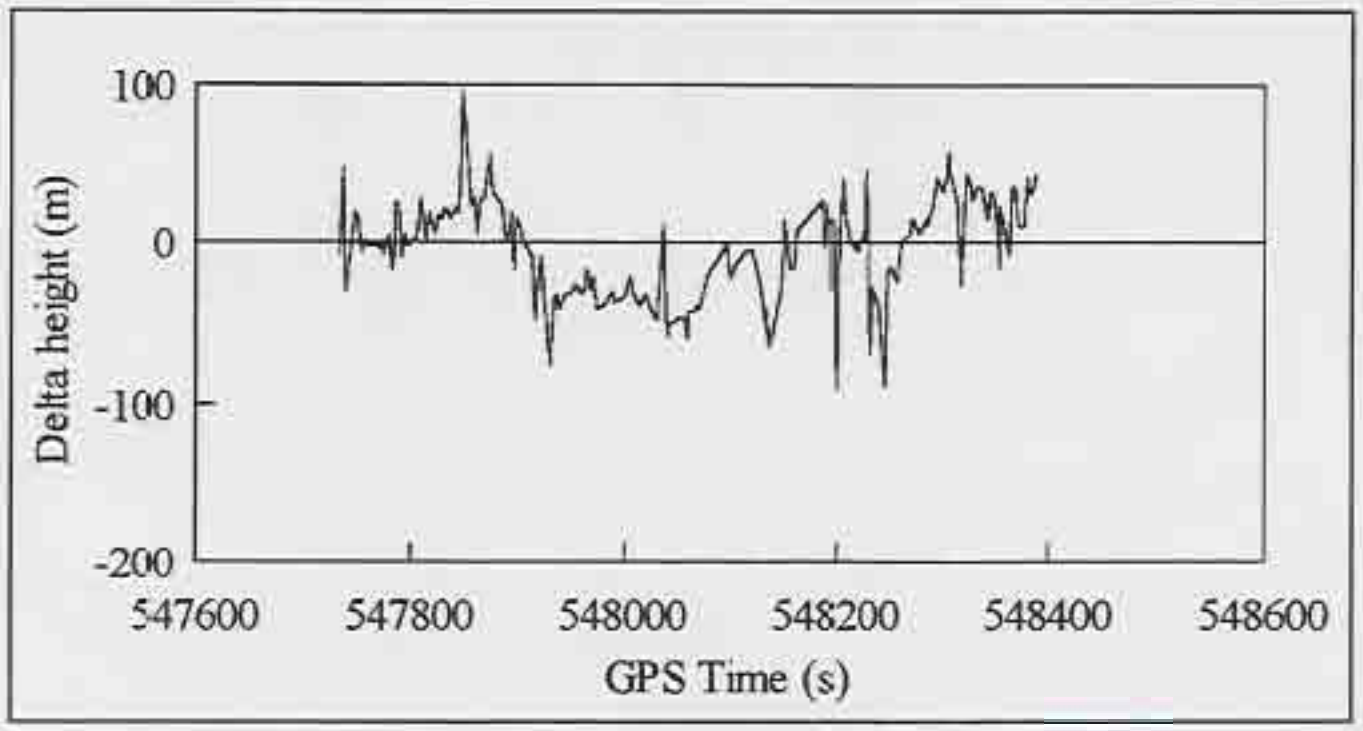

Figure 9.34 Difference in Height Between Map Aided GPS and Precise Fix in Tree Canopy, May 27, 1995

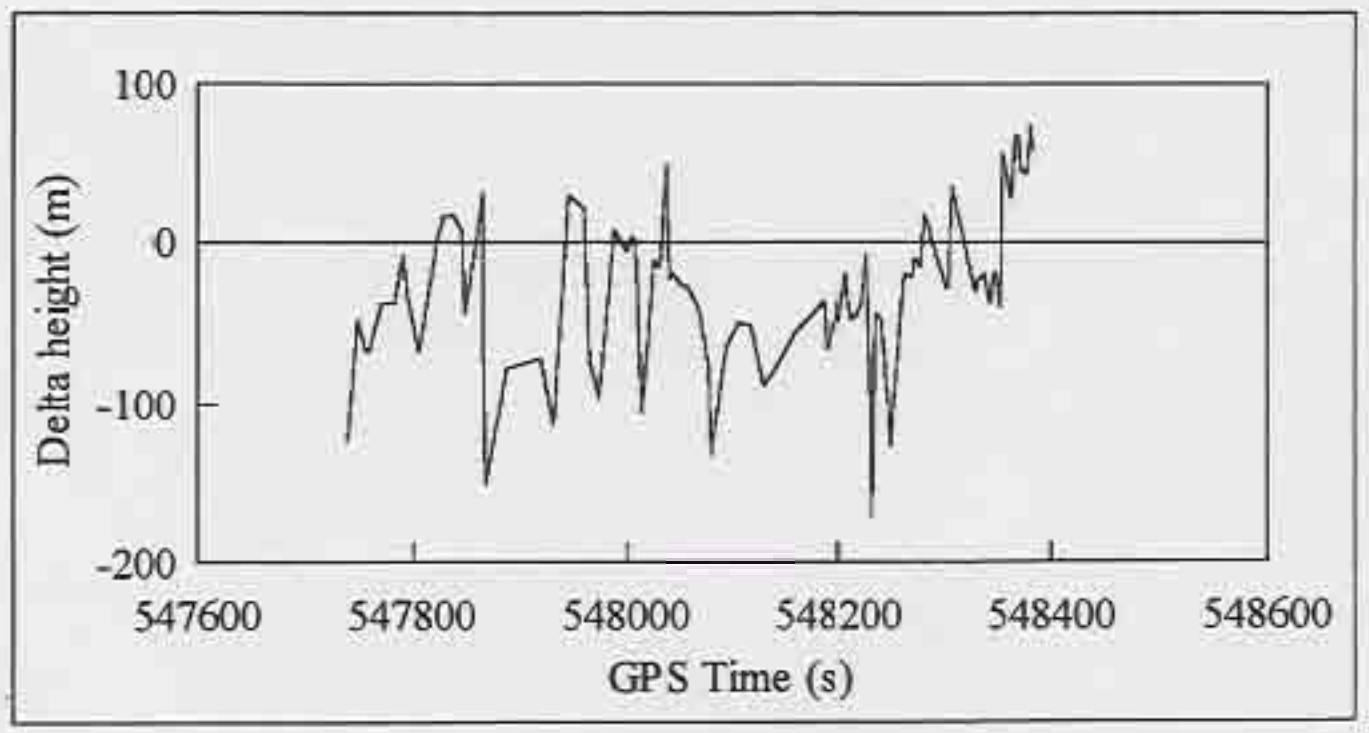

Figure 9.35 Difference in Height Between Best DOP Fix and Precise Fix in Tree Canopy, May 27, 1995

Test 2:

The second test under tree canopy conditions was done on May 30, 1995 and lasted for 962 seconds. Plots of the four solutions appear in Figures 9.36 to 9.39, and the HDOP and number of satellites available are shown in Figures 9.40 and 9.42. A total of 543 best DOP fixes (one every 1.77 seconds) were recorded, and 248 epochs (one every 3.88 seconds) were computed for the map aided GPS, least squares, and precise solutions.

Although the map aided GPS solution (Figure 9.36) is quite smooth, there is an area, marked by arrow A, where the incorrect road would have been displayed to the user in a map matching display. The actual road of travel was 12th Ave., and the direction was to the east. Examining the best DOP fix for this period (Figure 9.37) shows that SA was causing a large bias to the north at this time. Map aiding could not help the filter in this situation because the correct road of travel could not be identified. A navigable digital road map (see Section 4.1) would have helped in the road finding algorithm because 11th Ave. is a one way road in the west direction. Given the direction of the one way road, it could have been rejected based on the direction of travel of the vehicle. Even with this shortcoming, the map aided GPS solution was much better than the best DOP and least squares solutions in road identification.

Referring again to Figure 9.36, arrow B marks an area where the map aiding procedure helped the filter after overshooting a turn, and arrow C marks an area where the filter was helped after undershooting a turn. Arrow D shows an area where the road was overshot laterally after the map aiding process helped correct the filter. Again, setting the azimuth as described in Section 9.3 helps to remedy this problem.

In the precise plot (Figure 9.39), the section marked by arrow A is misleading. There was a period of about two blocks where GPSPACE was unable to compute a solution due to the high levels of multipath. The line segment is connecting the last known position along 14th Ave. to the next computed position, which is a point affected by multipath. The actual position of the road can be seen clearly in the short segment marked by arrow B.

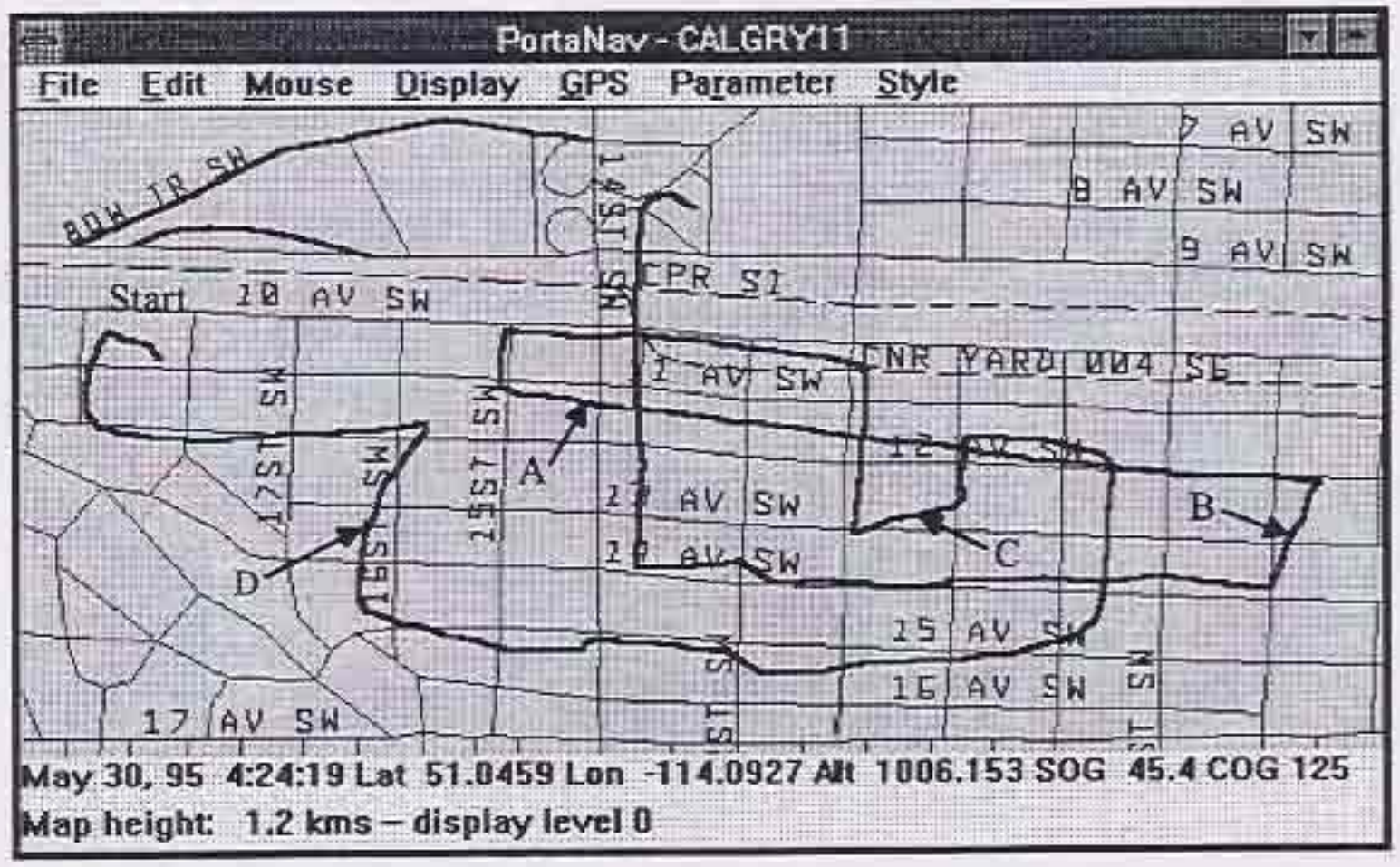

Figure 9.36 Map Aided GPS in Tree Canopy

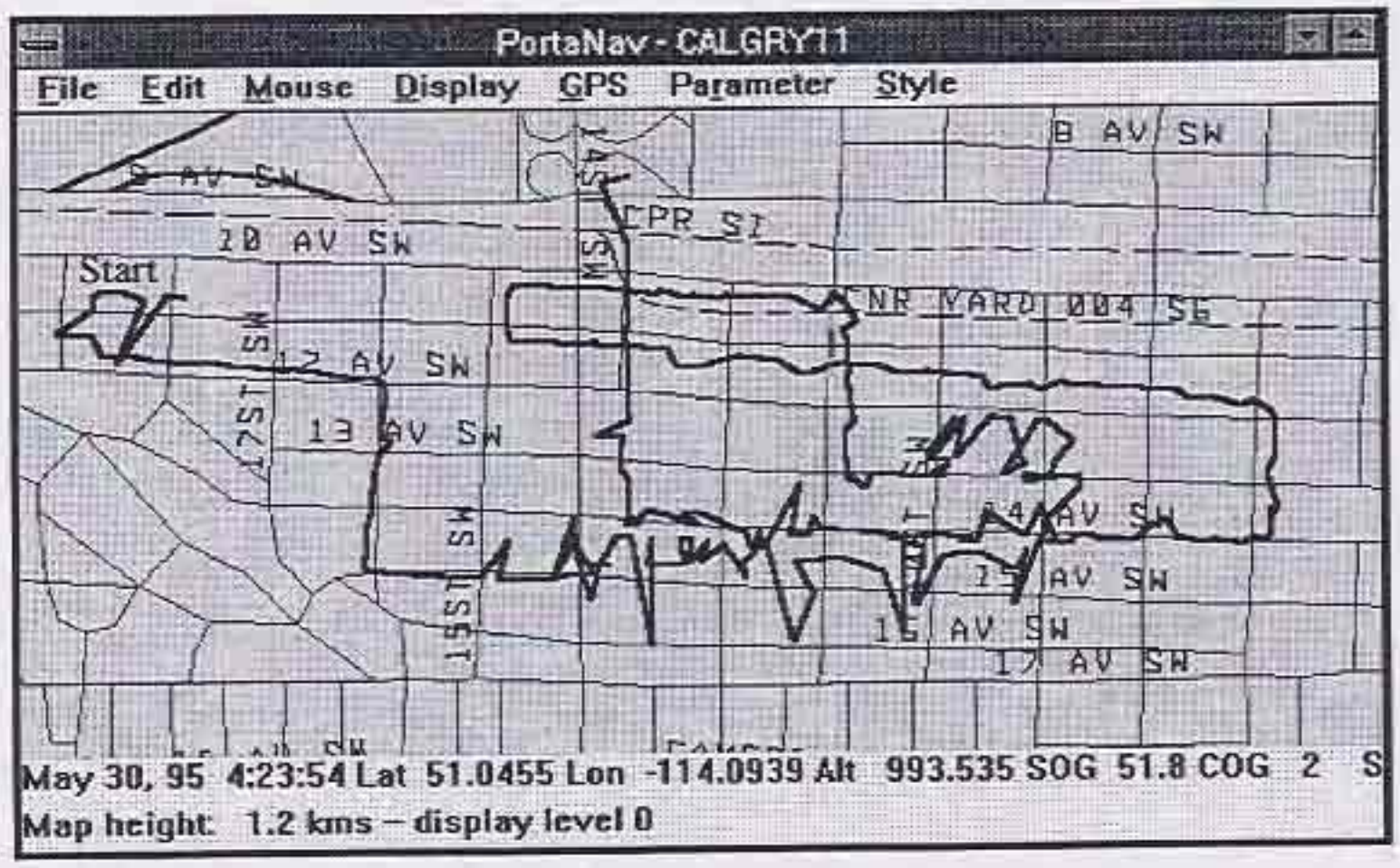

Figure 9.37 Best DOP Fix in Tree Canopy

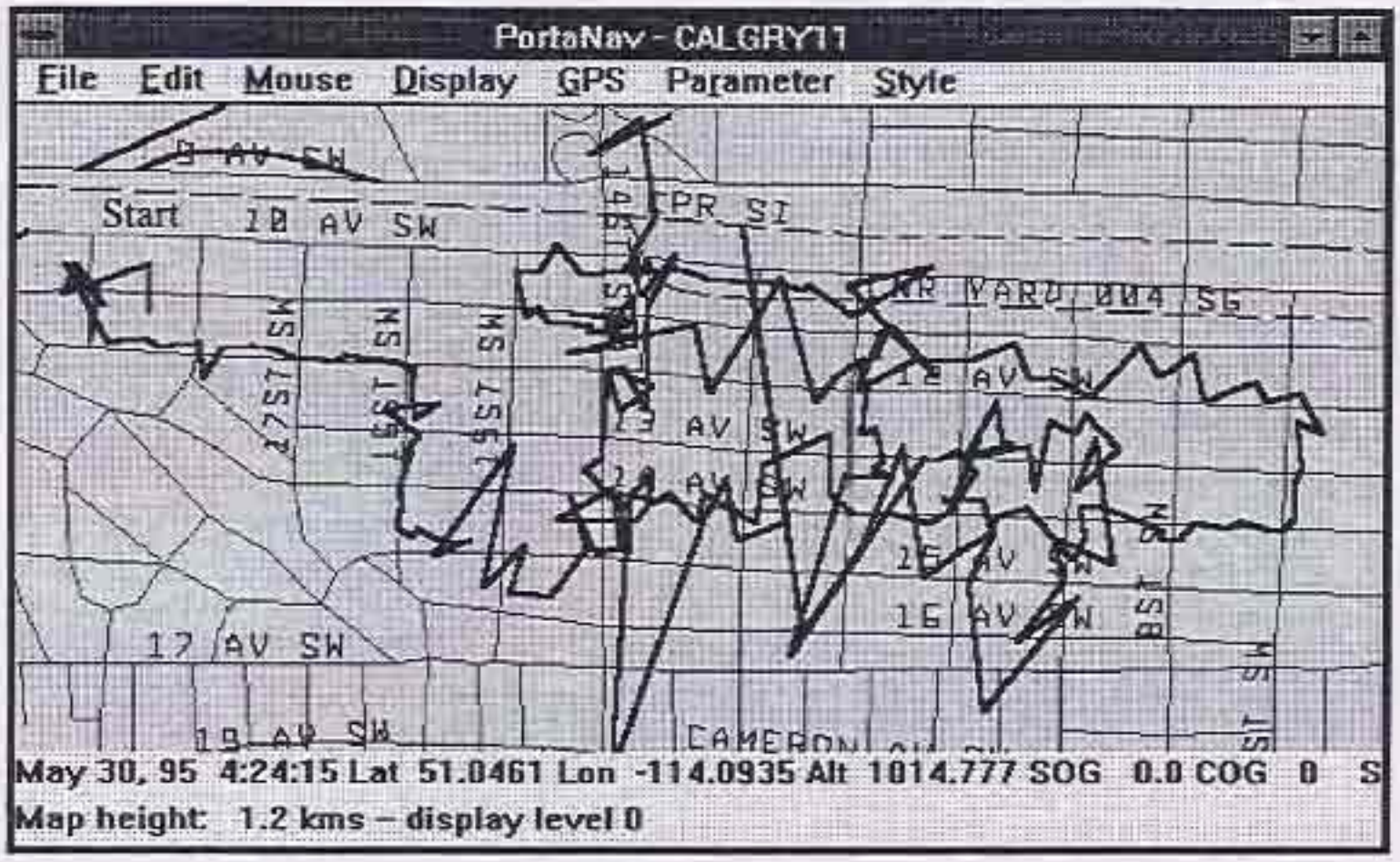

Figure 9.38 Least Squares Fix in Tree Canopy

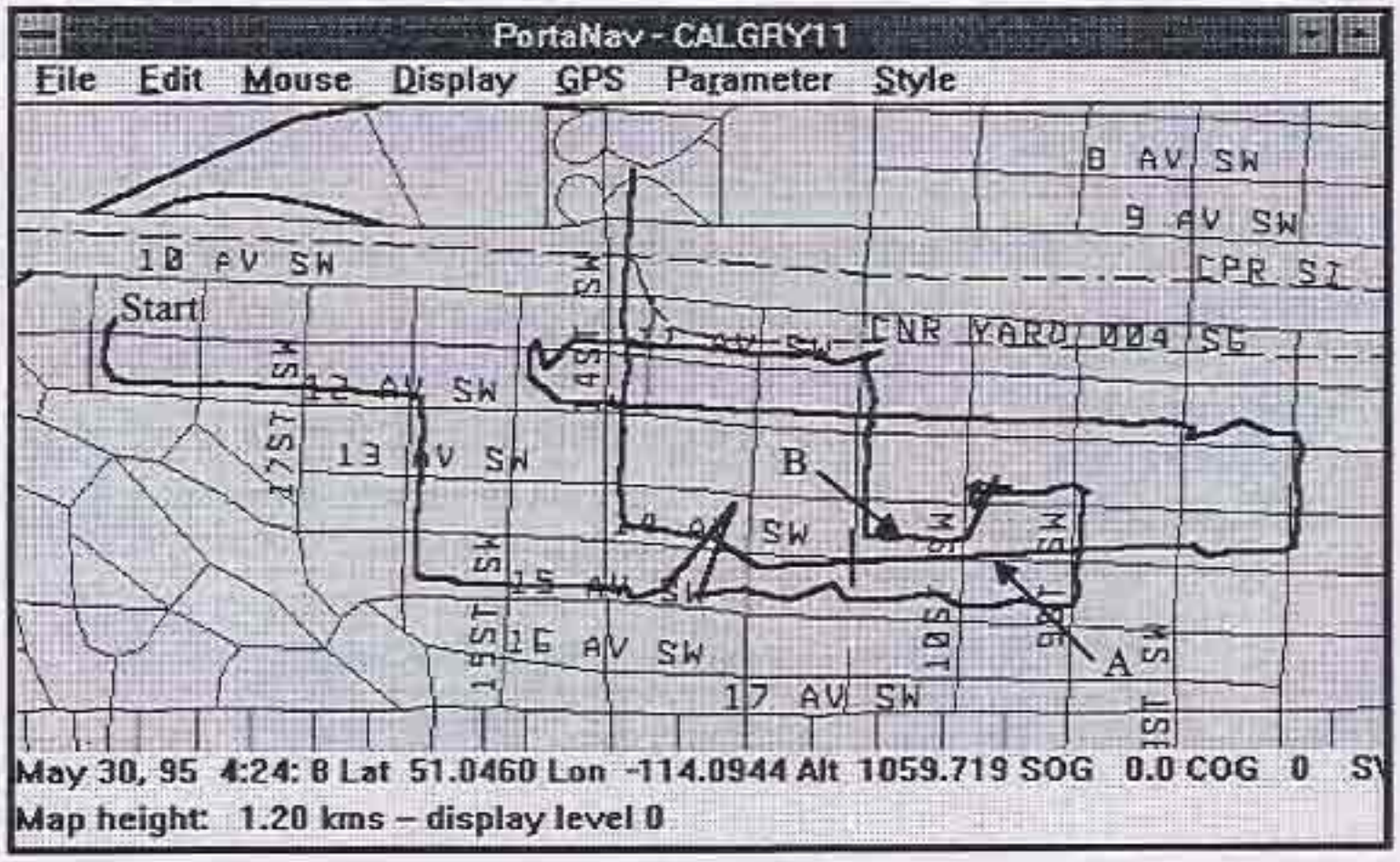

Figure 9.39 Precise Fix in Tree Canopy

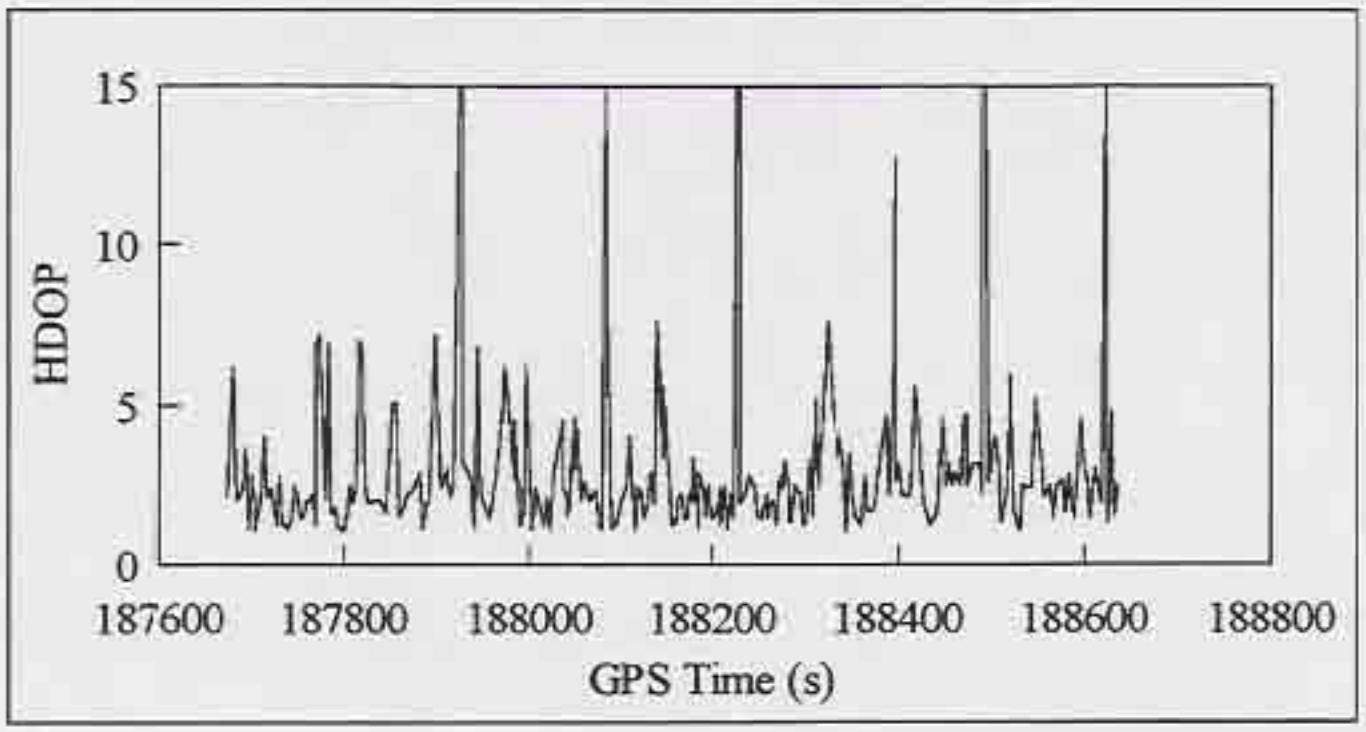

Figure 9.40 HDOP in Tree Canopy, May 30, 1995

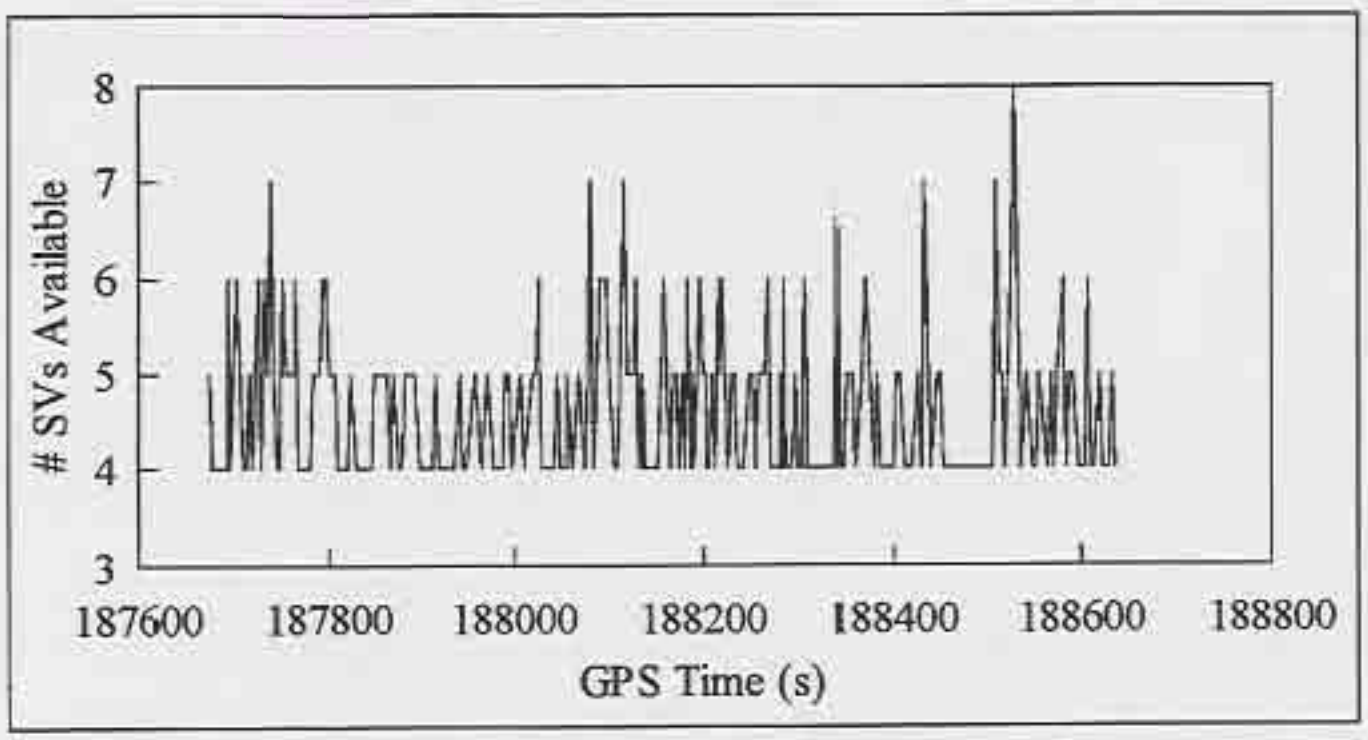

Figure 9.41 Number of Satellites Available in Tree Canopy, May 30, 1995

Test 3:

The third and final test under tree canopy conditions was performed on June 2, 1995 and lasted for 951 seconds. This run was done using the filter constraints described in Section 9.3 and without computing the least squares solution. The map aided GPS solution for this run appears in Figure 9.42, the plot of the best DOP fixes is in Figure 9.43, and the number of satellites available is shown in Figure 9.44. A total of 701 best DOP fixes (one every 1.36 seconds) were recorded, and 386 epochs (one every 2.46 seconds) were computed. Once again, the improved data rate can be attributed to the reduced computation load and the effect of the height aiding. A total of 210 epochs were of only three satellites. Without these epochs, the average data rate would have been one epoch every 3.79 seconds. The height aiding of the filter played a much larger role in improving the performance under tree canopy than it did in open road conditions.

The large shift marked with an arrow in the best DOP plot (Figure 9.43) is due to high multipath. At this point there were two large buildings lining the road, one to the north, and one to the south. This large multipath caused the map aided filter to get lost, as shown with arrow A in Figure 9.42. The filter was able to avoid the large shift to the south that is apparent in Figure 9.43, but a few epochs later, an over correction caused the large shift to the north. A blunder this large does not get absorbed completely by the filter. The filter should be modified to have better blunder detection and removal [Abousalem, 1993]. The good news is that the filter was able to find the correct position again within two blocks. In Kalman filtering, the solution has the potential to diverge after a large blunder is introduced.

Again, the trajectory of the map aided GPS solution is much smoother than the best DOP fix. Road identification is possible at all points in the trajectory except for the instance mentioned. The benefits of the 'kick starting' procedure can be seen in the sharp corners, two of which are indicated by arrows B and C in Figure 9.42.

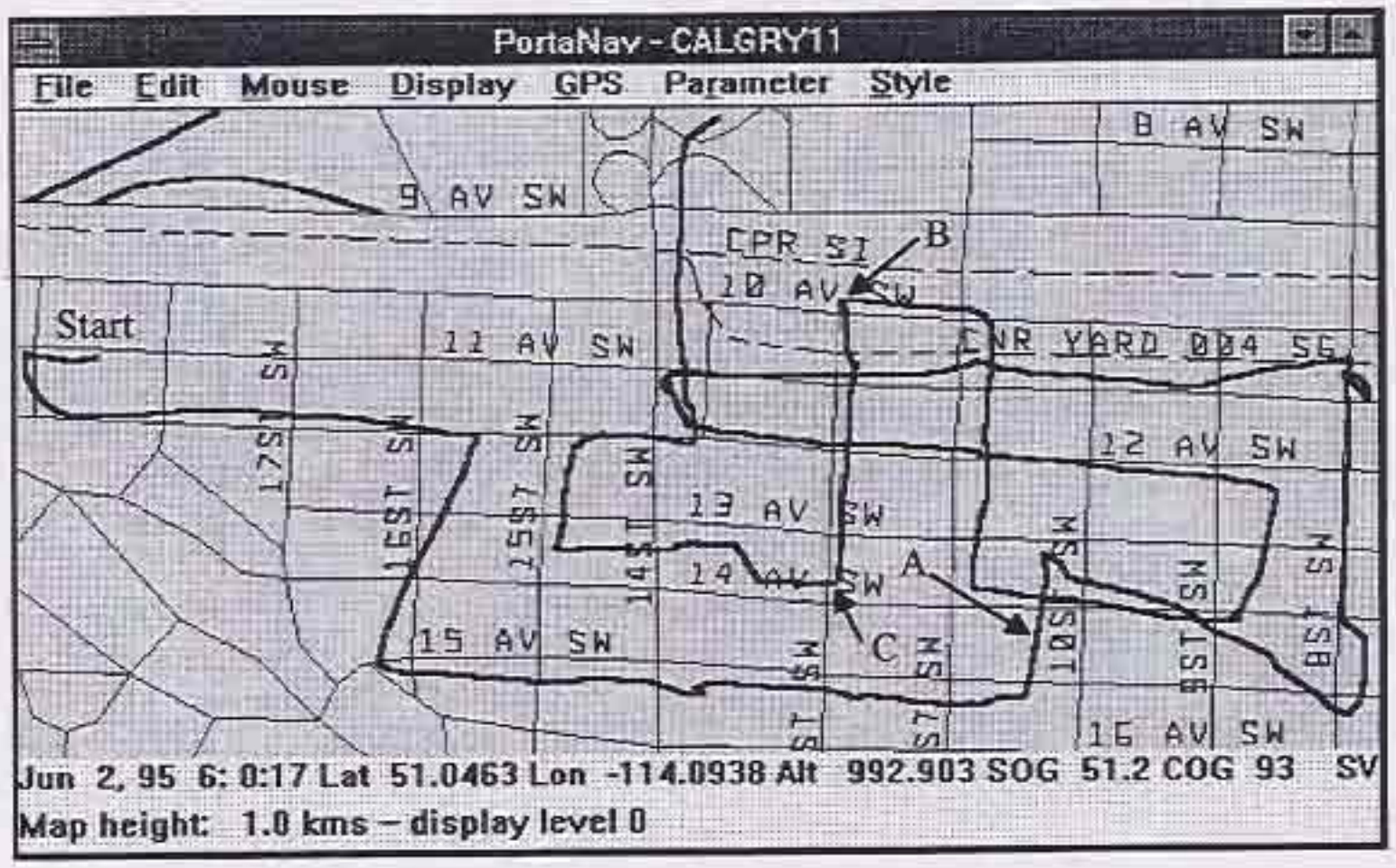

Figure 9.42 Map Aided GPS in Tree Canopy

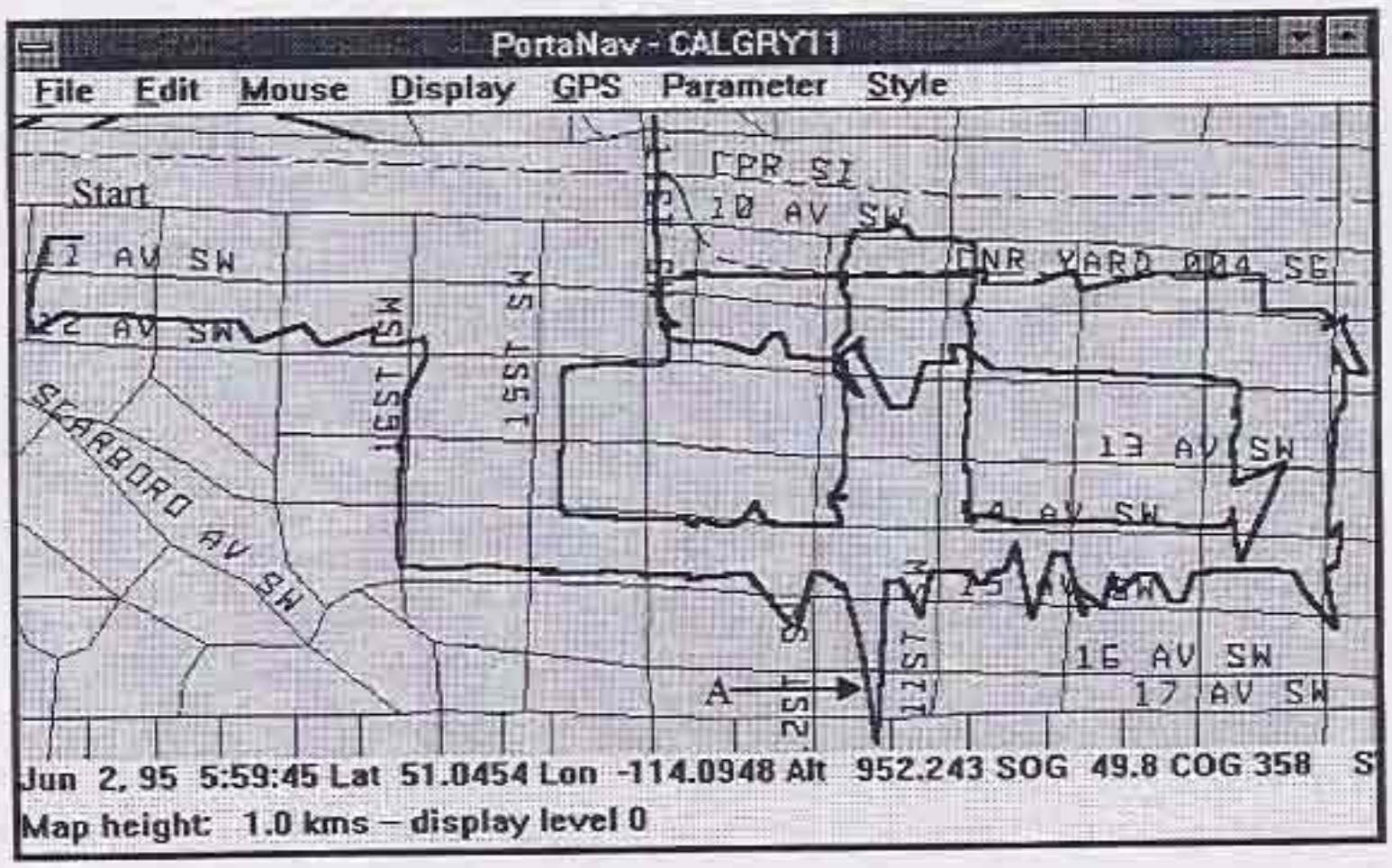

Figure 9.43 Best DOP Fix in Tree Canopy

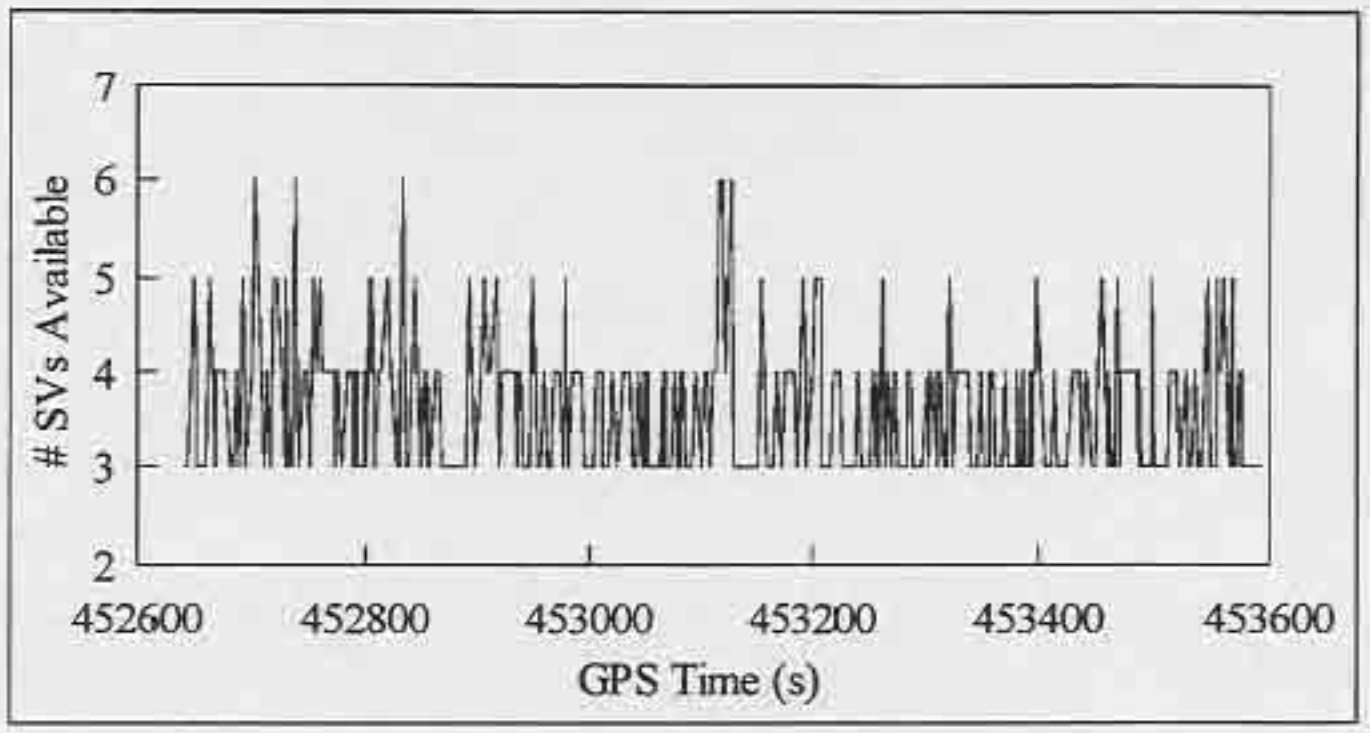

Figure 9.44 Number of Satellites Available in Tree Canopy, June 2, 1995

9.4.4 *Urban Canyon Tests*

The urban canyon environment is by far the most treacherous for GPS navigation. The signal blockages cause long periods between fixes and frequent instances of high multipath cause large shifts in the positions. The downtown core in Calgary is dense with buildings, many reaching 40 to 50 stories. Another performance degrading feature about the Calgary downtown area is the presence of overhead walkways between the buildings. To overcome the urban canyon problem, several navigation systems have used dead-reckoning sensors to extend the position through the regions of poor coverage. It is hypothesized that the map aiding approach will improve the performance of GPS in terms of coverage, identifying the correct road of travel and in the smoothness of the trajectory.

Test 1:

The first test in the urban canyon environment was done on May 30, 1995, and lasted for 640 seconds. Plots of the four solutions appear in Figures 9.45 to 9.48. A plot showing the HDOP for the period of the test is shown in Figure 9.49, and a plot showing the

number of satellites available for each epoch is shown in Figure 9.50. A total of 521 best DOP fixes (one every 1.23 seconds) were recorded, while a mere 119 epochs (one every 5.38 seconds) were computed by the least squares, map aided GPS and precise solutions.

The map aided GPS solution in Figure 9.45 has a smooth trajectory. The second turn was made on 4th Ave., not on 5th Ave. as indicated in this plot. The reason for missing the turn was due to the slow average data rate. After a few epochs, the filter found the correct position again, and was able to continue down the road. The missed turn is also evident in the plot showing the difference between the map aided solution and the precise solution in Figure 9.51. The large drop just after time 184 800 occurs along the northbound segment before the left turn. The bias starts at the intersection and grows rapidly. The slow data rate hinders the filter in catching up when the vehicle has started moving in a new direction. The distance between each epoch can grow quite large, but as long as an occasional epoch can be processed, the trajectory remains fairly smooth. Problems occur if there are many turns while few epochs are processed.

The northing difference between the best DOP and the precise fixes is shown in Figure 9.52. Here we can confirm that the large difference in the northing in Figure 9.51 was not due to multipath. The easting differences for the map aided solution and best DOP fix are shown in Figures 9.53 and 9.54 respectively. There is quite an improvement in the map aided solution. Finally, the height differences for the two solutions are shown in Figures 9.55 and 9.56. Again, there is not much difference here, since the map aiding process mainly affects the horizontal components of the position.

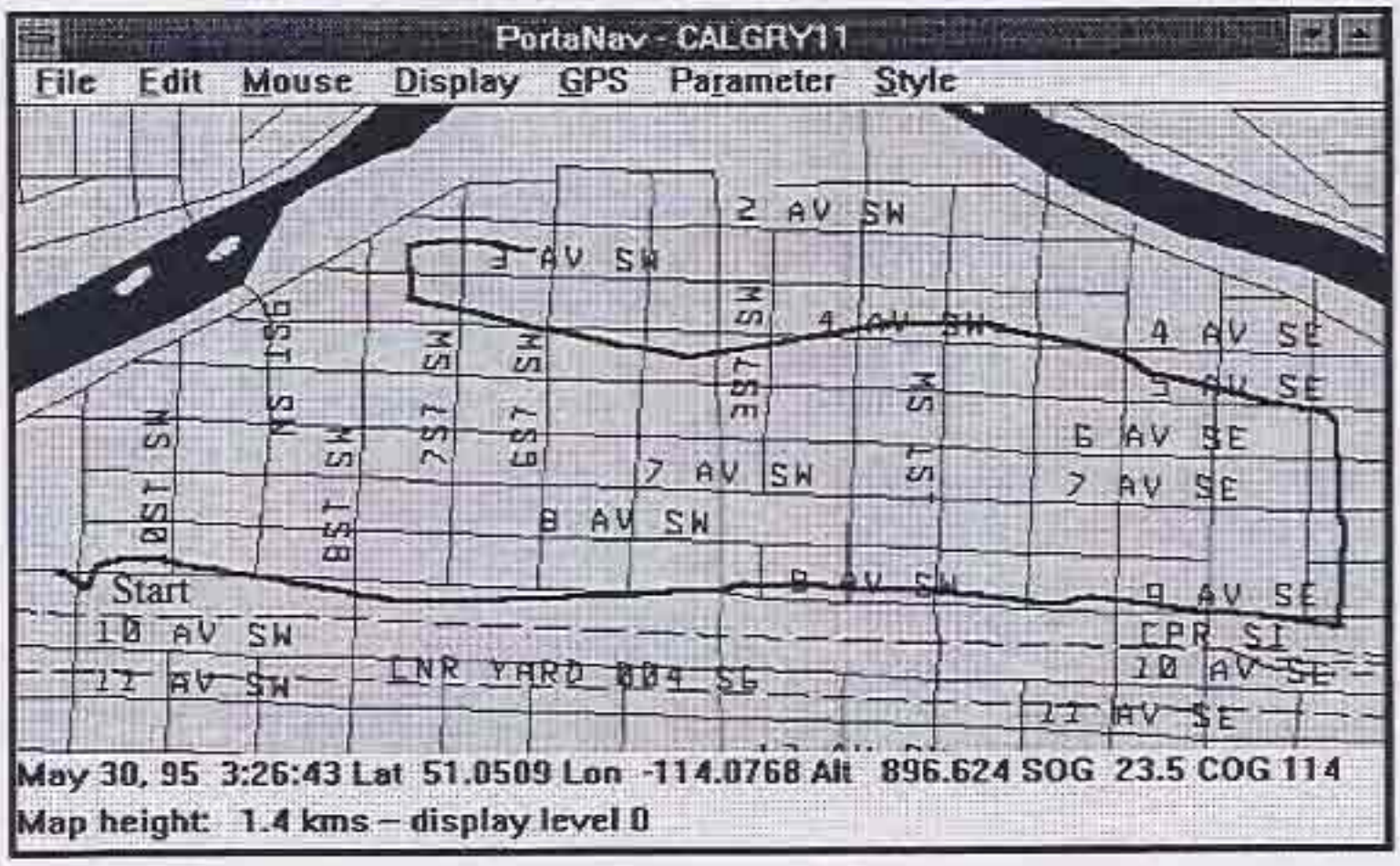

Figure 9.45 Map Aided GPS in Urban Canyon

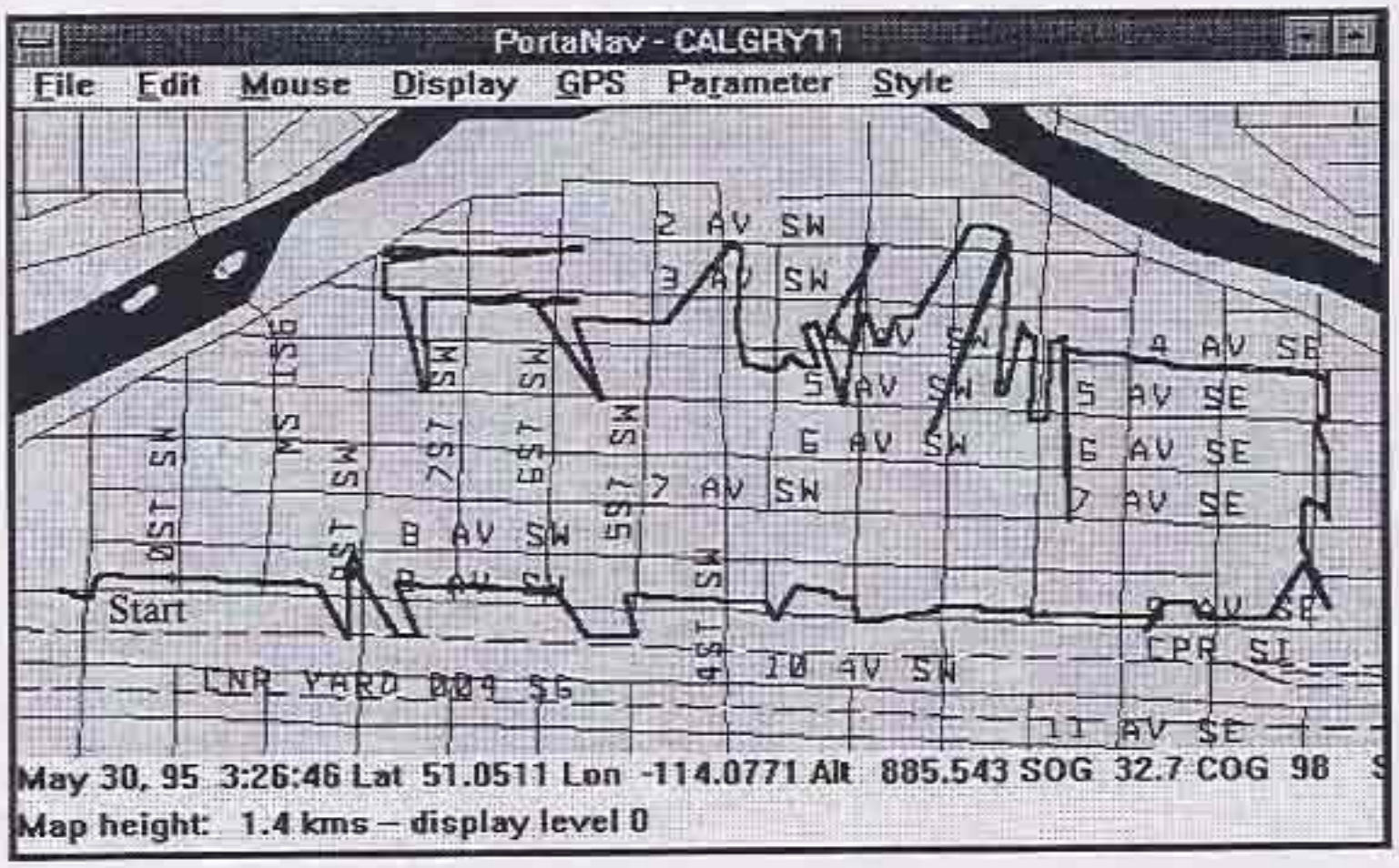

Figure 9.46 Best DOP Fix in Urban Canyon

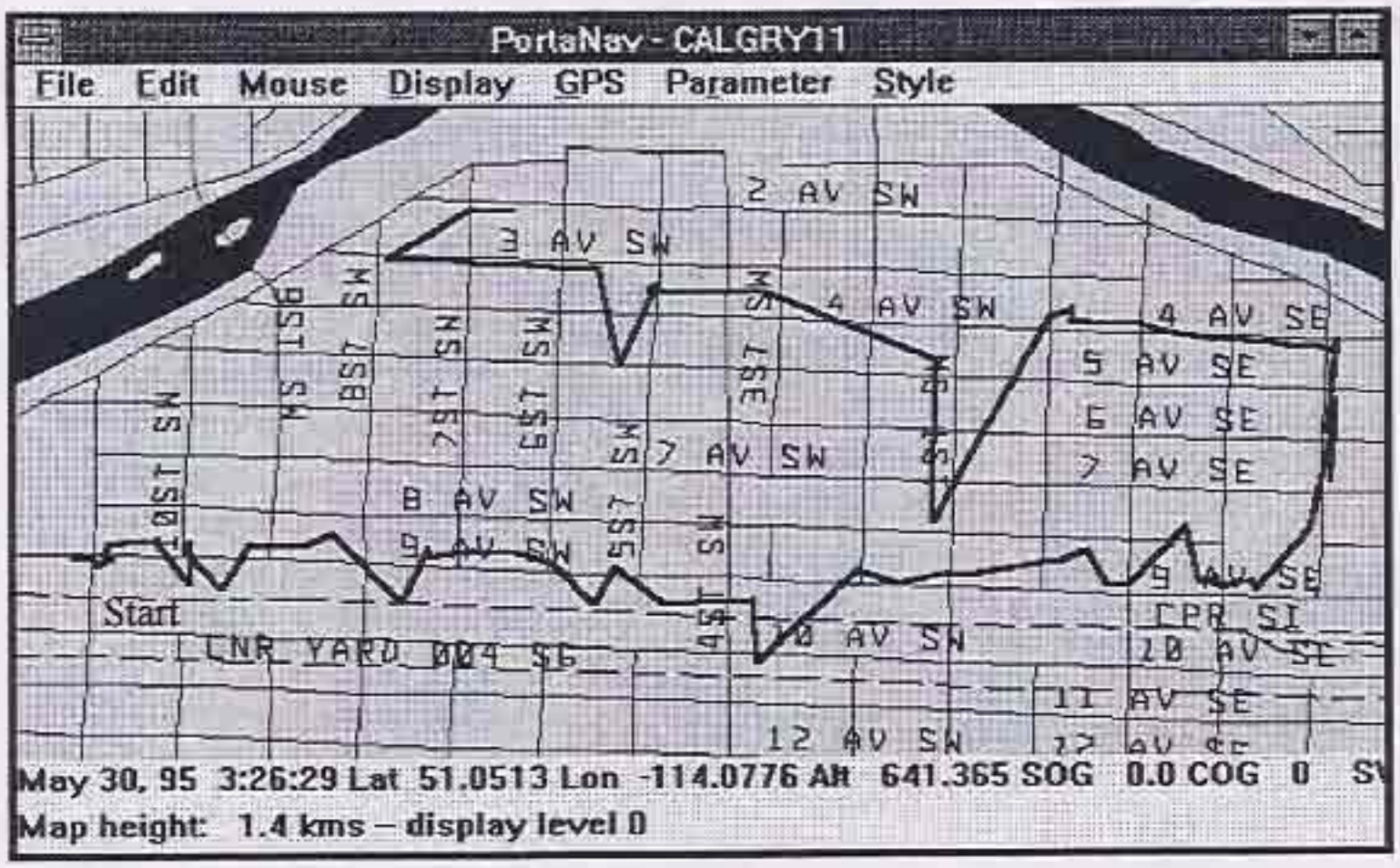

Figure 9.47 Least Squares Fix in Urban Canyon

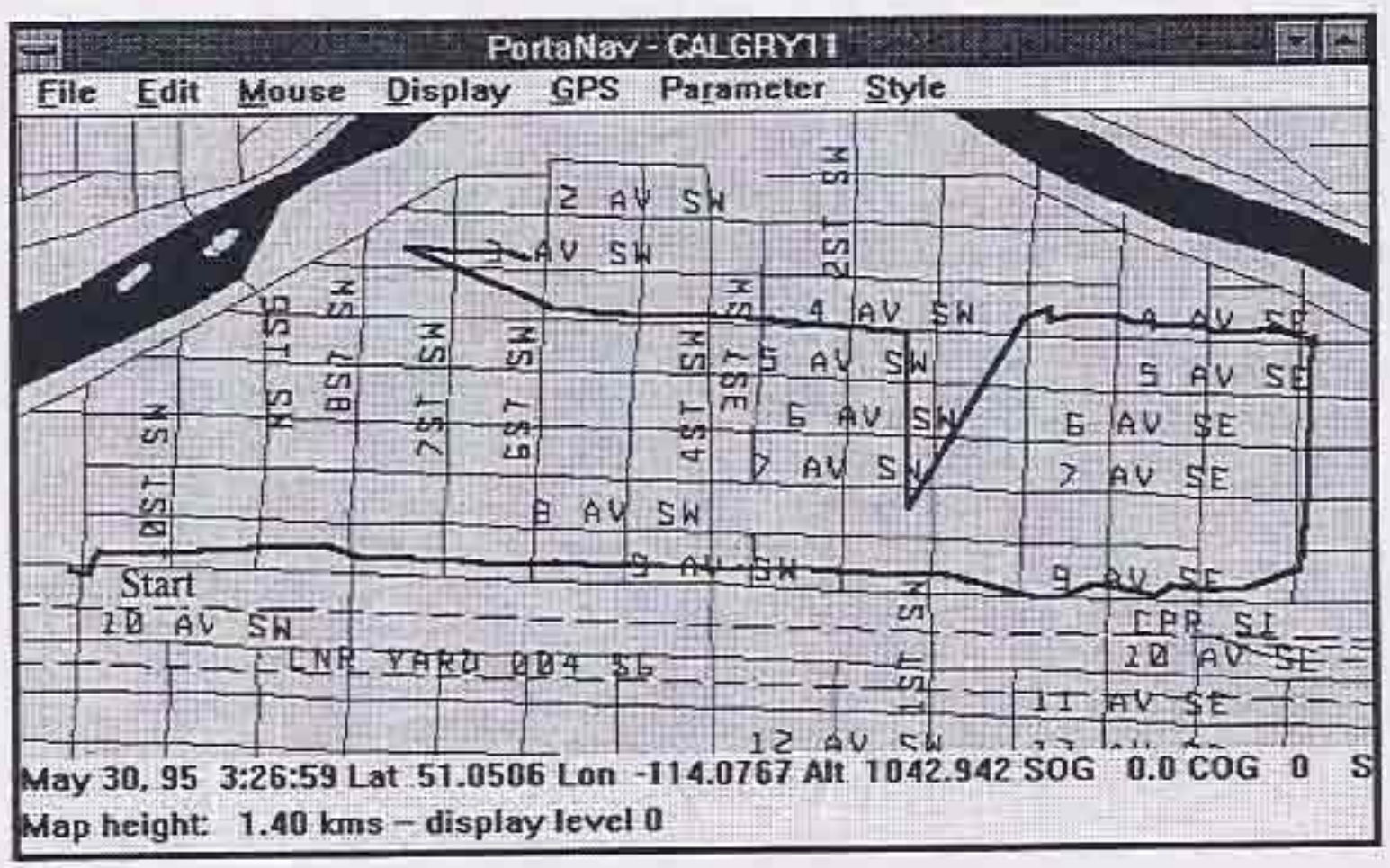

Figure 9.48 Precise Fix in Urban Canyon

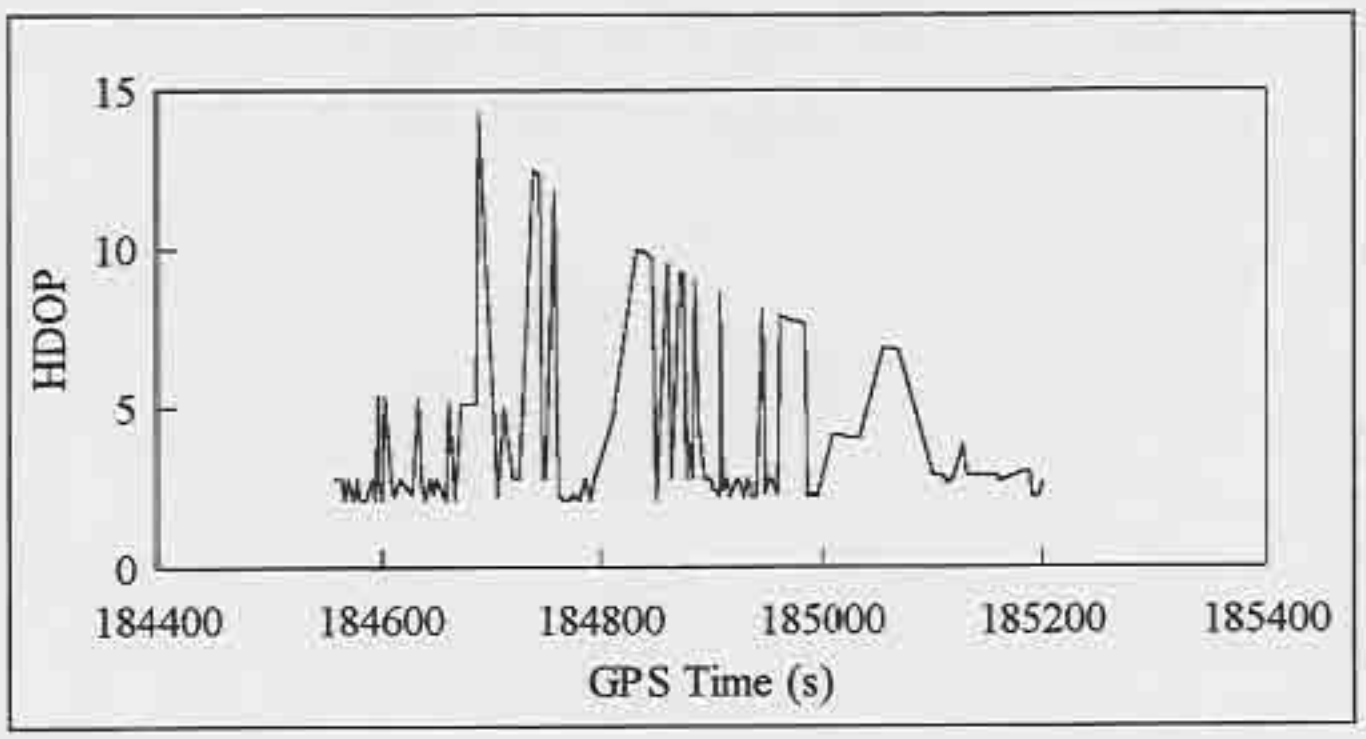

Figure 9.49 HDOP in Urban Canyon, May 30, 1995

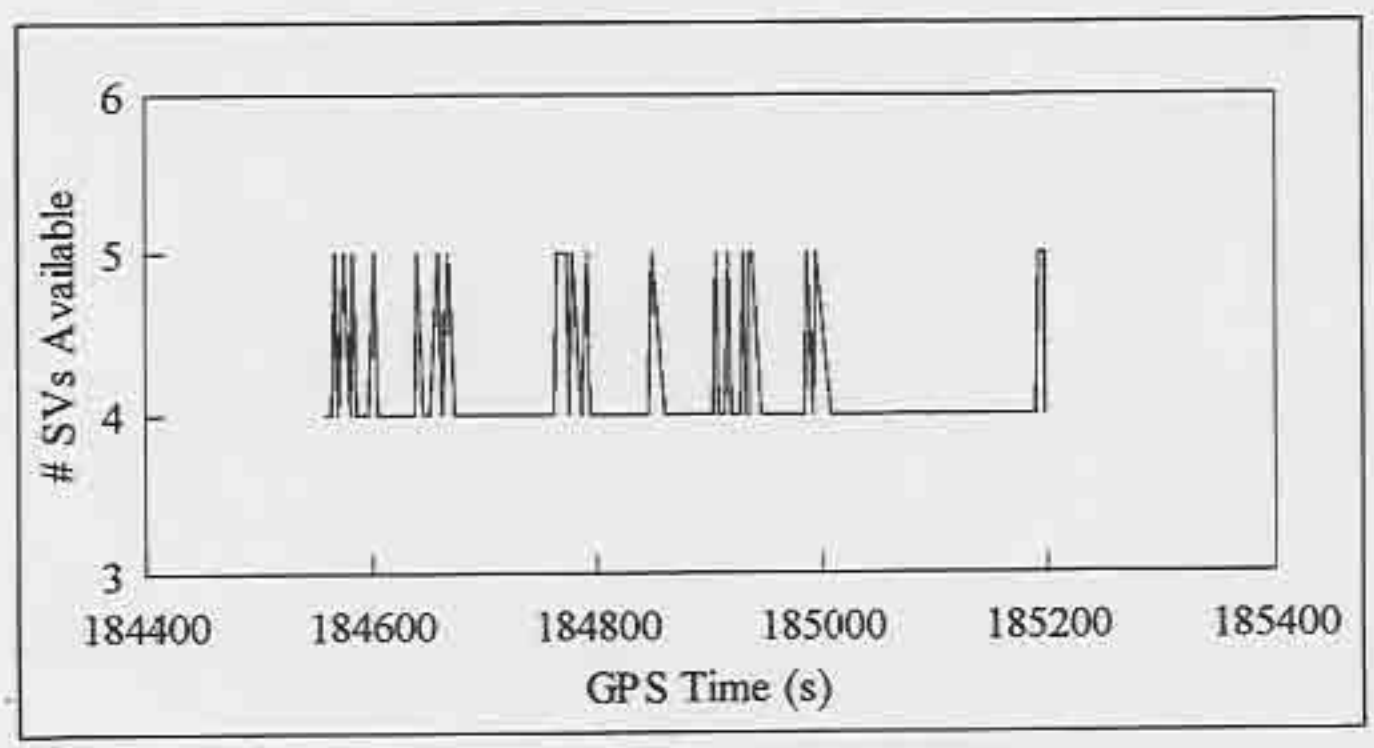

Figure 9.50 Number of Satellites Available in Urban Canyon, May 30, 1995

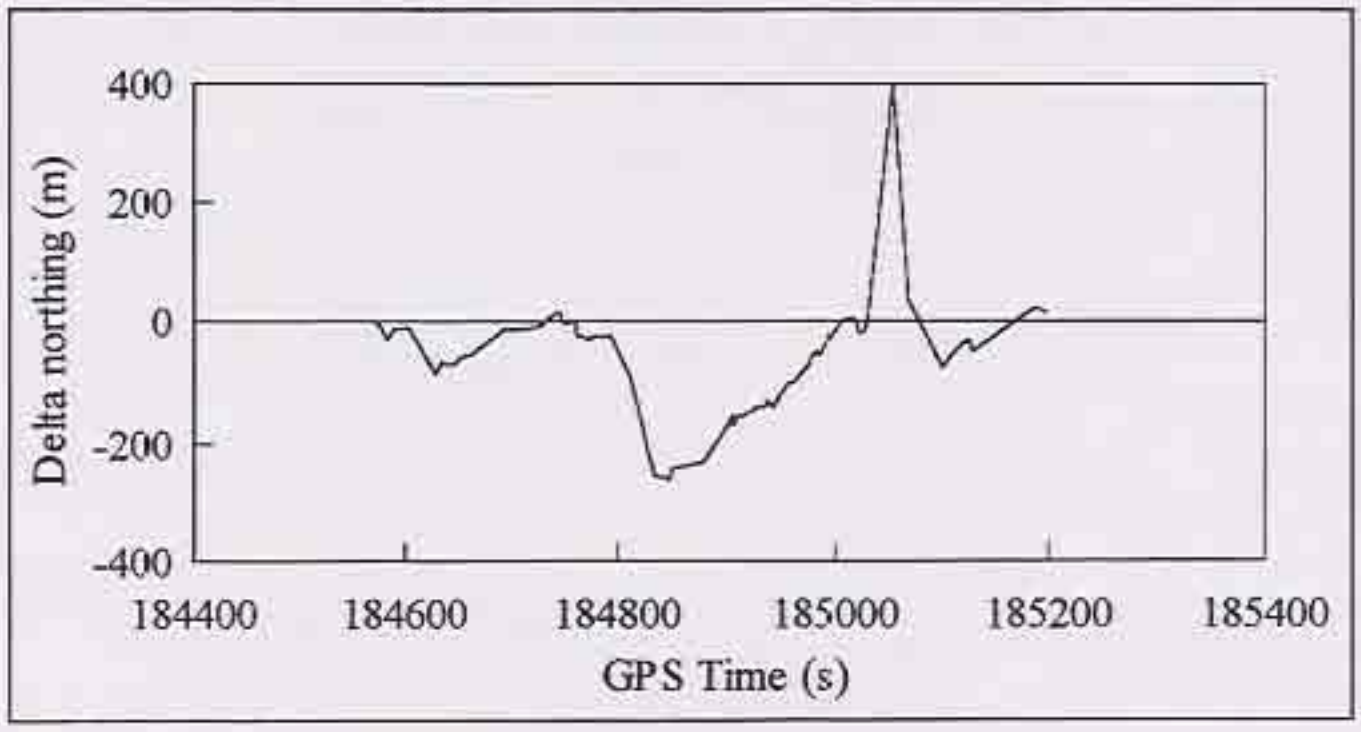

Figure 9.51 Difference in Northing Between Map Aided GPS and Precise Fix in Urban Canyon, May 30, 1995

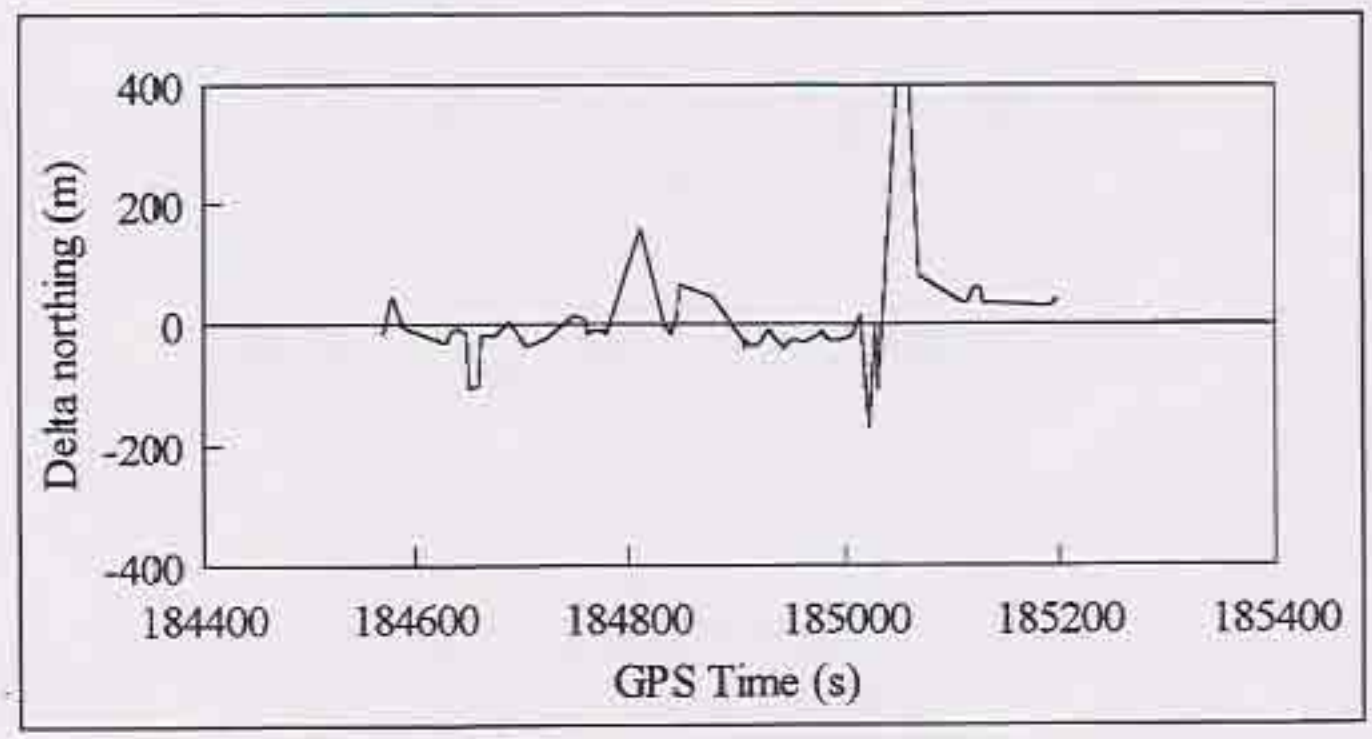

Figure 9.52 Difference in Northing Between Best DOP Fix and Precise Fix in Urban Canyon, May 30, 1995

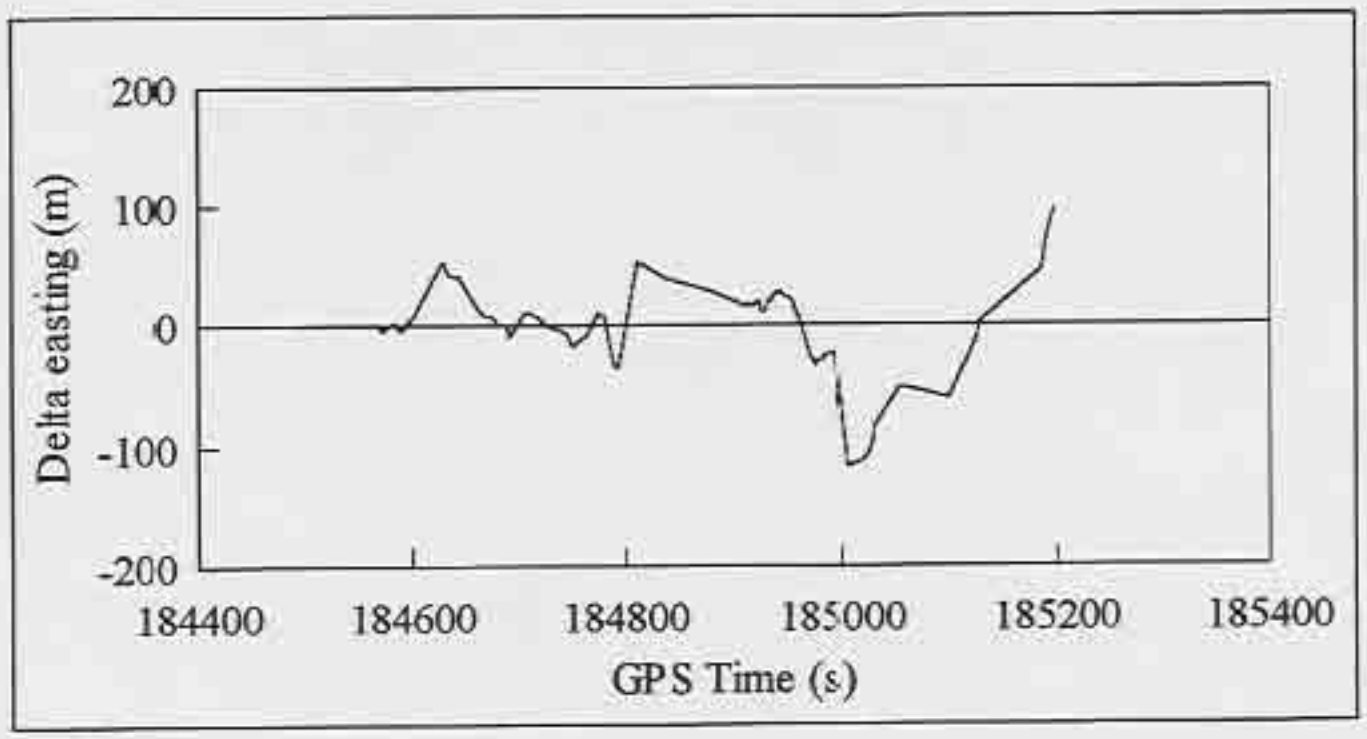

Figure 9.53 Difference in Easting Between Map Aided GPS and Precise Fix in Urban Canyon, May 30, 1995

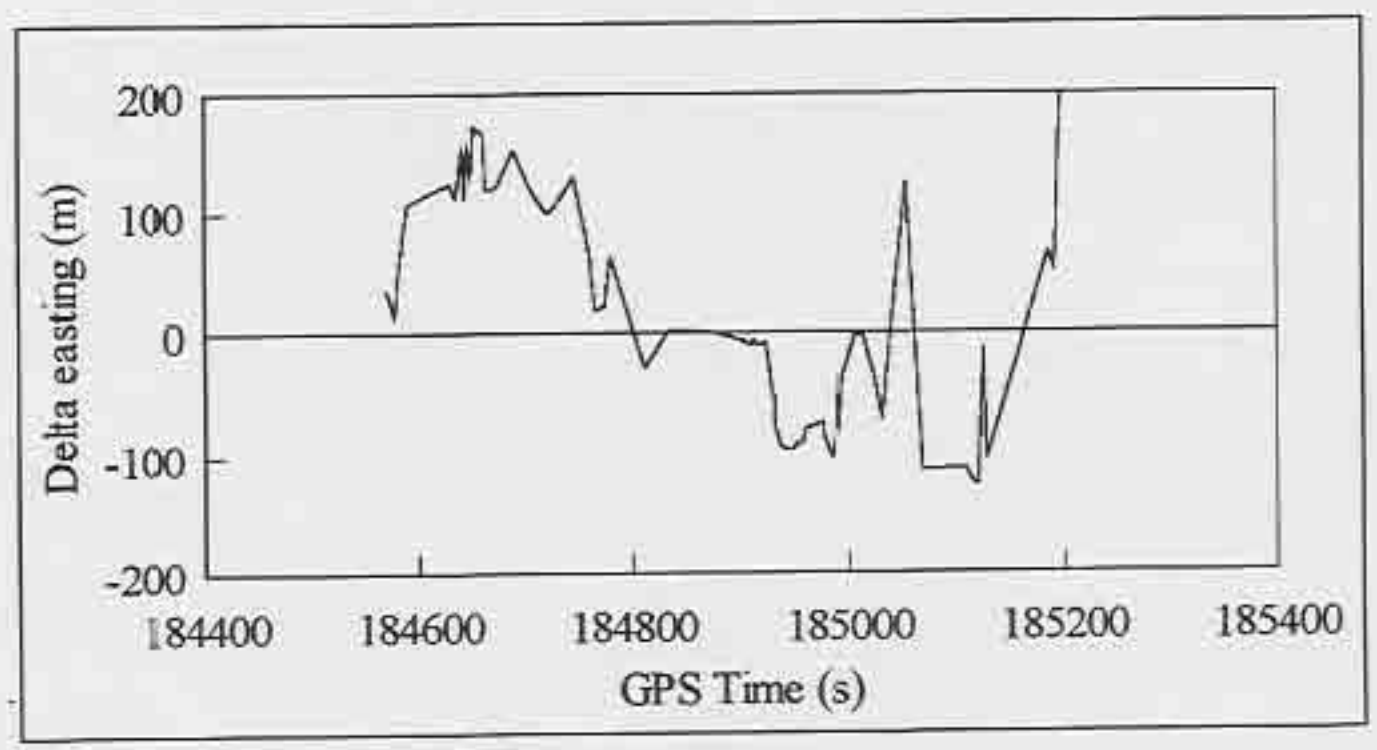

Figure 9.54 Difference in Easting Between Best DOP Fix and Precise Fix in Urban Canyon, May 30, 1995

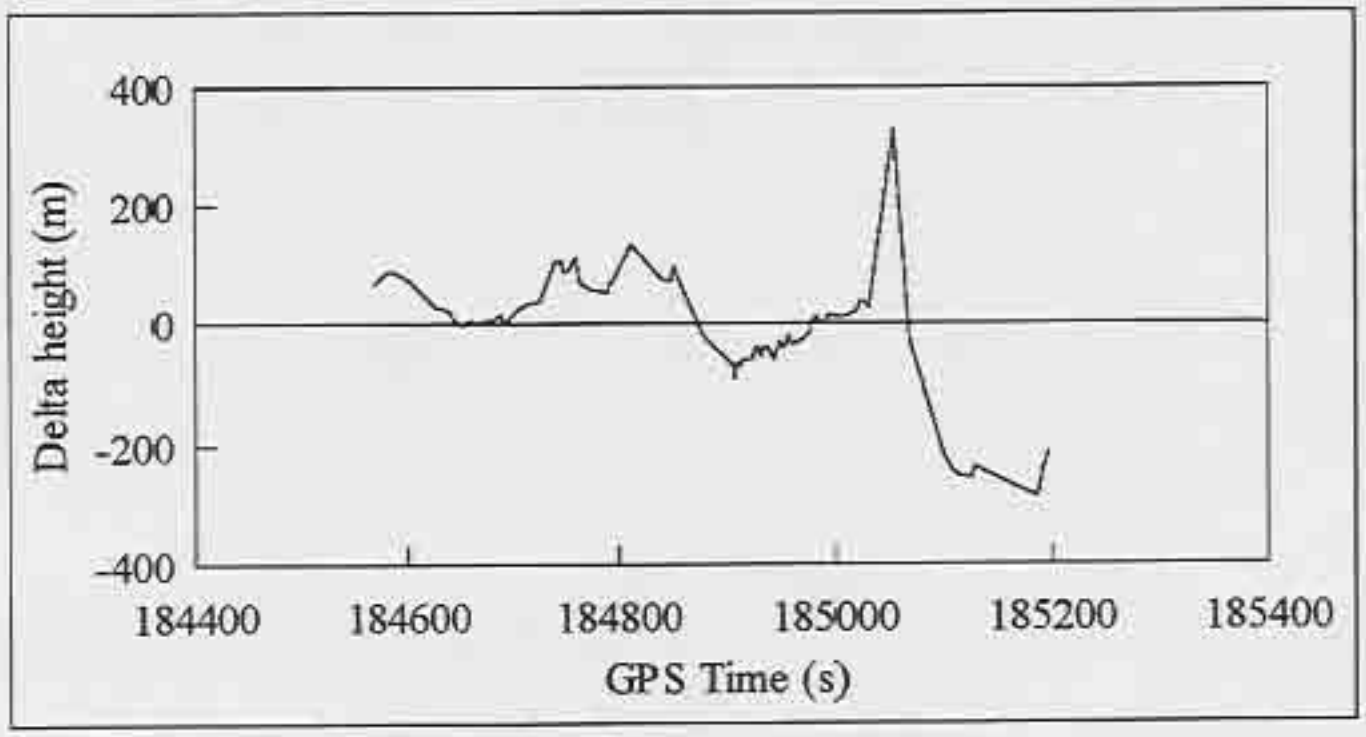

Figure 9.55 Difference in Height Between Map Aided GPS and Precise Fix in Urban Canyon, May 30, 1995

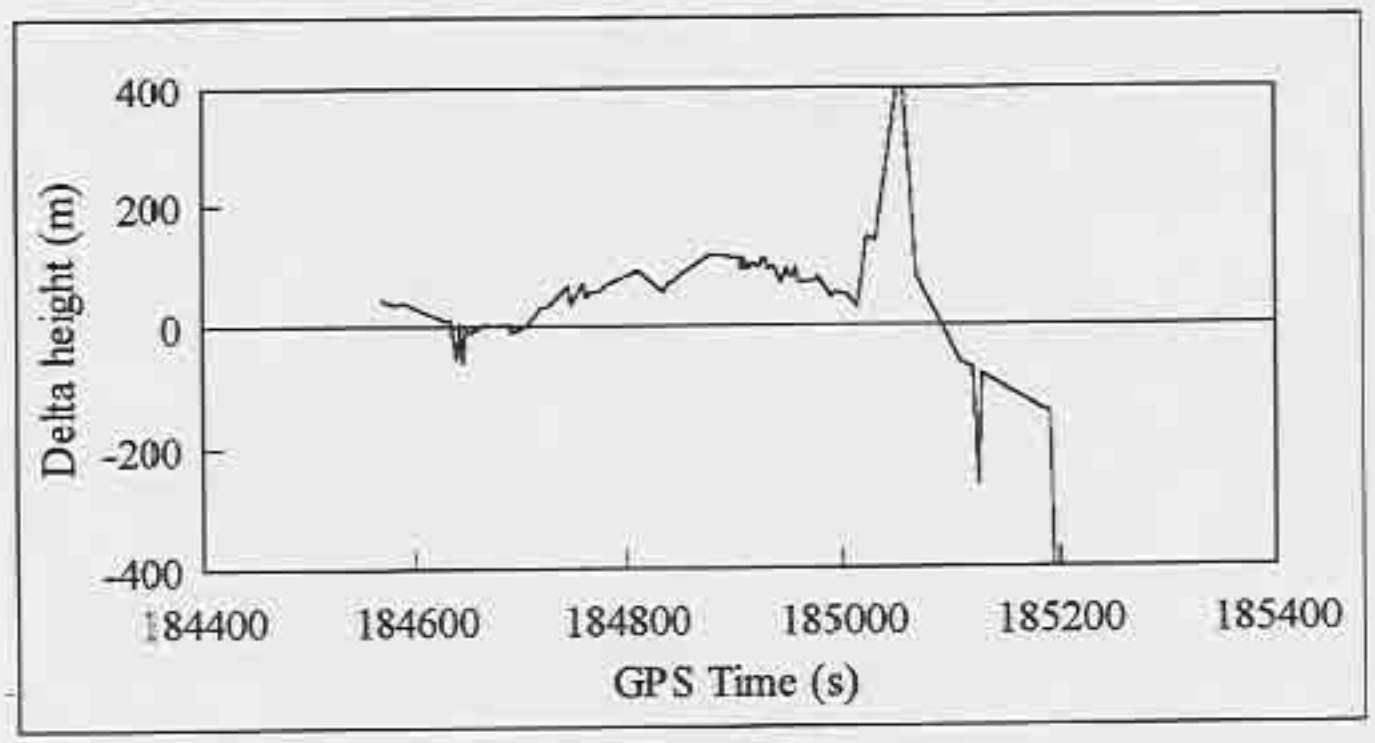

Figure 9.56 Difference in Height Between Best DOP Fix and Precise Fix in Urban Canyon, May 30, 1995

Test 2:

The second test was performed on May 31, 1995, and lasted 470 seconds. The map aided GPS solution is shown in Figure 9.57, the plot of the best DOP fixes is shown in Figure 9.58, and the number of satellites available for the period is shown in Figure 9.59. During this test, 388 best DOP fixes (one every 1.21 seconds) were recorded, and 123 epochs (one every 3.82 seconds) were computed.

The results of this run were much the same as for the previous run. Again, the filter had a problem on the northbound segment on the east side of downtown. This time, such a long period occurred between successive epochs (>20 s), that the filter was reset. Once reset, the filter looped as it found the current position. During this test, a maximum of four satellites were visible (Figure 9.59), explaining the problems in obtaining fixes.

The best DOP solution was quite poor in that the correct road of travel could rarely be identified. Even with the poor data rate and the resetting of the filter, the map aided GPS solution outperformed the best DOP fix in this category.

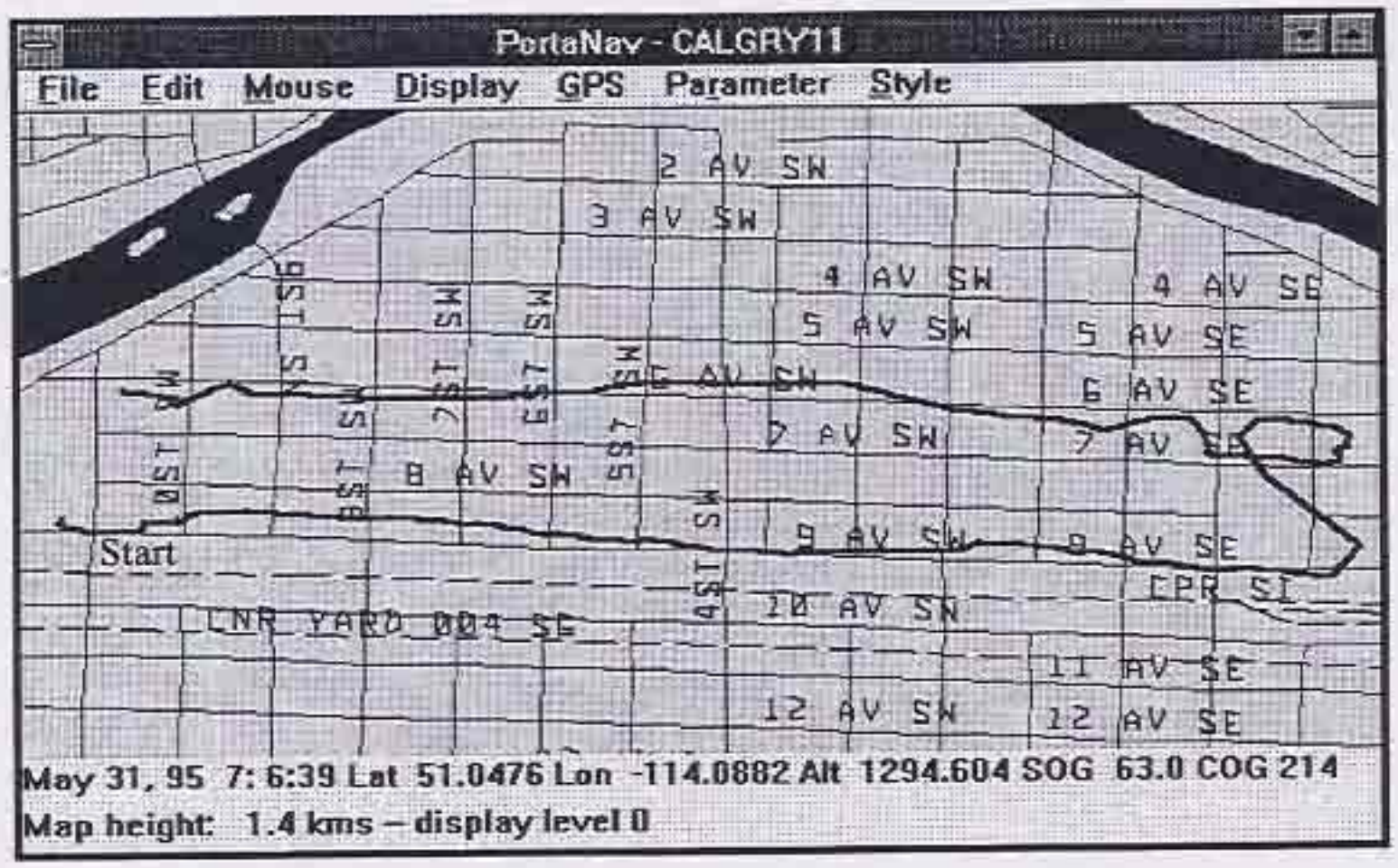

Figure 9.57 Map Aided GPS in Urban Canyon

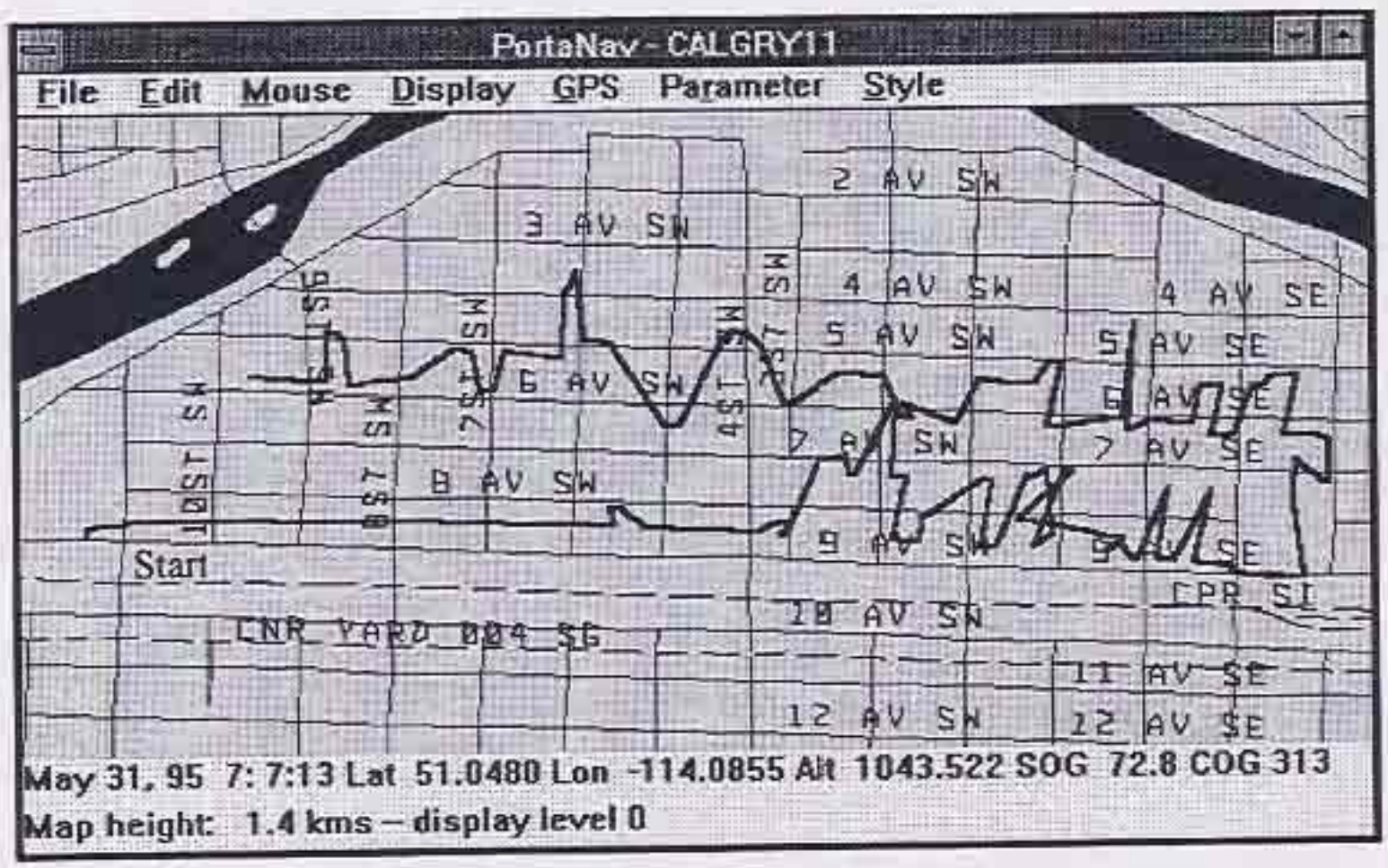

Figure 9.58 Best DOP Fix in Urban Canyon

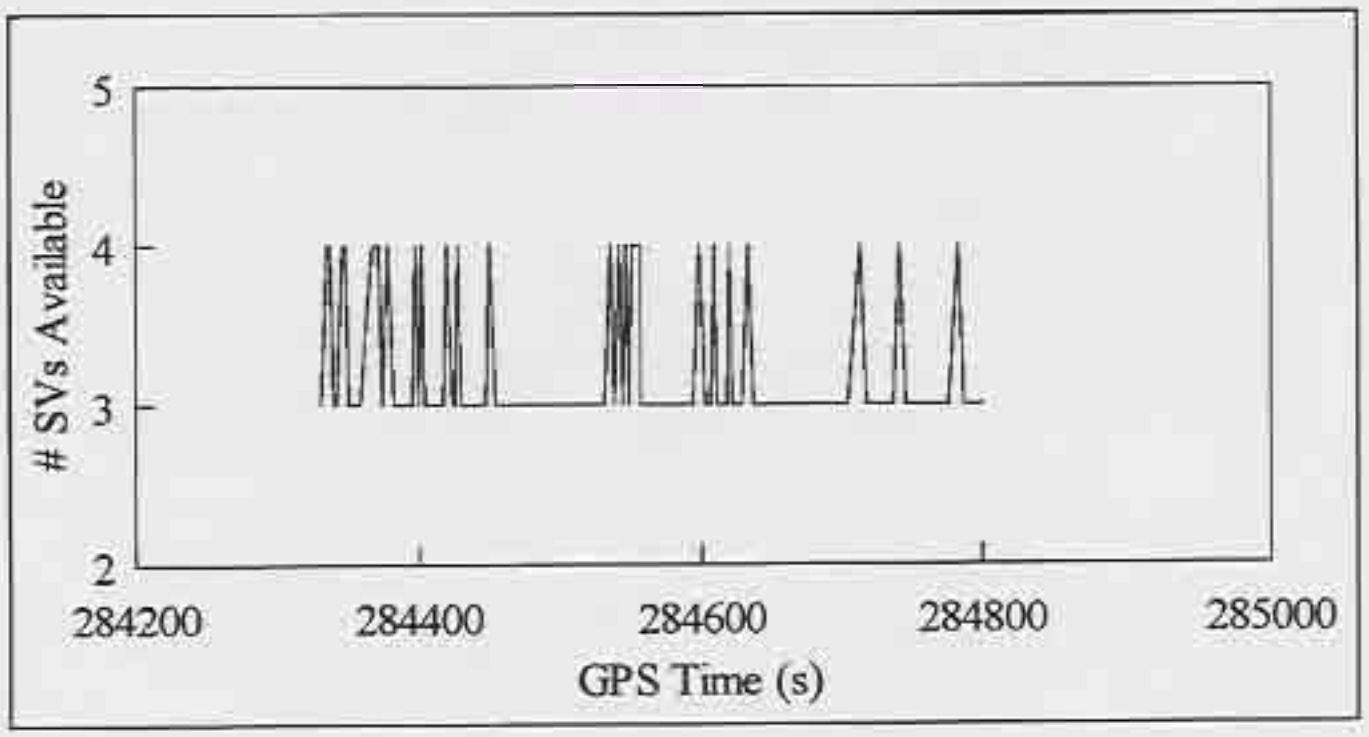

Figure 9.59 Number of Satellites Available in Urban Canyon, May 31, 1995

Test 3:

The final test was performed on June 2, 1995, and lasted 1 478 seconds. Recall that the tests on this day were done with the constraints implemented as discussed in Section 9.3.2. The height aiding had the desired effect; a total of 532 epochs (one every 2.78 seconds) were computed. Of these, 273 epochs consisted of only three satellites, so without the height aiding, the data rate would have been about one epoch every 5.71 seconds. There were 854 best DOP fixes recorded, which is one every 1.73 seconds on average.

The map aided GPS solution plotted in Figure 9.60 shows a smooth trajectory for the most part. The plot in Figure 9.61 shows that the best DOP fix had several shifts of up to three hundred metres due to multipath. The filter was able to absorb most of the multipath effects. With the best DOP solution, there are as many fixes near wrong roads as there are fixes near correct roads.

The only time the filter got completely lost is marked with arrow A in Figure 9.60. The actual path travelled was north on 6th St. to 3rd Ave., east until 2nd St., south until 4th Ave., then east to 9th St., where the filter finds the correct position. There are two other times where the filter is off course for a block. In the first, marked by arrow B, the vehicle was never on 4th Ave. The problem is caused by an incorrect map update, and was corrected when the vehicle made the next turn. The second instance, marked by arrow C, shows the vehicle traversing blocks diagonally. The actual path of the vehicle was south on 7th St. until 8th Ave., where it turned west. The problem was caused by a long period of blackout. Again, the filter was able to correct itself within two blocks.

Figure 9.62 shows that the satellite visibility for this test was improved over the last test. There are several epochs where five satellites were available, and a few epochs with six. The increased number of satellites helps the map aided GPS solution filter out the multipath errors.

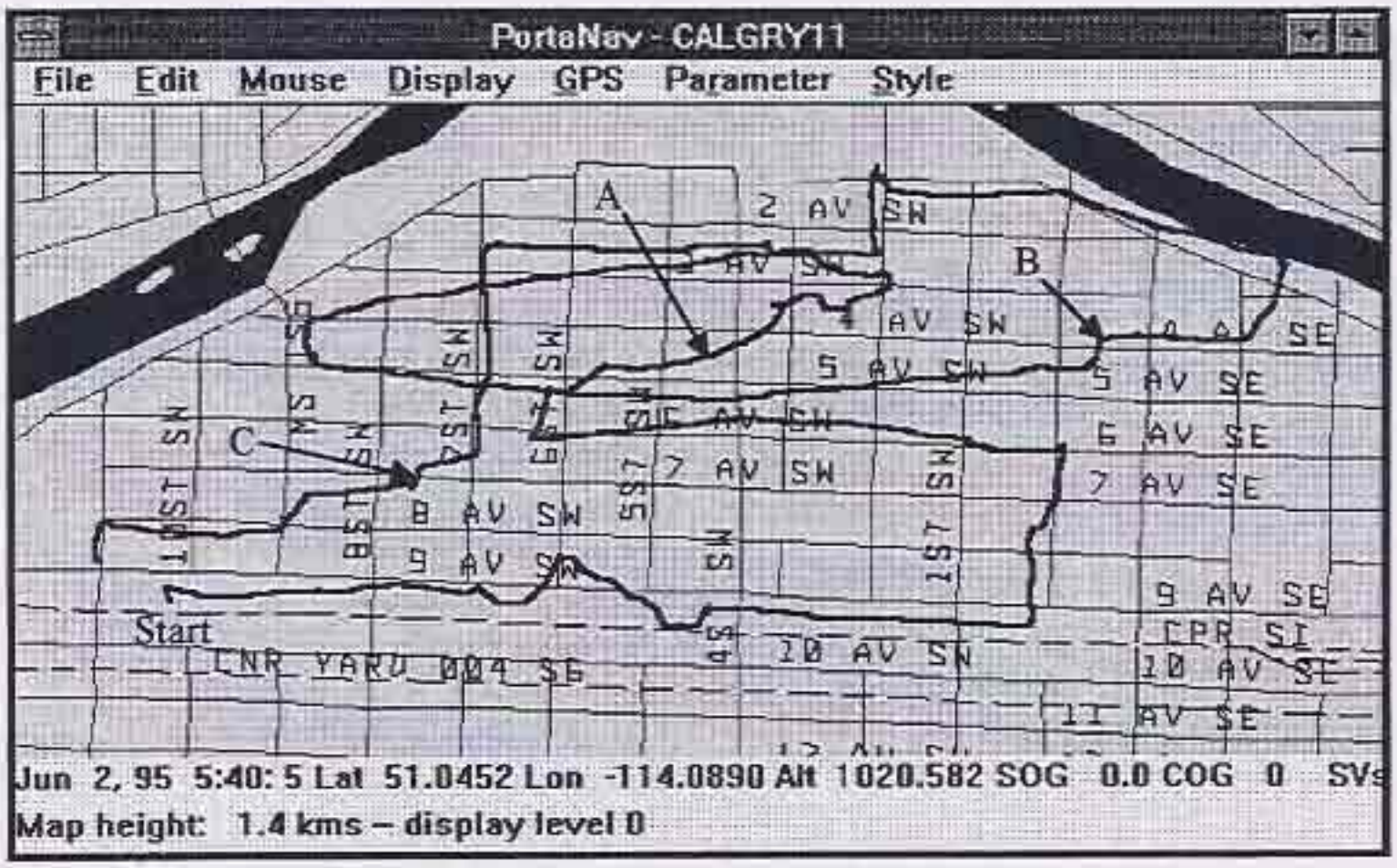

Figure 9.60 Map Aided GPS in Urban Canyon

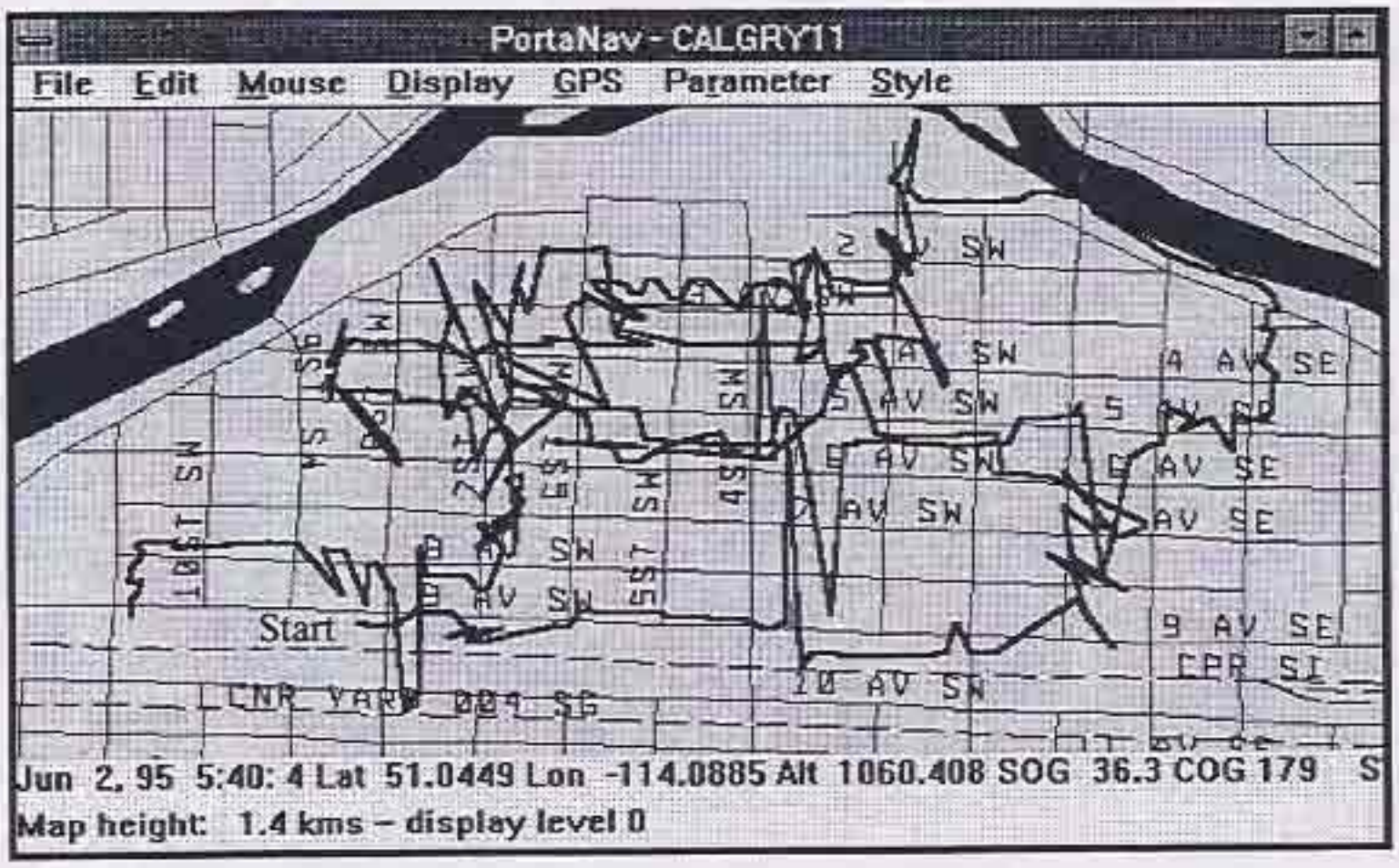

Figure 9.61 Best DOP Fix in Urban Canyon

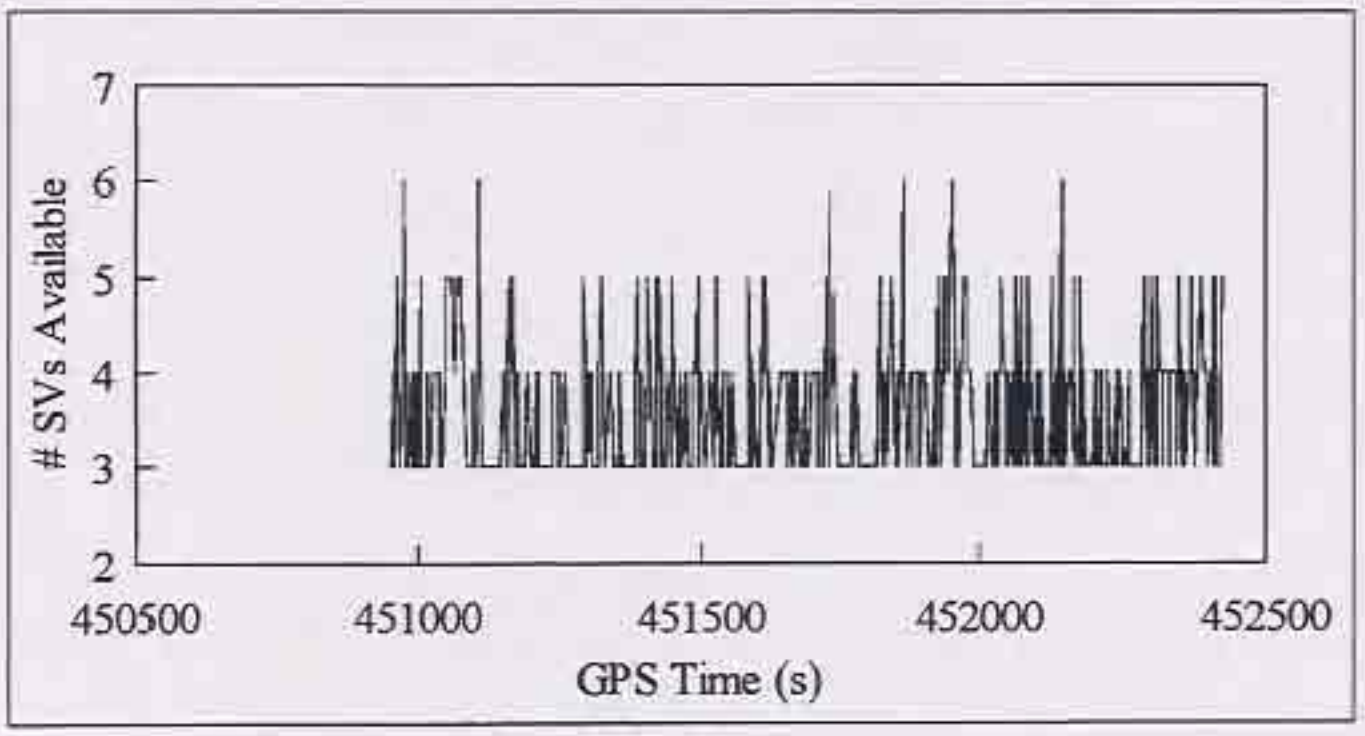

Figure 9.62 Number of Satellites Available in Urban Canyon, June 2, 1995

One last plot is shown in Figure 9.63 to demonstrate how poor conditions can get in an urban canyon environment. This run was done without the constraints on the Kalman filter. A severe case of multipath, combined with long periods between fixes resulted in the filter becoming badly lost on three separate occasions. The constraints on the filter help to minimize the occurrence and the severity of these periods.

9.5 Performance Summary of Solution Types

A few comments will be made to summarize the main characteristics of each solution type tested.

9.5.1 *Best DOP Unique Solution*

The first solution type discussed is the one that is computed on the Trimble MobileGPS receiver and logged by PortaNav as the fixes are reported. This solution proved to be quite stable, in that the trajectory does not experience very many large shifts. This is due to using a consistent constellation when available. When forced to switch constellations

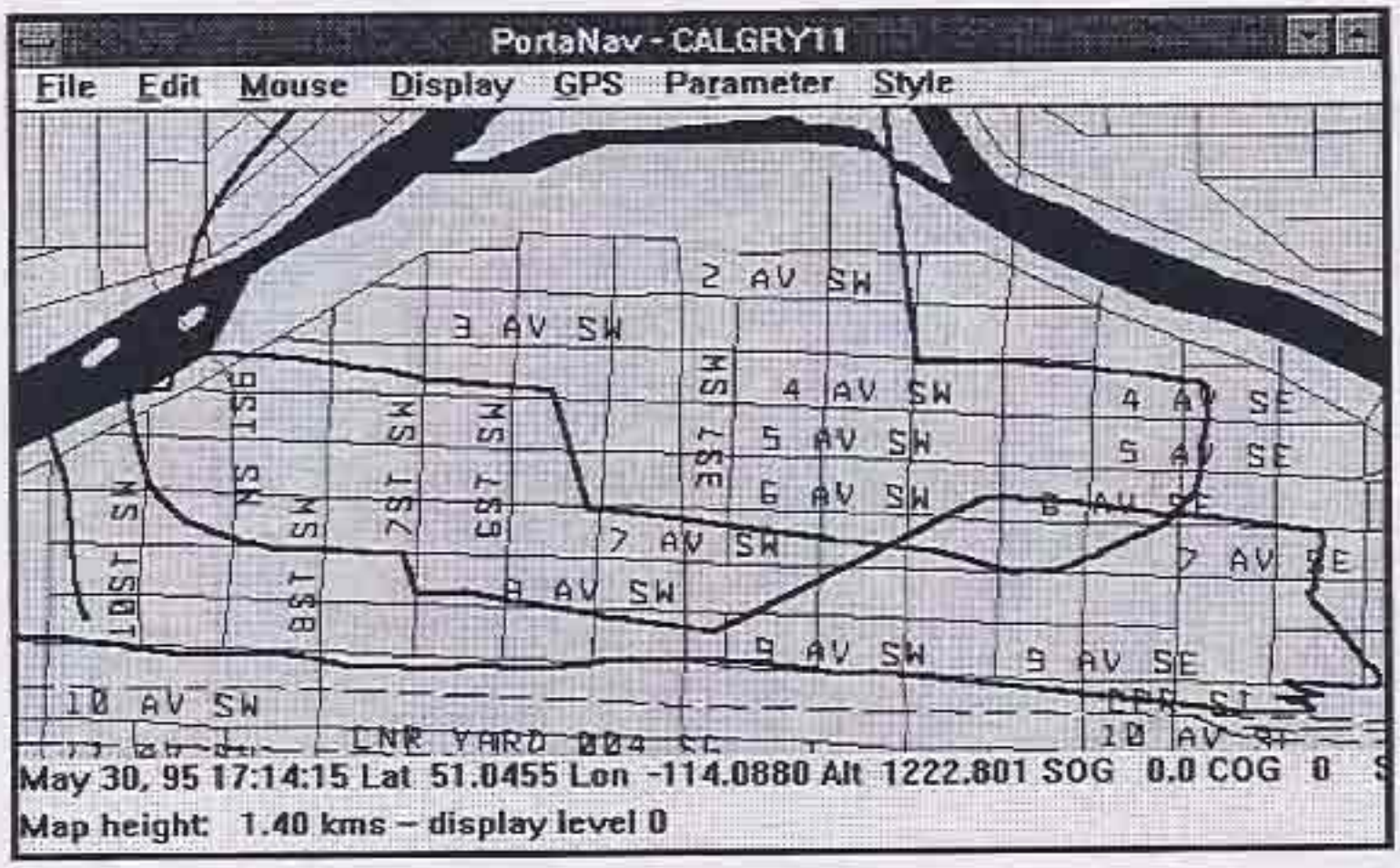

Figure 9.63 Map Aided GPS in Urban Canyon

because of the environment, the performance degrades significantly. In the open road, and in many of the tree canopy areas, the best DOP solution would have led to correct road identification in a map matching display. The problem occurs when a constellation change creates a large spike in the solution that in turn causes the map matching procedure to switch quickly between roads.

9.5.2 *Least Squares Solution*

The all-in-view least squares solution turned out to be the poorest for one main reason: constellation changes. In single point GPS, the effect of each pseudorange on a solution is very different due to SA. Thus when a different satellite is used from one epoch to the next, the computed solution can shift by several tens of metres. The receiver design had a large impact on the number of constellation changes. As discussed in Section 9.4.2, the sixth channel multiplexes through up to four satellite signals, causing an inconsistent data rate for these satellites. If a measurement to a satellite is not made, the constellation will

change. If the receiver used the six channels to simply track the highest six satellites, the least squares solution would be much more stable. This receiver was designed specifically for operation in the best DOP unique mode, and as can be seen, it performs quite nicely in that mode.

9.5.3 *Map Aided GPS Solution*

Overall, the map aided solution did as was expected, that is, augment the performance of GPS. The real question at hand, is whether map aiding alone is adequate for certain applications. The results from these tests indicate that the answer to this question is yes. The performance in all three environments clearly shows that the correct road can be identified and displayed by a map matching procedure. The only exception to this is when the filter becomes lost on occasion in urban canyons. When considering the needs of the average casual navigator, being lost once in a while is not a critical issue. In fact, when the filter becomes lost, it is immediately obvious, because the solution wanders around until it finds the correct position again. The user would be aware that the solution is wrong, and would then resort to traditional methods of navigating. The appealing feature of the map aiding approach is that it does not add any cost or hardware to the basic tools of navigation, namely, a computing device, a GPS receiver, and a digital road map.

The performance of the Kalman filter was evaluated with and without each of the state constraints described in Section 9.3.2. The static constraint helped the filter remain stable at intersections, and helped to prevent turn overshooting when the vehicle stopped before turning. A disadvantage of the static constraint is that when the filter becomes lost, it takes longer to return to the correct position again. The height constraint had the largest impact in the urban canyon, and a small impact under tree canopy. The azimuth constraint after a turn helped keep the filter from overshooting the roads laterally. The disadvantage to this constraint is that when an incorrect road is found, it takes longer for the true road to be found. The final adjustment to the filter was the 'kick start' applied after static periods, which helped the filter keep up in areas where quick turns were made.

The largest remaining problem with the map aided GPS Kalman filter is the data rate. Table 9.5 summarizes the data rates achieved for each of the nine tests. A significant improvement was realized in the third test of each environment. Recall that in these tests the height aiding was done and the least squares fix was not computed so as to reduce the computational burden. Each of these factors improved the average data rate, and consequently the performance of the filter. It should be possible to achieve the same data rate in the filter as was available in the best DOP fix.

Test		Total time of test run (s)	DOP fixes recorded	Average period between fixes (s)	Map aided epochs computed	Average period between epochs (s)
Open road:	Test 1	793	541	1.47	243	3.26
	Test 2	379	251	1.57	108	3.51
	Test 3	652	547	1.19	294	2.22
Tree canopy:	Test 1	707	444	1.59	205	3.45
	Test 2	962	543	1.77	248	3.88
	Test 3	951	701	1.36	386	2.46
Urban canyon:	Test 1	640	521	1.23	117	5.38
	Test 2	470	388	1.21	123	3.82
	Test 3	1 478	854	1.73	532	2.78

Table 9.5 Summary of Data Rates Achieved

9.5.4 *Precise Solution*

The solution computed using precise satellite clocks and precise orbits was intended to act as a baseline to help evaluate the performance of the various solution types. Unfortunately, this baseline is susceptible to multipath and receiver noise. The precise solution helped in clarifying the route taken and in determining whether ill effects were

due to SA or multipath or some other source of error. Also, the precise solution aided in determining an appropriate standard deviation for coordinates extracted from the digital road map.

Obtaining a baseline solution is always difficult in kinematic surveys. A better baseline could have been obtained by using a higher quality GPS receiver, differential GPS, or both. The baseline would still be susceptible to multipath errors, but the magnitude of the maximum multipath could be reduced. The largest gain with a higher quality receiver would be in the lower level of receiver noise. The post-mission precise solution proved adequate for the testing of PortaNav.

CHAPTER TEN

CONCLUSIONS AND RECOMMENDATIONS

10.1 Conclusions From Operational Tests

The map aiding approach taken to augment GPS greatly improves the smoothness and accuracy of the trajectory in vehicle navigation, particularly in the urban canyon and tree canopy environments. The computed solution enables the vehicle to be displayed on the correct road (with map matching in the display procedure) more often than with GPS alone. Map aiding enhances the performance of GPS for autonomous portable vehicle navigation at a low increase in the total cost of the system, and with no additional hardware. Map aided GPS provides output that is pleasing to the eye and mind if a user is willing to put up with the filter occasionally becoming lost in the urban canyon environments.

Some specific conclusions from the testing and development experience follow:

Map aiding:

- A digital road map with a horizontal accuracy of fifteen to twenty metres or better can be used to augment GPS through map aiding.
- A weighted point model update helps constrain the Kalman filter to a point on the road network.
- A straight line slope-intercept model update helps constrain the Kalman filter to a point along a road link in the road network.
- Both map-derived updates help reduce the effects of SA and multipath in GPS.
- Using map aiding with GPS allows the vehicle to be displayed on the correct road more consistently than with GPS alone.
- Map aiding helps the most in tree canopy and urban canyon environments.

Kalman filter performance:

- Height aiding greatly improves the coverage in urban canyon areas and marginally improves the coverage in tree canopy environments.
- Zeroing the velocities in the state vector when the vehicle is not moving helps to avoid wandering.
- 'Kick starting' the Kalman filter when the vehicle begins moving helps eliminate the lag effect.
- Applying the azimuth of the road to the Kalman filter velocity states helps to avoid overshooting roads laterally.
- Constricting the velocity in the up direction helped avoid large spikes due to multipath in the urban canyon environment.
- There is room for fine tuning the parameters of the Kalman filter, including the spectral densities, the correlation times, the initial state variances, and the observational variances.

GPS:

- With the Trimble MobileGPS receiver, a fix computed using a best DOP procedure is much more stable than an all-in-view least squares fix.
- When available, Doppler measurements should be used for velocity aiding in kinematic navigation applications.

Digital road map:

- A digital road map is very useful source of positioning observations.
- Road related information (directionality, turn restrictions, etc.) is a valuable resource in determining the most probable route of travel.
- A complete, consistent, and accurate road map is essential for use in land vehicle navigation.

Computing:

- The operating system is an important piece in the puzzle of a navigation system; a multi-tasking environment is highly desirable so that measurements can be recorded while an epoch is being processed.
- Even with a 25 MHz 80486 processor, a bottle neck occurs in the data processing for a real-time navigation system.

10.2 Recommendations For Future Development Directions

The first major recommendation is to solve the data latency problem and observe the improved performance of the filter with more frequent updates. It is hypothesized that the map aided filter will get lost even less in harsh environments if the updates can be achieved at an optimum one second data rate. This would involve optimizing the software to reduce the computational burden and also finding a way to avoid missing measurements as they are made by the receiver. This should be possible through multi-tasking or if a buffer of some sort can be used.

The second major recommendation is to implement a connectivity table for two purposes. First, the connectivity table can be used in the road finding algorithm to eliminate roads that are not connected directly to the location of the previous solution. Second, the connectivity chart can be used to keep track of possible routes of travel when the road of travel is ambiguous. Parallel filters can be run until such a point where one of the routes becomes impossible and is eliminated. When one filtered solution remains, it will have been filtered using the correct roads travelled on during the ambiguous time. Currently, if the road is ambiguous, no map updates are performed, and the solution loses the potential benefit of the road observations during the ambiguous time.

A potential extension to the concept of map aiding is the idea of using a digital terrain model (DTM) to perform height aiding. The accuracies of DTMs are improving with the development of better remote sensing techniques, and the cost of DTM data is decreasing. It should be possible to use a DTM that is good to about ten metres in height, to augment

GPS even further. The observational model for such a situation would be complex, but nevertheless possible.

No experiments were done to ascertain the stability of the map aided filter when using less than three satellites in an epoch. Mathematically, there is no reason to require three observations in an epoch and theoretically, the additional position information from the map should help to maintain stability in the filter.

Finally, it is recommended that a suitable form factor for PortaNav be developed so that it can be used more easily in a road vehicle or by a person on foot. Thus PortaNav will live up to its name of being a truly portable navigation system.

REFERENCES

Abousalem, M.A. (1993). "Development Of A Robust GPS Kinematic Positioning Module For Automatic Vehicle Location And Navigation." M.Sc. Thesis, Department of Geomatics Engineering, The University of Calgary, Canada.

Abousalem, M.A., J.F. McLellan, E. Whatley, and P.Galyean (1995). "International Wide Area Differential GPS Networks." *Proceedings of The Institute of Navigation National Technical Meeting 1995 (ION-NTM '95)*, January 18-20, Anaheim, California.

Alegiani, J.B., J.L. Buxton, and S.K. Honey (1989). "An In-Vehicle Navigation and Information System Utilizing Defined Software Services." *Proceedings of Vehicle Navigation and Information Systems (VNIS '89)*, September 11-13, Toronto, Ontario, Canada, pp. A3-A8.

Askenazi, V., T. Moore, C. Hill, P. Cross, W. Roberts, D. Hawksbee, K. Mollon, D. Winchester, and T. Jackson (1994). "Standards for Benchmarking Differential GPS." *Proceedings of Institute of Navigation GPS (ION GPS '94)*, September 20-23, Salt Lake City, Utah, pp. 1285-1290.

Azuma, S., K. Nishida, and S. Hori (1994). "The Future of In-Vehicle Navigation Systems." *Proceedings of the IEEE Position, Location, and Navigation Symposium, 1994 (PLANS '94)*, April 12-15, Las Vegas, Nevada, pp. 537-542.

Ballard, N. (1994). "State of PDAs and Other Pen-Based Systems." *Pen Compuing*, August 1994, Vol. 1, No. 1, pp. 14-18. Pen Computing Inc., Albany, New York.

Beser, J. and B.W. Parkinson (1981). "The Application of NAVSTAR Differential GPS in the Civilian Community." *Global Positioning System: Papers Published in Navigation*, Vol. II, 1984, pp. 167-196.

Blackwell, E.G. (1985). "Overview of Differential GPS Methods." *Global Positioning System: Papers Published in Navigation*, Vol. III, 1986, pp. 89-100.

Brown, R.G. and P.Y.C. Hwang (1992). *Introduction To Random Signals and Applied Kalman Filtering*. Second Edition, John Wiley & Sons Inc., New York.

Bullock, J.B. and E.J. Krakiwsky (1994). "Analysis of the Use of Digital Road Maps in Vehicle Navigation." *Proceedings of the IEEE Position, Location, and Navigation Symposium, 1994 (PLANS '94)*, April 12-15, Las Vegas, Nevada, pp. 494-501.

Bullock, J.B., E.J. Krakiwsky, and M.J. Casey (1995a). "The Diversity of Intelligent Ship Navigation Systems." *Proceedings of The Institute of Navigation National Technical Meeting 1995 (ION-NTM '95)*, January 18-20, Anaheim, California.

Bullock, J.B., E.J. Krakiwsky, N.G. Grant, and K.L. Grandia (1995b). "The Diversity of Intelligent Air Navigation Systems." *Proceedings of The Institute of Navigation National Technical Meeting 1995 (ION-NTM '95)*, January 18-20, Anaheim, California.

Cannon, M.E. (1991). "Airborne GPS/INS With An Application To Aerotriangulation." Ph.D. Thesis, Department of Geomatics Engineering, The University of Calgary, Canada.

Cannon, M.E. and G. Lachapelle (1992). "Analysis of a High Performance C/A Code GPS Receiver in Kinematic Mode." *Proceedings of The Institute of Navigation National Technical Meeting 1992 (ION-NTM '92)*, San Diego, California.

Cannon, M.E., J.B. Schleppe, J.F. McLellan, and T.E. Ollevier (1992). "Real-Time Heading Determination Using an Integrated GPS-Dead Reckoning System." *Proceedings of Institute of Navigation GPS (ION GPS '92)*, September 16-18, Albequerque, New Mexico, pp. 767-773.

Claussen, H. (1993). "Status and Directions of Digital Map Databases in Europe." *Proceedings of Vehicle Navigation and Information Systems (VNIS '93)*, October 12-15, Ottawa, Ontario, Canada, pp. 25-28.

Colestock, A. (1994). "A Batch Least Squares Implementation for Estimating Autonomous GPS Point Positions." *Proceedings of Institute of Navigation GPS (ION GPS '94)*, September 20-23, Salt Lake City, Utah, pp. 399-404.

Collier, W.C. and R.J. Weiland (1994). "Smart Cars, Smars Highways." *IEEE Spectrum*, April 1994, Vol. 31, No. 4, pp. 27-33. The Institute of Electrical and Electronics Engineers, New York, New York.

Dennehy, K. (1994). "Japanese Vehicle Navigation Market Update." Global Positioning & Navigation News, December 1, 1994, No. 12. Phillips Business Information Inc., Potomac, Maryland.

De Taeye, A. (1994). "The European Digital Road Map Triggered by Car Information Systems." *Proceedings of Vehicle Navigation & Information Systems (VNIS '94)*, August 31-September 2, Yokohama, Japan.

Dijkstra, E.W. (1959). "A Note On Two Problems on Connexion with Graphs." *Numerische Mathematik 1*, pp. 552-561.

Etak Inc. (1994). "MapDraw Library Programmer's Guide." Version 2.0.2. Etak Inc., Menlo Park, California.

French, R.L. (1987). "Historical Overview of Automobile Navigation Technology." *Proceedings of the 36th IEEE Vehicular Technology Conference*. Dallas, Texas, May 20-22, pp. 1-9.

French, R.L. (1989). "Map Matching Origins, Appoaches and Applications." *Proceedings of Land Vehicle Navigation.* July 4-7, 1989, pp. 91-116. Verlag TUV Rheinland GmbH., Koln, Germany.

French, R.L. and G.M. Lang (1973). "Automatic Route Control System." *IEEE Transactions on Vehicular Technology*, pp. 36-41. The Institute of Electrical and Electronic Engineers, New York, New York.

French, R.L. and C. Querèe (1993). "EGT Shuns Efforts to Set Up Data Pool for Euro Digital Mapping." *The Intelligent Highway*, September 1993, Vol. 4, Iss. 6, pp. 1-2.

Gao, Y. (1992). "A Robust Quality Control System For GPS Navigation and Kinematic Positioning." Ph.D. Thesis, Department of Geomatics Engineering, The University of Calgary, Canada.

Gelb, A. [editor] (1974). *Applied Optimal Estimation*. The MIT Press, Cambridge, Massachusetts.

Geomatics Canada (1994). "GPS Positioning from ACS Clocks and Ephemerides (GPSPACE)." User's guide, Version 2.0. Canadian Active Control System Operations, Geodetic Survey Division, Ottawa, Canada.

Goad, C.C. and L. Goodman (1974). "A Modified Hopfield Tropospheric Refraction Correction Model" Paper presented at the Fall Annual Meeting of the American Geophysical Union, San Francisco, California, December 12-17.

Greenspan, R.L. and J.I. Donna (1986). "Measurement Errors in GPS Observables." *Global Positioning System: Papers Published in Navigation*, Vol. IV, 1993, pp. 3-18.

Gurtner, W. (1994). "RINEX: The Receiver Independent Exchange Format Version 2." Astronomical Institute, University of Berne.

Harris, C.B. (1989). "Prototype For A Land Based Automatic Vehicle Location And Navigation System." M.Sc. thesis, Department of Geomatics Engineering, The University of Calgary, Canada.

Harris, C.B., L.A. Klesh, E.J. Krakiwsky, H.A. Karimi, and N.S.T. Lee (1988). "Digital Map Dependent Functions of Automatic Vehicle Location Systems." *Proceedings of the IEEE Position, Location, and Navigation Symposium, 1988 (PLANS '88)*, November 29 - December 2, Orlando, Florida.

Hofmann-Wellenhof, B., H. Lichtenegger, and J. Collins (1994). *GPS Theory and Practice.* Third, revised edition, Springer-Verlag Wien, New York, New York.

Jorgensen, P. (1986). "Relativity Correction in GPS User Equipment." *Proceedings of Position, Location, and Navigation Symposium, 1986 (PLANS '86)*, Las Vegas, Nevada, pp. 177-183.

Kalman, R.E. (1960). "A New Approach To Linear Filtering and Prediction." *Journal of Basic Engineering*, ASME, 82D.

Kao, W. (1991). "Integration of GPS and Dead-Reckoning Navigation Systems." *Proceedings of Vehicle Navigation & Information Systems Conference, 1991 (VNIS '91)*, October 20-23, Dearborne, Michigan, pp. 635-643.

Kee, C. and B. Parkinson (1994). "Calibration of Multipath Errors on GPS Pseudorange Measurements." *Proceedings of Institute of Navigation GPS (ION GPS '94)*, September 20-23, Salt Lake City, Utah, pp. 353-362.

Klobuchar, J.A. (1983). "Ionospheric Effects on Earth-Space Propagation." Air Force Geophysics Laboratory, TR-84-0004.

Klobuchar, J.A. (1986). "Design and Characteristics of the GPS Ionospheric Time Delay Algorithm For Single Frequency Users." *Proceedings of Position, Location, and Navigation Symposium, 1986 (PLANS '86)*, Las Vegas, Nevada, pp. 280-286.

Krakiwsky, E.J. (1991). "GPS and Vehicle Location and Navigation." Innovation Column, *GPS World*, May 1991, Vol. 2, No. 5. Advanstar Communications, Eugene Oregon.

Krakiwsky, E.J. (1992a). "GPS-Based IVHS Navigation Systems Will Continue To Overtake Purely Terrestrial Based Systems in 1993." *GPS World Showcase*, December 1992. Advanstar Communications, Eugene Oregon.

Krakiwsky, E.J. (1992b). *The Method of Least Squares: A Synthesis of Advances, ENGO 629 Lecture Notes*. Department of Geomatics Engineering, The University of Calgary, Canada.

Krakiwsky, E.J. and M.A. Abousalem (1995). *Adjustment of Observations, ENGO 361 Lecture Notes*. Department of Geomatics Engineering, The University of Calgary, Canada.

Krakiwsky, E.J., M.A. Abousalem, D.J. Szabo, and J.B. Bullock (1995). *IVHS Navigation Systems Database*, Version 4.5. Department of Geomatics Engineering, The University of Calgary, Canada.

Krakiwsky, E.J. and J.B. Bullock (1994). "Digital Road Data: Putting GPS On The Map." *GPS World*, May 1994, Vol. 5, No. 5, pp. 43-46. Advanstar Communications, Eugene, Oregon.

Krakiwsky, E.J., C.B. Harris, and R.V.C. Wong (1988). "A Kalman Filter For Integration of Dead Reckoning, Map Matching, and GPS Positioning." *Proceedings of the IEEE Position, Location, and Navigation Symposium, 1988 (PLANS '88)*, November 29 - December 2, Orlando, Florida.

Krakiwsky, E.J. and C.B. Harris (1994). "Communications for AVLN Systems." *GPS World*, November 1994, Vol. 5, No. 11. Advanstar Communications, Eugene, Oregon.

Krakiwsky, E.J., H.A. Karimi, C. Harris, and J. Geroge (1987). ""Research into Electronic Maps and Automatic Vehicle Location." *Proceedings of the Eighth International Symposium on Computer-Assisted Cartography, AUTO-CARTO 8*. Baltimore, Maryland, March 29 - April 3.

Krakiwsky, E.J and J.F. McLellan (1995). "Making GPS Even Better With Auxiliary Devices." *GPS World*, November 1994, Vol. 6, No. 3, pp. 46-53. Advanstar Communications, Eugene, Oregon.

Krakiwsky, E.J. and D.E. Wells (1971). "Coordinate Systems in Geodesy." The Department of Surveying Engineering, The University of New Brunswick, Fredricton, New Brunswick, May 1971. (Reprinted December 1990).

Lachapelle, G. (1993). *NAVSTAR GPS: Theory and Applications, ENGO 625 Lecture Notes*. Department of Geomatics Engineering, The University of Calgary, Canada.

Lachapelle, G. and J. Henriksen (1995). "GPS Under Cover: The Effects of Foliage On Vehicular Navigation." *GPS World*, March 1995, Vol. 6, No. 3, pp. 26-35. Advanstar Communications, Eugene Oregon.

Lachapelle, G., R. Klukas, D. Roberts, and W. Qiu (1994). "One-Meter Level Kinematic Point Positioning Using Precise Orbits and Satellite Clock Corrections." *Proceedings of Institute of Navigation GPS (ION GPS '94)*, September 20-23, Salt Lake City, Utah, pp. 1435-1443.

Lanigan, C.A., K. Pflieger, and P.K. Enge (1990). "Real-Time Differential Global Positioning System (DGPS) Data Link Alternatives." *Proceedings of Institute of Navigation GPS (ION GPS '90)*, September 19-21, Colorado Springs, Colorado, pp. 599-606.

Leick, A. (1995). *GPS Satellite Surveying*. Second Edition, John Wiley & Sons Inc., New York, New York.

Lezniak, T.W., R.W. Lewis, and R.A. McMillen (1977). "A Dead Rackoning/Map Correlation System for Automatic Vehicle Tracking." *IEEE Transactions on Vehicular Technology*. February 1977, Vol. 26, No. 1, pp. 47-60. The Institute of Electrical and Electronics Engineers, New York, New York.

Liikkuva Systems International Inc. (1994). "Knowing where you are is *only* the beginning..." Retki product brochure. Liikkuva Systems International Inc., Cameron Park, California.

Morrison, N. (1969). *Introduction To Sequential Smoothing and Prediction.* McGraw-Hill Book Company, New York, New York.

McLellan, J.F. (1992). "Design and Analysis of a Low-Cost GPS Aided Navigation System." M.Sc. Thesis, Department of Geomatics Engineering, The University of Calgary, Canada.

New Scientist (1984). "The Moving Map Makes Navigation Easy." *New Scientist*, September 1984, Haywards Heath, West Sussex, United Kingdom.

Nilsson, N.J. (1980). *Principals of Artificial Intelligence*. Tioga Publishing Co., Palo Alto, California.

Phail, F. (1991). "The Power of a Personal Computer for Car Information and Communications Systems." *Proceedings of Vehicle Navigation and Information Systems (VNIS '91)*, October 20-23, 1991, Dearborn, Michigan, pp.389-395.

Philips and Bosch (1988). *The Geographic Data File, Release 1.0, 1988-10-01.* Publication from Philips Consumer Electronics B.V., Eindhoven, The Netherlands.

Pulsearch Navigation Systems (1992). "Assessment of Digital Mapping Data for Use in Vehicle Navigation Systems." A report submitted to Alberta Forestry Lands and Wildlife Land Information Services Division in Edmonton, Alberta, Canada.

Qiu, W., G. Lachapelle, and M.E. Cannon (1994). "Ionospheric Effect Modelling for Single Frequency GPS Users." *Proceedings of Institute of Navigation GPS (ION GPS '94)*, September 20-23, Salt Lake City, Utah, pp. 911-919.

Reimer, J. (1994). "Getting Carded: So, What Are Those PCMCIA Cards All About?" *Pen Compuing*, August 1994, Vol. 1, No. 1, pp. 44-48. Pen Computing Inc., Albany, New York.

Road Scholar Software (1994). "City Streets Electronic Street Guide." City Streets product brochure. Road Scholar Software, Houston, Texas.

Rockwell International Corporation (1989). "NAVSTAR GPS Space Segment/Navigation User Interfaces." Interface Control Document ICD-GPS-200, Downey, California.

Schiff, T.H. (1993). "Data Sources and Consolidation Methods for Creating, Improving and Maintaining Navigation Databases." *Proceedings of Vehicle Navigation and Information Systems (VNIS '93)*, Oct. 12-15, Ottawa, Ontario, Canada, pp. 3-7.

Schwarz, K.P. (1987). "Kalman Filtering and Optimal Smoothing." *Papers For The CISM Adjustment And Analysis Seminars*. Second Edition, The Canadian Institute of Surveying and Mapping, Ottawa, Canada.

Schwarz, K.P., M.E. Cannon, and R.V.C. Wong (1989). "A Comparison of GPS Kinematic Models for the Determination of Position and Velocity Along a Trajectory." *Manuscripta Geodetica*, Vol. 14, No. 5, pp. 345-353.

Scott, C. (1994). "Improved GPS Positioning for Motor Vehicles Through Map Matching." *Proceedings of Institute of Navigation GPS (ION GPS '94)*, September 20-23, Salt Lake City, Utah, pp. 1391-1400.

Seeber, G. (1993). *Satellite Geodesy*. Walter de Gruyter, Berlin, Germany.

She, J. (1994). "High Accuracy Airborne Differential GPS Positioning Using a Multi-Receiver Configuration." M.Sc. Thesis, Department of Geomatics Engineering, The University of Calgary, Canada.

Shibata, M. and Y. Fujita (1989). "Current Status and Future Plans for Digital Map Databases in Japan." *Proceedings of Vehicle Navigation and Information Systems (VNIS '89)*, September 11-13, Toronto, Ontario, Canada, pp. 29-33.

Shields, T.R. (1994). "U.S. Trends In Navigable Digital Map Databases." *Proceedings of Vehicle Navigation & Information Systems (VNIS '94)*, August 31-September 2, Yokohama, Japan.

Shuldiner, H. (1985). "Here Now: Computerized Navigator for Your Car." *Popular Science*, June 1985, pp. 61-67. Times Mirror Magazines Inc., New York, New York.

Soviero, M.M. (1992). "Your World According To Newton." *Popular Science*, September 1992, Vol. 241, No. 3, pp. 45-49. Times Mirror Magazines Inc., New York, New York.

Sweetman, D. and C. Collier (1993). "Route Guidance Technology for Automatic GIS Database Maintenance." *Proceedings of The Institute of Navigation National Technical Meeting (ION '93)*, January 18-20, San Francisco, California.

Tapscott, M. (1994). "On the Road with GPS." *Defense Electonics*, September 1994, pp. 16-18.

Teunissen, P.J.G. and M.A. Salzmann (1988). "Performance Analysis of Kalman Filter." Technical Report #88.2, Geodetic Computing Centre, Delft University of Technology, The Netherlands.

Trimble Navigation (1994a). "Mobile GPS Programmer's Guide." Version 3.1. Trimble Navigation, Sunnyvale, California.

Trimble Navigation (1994b). "SVeeSix System Designer's Reference Manual." Part no. 25856-00, Trimble Navigation, Sunnyvale, California.

Van Dierendonck, A.J. (1995). "Understanding GPS Receiver Terminology: A Tutorial." *GPS World*, January 1995, Vol. 6, No. 1, pp. 34-44. Advanstar Communications, Eugene Oregon.

Vanicek, P. and E.J. Krakiwsky (1982). *Geodesy: The Concepts*. Second Edition, North-Holland Publishing Company, Amsterdam, The Netherlands.

Wells, D., N. Beck, D. Delikaraoglou, A. Kleusberg, E.J. Krakiwsky, G. Lachapelle, R.B. Langley, M. Nakiboglu, K.P. Schwarz, J.M. Tranquilla, and P. Vanicek (1986).

Guide to GPS Positioning. Canadian GPS Associates, Fredericton, New Brunswick, Canada.

White, M. (1987). "Digital Map Requirements of Vehicle Navigation." *Proceedings of the Eighth International Symposium on Computer-Assisted Cartography (AUTO-CARTO 8)*, March 29 - April 3, Baltimore, Maryland.

White, R. (1993). "In Search of the Ultimate Notebook." PC Computing, July 1993, Vol. 6, No. 7, pp. 184-204. Ziff-Davis Publishing Company, Boulder, Colorado.

Winston, P.H. (1984). *Artificial Intelligence*. Second Edition. Addison-Wesley Publishing Company, ch. 1, 4, 6, 8.

Wong, R.V.C. (1988). "Development Of A RLG Strapdown Inertial Survey System." Report Number 20027, Department of Geomatics Engineering, The University of Calgary, Canada.

Zavoli, W.B. (1989). "Navigation and Digital Maps Interface for Fleet Management and Driver Information Systems." *Proceedings of Vehicle Navigation and Information Systems (VNIS '89)*, September 11-13, Toronto, Ontario, Canada, pp. A9-A14.

Zavoli, W.B. and S.K. Honey (1986). "Map Matching Augmented Dead Reckoning." *Proceedings of Position, Location, and Navigation Symposium, 1986 (PLANS '86)*, Las Vegas, Nevada, pp. 359-362.